frontiers | Research Topics

Role of the immune system in renal transplantation: Importance, mechanism, and therapy

Edited by
Long Zheng, Ruiming Rong, Xuanchuan Wang and Liping Li

Published in
Frontiers in Immunology

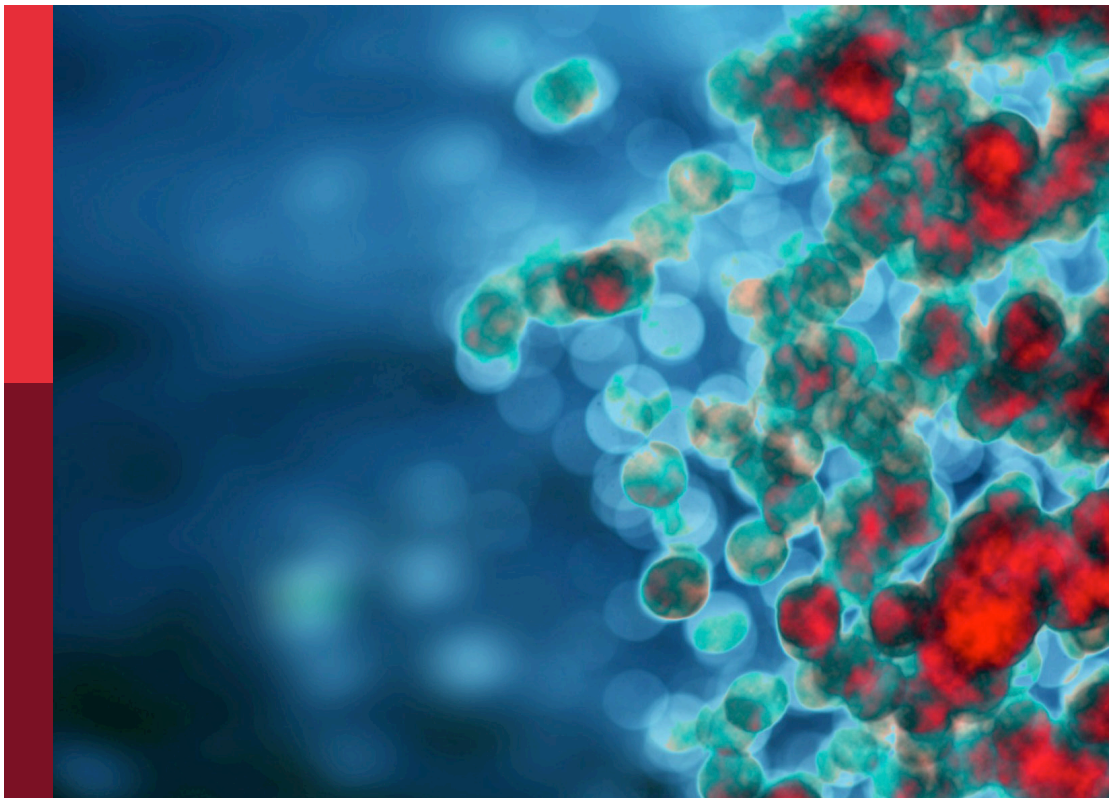

ISSN 1664-8714
ISBN 978-2-8325-4608-6
DOI 10.3389/978-2-8325-4608-6

About Frontiers

Frontiers is more than just an open access publisher of scholarly articles: it is a pioneering approach to the world of academia, radically improving the way scholarly research is managed. The grand vision of Frontiers is a world where all people have an equal opportunity to seek, share and generate knowledge. Frontiers provides immediate and permanent online open access to all its publications, but this alone is not enough to realize our grand goals.

Frontiers journal series

The Frontiers journal series is a multi-tier and interdisciplinary set of open-access, online journals, promising a paradigm shift from the current review, selection and dissemination processes in academic publishing. All Frontiers journals are driven by researchers for researchers; therefore, they constitute a service to the scholarly community. At the same time, the *Frontiers journal series* operates on a revolutionary invention, the tiered publishing system, initially addressing specific communities of scholars, and gradually climbing up to broader public understanding, thus serving the interests of the lay society, too.

Dedication to quality

Each Frontiers article is a landmark of the highest quality, thanks to genuinely collaborative interactions between authors and review editors, who include some of the world's best academicians. Research must be certified by peers before entering a stream of knowledge that may eventually reach the public - and shape society; therefore, Frontiers only applies the most rigorous and unbiased reviews. Frontiers revolutionizes research publishing by freely delivering the most outstanding research, evaluated with no bias from both the academic and social point of view. By applying the most advanced information technologies, Frontiers is catapulting scholarly publishing into a new generation.

What are Frontiers Research Topics?

Frontiers Research Topics are very popular trademarks of the *Frontiers journals series*: they are collections of at least ten articles, all centered on a particular subject. With their unique mix of varied contributions from Original Research to Review Articles, Frontiers Research Topics unify the most influential researchers, the latest key findings and historical advances in a hot research area.

Find out more on how to host your own Frontiers Research Topic or contribute to one as an author by contacting the Frontiers editorial office: frontiersin.org/about/contact

Role of the immune system in renal transplantation: Importance, mechanism, and therapy

Topic editors

Long Zheng — The second Affiliated Hospital of Zhejiang University School of Medicine, China

Ruiming Rong — Fudan University, China

Xuanchuan Wang — Fudan University, China

Liping Li — Geisinger Medical Center, United States

Citation

Zheng, L., Rong, R., Wang, X., Li, L., eds. (2024). *Role of the immune system in renal transplantation: Importance, mechanism, and therapy*. Lausanne: Frontiers Media SA. doi: 10.3389/978-2-8325-4608-6

Table of contents

frontiers | Frontiers in Immunology

TYPE Original Research
PUBLISHED 22 November 2022
DOI 10.3389/fimmu.2022.1039013

OPEN ACCESS

EDITED BY
Long Zheng,
The second Affiliated Hospital of Zhejiang University School of Medicine, China

REVIEWED BY
Yingzi Ming,
Central South University, China
Junnan Xu,
Chinese PLA General Hospital, China

*CORRESPONDENCE
Hanyu Xiao
xiaohanyu3399@foxmail.com
Juan Zhou
zj604050129@163.com

†These authors have contributed equally to this work and share first authorship

SPECIALTY SECTION
This article was submitted to Alloimmunity and Transplantation, a section of the journal Frontiers in Immunology

RECEIVED 07 September 2022
ACCEPTED 01 November 2022
PUBLISHED 22 November 2022

CITATION
Pang Q, Chen H, Wu H, Wang Y, An C, Lai S, Xu J, Wang R, Zhou J and Xiao H (2022) N6-methyladenosine regulators-related immune genes enable predict graft loss and discriminate T-cell mediate rejection in kidney transplantation biopsies for cause.
Front. Immunol. 13:1039013.
doi: 10.3389/fimmu.2022.1039013

N6-methyladenosine regulators-related immune genes enable predict graft loss and discriminate T-cell mediate rejection in kidney transplantation biopsies for cause

Qidan Pang[1†], Hong Chen[2†], Hang Wu[1†], Yong Wang[2], Changyong An[2], Suhe Lai[2], Jia Xu[1], Ruiqiong Wang[1], Juan Zhou[1*] and Hanyu Xiao[2*]

[1]Department of Nephrology, Bishan Hospital of Chongqing Medical University, Chongqing, China, [2]Department of General Surgery/Gastrointestinal Surgery, Bishan Hospital of Chongqing Medical University, Chongqing, China

Objective: The role of m6A modification in kidney transplant-associated immunity, especially in alloimmunity, still remains unknown. This study aims to explore the potential value of m6A-related immune genes in predicting graft loss and diagnosing T cell mediated rejection (TCMR), as well as the possible role they play in renal graft dysfunction.

Methods: Renal transplant-related cohorts and transcript expression data were obtained from the GEO database. First, we conducted correlation analysis in the discovery cohort to identify the m6A-related immune genes. Then, lasso regression and random forest were used respectively to build prediction models in the prognosis and diagnosis cohort, to predict graft loss and discriminate TCMR in dysfunctional renal grafts. Connectivity map (CMap) analysis was applied to identify potential therapeutic compounds for TCMR.

Results: The prognostic prediction model effectively predicts the prognosis and survival of renal grafts with clinical indications ($P< 0.001$) and applies to both rejection and non-rejection situations. The diagnostic prediction model discriminates TCMR in dysfunctional renal grafts with high accuracy (area under curve = 0.891). Meanwhile, the classifier score of the diagnostic model, as a continuity index, is positively correlated with the severity of main pathological

injuries of TCMR. Furthermore, it is found that METTL3, FTO, WATP, and RBM15 are likely to play a pivotal part in the regulation of immune response in TCMR. By CMap analysis, several small molecular compounds are found to be able to reverse TCMR including fenoldopam, dextromethorphan, and so on.

Conclusions: Together, our findings explore the value of m6A-related immune genes in predicting the prognosis of renal grafts and diagnosis of TCMR.

KEYWORDS

N6-methyladenosine (m6A), kidney transplantation, alloimmunity, graft loss, T-cell mediate rejection, biopsies for cause, prediction model

Introduction

As of now, kidney transplantation is still the most effective remedy for end-stage renal disease (1). However, transplant patients are still chronically challenged by graft rejection, infection, and recurrence of primary kidney disease, which may lead to allograft injury and dysfunction (2). Elevated serum creatinine, hematuria, proteinuria, and decreased urine output are the common clinical manifestations of allograft injury and dysfunction. When a kidney transplant recipient develops those indications, a biopsy for cause is usually needed to identify the pathogenesis, which is known to be the gold standard (3). Timely and targeted interventions may reverse active injuries, alleviate chronic lesions, and avoid graft loss. Although the reasons for graft injury and loss are multifactorial and time-dependent, immune factors still dominate (4). Two studies on transplant kidney histology have shown that the alloimmune processes account for 35%-64% of graft loss (5, 6), of which T cell-mediated rejection (TCMR) and antibody-mediated rejection (ABMR) are the most typical subtypes. Persistent alloimmunity can also aggravate interstitial fibrosis and tubular atrophy (IF/TA), which is regarded as an important prognostic factor of grafts and the final pathological outcome of graft injuries (4).

N6-methyladenosine (m6A) modification is one of the most prevalent and reversible modifications of RNA base in eukaryotes (7). Through three functional protease complexes: writers, erasers, and readers, m6A regulates RNA transport, export, splicing, localization, translation and stability at the post-transcriptional level, thus participating in various physiological and pathological processes. Recent studies show that the m6A modification plays an important role in shaping a balanced immune response (8). M6A can affect innate, adaptive and antiviral immune responses by modulating the mRNA of key genes in the immune pathway. For example, m6A-mediated degradation of interferon B (IFNB) transcripts weakens the type I interferon and antiviral innate immune responses (9). The m6A mechanism enhances the interleukin-STAT5 signaling pathway through the attenuation of SOCS mRNA, thereby promoting the proliferation of CD4+ T cells and the immunosuppressive function of Treg cells (10, 11). M6A methylation of the Tcf7 gene mediated by METTL3 stabilizes the transcripts of the Tcf7 gene and increases the expression of TCF-1. TCF-1 promotes the differentiation of T-helper and Tfh cells, thus facilitating B cell differentiation and plasma generation (12). The regulatory role of m6A in the immune system has been demonstrated to play a part in the tumor immune microenvironment (13) and many autoimmune diseases (14), including systemic lupus erythematosus, rheumatoid arthritis, and inflammatory bowel disease. However, there is no research to elucidate its role in the immune responses after kidney transplantation.

The maturity and reduced cost of sequencing technology have improved the accuracy of disease diagnosis and treatment. Genome-wide transcript microarray data can be derived from a morsel of graft tissue, which makes it feasible for us to explore the internal relations of diseases at a molecular level. The combined application of transcript data with machine algorithms has brought about a range of molecular classifiers and risk scoring models that facilitate diagnosis and predict prognosis. Histologic diagnosis is flawed by subjective interpretations among pathologists, nonspecific lesions, and arbitrary rules, making it not as reliable as we expect (15, 16). Given the absence of a reliable gold standard, classification criteria based on objective molecular expression data present an alternative approach and complement the histologic diagnosis. Reeve et al. (17) established the Molecular Microscope Diagnostic System (MMDx) based on microarray gene expression data of renal grafts, whose balanced accuracies for histology diagnoses of TCMR and ABMR reach 73% and 78%, respectively. The molecular risk score established by Einecke et al. (18) is able to reflect active injury and superior to either scarring or function in predicting graft failure.

This study aims to explore the relations between m6A modification and immune factors behind renal graft injury at

the molecular level by analyzing the microarray data of kidney transplantation biopsies for cause. By analyzing the gene expression data of discovery cohort, we found that m6A regulators are closely related to a variety of immune characteristics, which are mainly involved in alloimmune processes and T cell subsets, suggesting the unique value of m6A modifications in TCMR. Based on machine learning, we managed to build a risk score and a molecular classifier to predict graft outcomes and distinguish TCMR from other types of graft injury, respectively. In short, our findings suggest that m6A modification is involved in graft dysfunction after transplantation by regulating the immune response and provides a reference for subsequent studies.

Materials and method

Collection and processing of data

The microarray expression data used in this study were derived from research accession published in the Gene Expression Omnibus (GEO, https://www.ncbi.nlm.nih.gov/geo/) database. The inclusion criteria included: (1) consecutive cohort; (2) samples derived from kidney biopsies for clinical indications; and (3) including TCMR and ABMR pathologic diagnosis based on Banff criteria or graft survival data. We managed to screen out 4 datasets, of which GSE360591 (19) was used as the discovery cohort, GSE213742 (18) prognosis cohort, and GSE485813 (20) and GSE983204 (21) diagnosis cohorts. All microarray datasets were subjected to log2 transformation and normalized using the R "limma" package. Two expression matrices in the diagnosis cohort were transformed by z-score to increase the comparability between independent datasets.

Correlation analysis of m6A regulators with immune characteristics

We identified 23 m6A regulators from the previous literature (22), including 8 writers (METTL3, METTL14, METTL16, WTAP, VIRMA, ZC3H13, RBM15, RBM15B), 13 readers (YTHDC1, YTHDC2, YTHDF1, YTHDF2, YTHDF3, HNRNPC, FMR1, LRPPRC, HNRNPA2B1, IGFBP1, IGFBP2, IGFBP3, RBMX) and 2 erasers (FTO, ALKBH5). Characteristic gene data of 22 kinds of immune cells were collected from the CIBERSORTS (23) database (https://cibersortx.stanford.edu/), and the immune cell abundance of each sample in the discovery cohort was calculated using the CIBERSORT.R script. Immune gene ontology categories/gene sets were downloaded from the ImmPort (24) database (https://www.immport.org/), and the R "GSVA" package was used to perform the single sample gene set enrichment analysis (ssGSEA) to obtain an enrichment score for each sample based on immune gene sets. 35 key genes of allograft rejection pathway (map05330) were obtained from the Kyoto Encyclopedia of Genes and Genomes (KEGG, https://www.kegg.jp/) database, as well as the expression matrix of key genes in the cohort sample. We conducted the R cor.test () to figure out the correlation coefficient between m6A regulators gene expression and immune cell abundance, immune gene sets enrichment score as well as rejection key genes expression of samples in the cohort and the correlation heat map was plotted using the R "ggplot2" package.

Establishment and analysis of the prognostic prediction model

First, we performed the correlation analysis between 1795 (after removing 704 duplicates) immune genes of 17 immune categories and m6A regulators in the discovery cohort. Those immune genes were derived from ImmPort database. 278 m6A-related immune genes (MRIGs) (|correlation coefficients|> 0.6 and $P< 0.01$) were obtained, on which gene enrichment analysis was conducted *via* the R "clusterProfiler" package. Then, we performed the univariate cox regression analysis between MRIGs and graft survival data, which was assessed as the time between biopsy and graft failure/censoring, and obtained 108 prognostic m6A-related immune genes (P-MRIGs), taking $P<0.001$ as the cutoff value. Finally, the R "caret" package was used to randomly divide the prognosis cohort into train cohort and test cohort, with a ratio of 1:1. In the train cohort, we carried out the least absolute shrinkage and selection operator (Lasso) regression with 10-fold cross validation on P-MRIGs using R "glmnet" package and selected the P-MRIGs corresponding to the smallest lambda value for model building. The multivariate Cox regression was conducted to figure out the regression coefficient. The Risk Score was calculated with the following formula: Risk Score = $\sum_{i=1}^{n}(coef_i * expr_i)$, here $expr_i$represented the expression level of gene i and $coef_i$, the regression coefficient of gene i in the signature. The train cohort was divided into high- and low-risk groups, choosing median of risk score as the midpoint. The Kaplan-Meier survival curve was plotted using the R "survminer" package. Log Rank test was used to compare the differences in graft survival between the two risk groups and the ROC curve drew by R "timeROC" package plots evaluated the predictive performance of the signature. Similar proceedings were carried out in the test cohort. In addition, to verify the model's applicability, we conducted the graft survival analysis of high- and low-risk groups in the rejection group and non-rejection group respectively, ran the GSEA 4.1.0 software (25) to identify the underlying pathophysiology of the risk-group and compared the gene enrichment differences in the KEGG pathway between the high and low-risk groups.

Differential analysis of m6A regulators and immune characteristics in subgroups

The distribution differences of m6A regulators and immune characteristics, which were obtained from the proceedings above, including gene expression matrix, the abundance of immune cells, and immune gene set enrichment scores, were compared in the TCMR, ABMR, and non-rejection groups of the discovery cohort. The results were visualized using R "pheatmap," "ggplot2", and "ggpubr" packages.

Establishment and analysis of the diagnosis prediction model

We intended to build a diagnostic model of TCMR based on m6A-related immune genes. Firstly, we performed a gene differential analysis between TCMR and non-TCMR groups (including the mixed group) in the discovery cohort using R "limma" package and obtained 120 differentially expressed genes (DEGs, | Log Fc |> 1, P< 0.05), of which 64 DEGs are immune-related genes. Subsequently, we carried out a correlation analysis between 64 differentially expressed immune genes and m6A regulators, and further obtained 58 m6A-related immune genes (DE-MRIGs, |correlation coefficients|> 0.4 and P<0.05) in the diagnosis cohort (train). Cycloscape 3.8.0 software (26) was used to perform protein-protein interaction (PPI) analysis of DE-MRIGs and corresponding m6A regulators. The GlueGO pluglet (27) was used for enrichment analysis and visualization. Finally, we utilized R "randomForest" package to carry out the decision tree analysis of DE-MRIGs to select feature genes in the train cohort. The appropriate variables were selected on the basis of their importance to build the model and logistic regression was conducted to determine the variable regression coefficient. The classifier score was calculated with the following formula: Classifier Score = $\sum_{i=1}^{n}(coef_i * expr_i)$.,here $expr_i$ represented the expression level of gene, i and $coef_i$,the regression coefficient of gene i in the classifier. The diagnostic performance of classifier was evaluated by the Area Under Curve (AUC) of the ROC Curve. The Optimal cut-off point was determined based on Youden index. Classifier score was calculated and evaluated in the test cohort. Moreover, a violin plot was drawn based on the histological lesions in the test cohort to compare the distribution of classifier score in TCMR-related injuries of different degrees, in which Wilcoxon Rank Sum was used for comparison between two groups, Kruskal-Wallis test for comparison between multiple groups. We retrieved Connectivity Map (Cmap) Database (https://clue.io/) (28) to identify the potential compounds that could alleviate TCMR lesions. Potential drugs with absolute Cmap score over 95 were selected and visualized using the R ComplexHeatmap package.

Results

Characteristic of cohort and biopsy

A total of 4 consecutive study cohorts, including 2193 renal transplant biopsy samples and 1906 kidney transplant patients, are included in this study. The detailed information is shown in Table 1. 36%-62% of renal graft biopsies are performed due to rapid or slow deterioration of graft function. The median time of biopsy after transplantation ranges from 512 to 751 days, of which 55%-100% of renal allografts biopsies one year after transplantation. Biopsies with a definite pathological diagnosis or lesions associated with alloimmunity, including TCMR, ABMR, mixed ABMR and TCMR, borderline rejection, and transplant glomerulopathy (TG) are most common (24%-48%), among which TCMR and ABMR have similar incidence. 55%-83% of transplant patients are given maintenance immunosuppressive regimens, which include calcineurin inhibitors at the time of biopsy. 12%-29% of recipients undergo graft failure, with mean follow-up time after transplantation ranging from 469 to 1017days.

Correlation between m6A regulators and immune characteristics

To explore whether m6A is related to immune factors, especially alloimmunity at the molecular level in the process of graft dysfunction, we collected and processed the data with immune characteristics and performed the correlation analysis with m6A regulators. Most m6A regulators are significantly correlated with T cell subtypes, macrophages, dendritic cells, mast cells and eosinophils, but not B cells (Figure 1A). Similar findings are observed in the respective correlation analysis of m6A regulators and immune categories, as well as m6A regulators and rejection key genes, as shown in Figures 1B, C. Erasers are mainly negatively related to the corresponding immune characteristics (shown in blue wireframe) while writers are mainly positively related (shown in red wireframe). For readers, both positive and negative correlations can be found, which may be related to its property of adjustment.

M6A-related immune gene-based prognostic prediction model for graft loss

Given what we have discovered above, we assumed that m6A modification-related immune molecules may be able to affect the outcomes of renal grafts, on which we established a prognostic model of grafts. The flow of modeling is shown in Figure 2A. We found that most genes are enriched in T cell activation,

10.3389/fimmu.2022.1039013

TABLE 1 Characteristic at cohort and biopsy.

GEO accession	GSE36059	GSE21374	GSE48581	GSE98320
Cohort type in study	discovery cohort	prognosis cohort	diagnosis cohort (train)	diagnosis cohort (test)
Platform	GPL570	GPL570	GPL570	GPL15207
Sample tissue	kidney transplant biopsies	kidney transplant biopsies	kidney transplant biopsies	kidney transplant biopsies
Sample size	403	105/282*	300	1208
number of patients	315	105	264	1045
Indication for biopsy				
Primary nonfunction(including DGF)	10 (2%)	unknown	9 (3%)	53 (5%)
Deterioration of graft function	246 (61%)	65 (62%)	170 (57%)	436 (36%)
Stable impaired graft function	71 (18%)	7 (7%)	17 (6%)	79 (7%)
Investigate proteinuria/rejection/BK/creatinine	38 (9%)	15 (14%)	71 (24%)	175 (14%)
Follow-up from previous biopsy	unknown	6 (6%)	unknown	unknown
Others	23 (6%)	6 (6%)	17 (6%)	443 (37%)
Indication unknown	15 (4%)	6 (6%)	16 (5%)	22 (2%)
Time of biopsy after transplant (d)				
mean time	1437	1734	1705	unknown
median time (range)	512 (6-12831)	unknown	751 (3-9889)	591 (1-11453)
Early biopsies (< 1 year)	182 (45%)	0 (0%)	116 (39%)	507 (42%)
Late biopsies (≥ 1 year)	221 (55%)	100 (100%)	184 (61%)	701 (58%)
Diagnosis (conclusive)				
TCMR	32 (11%)	14 (13%)	35 (9%)	87 (7%)
ABMR	40 (13%)	11 (10%)	65 (16%)	24 (2%)
Mixed ABMR and TCMR	6 (2%)	3 (3%)	22 (5%)	41 (3%)
Borderline rejection	46 (15%)	11 (10%)	42 (10%)	109 (9%)
Transplant glomerulopathy(TG)	20 (7%)	unknown	4 (1%)	40 (3%)
Glomerulonephritis	40 (40%)	22 (21%)	41 (10%)	97 (8%)
BK virus	13 (4%)	1 (1%)	13 (4%)	37 (3%)
No major abnormalities	43 (14%)	unknown	76 (19%)	274 (23%)
Maintenance immunosuppression at biopsy (calcineurin inhibitors)				
Tacrolimus	176 (44%)	38 (36%)	127 (42%)	712 (59%)
Cyclosporine	101 (25%)	49 (47%)	38 (13%)	192 (16%)
Time of follow-up after biopsy (d, mean time)	1017	774	469	unknown
Failed grafts	80 (25%)	30 (29%)	33 (12%)	unknown

*GSE21374 provided a total of 282 samples, but was only able to find histological information for 105 of them.

regulation of response to biotic stimulus, cytokine receptor interaction, and PI3K-Akt signaling pathway (Supplementary 1) on gene set enrichment analysis of 278 m6A-related immune genes (MRIGs). A list of 108 m6A-related prognostic genes immune genes (P-MRIGs) with hazard ratios (HR) is recorded in Supplementary 2. Based on Lasso regression, 7 P-MRIGs (S100A6, TMSB10, NAMPT, IL15, PSMC6, NDRG1, NRG1) are determined for building the prognostic prediction model (Figure 2D). Each candidate gene is given a corresponding coefficient by multivariate Cox regression, and the risk score of each sample is calculated. Taking the median of risk score as the threshold, we stratified the train cohort into different risk groups, of which the graft survival probability of the high-risk group is significantly lower than that of the low-risk group (P<0.001, Figure 2E). The model shows good predictive performance (Figure 2F), as AUC for predicting graft survival of 3-year, 5 -year, 10- year, and 20-year are 0.91, 0.90, 0.90, and 0.87, respectively. The model was verified in the test cohort. Similarly, the high-risk group has remarkably poor graft survival (P< 0.007, Figure 2G), as AUC for predicting graft survival of 3-year, 5 -year, 10- year, and 20-year are 0.79, 0.83, 0.76, and 0.53, respectively (Figure 2H).

There is a significant difference in the distribution of risk scores between the rejection and non-rejection groups (Figure 3A), and the risk score is higher in the rejection group (p<0.001). Moreover, the KM survival curves show that graft survival of the high-risk group is much worse than that of the low-risk group regardless of with rejection or not (Figures 3B,

C), which indicates that the predictive performance of the model is not affected by rejection factors and possesses of strong applicability.

In order to explore the latent causes behind the poor graft survival of the high-risk group, we compared the gene enrichment of the two risk groups. In high-risk group, more genes are enriched in the pathways related to alloimmunity, such as allograft rejection and graft versus host disease, suggesting alloimmunity is the principal element accounting for graft loss.

M6A regulators and immune characteristics in rejection versus non-rejection

The gene expression differences of m6A regulators in the rejection group, including TCMR and ABMR, as well as non-rejection, are shown in Figure 4. For most of m6A regulators, their gene expression levels are significantly different between rejection group and non-rejection group (Figure 4A). Similarly, the expression levels of most of the m6A regulators are remarkably different between TCMR and non-TCMR groups. However, only a few m6A regulators show a significant difference in gene expression levels between ABMR and non-ABMR, as well as ABMR and TCMR (Figures 4B, D). Thus, we speculated that m6A regulators may play an important part in rejection, especially in TCMR, while its role in AMBR is limited.

The results of immune cell infiltration show that there are more CD4 or CD8 T cells, helper T cells, M1 macrophages, activated dendritic cells, and eosinophilia infiltrated in the TCMR group (Supplementary 3A, B), which are precisely the immune cell types significantly related to m6A regulators. The TCMR group has higher enrichment scores in a number of immune categories (Supplementary 2C, D), which are also significantly related to m6A regulators. Thus, it is justifiable to conclude that m6A-modified immune responses play a specific role in the pathogenesis of TCMR.

M6A-related immune gene-based diagnostic prediction model for TCMR

The process of establishing the prediction model is shown in Figure 5A. Several genes are enriched in T cells immunity, proliferation, and related pathway (Dark orange circles in Figure 5B) on the enrichment analysis of DE-MRIGs and their counterpart m6A regulators. Figure 5C shows the network of DE-MRIGs and m6A regulators, of which RBM15, WTAP, FTO, and METTL3 may be the hub genes that regulate the immune genes.

7 DE-MRIGs with the greatest mean decrease of Gini coefficient are selected for modeling by the Random Forest algorithm (Figure 6B). Figure 6A demonstrates that when the decision trees are accumulated to a certain number, the error of

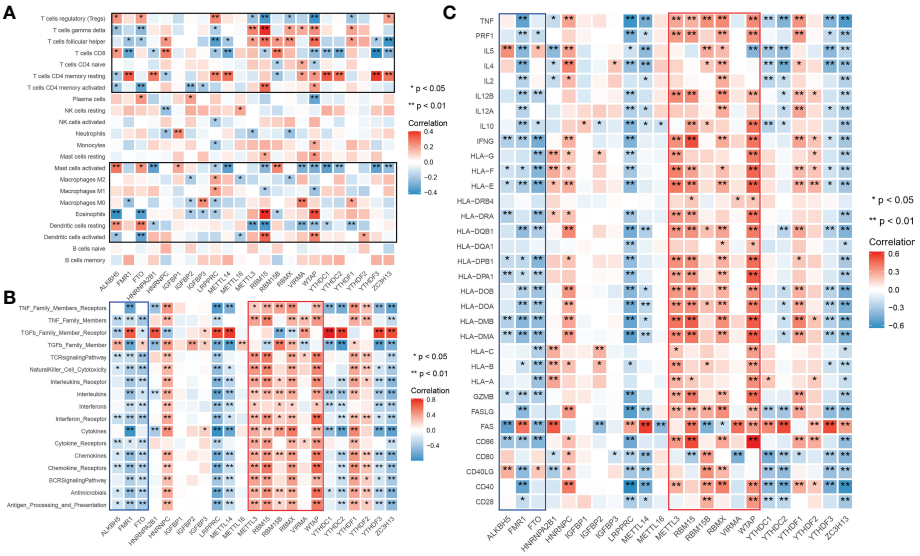

FIGURE 1
Landscape of correlationship between m6A regulators and immune characteristics. **(A)** Correlation heatmap of m6A regulators and immune cells. **(B)** Correlation heatmap of m6A regulators and immune gene categories. **(C)** Correlation heatmap of m6A regulators and rejection key genes. m6A regulators significantly correlated immune cells clustered in the black wireframe; Immune gene categories or rejection key genes significantly positive correlated m6A regulators clustered in the red wireframe; Immune gene categories or rejection key genes significantly negative correlated m6A regulators clustered in the blue wireframe.

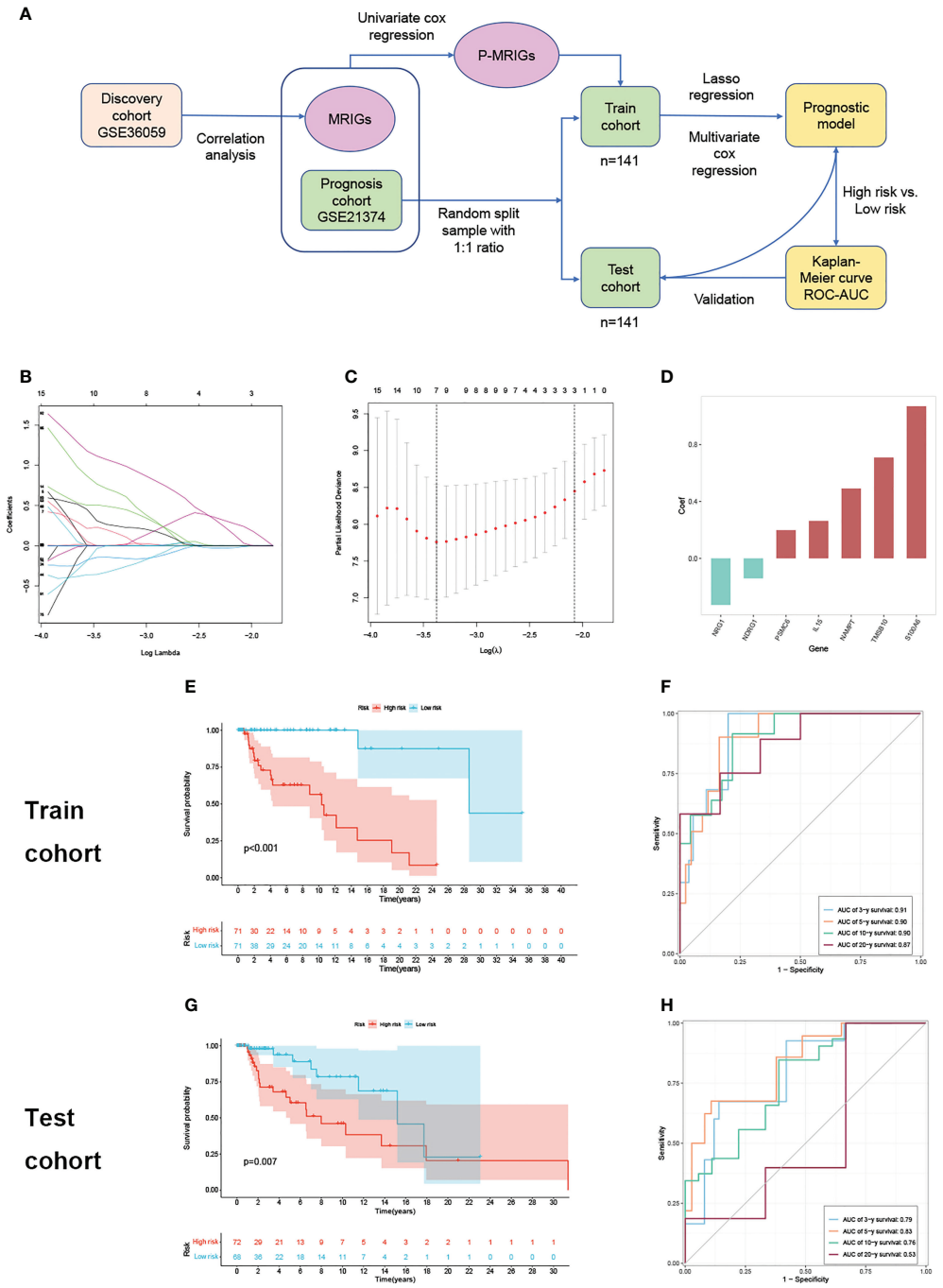

FIGURE 2
Construction and verification of prognostic prediction model. **(A)** Flow of constructing the prognostic prediction model. **(B)** Lasso coefficient profiles. **(C)** The partial likelihood deviance plot. **(D)** Coefficient of seven screened P-MRIGs in the prognostic prediction model. **(E)** The K-M curve showed that the high-risk group had a more inferior graft survival than the low-risk group in train set and **(G)** test set. **(F)** ROC curve of the model: the AUCs of 3-, 5-,10- and 20-year graft survival in the train set and **(H)** test set. Lasso, least absolute shrinkage and selection operator; P-MRIGs, prognostic m6A-related immune genes; K-M, Kaplan–Meier; ROC, receiver operating characteristic; AUC, areas under the curve.

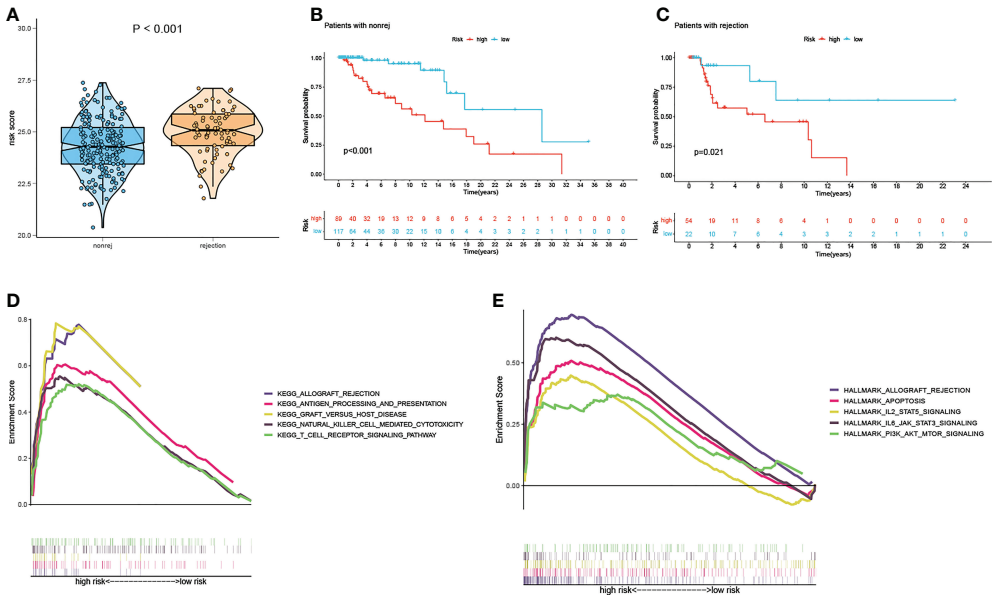

FIGURE 3
Test of suitability of the prognostic prediction model. **(A)** Violin plot of risk score in non-rejection and rejection group. **(B)** The K-M curve showed that the high-risk group had a more inferior graft survival than the low-risk group in non-rejection and **(C)** rejection group. **(D)** Gene enrichment analysis of KEGG pathway and **(E)** hallmark pathway in high-group versus low-group. K-M, Kaplan–Meier.

the random forest model falls between 10% and 12%. The regression coefficient of each DE-MRIG was obtained by Logistics regression, and then the classifier score of each sample in the train cohort was calculated. The expression levels of 7 DE-MRIGs in the sample and their corresponding histological and predicted diagnosis types are shown in Figure 6D. The classifier possesses excellent predictive performance for TCMR with an AUC of 0.891. The specificity

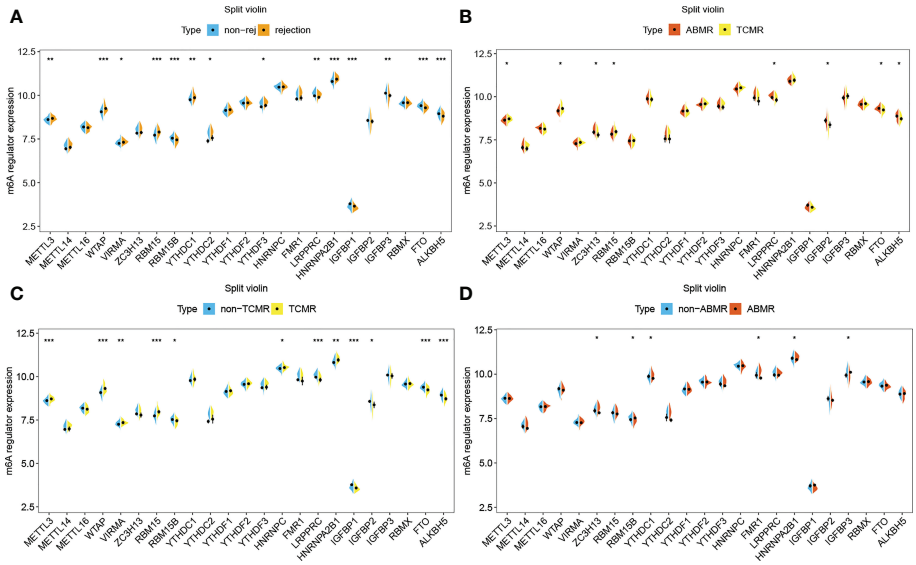

FIGURE 4
m6A regulators in rejection subtypes. **(A)** Split violin plot of m6A regulators' gene expression levels in non-rejection versus rejection group, **(B)** ABMR versus TCMR group, **(C)** non-TCMR versus TCMR group, and **(D)** non-ABMR versus ABMR group. *P< 0.05, **P< 0.01, ***P< 0.001.

and sensitivity of the model are 80.2% and 87.5%, respectively, when the optimal cut-off point is 1.070. We also verified the model in the test cohort, and it still shows good performance with an AUC of 0.854 when the optimal cut-off point is 1.657. The model was verified in the test cohort which also delivers good performance with an AUC of 0.854, and the optimal cut-off point is 1.070, affected by sequencing platforms. The specificity and sensitivity in the test cohort are 78.8% and 80.5%, respectively.

Banff lesions i, t, v, i-IFTA represent interstitial inflammation, tubulitis, intimal arteritis, and inflammation in areas of fibrosis/interstitial fibrosis and tubular atrophy, respectively. Those are the main pathological lesions of acute and chronic TCMR, and the diagnosis is exactly based on them. The distribution of the classifier score shows a significant gradient difference in injury indicators of TCMR, which means the classifier scores increases with the degree of injury (Figures 7A, C). Therefore, our model can be used to reflect the severity of pathological injury and facilitate in TCMR grading.

The Connectivity Map (CMap) database can explore the potential therapeutic small molecule compounds by comparing the uploaded gene signature with the in-house gene datasets, from which the corresponding correlation score is obtained, namely the CMap score. We screened out the compounds for TCMR in the CMap database based on the signature of the top 10 DE-MRIGs (Supplementary 4) in the diagnostic model. The potential therapeutic drugs with absolute CMap score over 95 are selected, and the most common mechanism of action is antagonizing adenosine receptor (Supplementary 5).

Discussion

The kidneys are a common target of systemic immune and autoimmune disorders, which is partly related to the size-selective and charge-dependent filtration process (29). In terms of transplanted kidneys, persistent and intense alloimmunity is the main culprit for graft loss. There is accumulating evidence suggesting new functions of m6A in regulating various aspects of immunity, including immune recognition, activation of innate and adaptive immune responses, and cell fate decisions (8). It is justifiable to speculate that m6A may also be involved in regulating alloimmunity and other immune responses in renal transplantation. Thus, we derived microarray expression data from transplanted kidney biopsies for cause and tried to explore the relations between m6A regulators and immune responses in

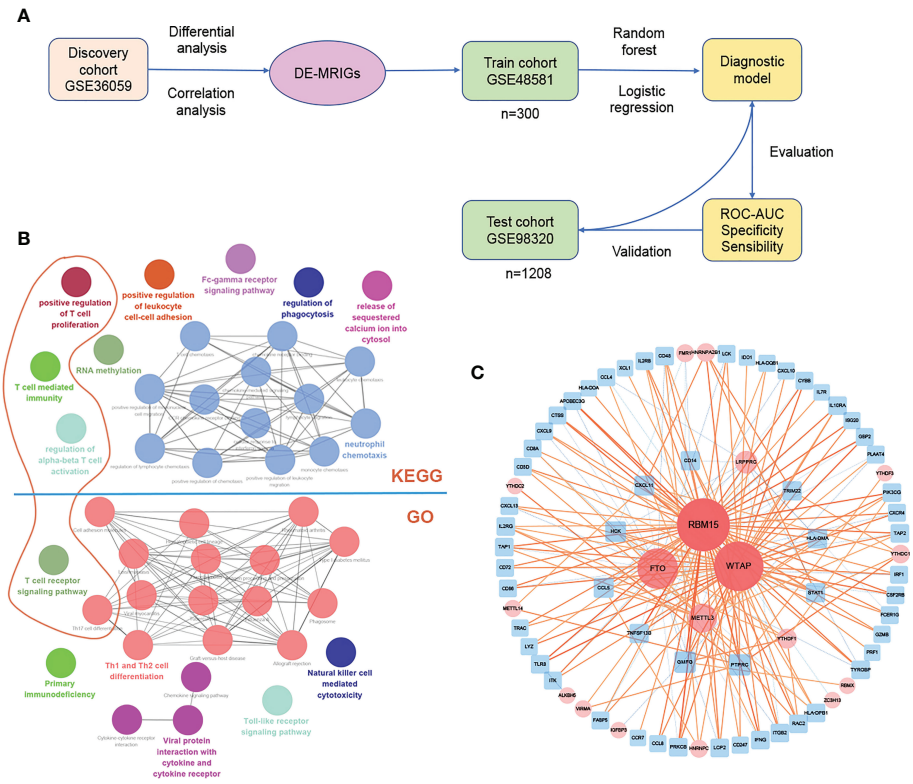

FIGURE 5
Construction and verification of diagnostic prediction model. **(A)** Flow of constructing the diagnostic prediction model. **(B)** Gene enrichment analysis and **(C)** network of DE-MRIGs and corresponding m6A regulators. DE-MRIGs, different expression m6A-related immune genes.

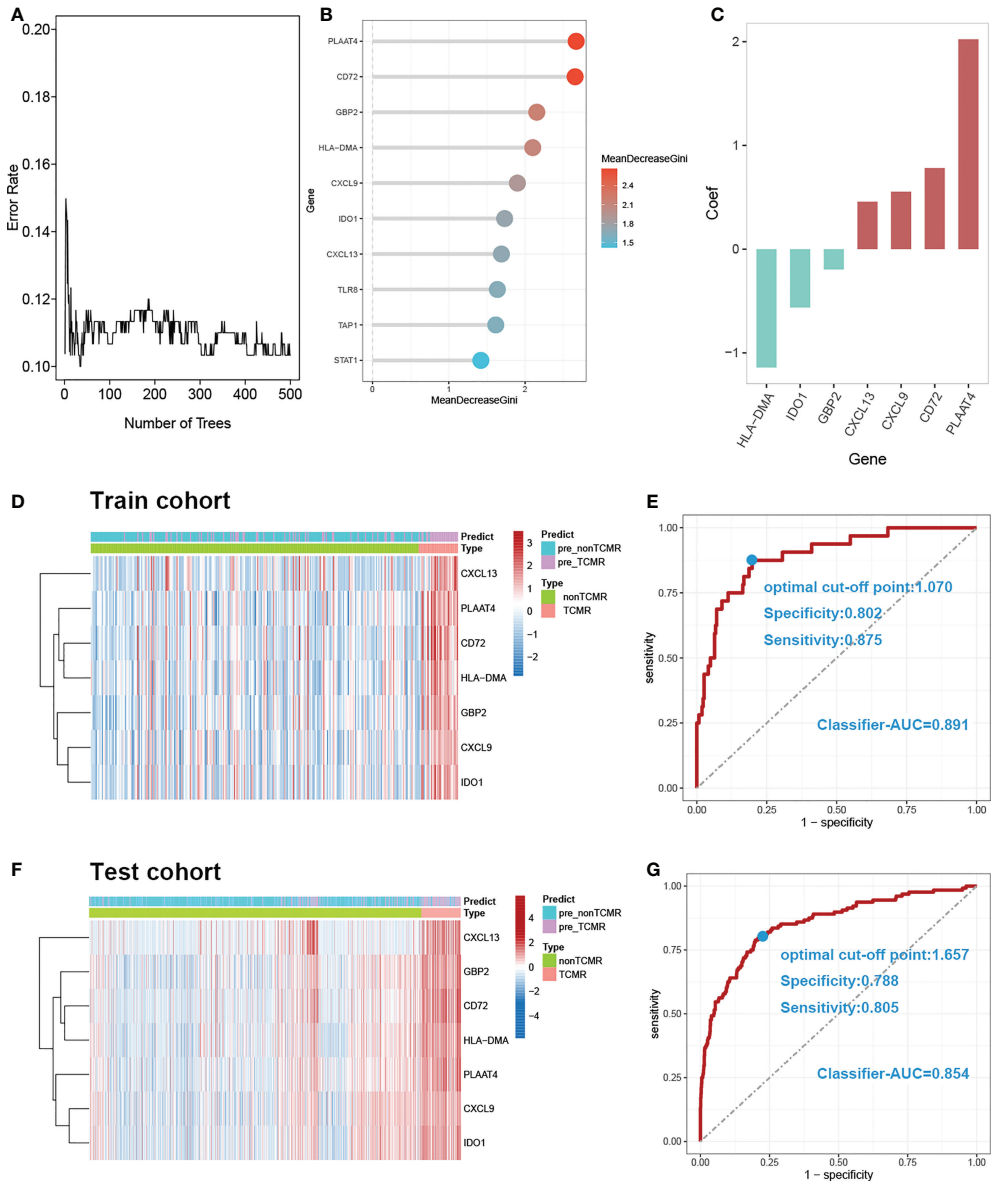

FIGURE 6
Construction and verification of diagnostic prediction model. **(A)** Random forest error rate plot. **(B)** Mean decreased gini of genes profiles. **(C)** Coefficient of seven screened DE-MRIGs in thedignostic prediction model. **(D)** Heatmap of identified DE-MRIGs in train cohort and **(F)** test cohort. **(E)** ROC curve of the model: the AUC, optimal cut-off point, specificity and sensitivity of classifier for discriminating TCMR in train cohort and **(G)** test cohort. DE-MRIGs, different expression m6A-related immune genes; ROC, receiver operating characteristic; AUC, areas under the curve.

renal transplantation at a molecular level, on which the diagnostic and prognostic models were built.

Einecke et al. (18) first reported a molecular classifier for predicting future graft loss in late kidney transplant biopsies. The transcripts that are associated with graft loss and used as a classifier, can only give us hints about tissue injury and fail to reflect the inflammatory state. Although transcripts in this research are limited to immune genes associated with m6A modifications, with an AUC of 0.9, they have better performance in predicting graft survival of 3-, 5-, and 10-years than the classifier in the previous study, whose AUC is 0.83. Moreover, our model is applicable for patients with or without rejections in predicting graft survival.

The m6A-related immune genes included in the prognostic model may also play a consequential role in the risk stratification of graft loss. S100A6 protein belongs to the S100 protein family

of Ca2+- binding proteins (30). Research revealed that interferon beta (INFβ) activity could be modulated *via* the binding of S100A6 protein (31). Yilmaz et al. (32) found that NAMPT can reflect endothelial dysfunction directly following renal transplantation. In kidney transplantation, IL-15 can stimulate CD4 + CD28 null T cells to generate alloreactivity (33) or acts as a biomarker for the assessment of antibody-mediated kidney allograft rejection (34).

In the wake of new immunosuppressive regimens, TCMR is less common but still remains the dominant early rejection phenotype and serves as the endpoint for clinical trials (35). The latest Banff classification outlines the diagnostic criteria of TCMR based on four histological lesions: interstitial inflammation (i2 or i3), tubulitis (t2 or t3), intimal arteritis (v1, v2 or v3), and inflammation in areas of interstitial fibrosis and tubular atrophy (i-IFTA2 or i-IFTA3) (36). This scoring system is largely opinion-based and inconsecutive with arbitrary cutoffs (37). Moreover, the histological lesions for TCMR are nonspecific. For example, interstitial inflammation and tubulitis are also found in acute kidney injury (AKI), possibly rendering false positives, and difficult to assess in scarred tissue, causing false negatives (20). Advantages of molecular assessment over histological approaches include objectivity, repeatability and quantification, which can emerge as an amelioration to pathological diagnosis (37).

In the pathogenesis of TCMR, effector T cells, dendritic cells and activated macrophages are the main acting cells (37), which are also significantly associated with m6A regulators in the discovery cohort. At the same time, there is a remarkable difference in the expression of most of these m6A regulators between TCMR and non-TCMR, indicating that m6A modification may play a part in TCMR, on which we established a diagnostic prediction model to identify TCMR in grafts dysfunction. The classifier score of our model outperforms the published molecular test - TCMR score in diagnostic performance with an AUC of 0.89 vs 0.8412. In addition, further analysis revealed that the classifier score is positively related to the degree of main pathological lesions of TCMR, enabling it to evaluate pathological injury degree and further grade TCMR.

Through network analysis, we found that METTL3, FTO, WATP and RBM15 may play a pivotal part in the regulation of immune responses in TCMR (Figure 8). It has been proven that METTL3 regulates T cell homeostasis (38), M1 macrophage polarization (39) and dendritic cell maturation (40); FTO enhances M1 and M2 macrophage activation (41); WTAP

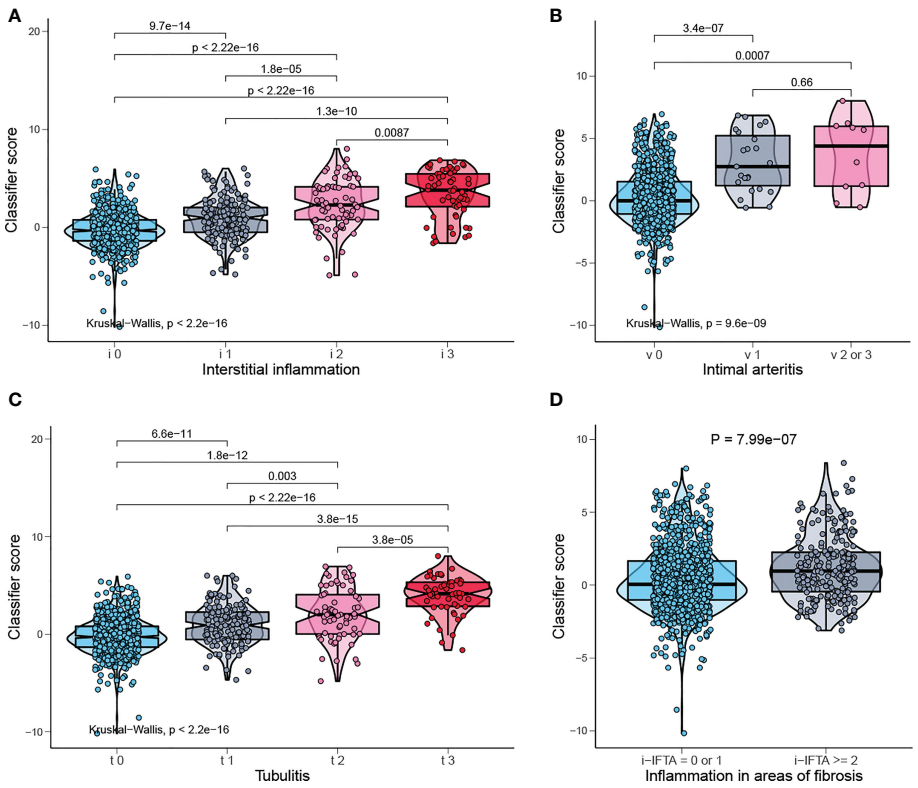

FIGURE 7
Classifier score in TCMR-related pathological lesion. **(A)** Classifier score in i0, i1, i2, i3, **(B)** v0, v1, v2 or 3, **(C)** t0, t1, t2, t3, and **(D)** i-IFTA=0 or 1, i-IFTA > =2. i, interstitial inflammation; t, tubulitis; v, intimal arteritis; i-IFTA, inflammation in areas of fibrosis.

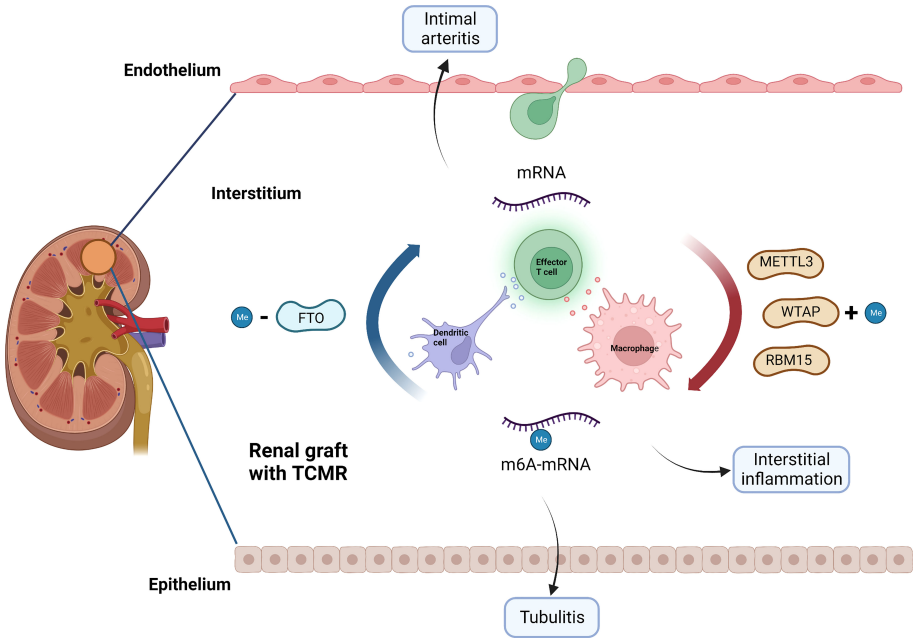

FIGURE 8
Potential role of m6A modification in TCMR. METTL3, WTAP, RBM15 and FTO may be involved in the pathogenesis of TCMR by regulating immune response, thereby causing interstitial inflammation, tubulitis and intimal arteritis. TCMR, T cell mediated rejection; Me, N6-methyladenosine.

controls T cell receptor signaling and survival of T cells (42). It is noted that the m6A-related immune genes, which were finally screened out to build our model, namely, CD72 (43), CXCL9 (44) and CXCL13 (45), have also been reported to emerge as biomarkers for TCMR-exclusive.

Furthermore, we managed to select some small molecule compounds that may be able to reverse TCMR damage. Among the compounds with highest CMap scores, fenoldopam has been proven to be able to alleviate acute kidney injury (46) and is promising for reversing delayed graft function (DGF) (47); dextromethorphan can reduce renal complications of diabetes (48). We identified the potential therapeutic drugs with absolute CMap score over 95, and the most common mechanism of action is antagonizing adenosine receptor. Debra et al. (49) confirmed in mice experiment that adenosine receptor antagonists could protect against kidney injury.

This study has some limitations: on one hand, there is no clinically relevant population being studied, which is referred to as "limited challenge bias" (36); on the other hand, the hypothesis requires *in vivo* and vitro experiments to verify. There are also some common problems in the buildup of transcriptome models: firstly, there is inevitable inaccuracy in adopting histology based on Banff classification as the gold standard of diagnosis. Secondly, the deviation can be generated from the transcript data obtained from different experimental platforms. Due to this bias, the optimal cutoff points derived from train and test cohorts in the diagnostic model are quite discrepant in this study. Finally, for-cause biopsies are mainly performed for those patients with clinical indications. The inclusion itself has already resulted in selection bias, which may overestimate the model's performance. Therefore, it is better to study the relations between m6A and transplant rejection in patients with protocol biopsy and diagnose rejection at an earlier stage. Anyhow, our study is pioneering and enlightening,and provides valuable clues for future studies on the role of m6A modification in renal graft dysfunction.

Conclusion

Collectively, our findings demonstrated that m6A-related immune genes could be used for prediction of graft loss and diagnosis of TCMR, which may be involved in the process of renal graft dysfunction. The results of this study offer novel schemes for molecular assessment of disease states in kidney transplant and provide a ponderable direction for the future research.

Data availability statement

Publicly available datasets were analyzed in this study. This loosedata can be found here: GSE360591 GSE213742 GSE485813 GSE983204.

Author contributions

QP and HX conceived and designed the study. HX, HC, HW, YW, and CA performed the data analysis. QP wrote the original draft. JZ, SL, JX, RW, and HX reviewed and revised the manuscript. All authors contributed to the article and approved the submitted version.

Acknowledgments

We appreciate Professor Philip F. Halloran and researchers of Alberta Transplant Applied Genomics Centre for their contribution to the molecular assessment of disease states in kidney transplant biopsy samples and their data available in the GEO database.

Conflict of interest

The authors declare that the research was conducted in the absence of any commercial or financial relationships that could be construed as a potential conflict of interest.

Publisher's note

Supplementary material

The Supplementary Material for this article can be found online at: https://www.frontiersin.org/articles/10.3389/fimmu.2022.1039013/full#supplementary-material

SUPPLEMENTARY 1
Gene enrichment analysis of m6A-related immune genes. **(A)** Bubble plot of GO analysis. **(B)** Bubble plot of KEGG analysis.

SUPPLEMENTARY 2
Univariate Cox regression analysis revealed that the selected m6Arelated immune-genes significantly correlated with clinical prognosis.

SUPPLEMENTARY 3
Immune characteristics in rejection subtypes. **(A)** Heatmap and **(B)** boxplot of immune cell infiltration in non-rejection, TCMR and ABMR. **(C)** Heatmap and **(B)** boxplot of enrichment score of immune categories in non-rejection, TCMR and ABMR.

SUPPLEMENTARY 4
Results of CMap analysis with absolute CMap score over 95 of top 10 important m6A-related immune genes.

SUPPLEMENTARY 5
The mechanisms of action shared by small molecular compounds based on CMap analysis.

References

1. Wekerle T, Segev D, Lechler R, Oberbauer R. Strategies for long-term preservation of kidney graft function. *LANCET* (2017) 389:2152–62. doi: 10.1016/S0140-6736(17)31283-7

2. Hariharan S, Israni AK, Danovitch G. Long-term survival after kidney transplantation. *N Engl J Med* (2021) 385:729–43. doi: 10.1056/NEJMra2014530

3. Williams WW, Taheri D, Tolkoff-Rubin N, Colvin RB. Clinical role of the renal transplant biopsy. *Nat Rev Nephrol* (2012) 8:110–21. doi: 10.1038/nrneph.2011.213

4. Van Loon E, Bernards J, Van Craenenbroeck AH, Naesens M. The causes of kidney allograft failure: More than alloimmunity. a viewpoint article. *TRANSPLANTATION* (2020) 104:e46–56. doi: 10.1097/TP.0000000000003012

5. El-Zoghby ZM, Stegall MD, Lager DJ, Kremers WK, Amer H, Gloor JM, et al. Identifying specific causes of kidney allograft loss. *Am J Transplant* (2009) 9:527–35. doi: 10.1111/j.1600-6143.2008.02519.x

6. Sellares J, de Freitas DG, Mengel M, Reeve J, Einecke G, Sis B, et al. Understanding the causes of kidney transplant failure: the dominant role of antibody-mediated rejection and nonadherence. *Am J Transplant* (2012) 12:388–99. doi: 10.1111/j.1600-6143.2011.03840.x

7. Jiang X, Liu B, Nie Z, Duan L, Xiong Q, Jin Z, et al. The role of m6A modification in the biological functions and diseases. *Signal Transduct Target Ther* (2021) 6:74. doi: 10.1038/s41392-020-00450-x

8. Shulman Z, Stern-Ginossar N. The RNA modification N(6)-methyladenosine as a novel regulator of the immune system. *Nat Immunol* (2020) 21:501–12. doi: 10.1038/s41590-020-0650-4

9. Winkler R, Gillis E, Lasman L, Safra M, Geula S, Soyris C, et al. m(6)A modification controls the innate immune response to infection by targeting type I interferons. *Nat Immunol* (2019) 20:173–82. doi: 10.1038/s41590-018-0275-z

10. Seki Y, Yang J, Okamoto M, Tanaka S, Goitsuka R, Farrar MA, et al. IL-7/STAT5 cytokine signaling pathway is essential but insufficient for maintenance of naive CD4 T cell survival in peripheral lymphoid organs. *J Immunol* (2007) 178:262–70. doi: 10.4049/jimmunol.178.1.262

11. Tong J, Cao G, Zhang T, Sefik E, Amezcua VM, Broughton JP, et al. m(6)A mRNA methylation sustains treg suppressive functions. *Cell Res* (2018) 28:253–6. doi: 10.1038/cr.2018.7

12. Yao Y, Yang Y, Guo W, Xu L, You M, Zhang YC, et al. METTL3-dependent m(6)A modification programs T follicular helper cell differentiation. *Nat Commun* (2021) 12:1333. doi: 10.1038/s41467-021-21594-6

13. Li X, Ma S, Deng Y, Yi P, Yu J. Targeting the RNA m(6)A modification for cancer immunotherapy. *Mol Cancer* (2022) 21:76. doi: 10.1186/s12943-022-01558-0

14. Tang L, Wei X, Li T, Chen Y, Dai Z, Lu C, et al. Emerging perspectives of RNA n (6)-methyladenosine (m(6)A) modification on immunity and autoimmune diseases. *Front Immunol* (2021) 12:630358. doi: 10.3389/fimmu.2021.630358

15. Furness PN, Taub N, Assmann KJ, Banfi G, Cosyns JP, Dorman AM, et al. International variation in histologic grading is large, and persistent feedback does not improve reproducibility. *Am J Surg Pathol* (2003) 27:805–10. doi: 10.1097/00000478-200306000-00012

16. Schinstock CA, Sapir-Pichhadze R, Naesens M, Batal I, Bagnasco S, Bow L, et al. Banff survey on antibody-mediated rejection clinical practices in kidney transplantation: Diagnostic misinterpretation has potential therapeutic implications. *Am J Transplant* (2019) 19:123–31. doi: 10.1111/ajt.14979

17. Reeve J, Bohmig GA, Eskandary F, Einecke G, Gupta G, Madill-Thomsen K, et al. Generating automated kidney transplant biopsy reports combining molecular measurements with ensembles of machine learning classifiers. *Am J Transplant* (2019) 19:2719–31. doi: 10.1111/ajt.15351

18. Einecke G, Reeve J, Sis B, Mengel M, Hidalgo L, Famulski KS, et al. A molecular classifier for predicting future graft loss in late kidney transplant biopsies. *J Clin Invest* (2010) 120:1862–72. doi: 10.1172/JCI41789

19. Reeve J, Sellares J, Mengel M, Sis B, Skene A, Hidalgo L, et al. Molecular diagnosis of T cell-mediated rejection in human kidney transplant biopsies. *Am J Transplant* (2013) 13:645–55. doi: 10.1111/ajt.12079

20. Halloran PF, Pereira AB, Chang J, Matas A, Picton M, De Freitas D, et al. Potential impact of microarray diagnosis of T cell-mediated rejection in kidney transplants: The INTERCOM study. *Am J Transplant* (2013) 13:2352–63. doi: 10.1111/ajt.12387

21. Reeve J, Bohmig GA, Eskandary F, Einecke G, Lefaucheur C, Loupy A, et al. Assessing rejection-related disease in kidney transplant biopsies based on archetypal analysis of molecular phenotypes. *JCI Insight* (2017) 2(12):e94197. doi: 10.1172/jci.insight.94197

22. Li Y, Gu J, Xu F, Zhu Q, Chen Y, Ge D, et al. Molecular characterization, biological function, tumor microenvironment association and clinical significance of m6A regulators in lung adenocarcinoma. *Brief Bioinform* (2021) 22(4):bbaa225. doi: 10.1093/bib/bbaa225

23. Newman AM, Liu CL, Green MR, Gentles AJ, Feng W, Xu Y, et al. Robust enumeration of cell subsets from tissue expression profiles. *Nat Methods* (2015) 12:453–7. doi: 10.1038/nmeth.3337

24. Bhattacharya S, Andorf S, Gomes L, Dunn P, Schaefer H, Pontius J, et al. ImmPort: disseminating data to the public for the future of immunology. *Immunol Res* (2014) 58:234–9. doi: 10.1007/s12026-014-8516-1

25. Subramanian A, Tamayo P, Mootha VK, Mukherjee S, Ebert BL, Gillette MA, et al. Gene set enrichment analysis: a knowledge-based approach for interpreting genome-wide expression profiles. *Proc Natl Acad Sci U.S.A.* (2005) 102:15545–50. doi: 10.1073/pnas.0506580102

26. Shannon P, Markiel A, Ozier O, Baliga NS, Wang JT, Ramage D, et al. Cytoscape: a software environment for integrated models of biomolecular interaction networks. *Genome Res* (2003) 13:2498–504. doi: 10.1101/gr.1239303

27. Bindea G, Mlecnik B, Hackl H, Charoentong P, Tosolini M, Kirilovsky A, et al. ClueGO: a cytoscape plug-in to decipher functionally grouped gene ontology and pathway annotation networks. *BIOINFORMATICS* (2009) 25:1091–3. doi: 10.1093/bioinformatics/btp101

28. Subramanian A, Narayan R, Corsello SM, Peck DD, Natoli TE, Lu X, et al. A next generation connectivity map: L1000 platform and the first 1,000,000 profiles. *CELL* (2017) 171:1437–52. doi: 10.1016/j.cell.2017.10.049

29. Kurts C, Panzer U, Anders HJ, Rees AJ. The immune system and kidney disease: basic concepts and clinical implications. *Nat Rev Immunol* (2013) 13:738–53. doi: 10.1038/nri3523

30. Donato R, Sorci G, Giambanco I. S100A6 protein: functional roles. *Cell Mol Life Sci* (2017) 74:2749–60. doi: 10.1007/s00018-017-2526-9

31. Kazakov AS, Sofin AD, Avkhacheva NV, Denesyuk AI, Deryusheva EI, Rastrygina VA, et al. Interferon beta activity is modulated *via* binding of specific S100 proteins. *Int J Mol Sci* (2020) 21(24):9473. doi: 10.3390/ijms21249473

32. Yilmaz MI, Saglam M, Carrero JJ, Qureshi AR, Caglar K, Eyileten T, et al. Normalization of endothelial dysfunction following renal transplantation is accompanied by a reduction of circulating visfatin/NAMPT. a novel marker of endothelial damage? *Clin Transplant* (2009) 23:241–8. doi: 10.1111/j.1399-0012.2008.00921.x

33. Dedeoglu B, Litjens N, Klepper M, Kraaijeveld R, Verschoor W, Baan CC, et al. CD4(+) CD28(null) T cells are not alloreactive unless stimulated by interleukin-15. *Am J Transplant* (2018) 18:341–50. doi: 10.1111/ajt.14480

34. Van Loon E, Gazut S, Yazdani S, Lerut E, de Loor H, Coemans M, et al. Development and validation of a peripheral blood mRNA assay for the assessment of antibody-mediated kidney allograft rejection: A multicentre, prospective study. *EBIOMEDICINE* (2019) 46:463–72. doi: 10.1016/j.ebiom.2019.07.028

35. Halloran PF. T Cell-mediated rejection of kidney transplants: a personal viewpoint. *Am J Transplant* (2010) 10:1126–34. doi: 10.1111/j.1600-6143.2010.03053.x

36. Loupy A, Haas M, Roufosse C, Naesens M, Adam B, Afrouzian M, et al. The banff 2019 kidney meeting report (I): Updates on and clarification of criteria for T cell- and antibody-mediated rejection. *Am J Transplant* (2020) 20:2318–31. doi: 10.1111/ajt.15898

37. Halloran PF, Famulski KS, Reeve J. Molecular assessment of disease states in kidney transplant biopsy samples. *Nat Rev Nephrol* (2016) 12:534–48. doi: 10.1038/nrneph.2016.85

38. Li HB, Tong J, Zhu S, Batista PJ, Duffy EE, Zhao J, et al. m(6)A mRNA methylation controls T cell homeostasis by targeting the IL-7/STAT5/SOCS pathways. *NATURE* (2017) 548:338–42. doi: 10.1038/nature23450

39. Lei H, He M, He X, Li G, Wang Y, Gao Y, et al. METTL3 induces bone marrow mesenchymal stem cells osteogenic differentiation and migration through facilitating M1 macrophage differentiation. *Am J Transl Res* (2021) 13:4376–88.

40. Wang H, Hu X, Huang M, Liu J, Gu Y, Ma L, et al. Mettl3-mediated mRNA m(6)A methylation promotes dendritic cell activation. *Nat Commun* (2019) 10:1898. doi: 10.1038/s41467-019-09903-6

41. Gu X, Zhang Y, Li D, Cai H, Cai L, Xu Q. N6-methyladenosine demethylase FTO promotes M1 and M2 macrophage activation. *Cell Signal* (2020) 69:109553. doi: 10.1016/j.cellsig.2020.109553

42. Ito-Kureha T, Leoni C, Borland K, Cantini G, Bataclan M, Metzger RN, et al. The function of wtap in N(6)-adenosine methylation of mRNAs controls T cell receptor signaling and survival of T cells. *Nat Immunol* (2022) 23:1208–21. doi: 10.1038/s41590-022-01268-1

43. Halloran PF, Venner JM, Madill-Thomsen KS, Einecke G, Parkes MD, Hidalgo LG, et al. Review: The transcripts associated with organ allograft rejection. *Am J Transplant* (2018) 18:785–95. doi: 10.1111/ajt.14600

44. Rabant M, Amrouche L, Lebreton X, Aulagnon F, Benon A, Sauvaget V, et al. Urinary c-X-C motif chemokine 10 independently improves the noninvasive diagnosis of antibody-mediated kidney allograft rejection. *J Am Soc Nephrol* (2015) 26:2840–51. doi: 10.1681/ASN.2014080797

45. Schiffer L, Wiehler F, Brasen JH, Gwinner W, Greite R, Kreimann K, et al. Chemokine CXCL13 as a new systemic biomarker for b-cell involvement in acute T cell-mediated kidney allograft rejection. *Int J Mol Sci* (2019) 20(10):2552. doi: 10.3390/ijms20102552

46. Gillies MA, Kakar V, Parker RJ, Honore PM, Ostermann M. Fenoldopam to prevent acute kidney injury after major surgery-a systematic review and meta-analysis. *Crit Care* (2015) 19:449. doi: 10.1186/s13054-015-1166-4

47. Ponticelli C. Ischaemia-reperfusion injury: a major protagonist in kidney transplantation. *Nephrol Dial Transplant* (2014) 29:1134–40. doi: 10.1093/ndt/gft488

48. Roshanravan H, Kim EY, Dryer SE. NMDA receptors as potential therapeutic targets in diabetic nephropathy: Increased renal NMDA receptor subunit expression in akita mice and reduced nephropathy following sustained treatment with memantine or MK-801. *DIABETES* (2016) 65:3139–50. doi: 10.2337/db16-0209

49. Dorotea D, Cho A, Lee G, Kwon G, Lee J, Sahu PK, et al. Orally active, species-independent novel A3 adenosine receptor antagonist protects against kidney injury in db/db mice. *Exp Mol Med* (2018) 50:1–14. doi: 10.1038/s12276-018-0053-x

frontiers | Frontiers in Immunology

TYPE Original Research
PUBLISHED 23 November 2022
DOI 10.3389/fimmu.2022.1063957

OPEN ACCESS

EDITED BY
Long Zheng,
The Second Affiliated Hospital of Zhejiang University School of Medicine, China

REVIEWED BY
Yuanyuan Tian,
Hackensack Meridian Health, United States
Manuel Muro,
Hospital Universitario Virgen de la Arrixaca, Spain
Xing Fang,
University of Mississippi Medical Center, United States

*CORRESPONDENCE
Yingzi Ming
mingyz_china@csu.edu.cn;
myz_china@aliyun.com

†These authors have contributed equally to this work and share first authorship

SPECIALTY SECTION
This article was submitted to Alloimmunity and Transplantation, a section of the journal Frontiers in Immunology

RECEIVED 07 October 2022
ACCEPTED 08 November 2022
PUBLISHED 23 November 2022

CITATION
Peng B, Yang M, Zhuang Q, Li J, Zhang P, Liu H, Cheng K and Ming Y (2022) Standardization of neutrophil CD64 and monocyte HLA-DR measurement and its application in immune monitoring in kidney transplantation. *Front. Immunol.* 13:1063957. doi: 10.3389/fimmu.2022.1063957

Standardization of neutrophil CD64 and monocyte HLA-DR measurement and its application in immune monitoring in kidney transplantation

Bo Peng[1,2†], Min Yang[1,2†], Quan Zhuang[1,2], Junhui Li[1,2], Pengpeng Zhang[1,2], Hong Liu[1,2], Ke Cheng[1,2] and Yingzi Ming[1,2*]

[1]Transplantation Center, The Third Xiangya Hospital, Central South University, Changsha, China, [2]Engineering and Technology Research Center for Transplantation Medicine of National Health Commission, Changsha, China

Background: Infections cause high mortality in kidney transplant recipients (KTRs). The expressions of neutrophil CD64 (nCD64) and monocyte HLA-DR (mHLA-DR) provide direct evidence of immune status and can be used to evaluate the severity of infection. However, the intensities of nCD64 and mHLA-DR detected by flow cytometry (FCM) are commonly measured by mean fluorescence intensities (MFIs), which are relative values, thus limiting their application. We aimed to standardize nCD64 and mHLA-DR expression using molecules of equivalent soluble fluorochrome (MESF) and to explore their role in immune monitoring for KTRs with infection.

Methods: The study included 50 KTRs diagnosed with infection, 65 immunologically stable KTRs and 26 healthy controls. The blood samples were collected and measured simultaneously by four FCM protocols at different flow cytometers. The MFIs of nCD64 and mHLA-DR were converted into MESF by Phycoerythrin (PE) Fluorescence Quantitation Kit. The intraclass correlation coefficients (ICCs) and the Bland-Altman plots were used to evaluate the reliability between the four FCM protocols. MESFs of nCD64 and mHLA-DR, nCD64 index and sepsis index (SI) with the TBNK panel were used to evaluate the immune status. Comparisons among multiple groups were performed with ANOVA one-way analysis. Receiver operating characteristics (ROC) curve analysis was performed to diagnose infection or sepsis. Univariate and multivariate logistic analysis examined associations of the immune status with infection.

Results: MESFs of nCD64 and mHLA-DR measured by four protocols had excellent reliability (ICCs 0.993 and 0.957, respectively). The nCD64, CD64 index and SI in infection group were significantly higher than those of stable KTRs group. Patients with sepsis had lower mHLA-DR but higher SI than non-sepsis patients. ROC analysis indicated that nCD64 had the highest area under

the curve (AUC) for infection, and that mHLA-DR had the highest AUC for sepsis. Logistic analysis indicated that nCD64 > 3089 and B cells counts were independent risk factors for infection.

Conclusion: The standardization of nCD64 and mHLA-DR made it available for widespread application. MESFs of nCD64 and mHLA-DR had good diagnostic performance on infection and sepsis, respectively, which could be promising indicators for immune status of KTRs and contributed to individualized treatment.

KEYWORDS

nCD64, mHLA-DR expression, infection, sepsis, kidney transplantation, immune monitoring, prognosis

Introduction

Kidney transplantation (KTx) is currently regarded as the most effective therapeutic approach for end-stage renal disease (ESRD) (1). Although the graft and patient survivals post KTx have been enhanced greatly in recent decades, infection is still the second leading cause of mortality in kidney transplant recipients (KTRs) (roughly 15% – 20%) (1). More seriously, KTRs with sepsis, which is characterized by dysregulation of the immune response following infection, have even higher mortality rate (2–4). Due to the intense induction therapy and long-term maintenance immunosuppressive regimen, the pathophysiology of KTRs with infection is heterogeneous and comprises both hyperinflammatory and immunosuppressive phenotypes. Although some biomarkers have been reported to predict infection in KTRs, it is still pivotal to identify optimal immunologic parameters to assess host immune status for early diagnosis and individualized treatment (5, 6).

A wide range of studies have revealed that elevated expression of neutrophil CD64 (nCD64) is linked to pro-inflammatory reaction, while decreased expression of monocyte HLA-DR (mHLA-DR) is linked to immunosuppression (7). CD64, a high affinity immunoglobulin (Ig)-G Fc receptor (FcγR), is characterized by a rapid and intense increase in expression on neutrophils in response to infection or pro-inflammatory cytokines (8). Some literatures have revealed that nCD64 is an effective biomarker for the diagnosis of infections, the assessment of sepsis severity and the prediction of prognosis (9, 10). Meanwhile, mHLA-DR, which presents antigens to T cells to initiate the adaptive immune response, is also an important indicator to assess the immune status (10). Several studies have found that low expression of mHLA-DR is associated with increased risk of acquiring secondary infections and mortality (10, 11). The predictive value of mHLA-DR in prognosis on various conditions, including sepsis (10, 11), nosocomial infection (12), SARS-CoV-2 infection (13) and solid organ transplantation (14, 15), has also been verified by various clinical investigations. Our previous study indicated that KTRs with pneumonia appeared lower expression of mHLA-DR and higher expression of nCD64, which were important parameters to predict the prognosis of pneumonia using machine learning models (16).

Although the value and effect of nCD64 and mHLA-DR for immune monitoring have been validated, it is difficult for horizontal comparison. In the majority of previous studies, the expression of nCD64 and mHLA-DR were assessed by the mean fluorescence intensity (MFI) *via* flow cytometry (FCM), which was a relative value. MFI is determined not only by the expression intensity but also by the flow cytometer settings and the antibody selected, thus limiting its widespread application. It is urgently required to establish standardized quantification of nCD64 and mHLA-DR for further clinical application.

In this study, we standardized the measurement of nCD64 and mHLA-DR by converting their MFI values into molecules of equivalent soluble fluorochrome (MESF) (17). Furthermore, a prospective longitudinal analysis of the standardized nCD64 and mHLA-DR in KTRs was performed to explore their performance in immune monitoring.

Materials and methods

Study design and population

In this prospective, longitudinal, observational study, 72 consecutive KTRs suspected of infection were recruited from the Transplantation Center, The Third Xiangya Hospital, Central South University from November 1, 2021, to June 31, 2022. The immune monitoring panels including both the standardized nCD64 and mHLA-DR panels and the TBNK

panel were performed at two time points, namely, 1 – 3 days and 5 – 8 days post admission. All the patients were 18 – 65 years old, and those who did not meet the diagnostic criteria of infection were excluded (Figure 1). The stable outpatient KTRs (n = 65) and another group of healthy controls (HCs, n = 26) were also recruited and received the immune monitoring panels once. The inclusion criteria for stable KTRs were as followings: (1) more than 3 months post KTx; (2) no signs of rejection, tumor or infection; (3) stable allograft function (the creatinine less than 171 μmol/L). Informed consent was obtained for each patient, and the study was approved by the Institutional Review Board of Third Xiangya Hospital, Central South University (No. 21176).

All KTRs received KTx from donation after citizens' death (DCD) after 2012 or from close family members. The allografts from DCD were attributed by the China Organ Transplant Response System. All transplants performed were approved by the Ethics Committee of the Third Xiangya Hospital, Central South University. Routine induction therapy included anti-thymocyte globulin (ATG, 1.00 mg/kg daily for 3 days) or basiliximab (20 mg at days 0 and 4), and the standard triple immunosuppressive regimen, namely, calcineurin inhibitor (CNI), mycophenolate mofetil/entericcoated mycophenolate sodium, and corticosteroid was given as a maintenance regimen.

Diagnostic criteria of infection and sepsis

Diagnostic criteria of infection (pneumonia, urinary infection or other infections) were as followings: (1) obvious clinical symptoms including fever, cough, pollakiuria, diarrhea, etc.; 2, positive laboratory tests including blood routine examination, serum procalcitonin, (1-3)-beta-D-glucan/galactomannan test (G/GM test) or pathogenic evidence; 3, significant imaging findings from X-ray or computed tomography (CT) (Figure 1). Sepsis was defined according to The Third International Consensus Definitions for Sepsis and Septic Shock (Sepsis-3), and organ dysfunction was defined as Sequential Organ Failure Assessment (SOFA) score of 2 points or more (4). Due to the fact that stable KTRs might maintain a relatively poorer renal function than the HCs, strict assessment of renal function according to the SOFA score would overestimate the severity of infection. Therefore, only KTRs with the creatinine equal to or greater than 171 μmol/L (SOFA score ≥ 2 points for renal function), or KTRs with obvious increase of creatinine during infection, were regarded as renal dysfunction for SOFA scoring.

Standardization protocol of nCD64 and mHLA-DR

Two panels were used to detect the MFIs of nCD64 and mHLA-DR using the following fluorochrome-conjugated monoclonal antibodies: anti-CD45-KRO (clone 22202012, Beckman Coulter), anti-CD14-APC (clone 22205028, Beckman Coulter), anti-HLA-DR-PE (clone Immu-357, Beckman Coulter) and anti-CD64-PE (clone 200053, Beckman Coulter). The nCD64 panel contained the anti-CD45 and anti-CD64

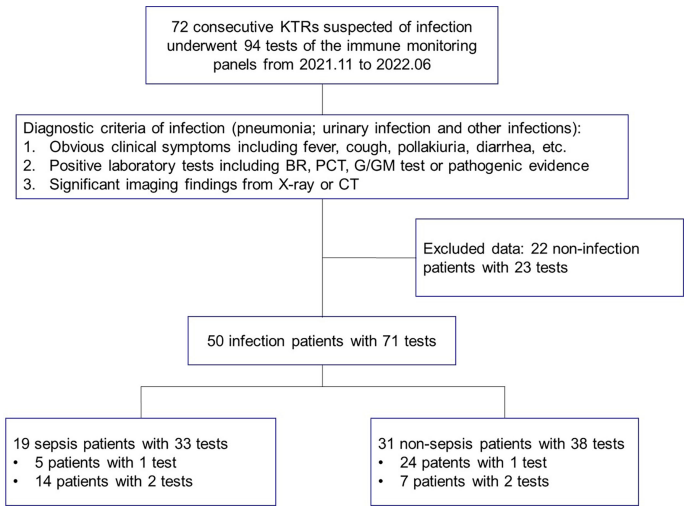

FIGURE 1
The study flow and diagnostic criteria of infection. 72 KTRs with 94 tests of immune function panels were first enrolled. 50 KTRs conformed of infection were further classified into the sepsis group and non-sepsis group according to the definition for sepsis. KTRs, kidney transplant recipients; BR, blood routine examination; PCT, serum procalcitonin; G/GM test, (1-3)-beta-D-glucan or galactomannan test; CT, computed tomography.

antibodies, while the mHLA-DR panel contained the anti-CD14 and anti-HLA-DR antibodies. Briefly, 50 µl whole blood from the identical EDTA anticoagulation tube was used for detection in each panel. After erythrolysis, cells and monoclonal antibodies were incubated in the dark for 15 minutes. After washing and resuspending, samples were detected and the MFIs of nCD64 and mHLA-DR were acquired with the two panels, respectively. The gating strategy was shown in the Supplementary Figure 1.

A total of four settings on two flow cytometers (BD FACSCanto II and Beckman Coulter DxFlex) were used to evaluate the reliability of the standardization protocol of nCD64 and mHLA-DR. On BD FACSCanto II, the voltage of PE channel (detecting the MFIs of nCD64 and mHLA-DR) was set at high, medium and low levels. On Beckman Coulter DxFlex, a fixed, proper voltage of PE channel was set. The MFIs of nCD64 and mHLA-DR for the identical sample were acquired under these four settings.

Then, the MFIs were converted to MESFs using PE Fluorescence Quantitation Kit (BD Quantibrite™ Beads, BD Biosciences). In this kit, beads were conjugated with calibrated four levels of PE molecules. The kit was run under the above four settings. A linear regression of Log_{10} MFI against Log_{10} PE molecules per bead (namely the MESF value) was performed. With the parameters of the linear regression, the MFIs of nCD64 and mHLA-DR were converted to MESFs. The mean value of the four results under the four settings mentioned above was used for further analysis.

nCD64 index and sepsis index

The formula for calculating the nCD64 index was shown as following: nCD64 index = (nCD64/lymCD64)/(mCD64/nCD64) (9). lymCD64 was the expression of CD64 on lymphocytes and mCD64 was expression of CD64 on monocytes. Sepsis Index (SI) was shown as following: SI = nCD64/mHLA-DR×100 (18). All parameters were calculated with the MESF values.

TBNK panel and lymphocyte counts

Another panel for immune monitoring was BD Multitest 6-color TBNK reagent with BD Trucount tubes, which identified the percentages and absolute counts of $CD3^+CD4^+$ T cells, $CD3^+CD8^+$ T cells, $CD19^+$ B cells and NK cells. This panel was performed according to the manufacture's instruction and analyzed by BD FACSCanto clinical software (BD Biosciences, San Jose, CA, USA).

Statistical analysis

Continuous data were presented as the mean ± standard deviation (SD) or median with interquartile range (IQR), and were compared using Student's t test or Welch's t test, where appropriate. Categorical data were compared using Pearson's chi-squared (χ^2) test or Fisher's exact test, where appropriate. Comparisons among multiple groups were performed with ANOVA one-way analysis. The least significant difference (LSD) test was used for back testing of multivariate ANOVA. The intraclass correlation coefficients (ICCs) and the Bland-Altman plots were used to evaluate the reliability of standardization protocol of nCD64 and mHLA-DR. Receiver operating characteristics (ROC) curve analysis was performed to evaluate the diagnostic efficiency of infection or sepsis. Univariate and multivariate logistic analysis examined the associations of immune status and infection. Statistical analysis was performed using SPSS version 22.0 (SPSS, Inc., Chicago, IL, USA) and GraphPad Prism 9.0. $P < 0.05$ was considered to be statistically significant.

Results

Patient characteristics

Seventy-two KTRs suspected of infection, 65 stable KTRs and 26 HCs were recruited and 185 tests of immune monitoring panels were performed. The immune monitoring panels included both the standardized nCD64 and mHLA-DR panels and the TBNK panel. Based on the diagnostic criteria of infection, 50 patients were conformed diagnosis of infection. Within the infection group, 19 patients were further categorized as the sepsis subgroup according to the definition of sepsis. Fourteen of the 19 sepsis patients received the immune monitoring panels twice, but 5 patients received only once due to their limited hospital stay. The study flow and details were shown in Figure 1.

Table 1 shows the clinical characteristics of the HCs and KTRs. There was a significant difference of age between the HCs and KTRs ($P < 0.001$), but no difference between the stable and infection groups ($P = 0.112$). More male patients were in the stable group ($P = 0.036$). Compared with the stable group, the infection group had lower lymphocyte count and higher serum creatinine at admission ($P < 0.001$ and $P < 0.001$, respectively). There was no statistical difference of donor source, calcineurin inhibitor, time from transplant to 1st test, neutrophil count or white blood cell (WBC) counts between the stable and infection groups.

TABLE 1 Clinical characteristics of the HCs and KTRs.

Parameters	HCs (n = 26)	KTRs			*P* value*	*P* value#
		All KTRs (n = 115)	Stable KTRs (n = 65)	Infection KTRs (n = 50)		
Male recipient, n (%)	15 (57.7%)	70 (60.9%)	45 (69.2%)	25 (50.0%)	0.036	0.428
Age, yrs ± SD	31.31 ± 10.65	42.02 ± 12.16	44.55 ± 9.56	44.30 ± 13.05	0.112	< 0.001
Donor, n (%)	NA				0.743	NA
DCD		83 (72.2%)	49 (69.2%)	34 (68.0%)		
Relative		32 (27.8%)	16 (30.8%)	16 (32.0%)		
Infection site, n (%)	NA	NA	NA		NA	NA
Pneumonia				27 (54%)		
Urinary infection				17 (34%)		
Other infection				6 (12%)		
Calcineurin inhibitor, n (%)	NA				0.412	NA
Tacrolimus		108 (93.9%)	60 (92.3%)	48 (96.0%)		
Cyclosporine A		7 (6.1%)	5 (7.7%)	2 (4.0%)		
Time from transplant to 1st test, months ± SD	NA	62.64± 52.90	69.86 ± 48.69	53.26 ± 57.06	0.295	NA
WBC (10^9/L)	NA	7.29 ± 3.27	6.78 ± 2.10	7.94 ± 4.28	0.076	NA
Neu (10^9/L)	NA	7.02 ± 10.83	6.48 ± 11.18	7.74 ± 10.43	0.537	NA
Lym (10^9/L)	NA	1.32 ± 0.74	1.64 ± 0.69	0.90 ± 0.58	< 0.001	NA
Cr admission (μmol/L)	NA	143.73 ± 88.42	121.91 ± 54.94	172.10 ± 113.10	< 0.001	NA

*Comparison between the stable KTRs and the infection KTRs.
#Comparison among the three groups.
HCs, healthy controls; KTRs, kidney transplant recipients; SD, standard deviation; DCD, donation after citizens' death; WBC, white blood cell counts; Neu, neutrophils count; Lym, lymphocyte counts; Cr, serum creatinine; NA, not available.

The standardization protocol of nCD64 and mHLA-DR showed excellent inter-rater reliability

Through the calibrated beads with known number of PE molecules, the MFIs of nCD64 and mHLA-DR were converted to MESFs. The linear regression equations under the four settings were shown in the Supplementary Figure 2. Every sample was detected under the four settings as mentioned above, thus four MESF results for each sample were calculated. Then, the variability of the four results for each sample was evaluated using the ICC. Both the MESFs of nCD64 and mHLA-DR showed excellent reliability, with ICCs of 0.993 and 0.957, respectively (supplementary Table 1). Furthermore, the Bland-Altman test revealed a good agreement over the full range between the mean value of the four results and each result under the four settings. (Figure 2 for nCD64 and Figure 3 for mHLA-DR). To deal with the outliers which were defined as more than 3 SD in the Bland-Altman plots, the outliers were excluded and the mean value of the remaining results were used for further analysis. After removing the outliers, the Bland-Altman test showed better consistency (Supplementary Figure 3 for nCD64 and Supplementary Figure 4 for mHLA-DR). Overall, the standardization protocol of nCD64 and mHLA-DR showed excellent inter-rater reliability under different conditions.

The infection KTRs had higher nCD64 but similar mHLA-DR compared with the stable KTRs

To determine the performance of the immune monitoring panels in infection, the MESFs of nCD64 and mHLA-DR, CD64 index and SI were compared among the HCs, the infection group and the stable group (Figure 4 and Table 2). For patients with multiple tests, the result of the first test was used for comparison. The stable group (1697.89 ± 1056.32) had slightly higher nCD64 than the HCs (1192.58 ± 537.61), but the nCD64 of the infection group (9424.08 ± 8574.58) was tremendously elevated compared with the other two groups. Surprisingly, the mHLA-DR showed no significant difference among the three groups (P = 0.273). Although the mHLA-DR of the infection group was a little lower than that of the stable group (2558.66 ± 1360.77 *vs.* 2728.62 ± 854.87), it showed no significant difference (P = 0.392). Due to the tremendous increase of nCD64, the CD64 index and SI of the infection group were also significantly higher than the other two groups. The ROC curves also showed that the nCD64, CD64 index and SI had high AUCs for identification of infection (AUCs 0.85, 0.83, 0.84, respectively, all P values less than 0.001), but the mHLA-DR showed no significant difference (P = 0.15, Figure 5).

For the TBNK panel, there were significant differences of the cell counts of $CD3^+$ T cells, $CD8^+$ T cells, $CD4^+$ T cells, NK cells

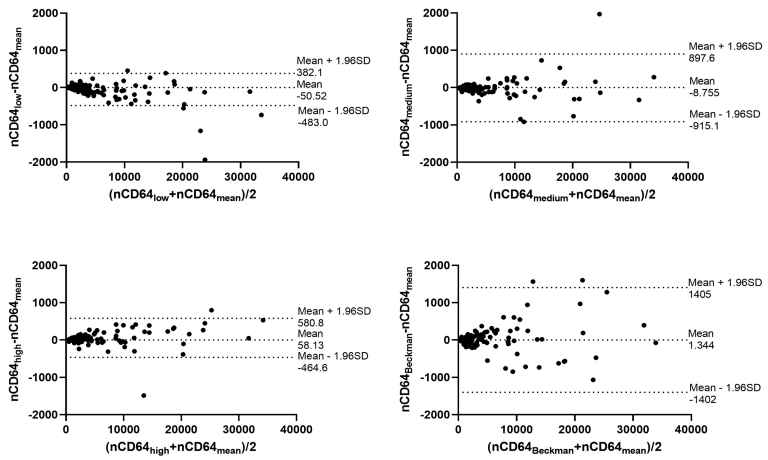

FIGURE 2
The Bland-Altman plot for the four MESFs of nCD64 under BD FACSCanto II with high/medium/high voltages and Beckman Coulter DxFlex with proper voltage. The agreement between the mean value of the four results and each result of nCD64 was assessed over the full range. The fixed range was defined as mean ± 1.96SD. nCD64, neutrophil CD64; SD, standard deviation; MESF, molecules of equivalent soluble fluorochrome.

and B cells among the three groups ($P \leq 0.001$). Compared with the stable group, the infection group was characterized by significantly lower cell counts of $CD3^+$ T cells (1141.11 ± 537.85 *vs.* 628.52 ± 469.07, $P < 0.001$), $CD8^+$ T cells (471.15 ± 242.78 *vs.* 284.68 ± 243.10, $P < 0.001$), $CD4^+$ T cells (598.42 ± 322.91 *vs.* 301.36 ± 228.33, $P < 0.001$), NK cells (223.26 ± 204.71 *vs.* 123.40 ± 104.91, $P < 0.001$) and B cells (162.00 ± 113.84 *vs.* 67.17 ± 66.67, $P < 0.001$) (Supplementary Table 2). However, the percentages of each subset showed no significant difference.

nCD64 helped distinguish different pathogenic pathogens of the infection

According to the different pathogenic pathogens, the infection group (n = 50) were further stratified into the bacterial (n = 26), the viral (n = 13) and the fungal (n = 11) infection subgroups. MESFs of nCD64 and mHLA-DR, CD64 index and SI were compared among the infection subgroups according to the pathogenic pathogens. The expression of

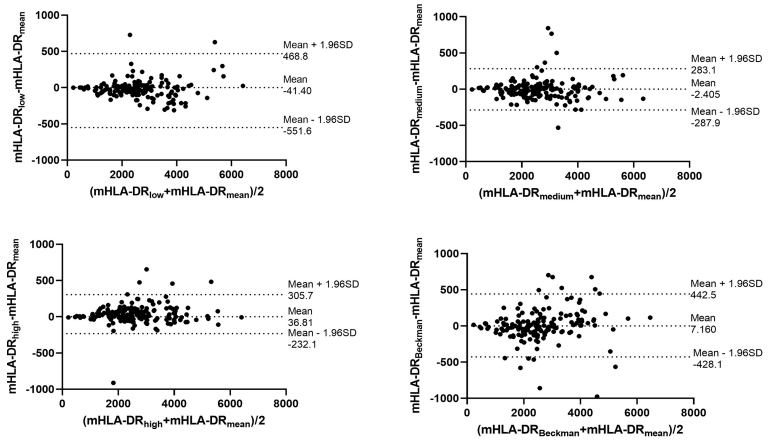

FIGURE 3
The Bland-Altman plot for the four MESFs of mHLA-DR under BD FACSCanto II with high/medium/high voltages and Beckman Coulter DxFlex with proper voltage. The agreement between the mean value of the four results and each result of mHLA-DR was assessed over the full range. The fixed range was defined as mean ± 1.96SD. mHLA-DR, monocyte HLA-DR; SD, standard deviation; MESF, molecules of equivalent soluble fluorochrome.

10.3389/fimmu.2022.1063957

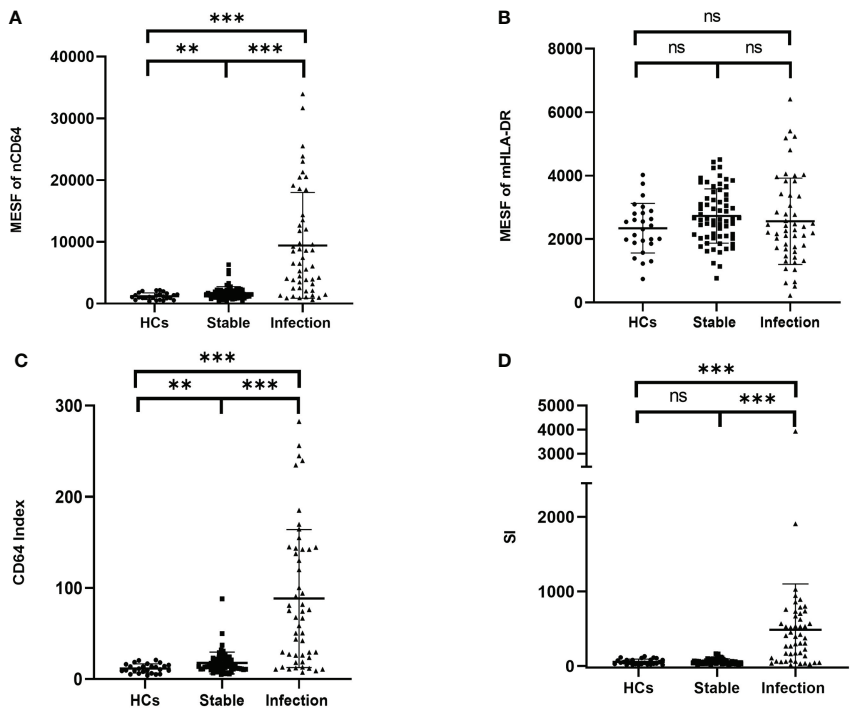

FIGURE 4
Comparison of the MESF of nCD64 **(A)**, MESF of mHLA-DR **(B)**, CD64 index **(C)** and SI **(D)** between HCs, stable KTRs and infection KTRs. Tested by the least significant difference test for back testing of multivariate ANOVA. *** means P < 0.001, and ** means P < 0.01. nCD64, neutrophil CD64; mHLA-DR, monocyte HLA-DR; HC, Healthy controls; KTRs, kidney transplant recipients; MESF, molecules of equivalent soluble fluorochrome; SI, Sepsis index; MESF, molecules of equivalent soluble fluorochrome. ns, no significance.

nCD64 was significantly higher in the bacterial and fungal infection subgroups than that in the viral infection subgroup. Although the mHLA-DR in the viral infection subgroup slightly increased, there was no statistical difference (Table 3). For the comparisons between every two subgroups, the bacterial and the fungal infection subgroups showed similar characteristics of nCD64, CD64 index and SI, while these parameters were lower in the viral infection subgroup (Figure 6).

mHLA-DR and SI identified sepsis in KTRs with infection

Sepsis was life-threatening organ dysfunction caused by a dysregulated host response to infection. KTRs with sepsis had a much higher mortality rate than the non-sepsis patients. Because the stable KTRs might maintain a relatively poorer renal function than the HCs, the SOFA score relating to the renal function was adjusted as mentioned in the methods. Although

TABLE 2 The expressions of nCD64 and mHLA-DR of the HCs and KTRs.

Parameters	All cases (n = 141)	HCs (n = 26)	KTRs			*P* value[#]
			Stable KTRs (n = 65)	Infection KTRs (n = 50)	*P* value*	
MESF of nCD64	4344.50 ± 6372.37	1192.58 ± 537.61	1697.89 ± 1056.32	9424.08 ± 8574.58	< 0.001	< 0.001
MESF of mHLA-DR	2596.92 ± 1054.52	2341.27 ± 781.75	2728.62 ± 854.87	2558.66 ± 1360.77	0.392	0.273
CD64 Index	41.58 ± 57.36	11.63 ± 4.97	17.60 ± 12.03	88.33 ± 75.69	< 0.001	< 0.001
SI	213.91 ± 417.41	58.86 ± 35.74	64.50 ± 32.69	488.76 ± 613.43	< 0.001	< 0.001

*Comparison between the stable KTRs and the infection KTRs.
[#]Comparison among the three groups.
Tested by the least significant difference test for back testing of multivariate ANOVA.
HCs, Healthy controls; KTRs, kidney transplant recipients, nCD64, neutrophil CD64; mHLA-DR, monocyte HLA-DR; MESF, molecules of equivalent soluble fluorochrome; SI, sepsis index.

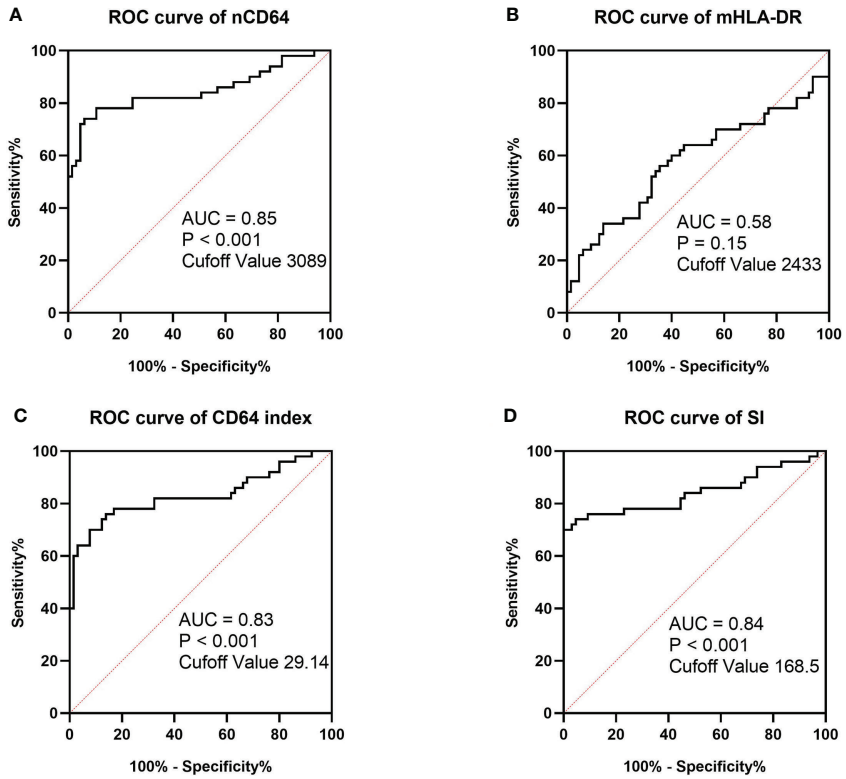

FIGURE 5
ROC curves of MESF of nCD64 **(A)**, MESF of mHLA-DR **(B)**, SI **(C)** and CD64 index **(D)** for diagnosis of infection in KTRs. The cut-off values were determined by the Youden index. ROC, Receiver operating characteristics; AUC, area under the curve; nCD64, neutrophil CD64; mHLA-DR, monocyte HLA-DR; KTRs, kidney transplant recipients; SI, Sepsis index; MESF, molecules of equivalent soluble fluorochrome.

the MESFs of nCD64 and mHLA-DR, CD64 index and SI showed significant differences among the stable, the sepsis and the non-sepsis groups, nCD64 and CD64 index could not distinguish between sepsis and non-sepsis patients (Table 4 and Figure 7). The sepsis patients had much lower mHLA-DR than the non-sepsis and the stable groups, but the nCD64 of the sepsis and the non-sepsis patients was close (both of them were higher than the stable group). Therefore, the sepsis group had the highest SI among the three groups. The non-sepsis group had the second highest SI, although the mHLA-DR showed no significant difference between the non-sepsis and the stable groups. The ROC curves confirmed that mHLA-DR and SI had good performance to identify sepsis in KTRs, with AUCs of 0.80 and 0.74, respectively (Figure 8).

As shown in Figure 1, 21 infection patients received the immune monitoring panels twice at the interval of approximately 1 week. These patients were also assessed by the SOFA score twice when they received the immune monitoring tests. According to the change of SOFA scores, which presented the severity of the infection, the patients were stratified into the exacerbation group ($\Delta SOFA > 0$) and the non-exacerbation group ($\Delta SOFA \leq 0$). The exacerbation group had a

TABLE 3 The expressions of nCD64 and mHLA-DR of infection KTRs with different pathogens.

Parameters	Bacterial (n = 26)	Viral (n = 13)	Fungal (n = 11)	*P* value[#]
MESF of nCD64	11361.46 ± 9428.95	4099.15 ± 5347.64	11137.91 ± 7337.20	0.03
MESF of mHLA-DR	2426.73 ± 1187.87	3176.31 ± 1601.28	2140.55 ± 1317.32	0.14
CD64 index	102.42 ± 81.11	44.75 ± 55.29	106.51 ± 67.89	0.051
SI	504.29 ± 376.84	170.73 ± 262.07	827.91 ± 1071.35	0.029

[#]Comparison among the three groups.
Tested by the least significant difference test for back testing of multivariate ANOVA.
KTRs, kidney transplant recipients; nCD64, neutrophil CD64; mHLA-DR, monocyte HLA-DR; MESF, molecules of equivalent soluble fluorochrome; SI, sepsis index.

10.3389/fimmu.2022.1063957

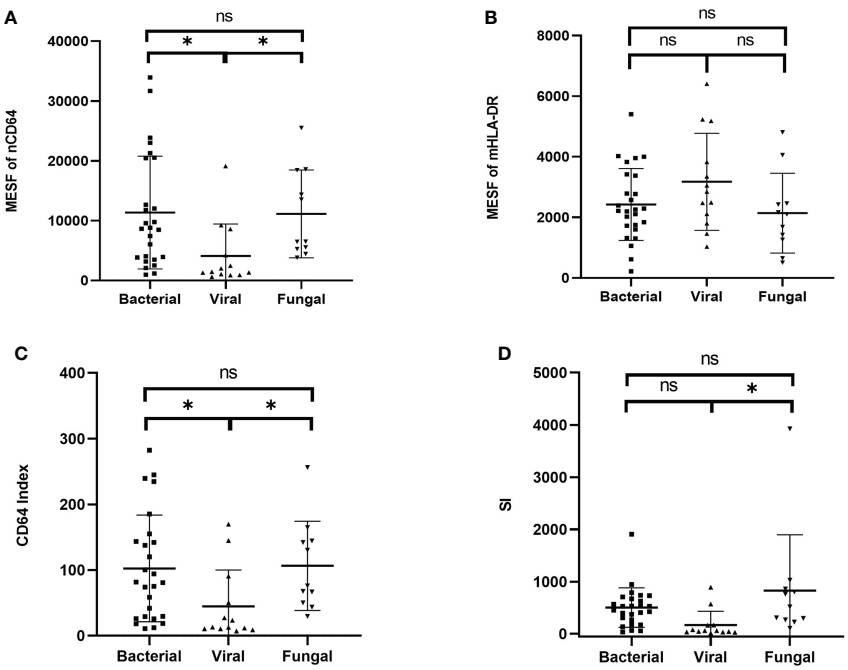

FIGURE 6
Comparison of the MESF of nCD64 **(A)**, MESF of mHLA-DR **(B)**, CD64 index **(C)** and SI **(D)** between the bacterial, the viral and the fungal infection subgroups. Tested by the least significant difference test for back testing of multivariate ANOVA. * means P < 0.05. nCD64, neutrophil CD64; mHLA-DR, monocyte HLA-DR; HC, Healthy controls; KTRs, kidney transplant recipients; MESF, molecules of equivalent soluble fluorochrome; ns, no significance.

sharp decline of mHLA-DR but a significant increase of SI, which suggested that dynamic changes of mHLA-DR and SI were related to the prognosis of the infection (Table 5 and Figure 9). In addition, the dynamic change of the nCD64 and CD64 index showed no significant relation to the prognosis.

nCD64 and B cell counts were independent risk factors of infection

To identify the risk factors of infection in KTRs, logistic analysis was performed with nCD64, mHLA-DR and parameters of the TBNK panel. Among them, nCD64 and mHLA-DR were transformed into binary variables with the cut-off values determined by the Youden index. As shown in Table 6, univariate logistic analysis revealed that nCD64 > 3089 (unadjusted odds ratio (OR) 43.404; 95% confidence interval (CI) 13.168 – 143.065; P < 0.001), mHLA-DR > 2433 (unadjusted OR 0.430; 95% CI 0.202 – 0.916; P = 0.029), the cell counts of $CD3^+$ T cells (unadjusted OR 0.998; 95% CI 0.997 – 0.999; P < 0.001), the cell counts of $CD8^+$ T cells (unadjusted OR 0.996; 95% CI 0.995 – 0.998; P < 0.001), the cell counts of $CD4^+$ T cells (unadjusted OR 0.996; 95% CI 0.994 – 0.998; P < 0.001), the cell counts of NK cells (unadjusted OR 0.995; 95% CI

TABLE 4 The expressions of nCD64 and mHLA-DR of infection KTRs with sepsis.

Parameters	Stable KTRs (n = 65)	Infection KTRs (n = 50)			*P* value[#]
		Sepsis (n = 19)	Non-sepsis (n = 31)	*P* value*	
MESF of nCD64	1697.89 ± 1056.32	10265.47 ± 8293.09	8908.39 ± 8837.41	0.416	< 0.001
MESF of mHLA-DR	2728.62 ± 854.87	1803.47 ± 1192.66	3021.52 ± 1260.32	< 0.001	< 0.001
CD64 index	17.60 ± 12.03	100.47 ± 74.46	80.98 ± 76.68	0.186	< 0.001
SI	64.50 ± 32.69	773.96 ± 868.31	313.96 ± 281.34	< 0.001	< 0.001

*Comparison between the sepsis patients and non-sepsis patients.
[#]Comparison among the three groups.
Tested by the least significant difference test for back testing of multivariate ANOVA.
KTRs, kidney transplant recipients; nCD64, neutrophil CD64; mHLA-DR, monocyte HLA-DR; MESF, molecules of equivalent soluble fluorochrome; SI, sepsis index.

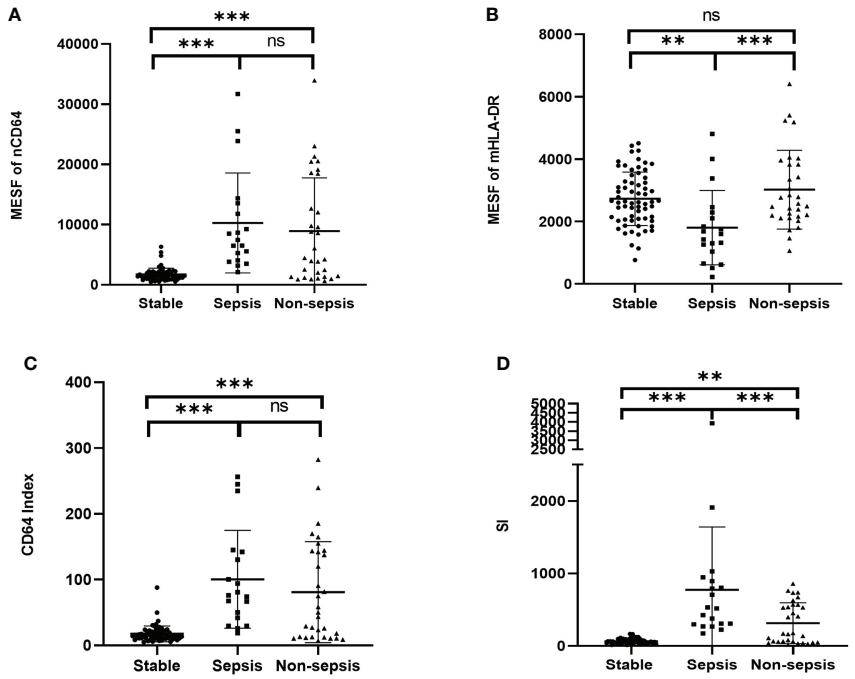

FIGURE 7
Comparison of the MESF of nCD64 **(A)**, MESF of mHLA-DR **(B)**, CD64 index **(C)** and SI **(D)** between the stable, the sepsis and the non-sepsis groups. Tested by the least significant difference test for back testing of multivariate ANOVA. *** means $P < 0.001$ and ** means $P < 0.01$. nCD64, neutrophil CD64; mHLA-DR, monocyte HLA-DR; HC, Healthy controls; KTRs, kidney transplant recipients; MESF, molecules of equivalent soluble fluorochrome; SI, Sepsis index. ns, no significance.

0.992 – 0.998; $P < 0.001$), and the cell counts of B cells (unadjusted OR 0.986; 95% CI 0.979 – 0.993; $P < 0.001$) were significantly associated with infection. Multivariate analysis further revealed that nCD64 > 3089 (unadjusted OR 49.378; 95% CI 11.015 – 221.347; $P < 0.001$) and the cell counts of B cells (unadjusted OR 0.989; 95% CI 0.979 – 0.998; $P = 0.022$) were independent risk factors for the infection in KTRs.

Discussion

In this study, we successfully established a standardization protocol of nCD64 and mHLA-DR and assessed their performance in KTRs with infection. nCD64 had the best diagnostic performance in KTRs with infection, and mHLA-DR distinguished sepsis and the dynamic change of mHLA-DR correlated with prognosis. mHLA-DR and nCD64 provided direct information of the immune status KTRs, and standardization measurement contributed to promotion and application of these parameters.

Infection is one of the most common but serious complications following KTx. Previous study using national data of KTRs indicated that the cumulative incidence of post-transplant infection was as high as 36.9% at 3 months, 53.7% at 1 year, 69.6% at 3 years, and 78.0% at 5 years (2). The most common post-transplant infections were urinary tract infection (46.8%) and pneumonia (28.2%). Because the optimal range balancing rejection and infection of the immunosuppressive drugs for KTRs is narrow, roughly adjusting the immunosuppressive drugs without precise immunological assessment during infection is likely to increase the risk of rejection or aggravate infection. Therefore, reliable immune biomarkers are needed to accurately assess immune status for KTRs with infection (19).

CD64 is constitutively expressed on monocytes, eosinophils, and neutrophils, but negatively expressed on lymphocytes. In a resting state, the expression of CD64 on monocytes is relatively high, but on neutrophils the expression is relatively low. However, a rapid 10-fold increase of CD64 expression is on neutrophils in a short period of time (4 – 6 hours) following an inflammatory response or pro-inflammatory cytokine stimulation, which plays an instrumental role in the immune response to infection (20). Meanwhile, the increase of CD64 expression on monocytes is limited. Therefore, nCD64 and CD64 index are effective and sensitive biomarkers for inflammation in the early stage. In our study, the stable KTRs had slightly higher nCD64 and CD64 index than the HCs,

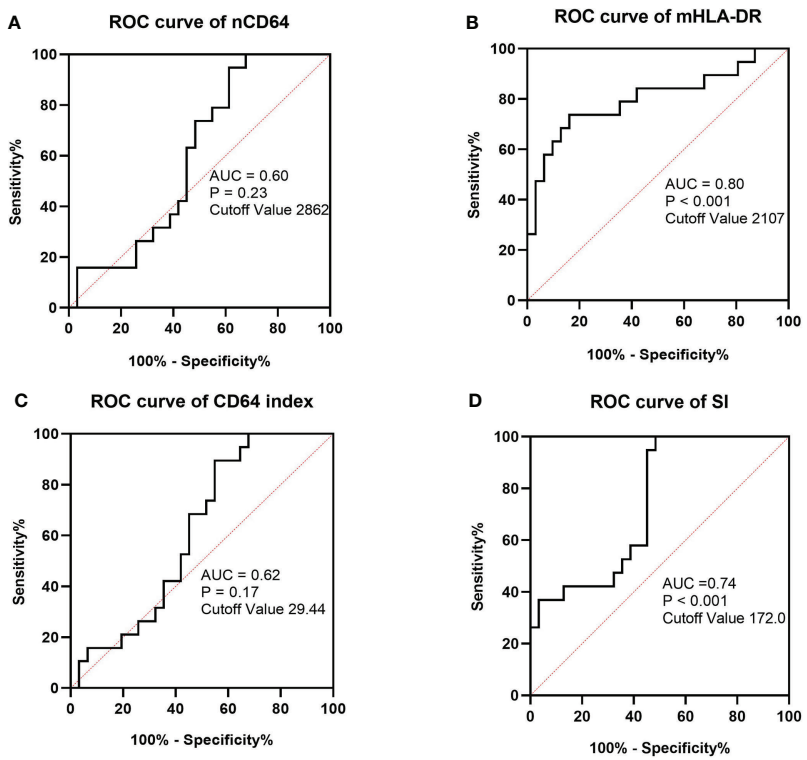

FIGURE 8
ROC curves of MESF of nCD64 **(A)**, MESF of mHLA-DR **(B)**, SI **(C)** and CD64 index **(D)** for diagnosis of sepsis in KTRs with infection. The cut-off values were determined by the Youden index. ROC, Receiver operating characteristics; AUC, area under the curve; nCD64, neutrophil CD64; mHLA-DR, monocyte HLA-DR; KTRs, kidney transplant recipients; SI, Sepsis index.

suggesting that mild inflammation response persisted in the stable KTRs. When the KTRs suffered from infection, both nCD64 and CD64 index rose sharply even if the KTRs received immunosuppressive drugs and were under immunosuppression. Therefore, nCD64 and CD64 index were still available biomarkers of infection for KTRs.

Different pathogenic pathogens of the infection showed different characteristics in the change of nCD64. It was reported that nCD64 expression was elevated in bacterial infections while it was normal in viral infections, which had potential for accurately distinguishing bacterial from COVID-19 or other viral infections in the emergency department (21). Pander G et al. indicated that quantitative detection of nCD64 in patients with severe alcoholic hepatitis could more accurately identify systemic bacterial infections and inflammation compared to other inflammatory markers (22). Consistently, our study also showed that KTRs with bacterial infections had significantly higher nCD64 and CD64 index than those with viral infections. The fungal infections, most of which were caused by Pneumocystis *jirovecii* in our study, also showed much higher nCD64 and CD64 index than the viral infections. When pathogens entered the human body, the innate immune

TABLE 5 The dynamic changes of nCD64 and mHLA-DR expression related to the prognosis of the infection KTRs.

Parameters	Infection KTRs (n = 21)	Exacerbation group (n = 3)	Non-exacerbation group (n = 18)	*P* value*
ΔnCD64	-5387.71 ± 8938.28	143.67 ± 5631.89	-6309.61 ± 9163.02	0.26
ΔmHLA-DR	513.29 ± 1671.85	-1273.33 ± 2049.93	811.06 ± 1461.78	0.042
ΔSI	-228.19 ± 635.51	701.67 ± 857.79	-383.17 ± 458.87	0.003
ΔCD64 index	-45.10 ± 70.38	0.33 ± 70.29	-52.67 ± 69.44	0.24

*Comparison between the exacerbation group and non-exacerbation group.
Tested by Student's t test or Welch's t test.
The exacerbation group was defined as ΔSOFA > 0 and the non-exacerbation group was defined as ΔSOFA ≤ 0. Δ means the results of the second test minus that of the first test.
KTRs, kidney transplant recipients; nCD64, neutrophil CD64; mHLA-DR, monocyte HLA-DR; MESF, molecules of equivalent soluble fluorochrome; SI, sepsis index.

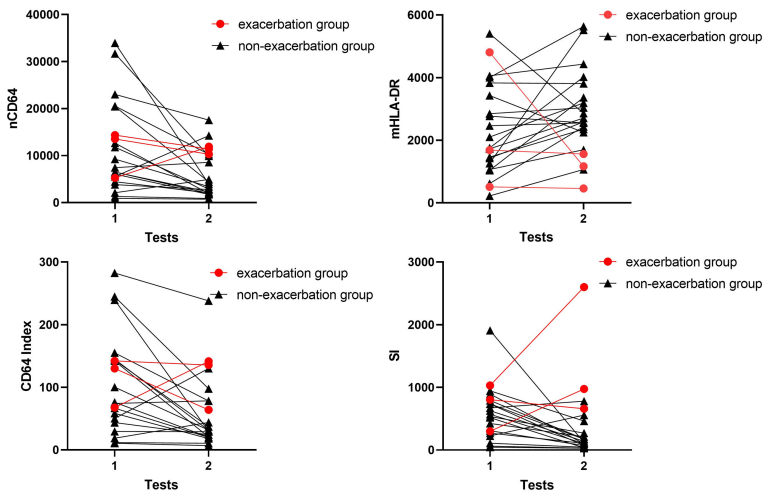

FIGURE 9
Longitudinal results of the immune monitoring panels in infection KTRs. The changes of MESFs of nCD64 and mHLA-DR, CD64 index and SI were shown for each patient. The exacerbation group was defined as ΔSOFA > 0 and the non-exacerbation group was defined as ΔSOFA ≤ 0. nCD64, neutrophil CD64; mHLA-DR, monocyte HLA-DR; KTRs, kidney transplant recipients; MESF, molecules of equivalent soluble fluorochrome; SI, Sepsis index; ΔSOFA, change of Sequential Organ Failure Assessment score.

system was activated by inducing cytokines, such as interferon (IFN), which was primarily involved in host defense against invading pathogens. IFNs were classified into three distinct types including type I, type II (gamma), and type III. *In vitro* and *in vivo* experiments demonstrated that IFN-γ intensely stimulated the expression of nCD64, but little effect was seen with type I and type III IFNs (23, 24). Upon bacterial infection, the activation of the immune system released pro-inflammatory cytokines including IFN-γ, which strongly induced the expression of nCD64 (24). Moreover, bacterial components such as lipopolysaccharide (LPS) could also induce CD64 expression on the surface of neutrophils (24). Similarly, the fungal infection, especially caused by Pneumocystis *jirovecii*, could also induce the secretion of IFN-γ, thus significantly upregulating the expression of nCD64 (25–27). In contrast, viral infection mainly induced the secretion of IFN type I, which slightly upregulated nCD64 (24). Yet it was worth noting that infections in KTRs were commonly mixed infections, thus nCD64 could only suggest but not confirm the pathogens of infection.

TABLE 6 Univariate and multivariate odds ratios for infection diagnosis among KTRs.

Parameters	Univariate analysis		Multivariate analysis	
	OR (95% CI)	*P* value	OR (95% CI)	*P* value
MESF of nCD64 > 3089	43.404 (13.168 – 143.065)	< 0.001	49.378 (11.015 - 221.347)	< 0.001
MESF of mHLA-DR > 2433	0.430 (0.202 – 0.916)	0.029	0.422 (0.130 – 1.372)	0.151
$CD3^+$ T cells/TBNK, mean ± SD (%)	0.991 (0.954 - 1.029)	0.644		
$CD3^+$ T cells, n ± SD (cells/μl)	0.998 (0.997 - 0.999)	< 0.001	0.996 (0.983 - 1.009)	0.548
$CD8^+$ T cells/TBNK, mean ± SD (%)	1.021 (0.977 - 1.067)	0.352		
$CD8^+$ T cells, n ± SD (cells/μl)	0.996 (0.995 - 0.998)	< 0.001	1.008 (0.993 - 1.022)	0.284
$CD4^+$ T cells/TBNK, mean ± SD (%)	0.976 (0.943 - 1.011)	0.176		
$CD4^+$ T cells, n ± SD (cells/μl)	0.996 (0.994 - 0.998)	< 0.001	1.002 (0.989 - 1.014)	0.811
NK cells/TBNK, mean ± SD (%)	1.031 (0.984 - 1.079)	0.202		
NK cells, n ± SD (cells/μl)	0.995 (0.992 - 0.998)	0.005	1.001 (0.997 - 1.005)	0.600
B cells/TBNK, mean ± SD (%)	0971 (0.913 - 1.033)	0.359		
B cells, n ± SD (cells/μl)	0.986 (0.979 - 0.993)	< 0.001	0.989 (0.979 - 0.998)	0.022
CD4/CD8 ratio, mean ± SD	0.719 (0.413 - 1.251)	0.243		

OR, odds ratio; TBNK, T, B, and NK cells; NK cells, natural killer cells; nCD64, neutrophil CD64; mHLA-DR, monocyte HLA-DR; MESF, molecules of equivalent soluble fluorochrome.

Currently, some researches showed that nCD64 expression performed good diagnostic efficacy in bacterial infections and sepsis (22). In a prospective observational study, it concluded that serial measurement of nCD64 expression could facilitate sepsis diagnosis and monitor the clinical course in critically ill patients (17). However, a meta-analysis indicated that nCD64 expression was a helpful marker but not sufficient for early diagnosis of sepsis in critically ill adult patients (28), which yielded conflicting results. In our study, the sepsis group and non-sepsis group had close nCD64 and CD64 index, although both of them were much higher than the stable group and HCs. Therefore, our data suggested that nCD64 alone was not enough to distinguish sepsis in KTRs with infection.

mHLA-DR expression is the most recognized immune indicator to assess the degree of immunosuppression in critically ill patients (29). Under the condition of sepsis, monocytes with decreased HLA-DR expression exhibit an impaired capacity to mount a proinflammatory reaction upon a secondary bacterial challenge and impairment in antigen presentation capacity (30). A wide array of studies confirmed that decreased mHLA-DR expression was a predictor for sepsis or septic complications and correlated with prognosis (30). A multi-centre cohort study showed that lower mHLA-DR expression with increased neutrophil CD24 and neutrophil CD279 best predicted the clinical deterioration to sepsis (31). Leijte et al. also indicated that dynamic declination of mHLA-DR over time was associated with adverse clinical outcomes of septic shock, but mHLA-DR expression exhibited no significant association with causative pathogens (32). In KTRs, the long-term administration of immunosuppressive drugs indeed leads to persist immunosuppression, but the classic triple immunosuppressive regimens mainly suppress the adaptive immunity. Therefore, stable KTRs and even KTRs with infection showed no significant decrease of mHLA-DR in this study. Only KTRs with sepsis, which indicated that patients had severe infection and were severely immunosuppressed, had decreased expression of mHLA-DR. It was shown in our study that mHLA-DR exhibited the best performance to distinguish sepsis among KTRs with infection. The SI which combined mHLA-DR and nCD64 also contributed to identifying patients with sepsis. In addition, the persistent decline of mHLA-DR was correlated with aggravation of infection.

In our study, the cell count of B cells was identified as an independent risk factor for KTRs with infection in multivariate logistic regression analysis. Although B cells compromised a relatively small percentage of lymphocytes, they played a critical role in adaptive immunity to fight against infection (33). Patients with decreased B cells were predisposed to infection. In our previous study, KTRs with pneumonia were characterized with significantly lower cell count of B cells, which was in accordance with the results in this research (16). Rituximab, a monoclonal antibody that depleted B cells, was reported to cause hypogammaglobulinemia and increased risk of severe infection (34). For KTRs, the use of rituximab after transplantation was also associated with higher risk of infectious disease and lower survival rate (35). Therefore, we should pay more attention to the B cells as a biomarker for immune monitoring.

In previous studies, nCD64 and mHLA-DR were quantified by the percentage of cells positively expressed these markers or the MFI values. Indeed, both CD64 and HLA-DR were continuously expressed on cells, which meant that it was technically difficult to determine the cut-off values for gating the positive cells. In addition, different gating strategies notably affected the results. For nCD64, almost all neutrophils positively expressed CD64 when patients suffered from infection, thus making it meaningless for comparison. The value of MFI was indeed quantified and widely used. However, MFI was a relative value, which was also determined by the instrument settings (such as voltage of the photomultipliers, optical filters, etc.) and antibodies selected. Therefore, the results of nCD64 and mHLA-DR quantified by MFIs varied in different studies, and it was meaningless for comparison between different studies. In this study, a standardization protocol of nCD64 and mHLA-DR was established. The MFI was converted into MESF by the calibrated beads with known number of PE molecules. It proved good reliability under different settings and instruments, making it possible for lab-to-lab comparison. In this protocol, some details should be noted. There should be no compensation for the channel chosen for standardization in the multicolor flow cytometry panel. The voltage for the channel should be fixed and the routine calibration of the flow cytometer should be performed.

There were some limitations in this study. The sample size was relatively limited, and the patients were recruited from a single institution. nCD64 and mHLA-DR were detected at only two points over two weeks, and some patients did not complete all tests because they were discharged. Due to the timely treatment, KTRs with infection had a relatively good prognosis in this study. Therefore, the prognostic value of nCD64 and mHLA-DR for infection needed further research.

In conclusion, we established a standardization protocol for detection of nCD64 and mHLA-DR, making it available for the lab-to-lab comparison and widespread application. nCD64 and mHLA-DR had good diagnostic performance in KTRs with infection and sepsis, respectively, which could be promising indicators for immune monitoring of KTRs and contributed to individualized treatment.

Data availability statement

The raw data supporting the conclusions of this article will be made available by the authors, without undue reservation.

Ethics statement

The studies involving human participants were reviewed and approved by The Ethics committee of Third Xiangya Hospital, Central South University. The patients/participants provided their written informed consent to participate in this study. Written informed consent was obtained from the individual(s) for the publication of any potentially identifiable images or data included in this article.

Author contributions

BP and YM: critical analysis, interpretation of the data, and drafting of the manuscript. MY and QZ: sample processing and cohort management. MY and JL: clinical data collection and sample acquisition. PZ, HL, and KC: guidance of experiment and technical support. BP and YM: conceived and designed the study. All authors contributed to the article and approved the submitted version.

Funding

This study was supported by the National Natural Science Foundation of China (81771722) and the Hunan Provincial Natural Science Foundation of China (2020JJ5863). The funders had no role in study design, data collection, analysis and interpretation, writing and submission of the manuscript.

Acknowledgments

We thank all the individuals for their participation in this study.

Conflict of interest

The authors declare that the research was conducted in the absence of any commercial or financial relationships that could be construed as a potential conflict of interest.

Publisher's note

Supplementary material

The Supplementary Material for this article can be found online at: https://www.frontiersin.org/articles/10.3389/fimmu.2022.1063957/full#supplementary-material

References

1. Coemans M, Callemeyn J, Naesens M. Long-term survival after kidney transplantation. *New Engl J Med* (2022) 386(5):497–8. doi: 10.1056/NEJMc2115207

2. Jackson KR, Motter JD, Bae S, Kernodle A, Long JEJ, Werbel W, et al. Characterizing the landscape and impact of infections following kidney transplantation. *Am J Transplant* (2021) 21(1):198–207. doi: 10.1111/ajt.16106

3. Schachtner T, Stein M, Reinke P. Sepsis after renal transplantation: Clinical, immunological, and microbiological risk factors. *Transplant Infect Dis* (2017) 19 (3):e12695. doi: 10.1111/tid.12695

4. Singer M, Deutschman CS, Seymour CW, Shankar-Hari M, Annane D, Bauer M, et al. The third international consensus definitions for sepsis and septic shock (Sepsis-3). *Jama Journal Am Med Assoc* (2016) 315(8):801–10. doi: 10.1001/jama.2016.0287

5. Fernandez-Ruiz M, Lopez-Medrano F, Aguado JM. Predictive tools to determine risk of infection in kidney transplant recipients. *Expert Rev Anti Infect Ther* (2020) 18(5):423–41. doi: 10.1080/14787210.2020.1733976

6. Boix F, Alfaro R, Jimenez-Coll V, Mrowiec A, Martinez-Banaclocha H, Botella C, et al. A high concentration of tgf-beta correlates with opportunistic infection in liver and kidney transplantation. *Hum Immunol* (2021) 82(6):414–21. doi: 10.1016/j.humimm.2021.03.007

7. Sanju S, Jain P, Priya VV, Varma PK, Mony U. Quantitation of mhla-Dr and Ncd64 by flow cytometry to study dysregulated host response: The use of quantibrite™ pe beads and its stability. *Appl Biochem Biotechnol* (2022), 194 (1):1–6. doi: 10.1007/s12010-022-03819-6

8. Nuutila J, Hohenthal U, Oksi J, Jalava-Karvinen P. Rapid detection of bacterial infection using a novel single-tube, four-colour flow cytometric method: Comparison with pct and crp. *Ebiomedicine* (2021) 74:103724. doi: 10.1016/j.ebiom.2021.103724

9. Liu QQ, Gao Y, Yang T, Zhou Z, Lin K, Zhang W, et al. Ncd64 index as a novel inflammatory indicator for the early prediction of prognosis in infectious and non-infectious inflammatory diseases: An observational study of febrile patients. *Front Immunol* (2022) 13:905060. doi: 10.3389/fimmu.2022.905060

10. Bodinier M, Peronnet E, Brengel-Pesce K, Conti F, Rimmele T, Textoris J, et al. Monocyte trajectories endotypes are associated with worsening in septic patients. *Front Immunol* (2021) 12:795052. doi: 10.3389/fimmu.2021.795052

11. Tamulyte S, Kopplin J, Brenner T, Weigand MA, Uhle F. Monocyte hla-Dr assessment by a novel point-of-Care device is feasible for early identification of icu patients with complicated courses -a proof-of-Principle study. *Front Immunol* (2019) 10:432. doi: 10.3389/fimmu.2019.00432

12. Denstaedt SJ, Singer BH, Standiford TJ. Sepsis and nosocomial infection: Patient characteristics, mechanisms, and modulation. *Front Immunol* (2018) 9:2446. doi: 10.3389/fimmu.2018.02446

13. Carter MJ, Fish M, Jennings A, Doores KJ, Wellman P, Seow J, et al. Peripheral immunophenotypes in children with multisystem inflammatory syndrome associated with sars-Cov-2 infection. *Nat Med* (2020) 26(11):1701–+. doi: 10.1038/s41591-020-1054-6

14. Alingrin J, Coiffard B, Textoris J, Nicolino-Brunet C, Gossez M, Jarrot PA, et al. Sepsis is associated with lack of monocyte hla-Dr expression recovery without modulating T-cell reconstitution after lung transplantation. *Transplant Immunol* (2018) 51:6–11. doi: 10.1016/j.trim.2018.08.001

15. Bottomley MJ, Harden PN, Wood KJ, Hester J, Issa F. Dampened inflammatory signalling and myeloid-derived suppressor-like cell accumulation reduces circulating monocytic hla-Dr density and may associate with malignancy risk in long-term renal transplant recipients. *Front Immunol* (2022) 13:901273. doi: 10.3389/fimmu.2022.901273

16. Peng B, Gong H, Tian H, Zhuang Q, Li JH, Cheng K, et al. The study of the association between immune monitoring and pneumonia in kidney transplant recipients through machine learning models. *J Trans Med* (2020) 18(1):370. doi: 10.1186/s12967-020-02542-2

17. Mittag A, Tarnok A. Basics of Standardization and Calibration in Cytometry- a Review. *Journal of Biophotonics* (2009) 2(8-9):470–81. doi: 10.1002/jbio.200910033

18. Pradhan R, Jain P, Paria A, Saha A, Sahoo J, Sen A, et al. Ratio of neutrophilic Cd64 and monocytic hla-Dr: A novel parameter in diagnosis and prognostication of neonatal sepsis. *Cytometry Part B Clinical Cytometry* (2016) 90 (3):295–302. doi: 10.1002/cyto.b.21244

19. Dendle C, Mulley WR, Holdsworth S. Can immune biomarkers predict infections in solid organ transplant recipients? a review of current evidence. *Transplant Rev* (2019) 33(2):87–98. doi: 10.1016/j.trre.2018.10.001

20. Liu QQ, Gao Y, Ou QF, Xu YZ, Zhou Z, Li T, et al. Differential expression of Cd64 in patients with mycobacterium tuberculosis infection: A potential biomarker for clinical diagnosis and prognosis. *J Cell Mol Med* (2020) 24(23):13961–72. doi: 10.1111/jcmm.16004

21. Bourgoin P, Soliveres T, Barbaresi A, Loundou A, Belkacem IA, Arnoux I, et al. Cd169 and Cd64 could help differentiate bacterial from covid-19 or other viral infections in the emergency department. *Cytometry Part A* (2021) 99(5):435–45. doi: 10.1002/cyto.a.24314

22. Pandey G, Singh H, Chaturvedi S, Hatti M, Kumar A, Mishra R, et al. Utility of neutrophil Cd64 in distinguishing bacterial infection from inflammation in severe alcoholic hepatitis fulfilling sirs criteria. *Sci Rep* (2021) 11(1):19726. doi: 10.1038/s41598-021-99276-y

23. Comins-Boo A, Gutiérrez-Larrañaga M, Roa-Bautista A, Guiral Foz S, Renuncio García M, González López E, et al. Validation of a quick flow cytometry-based assay for acute infection based on Cd64 and Cd169 expression. new tools for early diagnosis in covid-19 pandemic. *Front Med (Lausanne)* (2021) 8:655785. doi: 10.3389/fmed.2021.655785

24. Bourgoin P, Biéchelé G, Ait Belkacem I, Morange PE, Malergue F. Role of the interferons in Cd64 and Cd169 expressions in whole blood: Relevance in the balance between viral- or bacterial-oriented immune responses. *Immunity Inflammation Dis* (2020) 8(1):106–23. doi: 10.1002/iid3.289

25. Gozalbo D, Maneu V, Gil ML. Role of ifn-gamma in immune responses to candida albicans infections. *Front Biosci (Landmark edition)* (2014) 19(8):1279–90. doi: 10.2741/4281

26. Dos Santos AR, Fraga-Silva TF, de Fátima Almeida-Donanzam D, Dos Santos RF, Finato AC, Soares CT, et al. Ifn-Γ mediated signaling improves fungal clearance in experimental pulmonary mucormycosis. *Mycopathologia* (2022) 187 (1):15–30. doi: 10.1007/s11046-021-00598-2

27. Shen HP, Tang YM, Song H, Xu WQ, Yang SL, Xu XJ. Efficiency of interleukin 6 and interferon gamma in the differentiation of invasive pulmonary aspergillosis and pneumocystis pneumonia in pediatric oncology patients. *Int J Infect Dis IJID Off Publ Int Soc Infect Dis* (2016) 48:73–7. doi: 10.1016/j.ijid.2016.05.016

28. Wang X, Li ZY, Zeng L, Zhang AQ, Pan W, Gu W, et al. Neutrophil Cd64 expression as a diagnostic marker for sepsis in adult patients: A meta-analysis. *Crit Care* (2015) 19:172. doi: 10.1186/s13054-015-0972-z

29. Tawfik DM, Vachot L, Bocquet A, Venet F, Rimmele T, Monneret G, et al. Immune profiling panel: A proof-of-Concept study of a new multiplex molecular tool to assess the immune status of critically ill patients. *J Infect Dis* (2020) 222:S84–95. doi: 10.1093/infdis/jiaa248

30. Venet F, Lepape A, Monneret G. Clinical review: Flow cytometry perspectives in the icu - from diagnosis of infection to monitoring of injury-induced immune dysfunctions. *Crit Care* (2011) 15(5):231. doi: 10.1186/cc10333

31. Shankar-Hari M, Datta D, Wilson J, Assi V, Stephen J, Weir CJ, et al. Early prediction of sepsis using leukocyte surface biomarkers: The expres-sepsis cohort study. *Intensive Care Med* (2018) 44(11):1836–48. doi: 10.1007/s00134-018-5389-0

32. Leijte GP, Rimmele T, Kox M, Bruse N, Monard C, Gossez M, et al. Monocytic hla-Dr expression kinetics in septic shock patients with different pathogens, sites of infection and adverse outcomes. *Crit Care* (2020) 24(1):110. doi: 10.1186/s13054-020-2830-x

33. Akkaya M, Kwak K, Pierce SK. B cell memory: Building two walls of protection against pathogens. *Nat Rev Immunol* (2020) 20(4):229–38. doi: 10.1038/s41577-019-0244-2

34. Sacco KA, Abraham RS. Consequences of b-Cell-Depleting therapy: Hypogammaglobulinemia and impaired b-cell reconstitution. *Immunotherapy* (2018) 10(8):713–28. doi: 10.2217/imt-2017-0178

35. Kelesidis T, Daikos G, Boumpas D, Tsiodras S. Does rituximab increase the incidence of infectious complications? a narrative review. *Int J Infect Dis IJID Off Publ Int Soc Infect Dis* (2011) 15(1):e2–16. doi: 10.1016/j.ijid.2010.03.025

frontiers | Frontiers in Immunology

TYPE Case Report
PUBLISHED 29 November 2022
DOI 10.3389/fimmu.2022.1049444

OPEN ACCESS

EDITED BY
Xuanchuan Wang,
Zhongshan Hospital, Fudan University, China

REVIEWED BY
Wei Wang,
Tongji University, China
Jakob Nilsson,
University Hospital Zürich, Switzerland

*CORRESPONDENCE
Yun-Ying Shi
shiyunying@wchscu.cn
Yang-Juan Bai
whitewcums@126.com

†These authors have contributed equally to this work and share first authorship

SPECIALTY SECTION
This article was submitted to Alloimmunity and Transplantation, a section of the journal Frontiers in Immunology

RECEIVED 20 September 2022
ACCEPTED 11 November 2022
PUBLISHED 29 November 2022

CITATION
Chen X-M, Li H, Wu Y, Wang L-L, Bai Y-J and Shi Y-Y (2022) Case report: Dynamic antibody monitoring in a case of anti-recombinant human erythropoietin-mediated pure red cell aplasia with prolonged course after kidney transplantation.
Front. Immunol. 13:1049444.
doi: 10.3389/fimmu.2022.1049444

Case report: Dynamic antibody monitoring in a case of anti-recombinant human erythropoietin-mediated pure red cell aplasia with prolonged course after kidney transplantation

Xiao-Mei Chen[1†], Hui Li[2†], Yu Wu[3], Lan-Lan Wang[1], Yang-Juan Bai[1*] and Yun-Ying Shi[2*]

[1]Department of Laboratory Medicine/Research Centre of Clinical Laboratory Medicine, West China Hospital, Sichuan University, Chengdu, Sichuan, China, [2]Department of Nephrology, West China Hospital, Sichuan University, Chengdu, Sichuan, China, [3]Department of Hematology, West China Hospital, Sichuan University, Chengdu, Sichuan, China

Anti-erythropoietin (anti-EPO) antibody-mediated pure red cell aplasia (PRCA) is a rarely seen disease. Anti-EPO antibodies were mostly found in patients with chronic kidney disease who received recombinant human erythropoietin (rHuEPO) injections subcutaneously. The treatment against anti-EPO antibody-mediated PRCA included discontinuation of rHuEPO, immunosuppressive agents, intravenous immunoglobulin, plasmapheresis, or kidney transplantation. We reported a case of kidney transplant recipient with anti-EPO antibody-mediated PRCA, who had no trend of recovery after stopping rHuEPO, receiving regular induction and maintenance immunosuppressive regimens. He was further given 6 consecutive plasmapheresis sessions, cyclophosphamide, and adjusted maintenance immunosuppressive regimen into cyclosporine, sirolimus and prednisone. We monitored his anti-EPO antibody levels with a self-created simple mixing test. At 10 months post kidney transplant, his anti-EPO antibody finally turned negative, and his reticulocyte count dramatically increased. Cyclosporine, sirolimus and prednisone combined with roxadustat eventually alleviated the patient's anti-EPO antibody-mediated PRCA. Our self-created simple mixing test for anti-EPO antibody titer was very helpful in disease monitoring and therapeutic guidance.

KEYWORDS

anti-erythropoietin (anti-EPO) antibody, pure red cell aplasia, kidney transplant, immunosuppressive therapy, roxadustat

Introduction

Anti-EPO antibody-mediated PRCA is a very rare but severe transfusion-dependent anemia with an incidence of 0.02 to 0.03 per 1000 person-years (1). The incidence rate may be underestimated due to the availability of anti-EPO antibody testing. A slight modification in the production process of rHuEPO leads to some antigenicity of the manufactured hormone, which induces the generation of anti-EPO antibody (2–4). Causes of this disease included formulations without human serum albumin, subcutaneous administration, and uncoated rubber stoppers (1). The median duration of rHuEPO treatment prior to the occurrence of PRCA was 9-25 months (5). There was no guideline on the treatment for anti-EPO antibody-mediated PRCA, because there were too limited cases to perform prospective cohort studies and the patients in most case reports experienced rapid remission after kidney transplant (6). Since kidney transplant itself was an effective treatment for anti-EPO antibody-mediated PRCA, cases with prolonged course after kidney transplant were rarely reported. We reported a case of anti-EPO antibody-mediated PRCA diagnosed after kidney transplant with an abnormally prolonged course, and we successfully created a simple mixing test to monitor anti-EPO antibody titer and guide our treatment adjustment effectively.

Case presentation

A 38-year-old Chinese man who was diagnosed with end-stage renal disease (ESRD) due to chronic glomerulonephritis started maintenance hemodialysis three times a week in a local hospital since 2018. He received rHuEPO (Epiao, 3SBio, Shenyang, China) subcutaneously at 10,000 IU twice a week and roxadustat was added later due to his hemoglobin (Hb) below the target range (Figure 1). In June 2020, his Hb level suddenly decreased from 100 g/L to 34 g/L without evidence of active bleeding or hemolysis, and he required blood transfusion every month to maintain Hb around 60g/L ever since then. He underwent his first bone marrow aspirate and biopsy in February 2021 in West China Hospital, and his bone marrow smear showed hypercellularity with no red blood cell precursors. His blood routine examination showed that reticulocyte count was 0.0020×10^{12}/L and Hb was 50 g/L. His erythropoietin level was <0.60 mIU/mL and his ferritin level was >2000 ng/mL. In May 2021, he received a kidney transplant donated by his 58-year-old mother in West China Hospital of Sichuan University, and his Hb was enhanced to 90 g/L by transfusing leukodepleted red cell suspension prior to the surgery. Induction therapy including intravenous basiliximab and methylprednisolone pulse therapy was given, and the standard triple immunosuppressive regimen consisting of mycophenolate mofetil (MMF), tacrolimus (Tac), and prednisone was immediately applied. Trimethoprim-sulfamethoxazole and ganciclovir were administered as the general prophylaxis for pneumocystis pneumonia and cytomegalovirus (CMV) infection, respectively. The kidney graft functioned immediately after the surgery, and roxadustat combined with rHuEPO injection subcutaneously were continued for his anemia (Figure 1).

Approximately one month after kidney transplant, the patient was readmitted to the hospital due to severe anemia. His blood routine examination showed that reticulocyte count

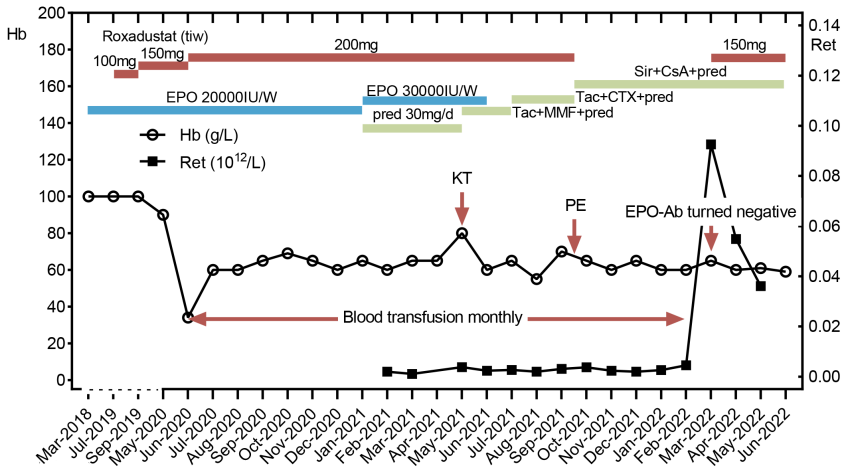

FIGURE 1
Clinical course. A kidney transplantation was performed in May 2021. Plasma exchange was performed in September 15, 2021. After the EPO antibody turned negative, the patient didn't rely on blood transfusion any more. Hb, hemoglobin; Ret, reticulocyte; Tac, tacrolimus; MMF, mycophenolate mofetil; pred, prednisone; CTX, cyclophosphamide; Sir, sirolimus; CsA, cyclosporine; KT, kidney transplant; PE, plasma exchange.

was 0.0020×10^{12}/L, Hb was 49 g/L, platelet (PLT) count was 60×10^{9}/L and white blood cell (WBC) count was 2.8×10^{9}/L with normal differentials. His graft function was stable with a creatinine level of 144 μmol/L. The erythropoietin and ferritin levels were similar to those before the transplant. Examinations to exclude other possible causes of anemia, including tumor markers, serum protein electrophoresis, serum immunofixation electrophoresis, anti-nuclear antibodies (ANA), extractable nuclear antigens (ENA), Coombs test, serum cytomegalovirus (CMV) DNA polymerase chain reaction (PCR) and Epstein-Barr virus (EBV) DNA PCR, were all negative. Computed tomography of the chest did not reveal thymoma. Fecal occult blood testing and DNA quantification of parvovirus B19 were also negative. No suspected family history or history of using drugs that might interfere hematopoietic function was found. Tacrolimus trough concentration was 6.86ng/mL. A second bone marrow biopsy was performed, and the bone marrow smear showed hypercellularity with 0.5% red blood cell precursors. Bone marrow biopsy revealed severe erythroid hypoplasia. The patient was diagnosed with PRCA accordingly. His serum was sent to 3SBio Pharmaceutical Company for the anti-EPO antibody examination, which showed positive by enzyme-linked immunosorbent assay (ELISA). The neutralization test of anti-EPO antibody was performed by a bioassay based on the fact that rHuEPO-neutralizing antibodies could inhibit the proliferation of rHuEPO on UT7/EPO-dependent cell lines. The patient was eventually diagnosed with anti-EPO antibody-mediated PRCA.

Due to the limited availability and long turn-around time of the anti-EPO antibody test, as well as the need for dynamic monitoring of the therapeutic effect, we created a simple mixing test to quantify the antibody titer (Supplementary Figure 1). The operating steps were as follows: the sera of both the patient and the health control were collected and then mixed in different proportions, which were used for the testing of EPO concentrations (IMMULITE 1000, SIEMENS). The maximum dilution multiple at which a positive EPO result was obtained was defined as the antibody titer, which was based on the fact that the neutralizing IgG antibodies against the protein component of exogenous erythropoiesis-stimulating agents (ESAs) would cross-react with endogenous hormones. The result of the simple mixing test was consistent with the neutralization test of anti-EPO antibodies from the 3SBio Pharmaceutical Company, which revealed a titer of 1:10 at diagnosis. Then, we adopted this simple method for the monthly anti-EPO antibody monitoring. It should be noted that the EPO level of the selected health control in each test must be fixed and above the upper limit of normal value to reduce errors. In our experiment, the fixed EPO level was 200mIU/ml. The dynamic changes of anti-EPO antibody titers and EPO levels of the patient are shown in Figure 2.

Once diagnosed in July 2021, rHuEPO was stopped immediately. The detailed treatment course is shown in Figure 1. Recombinant human granulocyte colony-stimulating factors were administered and Trimethoprim-sulfamethoxazole as well as ganciclovir were discontinued due to leukopenia. The

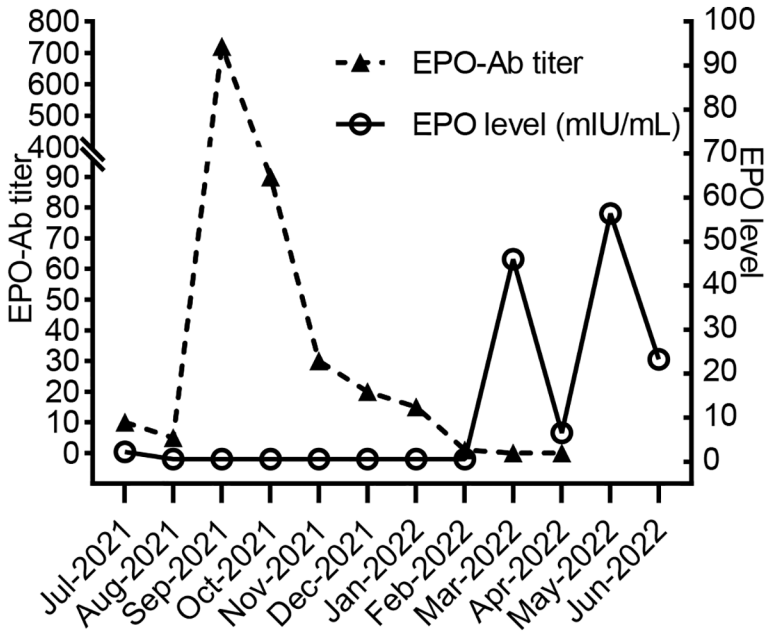

FIGURE 2
EPO antibody titer and EPO levels of the patient.

antibody titer decreased to 1:5 in August 2021, and then suddenly increased to 1:720 one month later after he received massive transfusion of 10 U leukodepleted red blood cell suspension in the local hospital. It was speculated that EPO existed in a small amount of plasma contained in the leukodepleted red blood cells, which may activate immunological memory response and induce the massive production of anti-EPO antibodies. In comparison, the residual plasma volume in washed red blood cells was less than that in leukodepleted red blood cell suspension (7). Therefore, we replaced the leukodepleted red blood cell suspension with a restrictive washed red blood cell transfusion. At the same time, the cumulative dose of cyclophosphamide reached 6 g but no effect was observed. Then, we performed plasmapheresis 6 times and adjusted immunosuppressive regimen into cyclosporine, sirolimus and methylprednisolone (because of mild liver dysfunction). The trough concentration of cyclosporine was maintained at 100-150 ng/ml, and sirolimus was maintained at 6-8 ng/ml. By the fifth month of the above treatment, antibodies were finally undetectable using the simple mixing test, and laboratory results were as follows: a Hb level of 51 g/L, a reticulocyte count of 0.0926×10^{12}/L, an EPO level of 46 mIU/mL, a creatinine level of 146 μmol/L, and an eGFR of 51.46 mL/min/1.73 m^2. A serum sample of the patient was sent to 3SBio Pharmaceutical company again for anti-EPO antibody test, which also confirmed the negative result. We did not schedule any more blood transfusions but started roxadustat treatment. For the following three months, although the patient's hemoglobin still fluctuated around 60 g/L, he no longer relied on blood transfusions. During the whole treatment, the graft function of the patient remained stable with serum creatinine level around 120-140umol/L, and no acute rejection or severe infection was occurred except a mild urinary tract infection and a herpes zoster infection.

Discussion

The main treatments for anti-EPO antibody-mediated PRCA include immediate cessation of rHuEPO, restrictive transfusion and immunosuppressive therapies (8). However, long-term blood transfusions are resource-consuming and may increase the risk of infection and antibody development. Kidney transplant appears to be a viable option for ESRD patients with PRCA (9). There may be antigenic differences between endogenous and exogenous erythropoietin, and kidney transplantation can inhibit the production of antibodies and restore EPO secretion from the transplanted kidney (10, 11). A retrospective study collected anti-EPO antibody-mediated PRCA cases in French and German from 1998 to 2003, which found that there were 6 cases in total and they all got recovered one month after undergoing kidney transplant (6). We also reviewed other case reports published afterward and found that 6 (85.7%) out of 7 ESRD cases with anti-EPO antibody-mediated PRCA got recovered with Hb levels above 100 g/L within 3 months after kidney transplantation (12–15). Only one case reported partial recovery at 28 months after transplantation with persistent anti-EPO antibodies but independent of blood transfusion (13). The clinical characteristics of 13 reported cases of anti-rHuEPO antibody-mediated PRCA who underwent kidney transplant were summarized in Table 1. Unlike previous reports, anemia in our case did not recover quickly after kidney transplant and intense immunosuppressive regimen. Instead, the antibodies disappeared after plasmapheresis therapy and immunosuppressive regimen adjustment. Although the anemia in this case was not completely corrected, we still consider the treatment to be successful because of the negative antibody result, increased reticulocyte count and detectable EPO concentration.

The patient was diagnosed 1 month after kidney transplantation after identifying anti-EPO antibodies, which highlights the importance of the timely detection of anti-EPO antibodies in suspected patients (16). The timely diagnosis before renal transplant can not only prevent the accumulation of rHuEPO but also guide the selection of immunosuppressive agents for subsequent treatment. Current assays for anti-EPO antibody examination include radioimmunoprecipitation (RIP), enzyme linked immunosorbent assay (ELISA), surface plasmon resonance (BIAcore) and bioassays that measure the proliferation of EPO-dependent primary erythroid cells or cell lines. Characteristics of the four assays used to measure anti-EPO antibodies are shown in Table 2. No single assay can both detect and fully characterize the presence of Abs and determine their neutralizing capabilities of them. Each assay has its own particular level of sensitivity and specificity for detecting Ab isotypes or binding affinities. At least two assays must be used for the analysis of EPO Abs, one assay for confirming the existence of Abs and the other (a bioassay) to demonstrate the Abs' ability to inhibit the biological activity of epoetin in living cells. Various laboratories have used different assays for detecting anti-EPO Abs. Due to the lack of standardized processes and reagents, it is difficult to compare the test results from different laboratories directly. In addition, laboratories capable of carrying out such tests were quite few, which leads to the extremely long turn-around-time for the anti-EPO antibody detection. Only a few previous cases have reported antibody titer monitoring during treatment with sophisticated bioassay methods. We recommended the aforementioned simple mixing test for the diagnosis and therapeutic monitoring of PRCA mediated by anti-EPO antibodies. Our simple mixing test is time-and cost-effective, which can be used for rapid differential diagnosis and timely therapeutic effect evaluation.

In this case, a large number of antibodies were removed from a titer of 1:720 to 1:30 after 6 rounds of plasmapheresis. To protect the graft kidney function, preventing the production of EPO-neutralizing antibodies and eliminating residual antibodies

TABLE 1 Clinical characteristics of 13 reported cases of anti-rHuEPO antibody-mediated PRCA who underwent kidney transplantation.

Case reports	Age (y)/ sex	Primary disease	Forms of rHuEPO given	Time from rHuEPO treatment to PRCA occurrence	Mean weekly dose	Diag-nosis before KT	Treatment before KT for PRCA	Induction therapy	Donor type	Immunosu-ppressive regi-mens after KT	Outcome		
											Hb (g/ L)	EPO-Ab	Time from KT to recovery
Verhelst et al., 2004 (6) *	NA	NA	NA	NA	NA	Yes	NA	IL-2 receptor antagonists or antilymphocyte globulins	NA	Tac or CsA, MMF, steroid	NA	NA	within 1 month
Kitpermkiat et al., 2022 (12)	46/F	LN	CERA, Biosimilar Retacrit® (alpha)	21 months	7200 IU	Yes	None	Rituximab, DFPP, IVIG, ATG, Tac, MMF, steroid,	living-related donor (brother)	Tac, MMF, steroid	127	NA	3 months
Nigg et al., 2004 (13)	25/F	MPGN	Eprex® (alpha), Recormon® (beta)	9 months	7500-12000 IU; 7000-20000 IU	Yes	CsA, CTX, steroids, ATG, thymectomy	NA	living-related donor (sister)	CsA, MMF, steroid	63-75	positive	28 months (partial remission)
Snanoudj et al., 2004 (14)	15/M	drug-induced (cyclosporine)	Eprex® (alpha), Neorecormon® (beta)	10 months	2000-8000 IU	Yes	CsA, AZA, steroid for liver transplantation	ATG, steroid	cadaveric donor	Tac, MMF, steroid	120	negative	6 weeks
Praditpornsilpa et al., 2005 (15)	15/ NA	NA	alpha and beta rHuEPO	30 months	267 IU/kg	Yes	Decadurabolin, steroid, CTX	Daclizumab	cadaveric donor	CsA, AZA, steroid	over 100	negative	12 weeks
	44/ NA	NA	beta and alpha rHuEPO	14 months	267 IU/kg	Yes	None	Daclizumab	cadaveric donor	CsA, AZA, steroid	over 100	negative	8 weeks
	52/ NA	NA	beta rHuEPO	22 months	267 IU/kg	Yes	None	Daclizumab	cadaveric donor	CsA, AZA, steroid	over 100	negative	12 weeks
	53/ NA	NA	alpha rHuEPO	26 months	267 IU/kg	Yes	None	Daclizumab	cadaveric donor	CsA, AZA, steroid	over 100	negative	10 weeks

*The retrospective study concluded 6 cases in total. rHuEPO, recombinant human erythropoietin; PRCA, pure red cell aplasia; KT, kidney transplant; EPO-Ab, anti-EPO antibody; LN, lupus nephritis; CERA, continuous erythropoietin receptor activator; Tac, tacrolimus; MMF, mycophenolate mofetil; DFPP, double-filtration plasmapheresis; IVIG, intravenous immunoglobulin; ATG, anti-thymocyte globulin; MPGN, membranoproliferative glomerulonephritis; CsA, cyclosporin A; CTX, cyclophosphamide; AZA, azathioprine; NA, data not available.

10.3389/fimmu.2022.1049444

10.3389/fimmu.2022.1049444

TABLE 2 Characteristics of the four assays used to measure anti-EPO antibodies.

Reference	Assays	Detection principles	Type of Anti-EPO antibodies detected	Lower limit of sensitivity	Advantages	Disadvantages	Measures Ab isotypes	Measures Ab affinities
Swanson et al., 2004 (17)	ELISA (conventional)	Indirect enzyme-linked immunosorbent assay	IgG	78IU/mL	Short detection time	Low affinity antibodies may not be able to detect	Yes, in some cases	No
					Relatively easy to use in the laboratory	Relatively low specificity and sensitivity		
					Detection reagents and instruments are relatively cheap	Unable to detect anti-EPO antibody IgM Not conducive to early diagnosis of disease		
					High throughput analysis - commonly used as a "screening assay" for anti EPO antibody detection			
Shin et al., 2012 (18)	ELISA (bridging)	Bridging enzyme-linked immunosorbent assay	IgG	40IU/mL	Dual-arm binding improves specificity (anti-EPO antibody needs to be recognized twice/to be detected)	Requires expensive enzyme-labeled antigens	Yes, in some cases	No
						Unable to detect anti-EPO antibody IgM		
Casadevall et al., 2002 (19)	RIP	Radioimmunoprecipitation assay	IgG	0.2IU/mL	High sensitivity and specificity	Difficult to automate; low-throughput analysis	No	No
					High throughput analysis	Risk of radionuclide contamination		
						Low affinity antibodies may not be able to detect		
						Difficult to detect anti-EPO IgM antibodies		
Swanson et al., 2004 (17)	BIAcore	Biosensor Immunoassay, surface plasmon resonance	IgG, IgM, subtype of antibody	8-10IU/mL	Detects the concentration of anti-EPO antibody, measures the affinity of the antibody, and also determines the subtype of the antibody	Expensive special testing equipment Available only in a few high-tech laboratories	Yes	No
					Can detect "low affinity" antibodies	Antigen degradation may result in false negatives during the procedure		

(Continued)

TABLE 2 Continued

Reference	Assays	Detection principles	Type of Anti-EPO antibodies detected	Lower limit of sensitivity	Advantages	Disadvantages	Measures Ab isotypes	Measures Ab affinities
					High specificity	Less sensitivity		
Casadevall et al., 2002 (19)	Bioassay	*In vitro* bioassays that measure proliferation of EPO-dependent primary erythroid cells or cell lines	Not mentioned	1IU/mL	Functional analysis to differentiate antibodies with neutralizing potential The only test that demonstrates the ability of antibodies to neutralize endogenous EPO	Complicated operation and time-consuming Validation difficult	No	Yes

is essential. Therefore, we finally chose cyclosporine, sirolimus and prednisone for immunosuppressive treatment. After four-month treatment of the adjusted regimen, the antibody titer dropped to 1:1, the reticulocyte count began to rise, and the transfusion frequency began to drop. At the fifth month of the treatment, EPO could be detected in the patient's serum, and the reticulocyte count was higher than the normal range, indicating that the bone marrow began to restore hematopoiesis. To our knowledge, this was the first reported case of successful remission of persistent PRCA after kidney transplantation using such treatment regimen. Moreover, this patient's PRCA was refractory with an abnormally prolonged disease course. Recently, studies had recommended initial treatment, including cyclosporine or cyclophosphamide combined with prednisone in PRCA (9, 11, 20). Tacrolimus may be considered as a substitute for cyclosporine (21). Chen et al. also reported the therapeutic effect of sirolimus in PRCA patients with a complete response of 58.3% and a median time of 4 (1–7) months to achieve the optimal effect (22).

In addition, roxadustat is an oral hypoxia-inducible factor prolyl hydroxylase inhibitor that simulates intracellular hypoxia to promote the production of endogenous EPO. Successful treatment with roxadustat in anti-EPO antibody-mediated PRCA has been noted in some case reports (23–25). However, it was reported that anti-EPO antibodies were found in patients who had never received rHuEPO (26), indicating that endogenous EPO may also induce the development of autoantibodies. Therefore, considering the possible interference of roxadustat in antibody production and its limited therapeutic effect when massive anti-EPO antibodies still existed, we stopped roxadustat treatment when anti-EPO antibody titer increased dramatically in Sep 2021 and restarted roxadustat when anti-EPO antibodies were below the lower limit of detection in Mar 2022. Our result demonstrated the safety of roxadustat in PRCA because no reproduction of anti-EPO antibody was found after restarting roxadustat. However, the data of our patient did not show the effectiveness of roxadustat, which may be related to the short observation time.

In conclusion, we reported a case of anti-EPO antibody-mediated persistent PRCA after renal transplant. Cyclosporine, sirolimus and methylprednisolone could be considered as maintenance immunosuppressive regimen and washed red blood cells should be used instead of leukodepleted red blood cells if transfusion was needed. Plasmapheresis was useful when anti-EPO antibody titers reached quite high. We created a simple mixing test for anti-EPO antibody titer, which was helpful in dynamic antibody monitoring especially when the examination of anti-EPO antibodies with RIPA, ELISA or biosensor assay was not available.

Data availability statement

The raw data supporting the conclusions of this article will be made available by the authors, without undue reservation.

Ethics statement

The studies involving human participants were reviewed and approved by Committee on Medical Ethics of West China Hospital, Sichuan University. The patients/participants provided their written informed consent to participate in this study. Written informed consent was obtained from the individual(s) for the publication of any potentially identifiable images or data included in this article.

Author contributions

The original manuscript was written by HL and X-MC and reviewed by Y-YS, Y-JB, L-LW and YW, while YW and Y-YS

participated in the treatments for the patients. The test for anti-EPO antibodies were conducted by X-MC and Y-JB. All authors contributed to the article and approved the submitted version.

Funding

Supported by 1·3·5 project for disciplines of excellence Clinical Research Incubation Project, West China Hospital, Sichuan University (ZYJC18004).

Conflict of interest

The authors declare that the research was conducted in the absence of any commercial or financial relationships that could be construed as a potential conflict of interest.

Publisher's note

Supplementary material

The Supplementary Material for this article can be found online at: https://www.frontiersin.org/articles/10.3389/fimmu.2022.1049444/full#supplementary-material

SUPPLEMENTARY FIGURE 1
The flow chart of experiment

References

1. McKoy JM, Stonecash RE, Cournoyer D, Rossert J, Nissenson AR, Raisch DW, et al. Epoetin-associated pure red cell aplasia: Past, present, and future considerations. *Transfusion* (2008) 48(8):1754–62. doi: 10.1111/j.1537-2995.2008.01749.x

2. Casadevall N. Antibodies against rhuepo: Native and recombinant. *Nephrol Dialysis Transplant* (2002) 17(suppl_5):42–7.

3. Means RTJr. Pure red cell aplasia. *Blood* (2016) 128(21):2504–9. doi: 10.1182/blood-2016-05-717140

4. Boven K, Knight J, Bader F, Rossert J, Eckardt KU, Casadevall N. Epoetin-associated pure red cell aplasia in patients with chronic kidney disease: Solving the mystery. *Nephrol Dial Transplant* (2005) 20 Suppl 3:iii33–40. doi: 10.1093/ndt/gfh1072

5. Bennett CL, Luminari S, Nissenson AR, Tallman MS, Klinge SA, McWilliams N, et al. Pure red-cell aplasia and epoetin therapy. *N Engl J Med* (2004) 351:1403–8. doi: 10.1056/NEJMoa040528

6. Verhelst D, Rossert J, Casadevall N, Krüger A, Eckardt KU, Macdougall IC. Treatment of erythropoietin-induced pure red cell aplasia: A retrospective study. *Lancet (London England)* (2004) 363(9423):1768–71. doi: 10.1016/s0140-6736(04)16302-2

7. Dameshek W, Neber J. Transfusion reactions to plasma constituent of whole blood; their pathogenesis and treatment by washed red blood cell transfusions. *Blood* (1950) 5(2):129–47. doi: 10.1182/blood.V5.2.129.129

8. Sawada K, Fujishima N, Hirokawa M. Acquired pure red cell aplasia: Updated review of treatment. *Br J Haematology* (2008) 142(4):505–14. doi: 10.1111/j.1365-2141.2008.07216.x

9. Rossert J, Macdougall I, Casadevall N. Antibody-mediated pure red cell aplasia (Prca) treatment and re-treatment: Multiple options. *Nephrol Dial Transplant* (2005) 20 Suppl 4:iv23–6. doi: 10.1093/ndt/gfh1090

10. Shingu Y, Nakata T, Sawai S, Tanaka H, Asai O, Tamagaki K, et al. Antibody-mediated pure red cell aplasia related with epoetin-beta pegol (C.E.R.A.) as an erythropoietic agent: Case report of a dialysis patient. *BMC Nephrol* (2020) 21(1):275. doi: 10.1186/s12882-020-01934-2

11. Bennett CL, Cournoyer D, Carson KR, Rossert J, Luminari S, Evens AM, et al. Long-term outcome of individuals with pure red cell aplasia and antierythropoietin antibodies in patients treated with recombinant epoetin: A follow-up report from the research on adverse drug events and reports (Radar) project. *Blood* (2005) 106(10):3343–7. doi: 10.1182/blood-2005-02-0508

12. Kitpermkiat R, Thotsiri S, Arpornsujaritkun N, Sangkum P, Chantrathammachart P, Kitpoka P, et al. A 46-Year-Old Thai woman with secondary acquired pure red cell aplasia due to treatment with recombinant erythropoietin while on dialysis for end-stage renal disease who recovered following abo-incompatible kidney transplantation. *Am J Case Rep* (2022) 23:e935451. doi: 10.12659/ajcr.935451

13. Nigg L, Schanz U, Ambühl PM, Fehr J, Bachli EB. Prolonged course of pure red cell aplasia after erythropoietin therapy. *Eur J Haematology* (2004) 73(5):376–9. doi: 10.1111/j.1600-0609.2004.00317.x

14. Snanoudj R, Beaudreuil S, Arzouk N, Jacq D, Casadevall N, Charpentier B, et al. Recovery from pure red cell aplasia caused by anti-erythropoietin antibodies after kidney transplantation. *Am J Transplant Off J Am Soc Transplant Am Soc Transplant Surgeons* (2004) 4(2):274–7. doi: 10.1046/j.1600-6143.2003.00297.x

15. Praditpornsilpa K, Buranasot S, Bhokaisuwan N, Avihingsanon Y, Pisitkul T, Kansanabuch T, et al. Recovery from anti-Recombinant-Human-Erythropoietin associated pure red cell aplasia in end-stage renal disease patients after renal transplantation. *Nephrology dialysis Transplant Off Publ Eur Dialysis Transplant Assoc - Eur Renal Assoc* (2005) 20(3):626–30. doi: 10.1093/ndt/gfh666

16. KDIGO Clinical Practice Guideline Working Group. Chapter 1: Diagnosis and evaluation of anemia in ckd. *Kidney Int Suppl (2011)* (2012) 2(4):288–91. doi: 10.1038/kisup.2012.33

17. Swanson SJ, Ferbas J, Mayeux P, Casadevall N. Evaluation of methods to detect and characterize antibodies against recombinant human erythropoietin. *Nephron Clin Pract* (2004) 96(3):c88–95. doi: 10.1159/000076746

18. Shin SK, Moon SJ, Ha SK, Jo YI, Lee TW, Lee YS, et al. Immunogenicity of recombinant human erythropoietin in Korea: A two-year cross-sectional study. *Biologicals J Int Assoc Biol Standardization* (2012) 40(4):254–61. doi: 10.1016/j.biologicals.2012.02.003

19. Casadevall N, Nataf J, Viron B, Kolta A, Kiladjian JJ, Martin-Dupont P, et al. Pure red-cell aplasia and antierythropoietin antibodies in patients treated with recombinant erythropoietin. *New Engl J Med* (2002) 346(7):469–75. doi: 10.1056/NEJMoa011931

20. Gurnari C, Maciejewski JP. How I manage acquired pure red cell aplasia in adults. *Blood* (2021) 137(15):2001–9. doi: 10.1182/blood.2021010898

21. Hashimoto K, Harada M, Kamijo Y. Pure red cell aplasia induced by anti-erythropoietin antibodies, well-controlled with tacrolimus. *Int J Hematol* (2016) 104(4):502–5. doi: 10.1007/s12185-016-2047-6

22. Chen Z, Liu X, Chen M, Yang C, Han B. Successful sirolimus treatment of patients with pure red cell aplasia complicated with renal insufficiency. *Ann Hematol* (2020) 99(4):737–41. doi: 10.1007/s00277-020-03946-2

23. Cai KD, Zhu BX, Lin HX, Luo Q. Successful application of roxadustat in the treatment of patients with anti-erythropoietin antibody-mediated renal anaemia: A case report and literature review. *J Int Med Res* (2021) 49(4):3000605211005984. doi: 10.1177/03000605211005984

24. Wu R, Peng Y. Roxadustat on anti-erythropoietin antibody-related pure red cell aplasia in the patient with end-stage renal disease. *Semin Dial* (2021) 34(4):319–22. doi: 10.1111/sdi.12991

25. Xu B, Liu S, Li Y, Zhao L, Song X, Chen T. Roxadustat in the treatment of a hemodialysis patient with anti-erythropoietin antibody-mediated pure red cell aplasia. *Clin Kidney J* (2021) 14(11):2444–5. doi: 10.1093/ckj/sfab134

26. Casadevall N, Dupuy E, Molho-Sabatier P, Tobelem G, Varet B, Mayeux P. Autoantibodies against erythropoietin in a patient with pure red-cell aplasia. *N Engl J Med* (1996) 334(10):630–3. doi: 10.1056/nejm199603073341004

frontiers | Frontiers in Immunology

TYPE Review
PUBLISHED 01 February 2023
DOI 10.3389/fimmu.2023.1113560

OPEN ACCESS

EDITED BY
Liping Li,
Geisinger Medical Center, United States

REVIEWED BY
Yongbing Qian,
Shanghai Jiao Tong University, China
Zhiao Chen,
Fudan University, China

*CORRESPONDENCE
Min-Jie Ju
ju.minjie@zs-hospital.sh.cn
Zhe Luo
luo.zhe@zs-hospital.sh.cn

†These authors have contributed equally to this work

SPECIALTY SECTION
This article was submitted to Alloimmunity and Transplantation, a section of the journal Frontiers in Immunology

RECEIVED 01 December 2022
ACCEPTED 09 January 2023
PUBLISHED 01 February 2023

CITATION
Huang D-L, He Y-R, Liu Y-J, He H-Y, Gu Z-Y, Liu Y-M, Liu W-J, Luo Z and Ju M-J (2023) The immunomodulation role of Th17 and Treg in renal transplantation. *Front. Immunol.* 14:1113560. doi: 10.3389/fimmu.2023.1113560

The immunomodulation role of Th17 and Treg in renal transplantation

Dan-Lei Huang[1†], Yi-Ran He[1†], Yu-Jing Liu[2†], Hong-Yu He[1], Zhun-Yong Gu[3], Yi-Mei Liu[1], Wen-Jun Liu[1], Zhe Luo[1*] and Min-Jie Ju[1*]

[1]Department of Critical Care Medicine, Zhongshan Hospital, Fudan University, Shanghai, China, [2]Department of Nursing, Zhongshan Hospital, Fudan University, Shanghai, China, [3]Department of Urinary Surgery, Zhongshan Hospital, Fudan University, Shanghai, China

Kidney transplantation (KT) is an ultimate treatment of end-stage chronic kidney disease, which can meet a lot of complications induced by immune system. With under-controlled immunosuppression, the patient will obtain a good prognosis. Otherwise, allograft disfunction will cause severe organ failure and even immune collapse. Acute or chronic allograft dysfunction after KT is related to Th17, Treg, and Th17/Treg to a certain extent. Elevated Th17 levels may lead to acute rejection or chronic allograft dysfunction. Treg mainly plays a protective role on allografts by regulating immune response. The imbalance of the two may further aggravate the balance of immune response and damage the allograft. Controlling Th17 level, improving Treg function and level, and adjusting Th17/Treg ratio may have positive effects on longer allograft survival and better prognosis of receptors.

KEYWORDS

renal transplantation, T cell, Th17, Treg, Th17/Treg

Introduction

Kidney transplantation (KT), as the ultimate treatment of end-stage chronic kidney disease (CKD) (1), same as other solid organ transplantation, can meet a lot of complications induced by immune system. Once immunosuppression is under control, with allograft functioning well, the patient will achieve a relatively high quality of life. Otherwise, allograft disfunction will cause severe organ failure and even immune collapse.

The most valuable evaluation index after renal transplantation is renal function. Routine assessment of graft function usually includes monitoring of serum creatinine levels and screening for proteinuria. Sometimes, allograft biopsy may be required to clarify the abnormality of kidney function. Various immune mechanisms may cause abnormal renal function after renal transplantation. Acute or chronic rejection of allograft may be mediated by T cells, and T-cell–mediated rejection (TCMR) remains a major obstacle to the long-term survival of kidney transplant patients (1–3). It is reported that Th1/Th2 balance is thought to be the main mechanism of rejection (4) However, certain immune events occurring after KT cannot be explained by Th1/Th2 balance alone.

Multiple functions of T cells had been approximately classified into coordinators [i.e., T helper (Th) cells and regulatory T cells (Tregs)] and effectors (i.e., cytotoxic T cells) (5, 6). Th17 cells were first reported in the mechanism of autoimmune diseases, as the additional subsets of Th1 and Th2, and its related cytokines also play an important role in the occurrence of acute and chronic allograft injury after organ transplantation (7, 8). Treg has been confirmed to play a role in regulating tolerance and rejection in animal models of solid organ transplantation (9). Signaling cells can induce T cell differentiate from naïve T cell by secreting kinds of cytokines, a correlation of different subtypes can also affect the procedure, and multiple discovered or undiscovered mechanisms help to maintaining the balance of T-cell–associated immunity. However, changes in the proportions of T-cell subtypes can be observed in renal allograft rejection (4, 10).

In this review, we will briefly describe the differentiation of Th17 and Treg and narrate the relevance between Th17 and Treg. Last, we will discuss the relationship between renal allograft rejection and Th17, Treg, Th17/Treg imbalance, and some possible immunosuppression treatment aimed at them.

Differentiation of Th17 and Treg

Th17

Th17 cells are T helper cells that express retinoic acid receptor-related orphan receptor γt (RORγt) and secrete interleukin-17A (IL-17A) and IL-17F cytokine. In the peripheral blood, Th17 was discovered and owned its name because of IL-17, which is the characteristic cytokine of it (11). IL-17 induces a powerful proinflammatory response by stimulating secretion of proinflammatory molecules by combining ubiquitous IL-17 receptor on epithelial cells, endothelial cells, monocytes, and macrophages (12).

IL-6 and transforming growth factor–β (TGF-β) are the critical cytokines for Th17 differentiation, and there are three possible stages of Th17 differentiation in mice: first, combined effect of TGF-β and IL-6/IL-21 triggers differentiation of Th17 cells; then, IL-21 secreted by Th17 cells and TGF-β induced amplification of Th17 cell themselves; and, finally, IL-23 stabilizes Th17 cells (13). Combination of TGF-β and IL-21 has been shown to be sufficient to induce the differentiation of human Th17 cells from immature T cells; meanwhile, IL-1β and IL-6 are important for enhancing the differentiation and memory expansion of Th17 cells (14). Tumor necrosis factor-α (TNF-α) plays an accessory role in Th17 differentiation (15). Signal transducer and activator of transcription 3 (STAT3) plays a key role in positive regulation the differentiation of Th17. After being activated by cytokines such as IL-6, IL-21, IL-23, TNF-α, and TGF-β, STAT3 can upregulate RORγt and promote the differentiation of Th17 (16).

Four distinct mechanisms are described in inhibiting Th17 differentiation: IL-13 can decrease the production of IL-17 by stimulating Th17 cells to produce IL-10, which results in the downregulation of IL-6 (17); IL-27 and IFN-γ through STAT1 activation (12, 18); IL-2 and IL-4 through STAT5 activation (19); and the inhibition of RORγt by Foxp3 (20). Few STAT family members are involved in regulation of Th17 differentiation mediated through some cytokines (16, 18). IL-27, IL-13, and IFN-γ are responsible for inhibiting Th17 development in a STAT1-dependent manner (16, 18, 21, 22). IL-2 also participates in negative regulation of Th17 differentiation through STAT5 (19).

Th17 cells are involved in a variety of autoimmune diseases, including psoriasis, rheumatoid arthritis, inflammatory bowel disease, and multiple sclerosis (23, 24). Meanwhile, Th17 cells can also defend extracellular pathogens, including fungi and bacteria, colonizing the mucosal surface (25). It has been reported that Th17 deficiency can be associated with fungi co-infection, immunoparalysis development, and increased mortality (26–28).

Tregs

Tregs, either originating from the thymus [natural (n)Treg] or induced peripherally by antigen exposure and cytokines [induced (i) Treg], are CD25+ CD4+ Foxp3+ T cells, continuously expressing cytotoxic T-lymphocyte–associated protein-4 or CD152 and glucocorticoid-inducible tumor necrosis factor receptor (29, 30). Tregs characteristically express Foxp3 and are major immunoregulatory cells with an ability to suppress exaggerated pro-inflammatory action of effector T cells (i.e., activated Th1, Th2, Th3, Th9, Th17, and cytotoxic T cells) (31).

Tregs function by producing the inhibitory cytokines IL-10 and TGF-β (32, 33), interfering with T-cell survival through IL-2 depletion (34), and secreting molecules that directly eliminate effector cells and inhibit antigen-presenting cell maturation and functionality (34, 35). It means that Tregs may show an antagonistic effect against Th17 in an immune response dysregulation individual. TGF-β also plays an important role in the differentiation of Tregs through the induction of STAT5 transcription factor (36). Then, IL-2, through the induction of transcription factor STAT5, and retinoic acid further enhanced the differentiation toward Treg subset (37). In turn, STAT5 will enhance Foxp3 expression. Whereas, retinoic acid can promote TGF-β signaling and Foxp3 promoter activity and can inhibit Th17 differentiation by blocking IL-6 signaling simultaneously (38). IL-10 also plays a part in promoting differentiation of Tregs (39).

It is worth mentioning that, although knockdown of Foxp3 can significantly inhibit Treg function, because Foxp3 is induced upon TCR stimulation, it is possible that Foxp3 expression is not an ideal marker for human Tregs (40). Several lines of evidence suggest that the combination of CD4 and CD25 and the low expression of CD127 identify a subset of peripheral blood T cells, which are highly suppressive in functional assays and are the highest expression of FoxP3, suggesting that the IL-7 receptor (CD127) may be a better biomarker for human Treg (41).

Th17/Treg

Because it has been described that Foxp3 can inhibit RORγt function that turns out to reduce Th17 cell differentiation (20),

substantiating the balance between Foxp3 and RORγt is therefore a very important factor in the Th17/Treg balance. Although TGF-β can induce the development of both Tregs and Th17 cell from naïve T cells, Foxp3, induced by TGF-β as well, inhibits Th17 cell differentiation by inhibiting RORγt function when other inflammatory factors are absent (20). TGF-β–induced Foxp3 expression is inhibited by IL-6 (42), IL-21 (43), and IL-23 (20). IL-6 acts as proinflammatory cytokine in T cells by promoting Th17 differentiation and inhibiting Treg differentiation to regulate the balance between Th17 and Treg (18). Figure 1 shows some important mechanisms in the differentiation process of Treg and Th17, as well as the interaction between Th17 and Treg.

Because Th17 and Tregs play the opposite roles in the immune response and maintain a medium stage of immune activation, which is neither hyperactivation of immune response nor immunosuppression, Th17/Treg imbalance may produce a marked effect in immune dysfunction.

Relationship between Th17, Treg, and KT

Th17 and KT

In allograft rejection and dysfunction, it is important to identify the main causes of graft rejection due to the complexity and diversity of mechanisms. Th17 is now known to play a role in both acute allograft rejection and chronic allograft dysfunction.

Some studies have suggested that causes such as ischemia/reperfusion that occurs during transplantation, as well as collagen exposure (Col V), may promote the differentiation of naïve T cells into Th17 under conditions of low levels of TGF-β1 and high levels of IL-6. In addition, Col V is more expressed in bronchial and alveolar tissues. It is assumed that Th17 anti–Col V cell-mediated immunity may be related to graft rejection in lung transplantation (44).

IL-17, an important cytokine secreted by Th17, was found to have increased local expression in graft rejection. In addition, increased infiltration of Th17 cells was significantly associated with incomplete recovery, recurrent TCMR, steroid-resistant rejection, and lower graft survival after rejection (45). Several hypotheses have been proposed. The secretion of IL-17 by Th17 plays a role in the recruitment of neutrophils (46). At the same time, renal epithelial cells exposed to IL-17 produce inflammatory mediators and stimulate the early alloimmune response (47). Th17 cells can also further drive the alloimmune response by promoting lymphoid regeneration (7). Thus, it is assumed that Th17 cells induce a stronger and more durable alloimmune response and result in severe graft tissue damage.

IL-17 induces IL-6, IL-8, monocyte chemoattractant protein-1 (MCP-1), and complement component C3 through the src/mitogen-activated protein kinase pathway (48). In addition, IL-17 exerts its effects through the synergistic interaction with cd40 ligand and the activation of nuclear factor–κB (49).

In the heart transplantation model, antagonism of the IL-17 network (through expression of the IL-17R-immunoglobulin fusion protein) reduced the production of an intra-graft inflammatory cytokine (i.e., IFN-γ) and prolonged graft survival (50).

Studies have found that the Th17 levels in patients who develop CKD after KT are higher than that in patients with normal renal function who undergone KT. In addition, Th17 levels in patients with CKD who have not undergone KT are also lower than those after KT, suggesting that immune response is the cause of the development of CKD after transplantation (45, 51). Retrospective studies have found that the increase in the proportion of Th17 cells is consistent with the increase in the rate of graft failure (52). In addition, Th17 infiltration of allograft has a certain indicator effect on transplantation prognosis and anti-rejection response (53).

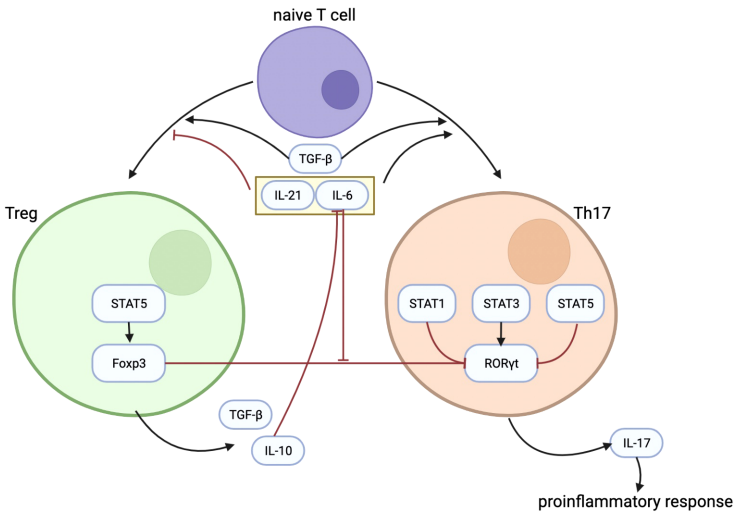

FIGURE 1
The figure shows some important mechanisms in the differentiation process of Treg and Th17, as well as the interaction between them. TGF-β plays an important role in the differentiation of Treg and Th17. IL-21 and IL-6 could inhibit the differentiation of Treg while promoting the differentiation of Th17. IL-10 secreted by Treg can inhibit the effect of IL-6. Treg regulates Th17 differentiation through the inhibitory effect of Foxp3 on RORγt, and the inhibitory effect of Foxp3 on RORγt is inhibited by IL-6. Treg, regulatory T cells; Th17, T helper cells 17; TGF-β, transforming growth factor–β; IL-21, interleukin-21; IL-6, interleukin-6; IL-10, interleukin-10; Foxp3, forkhead box protein 3; RORγt, receptor-related orphan receptor γt.

Treg and KT

Treg is considered as an important part in inhibiting activated T-cell function and regulating immunity. The main mechanisms are separated into two types: contact-dependent mechanisms that are dependent on the intercellular receptor and ligand contact, and contact-independent mechanisms that function on the secretion of cytokines (54). It is generally assumed that Tregs act by direct contact with cells, mediated by other active cells or by IFN-γ (55). *In vitro*, Tregs have the ability to inhibit the proliferation and cytokine production of responsive (CD4+ CD25− and CD8+) T cells and downregulate the responses of CD8+ T cells, NK cells, and CD4+ cells to specific antigens (56, 57). *In vivo*, it can play a role in preventing graft rejection (58).

On the basis of the effects of Th1, Th2, and Th17 on the rejection and dysfunction of solid transplanted organs, and the inhibitory effect of Treg on the above cells and their related immune responses, it can be assumed that the increase of Treg level has a certain protective effect on the transplanted organs.

Although the specific mechanism of Treg in promoting human organ transplantation tolerance in terms is unclear, Treg level has an obvious correlation with allograft survival rate (59), and cardiac transplantation related study has found that the local and total Treg and iTreg level is negatively related to the incidence of allograft rejection present (60), prompting that Treg may play a positive role in graft tolerance. In addition, some studies have found that FOXP3 gene hypomethylation may be used as a marker of the percentage of infiltrated Treg in the graft to predict the incidence of rejection events after the suppression of solid organs (61).

Th17/Treg and KT

As mentioned above, because the changes in the Th17 and Treg levels are related to the occurrence of renal rejection after KT, and on the basis of the interaction between Th17 and Treg, the ratio of local infiltration of Th17/Treg and the balance of Th17/Treg are also theoretically related to transplant organ rejection.

It has been suggested that kidney perfusate–derived extracellular vesicles (KP-EVs) released in allografts may signal the degree of ischemic stress and are considered playing an important role in the development of anti-donor immunity (62, 63). *In vitro* studies confirmed that stimulation of peripheral blood monocytes in this KP-EV environment resulted in a significant reduction in the proportion of Tregs, accompanied by an increase in the Th17/Treg ratio. The expression of miR-218-5p KP-EV increased in allograft of patients with chronic graft rejection. MiR-218-5p KP-EV may participate in the immune process and become a key regulator of T-cell activation through molecular processes, and its expression may be related to the change of Th17/Treg ratio (64).

Some studies have indicated that the imbalance of T-cell subtype proportion is related to the occurrence of CKD in patients after renal transplantation. Compared with normal and mild functional decline individuals, patients with significantly decreased renal function after KT have higher Th17 local infiltration and lower Treg local infiltration of allograft (10). Study has also confirmed that a higher Th17/Treg rate of infiltration in allografts is significantly correlated with decreased allograft function and more grievous interstitial and tubular injury (65).

Immunosuppression treatment aimed at Th17, Treg, and Th17/Treg

Th17-related immunosuppression treatment

T cells are inhibited by a combination of tacrolimus (Tac), mycophenolate, and steroids. In addition, induction therapy with the anti-CD25 monoclonal antibody Basiliximab can also inhibit the proliferation of t cells (66). Even if the short-term use of immunosuppressive therapy can avoid most short-term allograft rejection after KT, the long-term prognosis improvement is not ideal (67), suggesting that the current immunosuppressive therapy still has some limitations. Local infiltration of Th17 may lead to chronic allograft dysfunction, and some Th17-inhibiting drugs may be helpful for treatment.

Mammalian target of rapamycin (mTOR) plays an important role in T-cell differentiation, and inhibitors that limit its effect may be beneficial to patients after transplantation. Sirolimus (SRL) has been shown to reduce Th17 levels in patients after renal transplantation. Treatment with SRL instead of Tac can effectively control Th17 levels (68).

1α,25-Dihydroxyvitamin D3 combined with Tac can also play a role in regulating Th17 levels. It has been reported that the combination of the two can significantly inhibit peripheral Th17 and reduce IL-17 and IL-22 levels (69).

Treg in post-transplantation treatment

The role of Treg in the recovery of patients after KT may mainly lie in several points, promote the recovery of ischemia-reperfusion of transplanted kidney (54), negatively regulate a series of pro-inflammatory factors produced by effector T cells (70), and adjust the level of donor-specific antibodies to regulate humoral immunity (71).

Although part of the immune treatment medicine may play a role in immunosuppression, the limitation is that they may inhibit Treg level (72–75). Therefore, improving the level of Treg in the human body is a kind of auxiliary treatment idea, and achieving this goal means that there are two main methods: (1) Promote Treg proliferation and differentiation endogenously; (2) extract Treg and proliferate *in vitro* and back transfusion.

To promote the proliferation and differentiation of Treg, several drugs have attracted the attention of researchers. In addition to inhibiting Th17 proliferation, mTOR inhibitors can also promote the proliferation and differentiation of Treg (76). The use of alenzumab has also been shown to lead to the production/expansion of Treg (77). Erythropoietin can inhibit the proliferation of other effector T cells while preserving the proliferation of Treg (78). Finally, low-dose recombinant IL-2 is considered as a potential means to enlarge Treg (79).

At present, a series of trials are being conducted for adoptive Treg transplantation in renal transplantation patients. The main technical difficulties lie in how to perform stable and effective amplification after extraction, how to enhance the stability of *in vitro* induced Treg effect, and how to produce specificity for alloantigens during amplification, so as to finally achieve reliable therapeutic effect (54).

Treatment regulation of Th17/Treg

The changes in Th17 and Treg levels and the imbalance of the two subtypes are related to the allograft dysfunction after KT (10, 65). Adjusting the level of one subtype alone may aggravate the imbalance of the ratio. Therefore, regulating the ratio of the two may also become the research direction of immunosuppression therapy. Currently, there are limited studies on Th17/Treg ratio after renal transplantation as a therapeutic target. However, studies have found that thymoglobulin induction therapy is beneficial to change the ratio of T effector and Treg (80, 81). *In vivo* studies have shown that bortezomib can increase the number of Tregs, can significantly reduce the proportion of Th17 cells, and can also improve renal function and graft survival (82). In rats after KT under carbamylated erythropoietin (CEPO) treatment, it was found that CEPO significantly extended the survival time of the allograft, and flow cytometry showed that Th17/Treg ratio decreased significantly (83). These results indicate that effective treatment can prolong the survival time of kidney grafts, accompanied by the improvement of Th17/Treg ratio.

In recent years, mesenchymal stem cells (MSCs) have attracted more and more attention in the treatment of autoimmune diseases, especially systemic lipus erythematosus (SLE). This therapy can promote the proliferation of Th2 and Tregs; inhibit the activities of Th1, Th17, and B cells; improve the Th17/Treg ratio; and finally improve the signs and symptoms of refractory SLE (84). From the mechanistic point of view, although this kind of cell therapy in patients after transplantation still needs further study support, we can consider MSCs as a potential development direction.

Conclusions

Acute or chronic allograft dysfunction after KT is related to Th17, Treg, and Th17/Treg to a certain extent. Elevated Th17 levels may lead to acute rejection or chronic allograft dysfunction. Treg mainly plays a protective role on allografts by regulating immune response. The imbalance of the two may further aggravate the balance of immune response and damage the allograft. Controlling Th17 level, improving Treg function and level, and adjusting Th17/Treg ratio may have positive effects on longer allograft survival and better prognosis of receptors.

Author contributions

Work concept: D-LH, ZL, and M-JJ; Literature collection: D-LH, Y-RH, Y-JL, H-YH, Z-YG, Y-ML, and W-JL; Article writing: D-LH; Mistake correction: D-LH, Y-RH, ZL, and M-JJ; Writing guidance: ZL and M-JJ. All authors contributed to the article and approved the submitted version.

Funding

This work was supported by the Clinical Research Plan of SHDC (grant number SHDC2020CR4067) and by the Shanghai Science and Technology Commission (grant numbers 20S31905300 and 20Y11900900).

Conflict of interest

The authors declare that the research was conducted in the absence of any commercial or financial relationships that could be construed as a potential conflict of interest.

The reviewer ZC declared a shared parent affiliation with the authors to the handling editor at the time of the review.

Publisher's note

References

1. Suthanthiran M, Strom TB. Renal transplantation. *N Engl J Med* (1994) 331(6):365–76. doi: 10.1056/NEJM199408113310606

2. Wu O, Levy AR, Briggs A, Lewis G, Jardine A. Acute rejection and chronic nephropathy: a systematic review of the literature. *Transplantation* (2009) 87(9):1330–9. doi: 10.1097/TP.0b013e3181a236e0

3. Zhang Y, Yang Y, Li X, Chen D, Tang G, Men T. Thalidomide ameliorate graft chronic rejection in an allogenic kidney transplant model. *Int Immunopharmacol* (2019) 71:32–9. doi: 10.1016/j.intimp.2018.12.035

4. Liu Z, Fan H, Jiang S. CD4(+) T-cell subsets in transplantation. *Immunol Rev* (2013) 252(1):183–91. doi: 10.1111/imr.12038

5. Juno JA, van Bockel D, Kent SJ, Kelleher AD, Zaunders JJ, Munier CM. Cytotoxic CD4 T cells-friend or foe during viral infection? *Front Immunol* (2017) 8:19. doi: 10.3389/fimmu.2017.00019

6. Rabb H. The T cell as a bridge between innate and adaptive immune systems: Implications for the kidney. *Kidney Int* (2002) 61(6):1935–46. doi: 10.1046/j.1523-1755.2002.00378.x

7. Deteix C, Attuil-Audenis V, Duthey A, Patey N, McGregor B, Dubois V, et al. Intragraft Th17 infiltrate promotes lymphoid neogenesis and hastens clinical chronic rejection. *J Immunol* (2010) 184(9):5344–51. doi: 10.4049/jimmunol.0902999

8. Mitchell P, Afzali B, Lombardi G, Lechler RI. The T helper 17-regulatory T cell axis in transplant rejection and tolerance. *Curr Opin Organ Transplant* (2009) 14(4):326–31. doi: 10.1097/MOT.0b013e32832ce88e

9. Duran-Struuck R, Sondermeijer HP, Buhler L, Alonso-Guallart P, Zitsman J, Kato Y., et al. Effect of ex vivo-expanded recipient regulatory T cells on hematopoietic chimerism and kidney allograft tolerance across MHC barriers in cynomolgus macaques. *Transplantation* (2017) 101(2):274–83. doi: 10.1097/TP.0000000000001559

10. Ma L, Zhang H, Hu K, Lv G, Fu Y, Ayana D.A., et al. The imbalance between tregs, Th17 cells and inflammatory cytokines among renal transplant recipients. *BMC Immunol* (2015) 16:56. doi: 10.1186/s12865-015-0118-8

11. Bettelli E, Korn T, Oukka M, Kuchroo VK. Induction and effector functions of T (H)17 cells. *Nature* (2008) 453(7198):1051–7. doi: 10.1038/nature07036

12. Awasthi A, Kuchroo VK. Th17 cells: from precursors to players in inflammation and infection. *Int Immunol* (2009) 21(5):489–98. doi: 10.1093/intimm/dxp021

13. Korn T, Bettelli E, Oukka M, Kuchroo VK. IL-17 and Th17 cells. *Annu Rev Immunol* (2009) 27:485–517. doi: 10.1146/annurev.immunol.021908.132710

14. Yang L, Anderson DE, Baecher-Allan C, Hastings WD, Bettelli E, Oukka M, et al. IL-21 and TGF-beta are required for differentiation of human T(H)17 cells. *Nature* (2008) 454(7202):350–2. doi: 10.1038/nature07021

15. Veldhoen M, Hocking RJ, Atkins CJ, Locksley RM, Stockinger B. TGFbeta in the context of an inflammatory cytokine milieu supports *de novo* differentiation of IL-17-producing T cells. *Immunity* (2006) 24(2):179–89. doi: 10.1016/j.immuni.2006.01.001

16. Mangodt TC, Van Herck MA, Nullens S, Ramet J, De Dooy JJ, Jorens PJ, et al. The role of Th17 and treg responses in the pathogenesis of RSV infection. *Pediatr Res* (2015) 78(5):483–91. doi: 10.1038/pr.2015.143

17. Newcomb DC, Boswell MG, Huckabee MM, Goleniewska K, Dulek DE, Reiss S, et al. IL-13 regulates Th17 secretion of IL-17A in an IL-10-dependent manner. *J Immunol* (2012) 188(3):1027–35. doi: 10.4049/jimmunol.1102216

18. Kimura A, Kishimoto T. IL-6: regulator of Treg/Th17 balance. *Eur J Immunol* (2010) 40(7):1830–5. doi: 10.1002/eji.201040391

19. Laurence A, Tato CM, Davidson TS, Kanno Y, Chen Z, Yao Z, et al. Interleukin-2 signaling *via* STAT5 constrains T helper 17 cell generation. *Immunity* (2007) 26(3):371–81. doi: 10.1016/j.immuni.2007.02.009

20. Zhou L, Lopes JE, Chong MM, Ivanov II, Min R, Victora GD, et al. TGF-beta-induced Foxp3 inhibits T(H)17 cell differentiation by antagonizing RORgammat function. *Nature* (2008) 453(7192):236–40. doi: 10.1038/nature06878

21. Cruz A, Khader SA, Torrado E, Fraga A, Pearl JE, Pedrosa J, et al. Cutting edge: IFN-gamma regulates the induction and expansion of IL-17-producing CD4 T cells during mycobacterial infection. *J Immunol* (2006) 177(3):1416–20. doi: 10.4049/jimmunol.177.3.1416

22. Stumhofer JS, Laurence A, Wilson EH, Huang E, Tato CM, Johnson LM, et al. Interleukin 27 negatively regulates the development of interleukin 17-producing T helper cells during chronic inflammation of the central nervous system. *Nat Immunol* (2006) 7 (9):937–45. doi: 10.1038/ni1376

23. Wang YL, Chou FC, Chen SJ, Lin SH, Chang DM, Sytwu HK, et al. Targeting pre-ligand assembly domain of TNFR1 ameliorates autoimmune diseases - an unrevealed role in downregulation of Th17 cells. *J Autoimmun* (2011) 37(3):160–70. doi: 10.1016/j.jaut.2011.05.013

24. Yang J, Sundrud MS, Skepner J, Yamagata T. Targeting Th17 cells in autoimmune diseases. *Trends Pharmacol Sci* (2014) 35(10):493–500. doi: 10.1016/j.tips.2014.07.006

25. Peck A, Mellins ED. Precarious balance: Th17 cells in host defense. *Infect Immun* (2010) 78(1):32–8. doi: 10.1128/IAI.00929-09

26. Rendon JL, Choudhry MA. Th17 cells: critical mediators of host responses to burn injury and sepsis. *J Leukoc Biol* (2012) 92(3):529–38. doi: 10.1189/jlb.0212083

27. van de Veerdonk FL, Mouktaroudi M, Ramakers BP, Pistiki A, Pickkers P, van der Meer JW, et al. Deficient candida-specific T-helper 17 response during sepsis. *J Infect Dis* (2012) 206(11):1798–802. doi: 10.1093/infdis/jis596

28. Wu HP, Chung K, Lin CY, Jiang BY, Chuang DY, Liu YC, et al. Associations of T helper 1, 2, 17 and regulatory T lymphocytes with mortality in severe sepsis. *Inflammation Res* (2013) 62(8):751–63. doi: 10.1007/s00011-013-0630-3

29. Belkaid Y, Rouse BT. Natural regulatory T cells in infectious disease. *Nat Immunol* (2005) 6(4):353–60. doi: 10.1038/ni1181

30. Fontenot JD, Rudensky AY. A well adapted regulatory contrivance: regulatory T cell development and the forkhead family transcription factor Foxp3. *Nat Immunol* (2005) 6(4):331–7. doi: 10.1038/ni1179

31. Arce-Sillas A, Alvarez-Luquin DD, Tamaya-Dominguez B, Gomez-Fuentes S, Trejo-Garcia A, Melo-Salas M, et al. Regulatory T cells: Molecular actions on effector cells in immune regulation. *J Immunol Res* (2016) 2016:1720827. doi: 10.1155/2016/1720827

32. Hisano G, Hanna N. Murine lymph node natural killer cells: Regulatory mechanisms of activation or suppression. *J Natl Cancer Inst* (1982) 69(3):665–71.

33. Miyara M, Sakaguchi S. Natural regulatory T cells: mechanisms of suppression. *Trends Mol Med* (2007) 13(3):108–16. doi: 10.1016/j.molmed.2007.01.003

34. Shalev I, Schmelzle M, Robson SC, Levy G. Making sense of regulatory T cell suppressive function. *Semin Immunol* (2011) 23(4):282–92. doi: 10.1016/j.smim.2011.04.003

35. Huang CT, Workman CJ, Flies D, Pan X, Marson AL, Zhou G, et al. Role of LAG-3 in regulatory T cells. *Immunity* (2004) 21(4):503–13. doi: 10.1016/j.immuni.2004.08.010

36. Tran DQ. TGF-beta: the sword, the wand, and the shield of FOXP3(+) regulatory T cells. *J Mol Cell Biol* (2012) 4(1):29–37. doi: 10.1093/jmcb/mjr033

37. Zhou L, Chong MM, Littman DR. Plasticity of CD4+ T cell lineage differentiation. *Immunity* (2009) 30(5):646–55. doi: 10.1016/j.immuni.2009.05.001

38. de Jong E, Suddason T, Lord GM. Translational mini-review series on Th17 cells: development of mouse and human T helper 17 cells. *Clin Exp Immunol* (2010) 159 (2):148–58. doi: 10.1111/j.1365-2249.2009.04041.x

39. Tatura R, Zeschnigk M, Hansen W, Steinmann J, Vidigal PG, Hutzler M, et al. Relevance of Foxp3(+) regulatory T cells for early and late phases of murine sepsis. *Immunology* (2015) 146(1):144–56. doi: 10.1111/imm.12490

40. Gavin MA, Torgerson TR, Houston E, DeRoos P, Ho WY, Stray-Pedersen A, et al. Single-cell analysis of normal and FOXP3-mutant human T cells: FOXP3 expression without regulatory T cell development. *Proc Natl Acad Sci U.S.A.* (2006) 103(17):6659–64. doi: 10.1073/pnas.0509484103

41. Liu W, Putnam AL, Xu-Yu Z, Szot GL, Lee MR, Zhu S, et al. CD127 expression inversely correlates with FoxP3 and suppressive function of human CD4+ T reg cells. *J Exp Med* (2006) 203(7):1701–11. doi: 10.1084/jem.20060772

42. Bettelli E, Carrier Y, Gao W, Korn T, Strom TB, Oukka M, et al. Reciprocal developmental pathways for the generation of pathogenic effector TH17 and regulatory T cells. *Nature* (2006) 441(7090):235–8. doi: 10.1038/nature04753

43. Nurieva R, Yang XO, Martinez G, Zhang Y, Panopoulos AD, Ma L, et al. Essential autocrine regulation by IL-21 in the generation of inflammatory T cells. *Nature* (2007) 448(7152):480–3. doi: 10.1038/nature05969

44. Sullivan JA, Adams AB, Burlingham WJ. The emerging role of TH17 cells in organ transplantation. *Transplantation* (2014) 97(5):483–9. doi: 10.1097/TP.0000000000000000

45. Chung BH, Yang CW, Cho ML. Clinical significance of Th17 cells in kidney transplantation. *Korean J Intern Med* (2018) 33(5):860–6. doi: 10.3904/kjim.2018.095

46. Healy DG, Watson RW, O'Keane C, Egan JJ, McCarthy JF, Hurley J, et al. Neutrophil transendothelial migration potential predicts rejection severity in human cardiac transplantation. *Eur J Cardiothorac Surg* (2006) 29(5):760–6. doi: 10.1016/j.ejcts.2006.01.065

47. Loong CC, Hsieh HG, Lui WY, Chen A, Lin CY. Evidence for the early involvement of interleukin 17 in human and experimental renal allograft rejection. *J Pathol* (2002) 197(3):322–32. doi: 10.1002/path.1117

48. Hsieh HG, Loong CC, Lin CY. Interleukin-17 induces src/MAPK cascades activation in human renal epithelial cells. *Cytokine* (2002) 19(4):159–74. doi: 10.1006/cyto.2002.1952

49. Woltman AM, Simone DEH, Boonstra JG, Gobin SJP, Daha MR, Kooten CV, et al. Interleukin-17 and CD40-ligand synergistically enhance cytokine and chemokine production by renal epithelial cells. *J Am Soc Nephrol* (2000) 11(11):2044–55. doi: 10.1681/ASN.V11112044

50. Li J, Simeoni E, Fleury S, Dudler J, Fiorini E, Kappenberger L, et al. Gene transfer of soluble interleukin-17 receptor prolongs cardiac allograft survival in a rat model. *Eur J Cardiothorac Surg* (2006) 29(5):779–83. doi: 10.1016/j.ejcts.2006.01.052

51. Chung BH, Kim KW, Kim BM, Doh KC, Cho ML, Yang CW, et al. Increase of Th17 cell phenotype in kidney transplant recipients with chronic allograft dysfunction. *PLos One* (2015) 10(12):e0145258. doi: 10.1371/journal.pone.0145258

52. Dziarmaga R, Ke D, Sapir-Pichhadze R, Cardinal H, Phan V, Piccirillo CA, et al. Age- and sex-mediated differences in T lymphocyte populations of kidney transplant recipients. *Pediatr Transplant* (2022) 26(1):e14150. doi: 10.1111/petr.14150

53. Tehrani HA, Einollahi B, Ahmadpoor P, Nafar M, Nikoueinejad H, Parvin M, et al. The relationship between T-cell infiltration in biopsy proven acute T-cell mediated rejection with allograft function and response to therapy: A retrospective study. *Transpl Immunol* (2022) 71:101394. doi: 10.1016/j.trim.2021.101394

54. Martin-Moreno PL, Tripathi S, Chandraker A. Regulatory T cells and kidney transplantation. *Clin J Am Soc Nephrol* (2018) 13(11):1760–4. doi: 10.2215/CJN.01750218

55. Afzali B, Lombardi G, Lechler RI, Lord GM. The role of T helper 17 (Th17) and regulatory T cells (Treg) in human organ transplantation and autoimmune disease. *Clin Exp Immunol* (2007) 148(1):32–46. doi: 10.1111/j.1365-2249.2007.03356.x

56. Dieckmann D, Plottner H, Berchtold S, Berger T, Schuler G. Ex vivo isolation and characterization of CD4(+)CD25(+) T cells with regulatory properties from human blood. *J Exp Med* (2001) 193(11):1303–10. doi: 10.1084/jem.193.11.1303

57. Wing K, Lindgren S, Kollberg G, Lundgren A, Harris RA, Rudin A, et al. CD4 T cell activation by myelin oligodendrocyte glycoprotein is suppressed by adult but not cord blood CD25+ T cells. *Eur J Immunol* (2003) 33(3):579–87. doi: 10.1002/eji.200323701

58. Game DS, Hernandez-Fuentes MP, Chaudhry AN, Lechler RI. CD4+CD25+ regulatory T cells do not significantly contribute to direct pathway hyporesponsiveness in stable renal transplant patients. *J Am Soc Nephrol* (2003) 14(6):1652–61. doi: 10.1097/01.asn.0000067411.03024.a9

59. Sabia C, Picascia A, Grimaldi V, Amarelli C, Maiello C, Napoli C. The epigenetic promise to improve prognosis of heart failure and heart transplantation. *Transplant Rev (Orlando)* (2017) 31(4):249–56. doi: 10.1016/j.trre.2017.08.004

60. Boer K, Caliskan K, Peeters AM, van Groningen MC, Samsom JN, Maat AP, et al. Thymus-derived regulatory T cells infiltrate the cardiac allograft before rejection. *Transplantation* (2015) 99(9):1839–46. doi: 10.1097/TP.0000000000000730

61. Vasco M, Benincasa G, Fiorito C, Faenza M, De Rosa P, Maiello C, et al. Clinical epigenetics and acute/chronic rejection in solid organ transplantation: An update. *Transplant Rev (Orlando)* (2021) 35(2):100609. doi: 10.1016/j.trre.2021.100609

62. Dieude M, Turgeon J, Karakeussian Rimbaud A, Beillevaire D, Qi S, Patey N, et al. Extracellular vesicles derived from injured vascular tissue promote the formation of tertiary lymphoid structures in vascular allografts. *Am J Transplant* (2020) 20(3):726–38. doi: 10.1111/ajt.15707

63. Liu Q, Rojas-Canales DM, Divito SJ, Shufesky WJ, Stolz DB, Erdos G, et al. Donor dendritic cell-derived exosomes promote allograft-targeting immune response. *J Clin Invest* (2016) 126(8):2805–20. doi: 10.1172/JCI84577

64. Rutman AK, Negi S, Saberi N, Khan K, Tchervenkov J, Paraskevas S. Extracellular vesicles from kidney allografts express miR-218-5p and alter Th17/Treg ratios. *Front Immunol* (2022) 13:784374. doi: 10.3389/fimmu.2022.784374

65. Chung BH, Oh HJ, Piao SG, Sun IO, Kang SH, Choi SR, et al. Higher infiltration by Th17 cells compared with regulatory T cells is associated with severe acute T-cell-mediated graft rejection. *Exp Mol Med* (2011) 43(11):630–7. doi: 10.3858/emm.2011.43.11.071

66. Halloran PF. Immunosuppressive drugs for kidney transplantation. *N Engl J Med* (2004) 351(26):2715–29. doi: 10.1056/NEJMra033540

67. Guerra G, Srinivas TR, Meier-Kriesche HU. Calcineurin inhibitor-free immunosuppression in kidney transplantation. *Transpl Int* (2007) 20(10):813–27. doi: 10.1111/j.1432-2277.2007.00528.x

68. Yurchenko E, Shio MT, Huang TC, Da Silva Martins M, Szyf M, Levings MK, et al. Inflammation-driven reprogramming of CD4+ Foxp3+ regulatory T cells into pathogenic Th1/Th17 T effectors is abrogated by mTOR inhibition. *vivo. PLos One* (2012) 7(4):e35572. doi: 10.1371/journal.pone.0035572

69. Chung BH, Kim BM, Doh KC, Min JW, Cho ML, Kim KW, et al. Suppressive effect of 1alpha,25-dihydroxyvitamin D3 on Th17-immune responses in kidney transplant recipients with tacrolimus-based immunosuppression. *Transplantation* (2017) 101(7):1711–9. doi: 10.1097/TP.0000000000001516

70. Gandolfo MT, Jang HR, Bagnasco SM, Ko GJ, Agreda P, Satpute SR, et al. Foxp3+ regulatory T cells participate in repair of ischemic acute kidney injury. *Kidney Int* (2009) 76(7):717–29. doi: 10.1038/ki.2009.259

71. Liao T, Xue Y, Zhao D, Li S, Liu M, Chen J, et al. *In vivo* attenuation of antibody-mediated acute renal allograft rejection by ex vivo TGF-beta-Induced CD4(+)Foxp3(+) regulatory T cells. *Front Immunol* (2017) 8:1334. doi: 10.3389/fimmu.2017.01334

72. Bluestone JA, Liu W, Yabu JM, Laszik ZG, Putnam A, Belingheri M, et al. The effect of costimulatory and interleukin 2 receptor blockade on regulatory T cells in renal transplantation. *Am J Transplant* (2008) 8(10):2086–96. doi: 10.1111/j.1600-6143.2008.02377.x

73. Demirkiran A, Sewgobind VD, van der Weijde J, Kok A, Baan CC, Kwekkeboom J, et al. Conversion from calcineurin inhibitor to mycophenolate mofetil-based immunosuppression changes the frequency and phenotype of CD4+FOXP3+ regulatory T cells. *Transplantation* (2009) 87(7):1062–8. doi: 10.1097/TP.0b013e31819d2032

74. Riella LV, Liu T, Yang J, Chock S, Shimizu T, Mfarrej B, et al. Deleterious effect of CTLA4-ig on a treg-dependent transplant model. *Am J Transplant* (2012) 12(4):846–55. doi: 10.1111/j.1600-6143.2011.03929.x

75. Scotta C, Fanelli G, Hoong SJ, Romano M, Lamperti EN, Sukthankar M, et al. Impact of immunosuppressive drugs on the therapeutic efficacy of *ex vivo* expanded human regulatory T cells. *Haematologica* (2016) 101(1):91–100. doi: 10.3324/haematol.2015.128934

76. Gallon L, Traitanon O, Yu Y, Shi B, Leventhal JR, Miller J, et al. Differential effects of calcineurin and mammalian target of rapamycin inhibitors on alloreactive Th1, Th17, and regulatory T cells. *Transplantation* (2015) 99(9):1774–84. doi: 10.1097/TP.0000000000000717

77. Bloom DD, Chang Z, Fechner JH, Dar W, Polster SP, Pascual J, et al. CD4+ CD25+ FOXP3+ regulatory T cells increase *de novo* in kidney transplant patients after immunodepletion with campath-1H. *Am J Transplant* (2008) 8(4):793–802. doi: 10.1111/j.1600-6143.2007.02134.x

78. Purroy C, Fairchild RL, Tanaka T, Baldwin WM, Manrique J 3rd, Madsen JC, et al. Erythropoietin receptor-mediated molecular crosstalk promotes T cell immunoregulation and transplant survival. *J Am Soc Nephrol* (2017) 28(8):2377–92. doi: 10.1681/ASN.2016101100

79. Hartemann A, Bensimon G, Payan CA, Jacqueminet S, Bourron O, Nicolas N, et al. Low-dose interleukin 2 in patients with type 1 diabetes: a phase 1/2 randomised, double-blind, placebo-controlled trial. *Lancet Diabetes Endocrinol* (2013) 1(4):295–305. doi: 10.1016/S2213-8587(13)70113-X

80. Gurkan S, Luan Y, Dhillon N, Allam SR, Montague T, Bromberg JS, et al. Immune reconstitution following rabbit antithymocyte globulin. *Am J Transplant* (2010) 10(9):2132–41. doi: 10.1111/j.1600-6143.2010.03210.x

81. Tang Q, Leung J, Melli K, Lay K, Chuu EL, Liu W, et al. Altered balance between effector T cells and FOXP3+ HELIOS+ regulatory T cells after thymoglobulin induction in kidney transplant recipients. *Transpl Int* (2012) 25(12):1257–67. doi: 10.1111/j.1432-2277.2012.01565.x

82. Cheng H, Xu B, Zhang L, Wang Y, Chen M, Chen S, et al. Bortezomib alleviates antibody-mediated rejection in kidney transplantation by facilitating Atg5 expression. *J Cell Mol Med* (2021) 25(23):10939–49. doi: 10.1111/jcmm.16998

83. Na N, Zhao D, Zhang J, Wu J, Miao B, Li H, et al. Carbamylated erythropoietin regulates immune responses and promotes long-term kidney allograft survival through activation of PI3K/AKT signaling. *Signal Transduct Target Ther* (2020) 5(1):194. doi: 10.1038/s41392-020-00232-5

84. Li A, Guo F, Pan Q, Chen S, Chen J, Liu HF, et al. Mesenchymal stem cell therapy: Hope for patients with systemic lupus erythematosus. *Front Immunol* (2021) 12:728190. doi: 10.3389/fimmu.2021.728190

frontiers | Frontiers in Immunology

TYPE Original Research
PUBLISHED 06 February 2023
DOI 10.3389/fimmu.2023.1090373

OPEN ACCESS

EDITED BY
Xuanchuan Wang,
Fudan University, China

REVIEWED BY
Giuseppe Gianni Figueiredo Leite,
Federal University of São Paulo, Brazil
Hu Linkun,
Soochow University, China

*CORRESPONDENCE
Kunhong Xiao
kunhongkevin.xiao@ahn.org

†These authors have contributed equally to this work

SPECIALTY SECTION
This article was submitted to Alloimmunity and Transplantation, a section of the journal Frontiers in Immunology

RECEIVED 05 November 2022
ACCEPTED 23 January 2023
PUBLISHED 06 February 2023

CITATION
Fang F, Liu P, Song L, Wagner P, Bartlett D, Ma L, Li X, Rahimian MA, Tseng G, Randhawa P and Xiao K (2023) Diagnosis of T-cell-mediated kidney rejection by biopsy-based proteomic biomarkers and machine learning.
Front. Immunol. 14:1090373.
doi: 10.3389/fimmu.2023.1090373

Diagnosis of T-cell-mediated kidney rejection by biopsy-based proteomic biomarkers and machine learning

Fei Fang[1†], Peng Liu[2†], Lei Song[1†], Patrick Wagner[3], David Bartlett[3], Liane Ma[3], Xue Li[4], M. Amin Rahimian[5], George Tseng[2], Parmjeet Randhawa[6] and Kunhong Xiao[1,3,7,8*]

[1]Department of Pharmacology and Chemical Biology, School of Medicine, University of Pittsburgh, Pittsburgh, PA, United States, [2]Department of Biostatistics, University of Pittsburgh, Pittsburgh, PA, United States, [3]Allegheny Health Network Cancer Institute, Pittsburgh, PA, United States, [4]Department of Chemistry, Michigan State University, East Lansing, MI, United States, [5]Department of Industrial Engineering, University of Pittsburgh, Pittsburgh, PA, United States, [6]Department of Pathology, The Thomas E Starzl Transplantation Institute, University of Pittsburgh, Pittsburgh, PA, United States, [7]Center for Proteomics & Artificial Intelligence, Allegheny Health Network Cancer Institute, Pittsburgh, PA, United States, [8]Center for Clinical Mass Spectrometry, Allegheny Health Network Cancer Institute, Pittsburgh, PA, United States

Background: Biopsy-based diagnosis is essential for maintaining kidney allograft longevity by ensuring prompt treatment for graft complications. Although histologic assessment remains the gold standard, it carries significant limitations such as subjective interpretation, suboptimal reproducibility, and imprecise quantitation of disease burden. It is hoped that molecular diagnostics could enhance the efficiency, accuracy, and reproducibility of traditional histologic methods.

Methods: Quantitative label-free mass spectrometry analysis was performed on a set of formalin-fixed, paraffin-embedded (FFPE) biopsies from kidney transplant patients, including five samples each with diagnosis of T-cell-mediated rejection (TCMR), polyomavirus BK nephropathy (BKPyVN), and stable (STA) kidney function control tissue. Using the differential protein expression result as a classifier, three different machine learning algorithms were tested to build a molecular diagnostic model for TCMR.

Results: The label-free proteomics method yielded 800-1350 proteins that could be quantified with high confidence per sample by single-shot measurements. Among these candidate proteins, 329 and 467 proteins were defined as differentially expressed proteins (DEPs) for TCMR in comparison with STA and BKPyVN, respectively. Comparing the FFPE quantitative proteomics data set obtained in this study using label-free method with a data set we previously reported using isobaric labeling technology, a classifier pool comprised of features from DEPs commonly quantified in both data sets, was generated for TCMR prediction. Leave-one-out cross-validation result demonstrated that the random forest (RF)-based model achieved the best predictive power. In a follow-up blind test using an independent sample set, the RF-based model yields 80% accuracy for TCMR and 100% for STA. When applying the established RF-based model to two

public transcriptome datasets, 78.1%-82.9% sensitivity and 58.7%-64.4% specificity was achieved respectively.

Conclusions: This proof-of-principle study demonstrates the clinical feasibility of proteomics profiling for FFPE biopsies using an accurate, efficient, and cost-effective platform integrated of quantitative label-free mass spectrometry analysis with a machine learning-based diagnostic model. It costs less than 10 dollars per test.

KEYWORDS

biomarker, quantitative proteomics, machine learning, FFPE, kidney transplantation, diagnosis, mass spectrometry

Introduction

In the United States alone, over 200,000 people are now living with functioning kidney transplants, and rejection is the major cause for transplant loss (1, 2). Although short-term graft survival is now excellent (*i.e.*, 92% and 83% at 1 and 3 years respectively), the 10-year graft survival rate drops to ~60% due to a spectrum of allograft pathology with a variety of distinct mechanisms and therapeutic options (3). Timely diagnosis of pathology is imperative in preserving allograft longevity and has traditionally been achieved using conventional biopsy-based histologic methods. One major allograft injury mechanism is T-cell-mediated rejection (TCMR), a classic model for T-cell-mediated inflammatory diseases. With contemporary immunosuppression, TCMR is less frequent but remains the dominant early rejection phenotype and the end point in many clinical trials (4).

At present, TCMR is mainly diagnosed using the Banff lesion score *i* (Interstitial inflammation) to evaluate the degree of inflammation in non-scarred areas of cortex. This diagnostic method has significant limitations of being descriptive, non-quantitative, and empirically derived, with significant inter-observer variability (5, 6). These limitations could be avoided with a diagnostic method that evaluates molecular changes in the tissue that preceded morphologic legion development. Such a method would use small tissue samples obtained from biopsies and would ideally be evaluated using molecular markers (RNA, DNA or protein) that could be assayed by a more sensitive, reproducible, and quantitative technology.

As the base of commercially available diagnostic tests, mRNA profiling is available as a test that is marketed as the Molecular Microscope or MMDx® system. It offers prospects of improved disease classification but has several inherent limitations such as high cost of mRNA extraction (7, 8). In addition, it's easy to miss the core with real disease information since the developed technologies become dependent analysis of a small tissue fragment taken from a longer core sent for routine histology (9, 10).

We have focused on working with proteins extracted from formalin-fixed, paraffin-embedded (FFPE) biopsy specimens to develop such a diagnostic assay. Compared with traditional diagnostic methods, proteomics-based tests have many advantages, including superior specificity, sensitivity, and accuracy as well as being quantitative, high-throughput and low cost. These tests also can simultaneously monitor multiple biomarkers, therefore providing a better understanding of disease pathogenesis and a more systematic evaluation of disease status. Compared with conventional biopsy readings by human observers, biopsy-based proteomic profiling can be a powerful tool to enhance biopsy interpretation, especially when combined with computer modeling to predict outcomes.

Predictive modeling, a method of creating models that can identify the likelihood of disease, has been widely discussed in recent years (11, 12). In predictive modeling, machine learning algorithms employ a variety of statistical, probabilistic and optimization methods to learn from known knowledge and to detect useful patterns from large data sets that rely on labeled training data (13). Whereas a multitude of deep learning-based prediction models for kidney transplant pathology have been developed based on the transcriptomic data sets (14), prediction models incorporating proteomic data have yet to be fully explored.

In our previous work, a Tandem Mass Tag (TMT)-based quantitative proteomic workflow was developed for proteomic profiling of FFPE biopsies (15). However, the TMT-based workflow requires tedious procedures with expensive isobaric reagents that likely preclude its incorporation into routine clinical practice. In the current study, a more cost-efficient and easily manageable workflow using label-free proteomic profiling technology was developed to evaluate kidney allograft injuries. We used samples from patients with TCMR or Polyomavirus BK nephropathy (BKPyVN), which is easily confused with on routine light microscopy (9, 16), and samples from patients without either condition to demonstrate proof-of-concept for developing a clinical-friendly workflow. This system uses label-free proteomic profiling technology and machine learning to correctly differentiate three types of biopsy samples.

Materials and methods

Materials

All chemicals used in this study were of analytical grade and purchased from Sigma-Aldrich (St. Louis, MO) unless otherwise stated. LC-MS grade solvents, including water, formic acid (FA),

methanol and acetonitrile (ACN) were ordered from Fisher Scientific (Pittsburgh, PA). The 10-kDa centrifugal filter unit was purchased from Millipore Sigma (Burlington, MA). The complete mini protease inhibitor cocktail was from Roche (Indianapolis, IN).

Patients and sample collection

This study was approved by the University of Pittsburgh IRB (protocol 10110393). STA kidney specimens and biopsies diagnosed as TCMR or BKPyVN were selected from weekly clinical conferences conducted immediately prior to commencement of the study. Diabetes mellitus, hypertension, and glomerulonephritis were the three most common causes of end-stage kidney disease in these subjects. All patients received Thymoglobulin induction followed by dual maintenance immunosuppressive therapy consisting of mycophenolate mofetil and tacrolimus. Corticosteroids were tapered over the first 7 days and then discontinued. Histologic diagnoses were based on the Banff classification for kidney allograft pathology (17). Diagnostically relevant Banff scores for the TCMR patients were g0, v0, i2, ptc0, cg0, ci1, ct1 for all biopsies. The t -score was 2 in all biopsies, except for 1 biopsy in which it was t3. The core needle biopsy specimens (18 gauge) were fixed in formalin immediately and paraffin embedded within 24 h.

The patients (eight males, seven females) in the discovery cohort ranged in age from 32 to 84 years with mean values of 60.8, 56.2, and 51.6 in the STA, BKPyVN, and TCMR groups, respectively. Biopsies had been performed 23-526 days post-transplant (mean 263) and showed renal cortex with mild interstitial fibrosis and tubular atrophy. For the BKPyVN biopsies, the concentration of viral loads ranged from 2.38E+08 to 6.67E+10 copies per mL in the urine and 8.11E+03 to 3.85E+05 copies per mL in the plasma. All biopsies showed polyomavirus antigens on immunohistochemistry.

The patients (two males, seven females) in validation cohort ranged in age from 27 to 73 years with mean values of 52.7. Biopsies had been performed 74-106 days post-transplant (mean 88).

Deparaffinization and protein extraction

The biopsy tissue embedded in the paraffin blocks was extracted with a sharp scalpel, followed by cutting into 1 mm pieces. Each sample was deparaffinized by incubating with 1 mL of xylene at room temperature (RT) for 5 min, centrifugating at 3,000 × g for 2 min. The supernatant was discarded after centrifugation. The above xylene washing step was repeated three times. The deparaffinized sample was rehydrated by incubating with 1 mL of 100% ethanol at RT for 3 min. The sample was centrifugated at 3,000 × g for 2 min, with the supernatant discarded. The ethanol washing step was repeated three times. After ethanol washing, 40 μL of lysis buffer (2% sodium dodecyl sulfate (SDS), 20 mM tris(hydroxymethyl)aminomethane (Tris), 1% protease inhibitor, pH 8.0) was added to each sample, which was then subjected to a focused ultrasonication step (work 4s, suspend 6s, total time 2min) with Model 120 Sonic Dismembrator (Fisher Scientific, Pittsburgh, PA). After the focused ultrasonication repeated for five times, the disrupted samples were incubated at 98˚C for 120 min. With the supernatants collected by centrifugation at 10,000 × g for 10 min at 4˚C, the concentration of the obtained protein supernatant was measured by BCA Protein Assay Kit (Thermo Scientific, Waltham, MA).

In-gel digestion

For each FFPE sample, 10 μg of the extracted proteins were respectively subjected to in-gel trypsin digestion according to standard procedures with minor modifications (18, 19). Briefly, the protein concentration was adjusted to 1 mg/mL with lysis buffer. 4 × sample loading buffer was added to a final concentration of 1 x and Tris(2-carboxyethyl) phosphine (TCEP) was added to a final concentration of 10 mM. The protein samples were denatured and reduced by incubating at 90°C for 20 min. After cooling down to the room temperature, the samples were alkylated by incubating with 25 mM IAA at room temperature in the dark for 30 min. The protein samples were then loaded into the wells of an SDS-polyacrylamide gel electrophoresis (SDS-PAGE) gel (i.e., 4% stacking gel and 10% separating gel). The gel electrophoresis was stopped once the dye front migrated into the separating gel and reached about 1cm from the top of the separating gel. After Coomassie blue staining, the 1 cm long gel band corresponding to proteins were excised and chopped into about 20 small pieces. The gel pieces were distained by incubating with 50% ACN in 50 mM ammonium bicarbonate (NH_4HCO_3) for 15 min at 37°C with sharking for three times, followed by incubating with pure water for 1 h at 37°C with shaking for three times. Subsequently, the gel pieces were treated with 100% ACN, followed by rehydration with digestion buffer (50 mM NH_4HCO_3 buffer containing 2% ACN). Protein tryptic digestion was performed at 37°C for overnight with 10 ng/μl trypsin (Promega, Mannheim, Germany). Digestion was terminated with FA at a concentration of 1% (v/v). Finally, the tryptic digests were extracted by incubating with 50% ACN followed by 80% ACN, purified with stage-tip protocol (20) and lyophilized with a vacuum concentrator (Thermo Scientific, Waltham, MA).

On-filter digestion

For each FFPE sample, 10 μg of the extracted proteins were processed using a filter-aided sample preparation (FASP) method (21) with minor modifications. Briefly, the proteins were denatured and reduced by incubating with 100 mM TCEP for 10 min at 90°C. After the sample was cooled down to RT, 100 μL of 8 M urea (dissolved in 100 mM NH_4HCO_3) was added to the sample and mixed. Then the mixture of each sample was loaded onto a 10-kDa centrifugal filter unit (250 μL/unit) followed by centrifugation at 14,000 g for 20 min. After the proteins on the membrane were washed with 200 μL of 8 M urea once, 200 μL of 8 M urea containing 20 mM IAA was added to the membrane and incubated at RT for 30 min in the dark. Next, the proteins on the membrane were washed with 200 μL of 8 M urea three times followed by 100 mM NH_4HCO_3 three times. Finally, 150 μL of 100 mM NH_4HCO_3 (pH 8.0) containing 0.4 μg of trypsin was added to each unit and incubated at 37°C for overnight. After digestion, FA was used to acidify the protein digests to terminate digestion at 1% FA (v/v). The filtrate units were

centrifuged at 14,000 g for 15 min, and the flow-through containing the peptides was collected. To increase peptide recovery from the membrane, the membrane was further washed with 150 µL of water, with elutes lyophilized with a vacuum concentrator.

Liquid chromatography with tandem mass spectrometry

The LC-MS/MS experiments were performed using nanoACQUITY Ultra-Performance LC (UPLC) system (Waters, Milford, MA) coupled with a LTQ Orbitrap Velos mass spectrometer (Thermo Scientific, San Jose, CA). Peptide separation was performed on a C18 capillary column (10.5 cm, 3 µm, 120 Å) from New Objective (Woburn, MO). The two eluent buffers were H_2O with 2% ACN and 0.1% FA (mobile phase A), and ACN with 2% H_2O and 0.1% FA (mobile phase B), and both were at pH 3. The gradient of the mobile phase B was set as follows: sample loaded at 2% B for 10 min, then 2%-35% B in 45 min, 35%-98% B in 10 min, and maintained at 80% B for 10 min. After separation, the column was equilibrated at 2% B for 25 min. The flow rate was 350 nL/min.

The LTQ Orbitrap Velos mass spectrometer was operated in the data-dependent acquisition (DDA) mode. MS1 scans were acquired in the Orbitrap analyzer at a resolution of 1.5×10^4 over the *m/z* 350-1,500 range. The AGC targets were set as 1×10^6 and 5×10^3 for MS scans and MS/MS scans, respectively. The ion accumulation times were set as 60 ms for MS scans and 50 ms for MS/MS scans. To improve spectrum utility, only ions with charge state between 2 and 4 were subjected to fragmentation with a minimum signal threshold of 500. The 20 most intense ions were fragmented at a normalized collision energy of 35%. Tandem mass spectra were acquired in the ion trap. The dynamic exclusion time was set to 30 s, with the isolation window as 2 Da. For MS2, the selected precursor ions were fragmented with activation time of 20 ms while activation q as 0.25.

Data analysis

Raw data files were processed using Proteome Discoverer (Thermo Scientific, version 1.4) with SEQUEST search engine. MS/MS spectra were matched with a Uniprot *Homo sapiens* database (204,961 entries, May 2022) and *BK polyomavirus (strain AS)* (BKPyVN) database (5 entries, May 2022), using the following parameters: full trypsin digest with maximum 2 missed cleavages, static modification carbamidomethylation of cysteine (+57.021 Da), dynamic modification of phosphorylation at serine, threonine, or tyrosine (+79.966 Da) as well as oxidation at methionine (+15.995 Da). Precursor and fragment ion mass tolerance was 10 ppm and 0.8 Da, respectively. Peptide spectral matches were validated using percolator with 1% false discovery rate (FDR). To enable meaningful expression comparison of different proteins. The data across different phenotypes were quantile normalized with normalyzer software (22), which was implemented in R using Bioconductor packages. Principal component analysis (PCA) was performed by subjecting data to Perseus software (version 1.6.10.50, available online: https://maxquant.net/perseus/) (23) based on singular value decomposition (24).

Statistical analysis and bioinformatics analysis

Statistical analysis was performed using the empirical Bayes method implemented in R package LIMMA (25) to determine proteins with statistically significant difference in abundance across different biopsies. To minimize the inaccuracy issues associated with label-free quantitative proteomics, log transformation followed by quantile normalization were performed before quantification analysis (26). DEPs were selected using two criteria: 1) their expression levels in TCMR biopsies significantly changed (*i.e.*, the Benjamin–Hochberg procedure adjusted p value < 0.05) in comparison with STA samples; 2) fold changes (FC) of protein expression levels between TCMR and STA are >2 or <0.5.

Bioinformatics analysis, including protein localization and signaling pathways involved by the identified proteins, was performed using QIAGEN Ingenuity Pathway Analysis (IPA) (https://digitalinsights.qiagen.com). Database for Annotation, Visualization and Integrated Discovery (DAVID) (https://david.ncifcrf.gov/) was performed for the functional annotation of the identified proteins (27, 28). In addition, the protein-protein interaction was predicted using the STRING software (https://string-db.org/) with a confidence cutoff as 0.7, followed by visualization using Cytoscape software (https://cytoscape.org/).

Machine learning and validation

Three machine learning predictive models were used: linear discriminant analysis (LDA), support vector machine (SVM), and random forest (RF). LDA uses Gaussian assumptions and Bayes theorem to estimate the posterior probability of being classified as TCMR for each testing sample (29). Those with posterior probabilities greater than or equal to a specific cutoff are classified as TCMR. LDA was implemented by the "lda" function in the R package "MASS". The second method SVM separates the STA and TCMR samples by finding a higher-dimension hyperplane that maximizes the margin, which is the minimum distance of the objects to the hyperplane (30). SVM was implemented by the "svm" function in the R package "e1071". RF classifies the samples by a majority vote of random trees using the classification and regression tree algorithm. The trees are constructed by bootstrapping of samples and subsampling of features (31). This method was implemented using "randomForest" function in the R package "randomForest". To evaluate the prediction performance of the protein signatures panel to distinguish TCMR, STA and BKPyVN, we performed a leave-one-out cross-validation (32) and employed the three, above-mentioned learning algorithms (i.e. LDA, SVM and RF) respectively. In each leave-one-out cross-validation procedure, one sample was held out as testing sample and the remaining samples are used as training set (33–35). Missing values were imputed. DEP analysis for the TMT and label-free training sets with all protein features was performed using an empirical Bayes method by R package LIMMA (25). The co-differentially expressed protein (cDEP) features of TMT and label-free proteomics data were then selected. The label-free intensities of selected proteins were used to construct classifiers by implementing the three machine learning

algorithms. Then we predict the classification of the testing sample using the classifiers we constructed. Performance was evaluated by calculating sensitivity, specificity, and accuracy. The detailed machine learning code was described in Supplementary Materials.

Results

Development of a label-free quantitative proteomics workflow for kidney FFPE biopsies

We previously reported a quantitative proteomic workflow for FFPE specimens, consisting of a loss-less sample preparation method, a TMT10plex-proteomic protocol, and a systematic data analysis pipeline (Figure 1A) (15). In this work, to simplify the workflow, a modified FASP method, which showed a comparable performance with in-gel digestion strategy for biopsy specimens (data not shown here), was applied for the protein digestion. In addition, instead of labeling the tryptic peptides with isobaric reagents followed by fractionation, the tryptic digests of FFPE specimens were injected directly to the separation column for LC-MS/MS analysis without peptide fractionation (Figure 1B). After database search, the identified and quantified proteins were subjected to systematic statistical analysis using the bioinformatics tool of R package LIMMA to obtain DEPs (Figure 1C) before building a predictive model (Figure 1D). Using this workflow, we analyzed 15 FFPE biopsies containing 5 TCMR, 5 BKPyVN and 5 STA. A total of 800-1350 proteins were identified and quantified with high confidence in each individual sample (Supplementary Table S1–S3) using a 45 min LC gradient.

Label-free quantitative proteomics analysis distinguishes different kidney transplant injury biopsies

Each step in the label-free proteomics workflow was optimized for FFPE biopsies to improve reproducibility. As shown in Figure 2A, a Pearson's correlation coefficient as high as 0.9 among the replicate experiments was achieved using our label-free workflow, demonstrating a good reproducibility in analyzing FFPE biopsies. To test whether label-free proteomics could distinguish different kidney transplant pathologies from one another, PCA was performed to the label-free proteomic data (Supplementary Table S4). As shown in Figure 2B, the quantified FFPE proteins not only segregate TCMR biopsies from control specimens (TCMR *vs.* STA), but also distinguish the two tested disease phenotypes from each other (TCMR *vs.* BKPyVN).

Differential expression analysis reveals potential biomarkers for TCMR

To identify DEPs that can serve as biomarkers to distinguish TCMR from BKPyVN and STA, differential expression analysis was

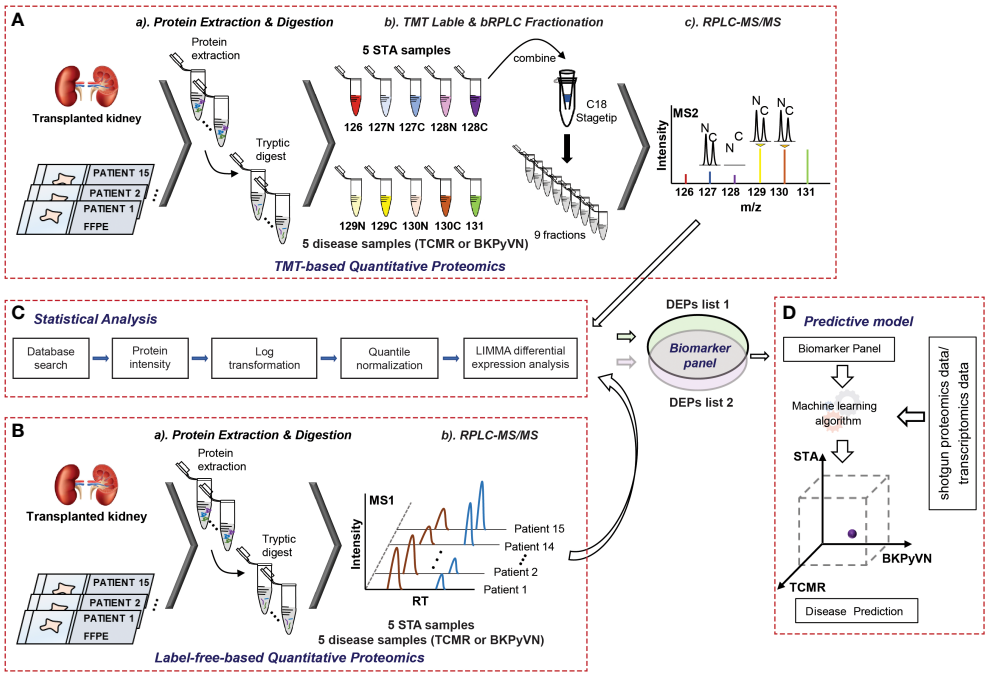

FIGURE 1
A flow chart showing the procedures to diagnose TCMR by FFPE biopsy-based proteomics and machine learning. **(A)** Experimental procedures for TMT-based quantitative proteomics. The proteins were extracted from 5 TCMR, 5 BKPyVN, and 5 STA biopsies, the digested peptides were labeled with TMT10-plex-reagents and separated by basic reverse phase C18 material. The fractionated peptides were subjected to LC-MS/MS analysis; **(B)** Experimental procedures for label-free quantitative proteomics. The proteins were extracted from 5 TCMR, 5 BKPyVN, and 5 STA biopsies, the digested peptides were directly subjected to LC-MS/MS analysis; **(C)** The proteins were subjected to a systematic statistical analysis consisting of log transformation, quantile normalization, and LIMMA analysis to obtain differentially expressed proteins; and **(D)** The machine learning algorithm was established based on the training data and validated with testing data.

performed using an empirical Bayes method implemented in R package LIMMA (25). In total, 329 out of the 924 quantified proteins were identified as DEPs for TCMR when comparing to STA (Supplementary Table S5), with the expression levels of 86 proteins upregulated and 243 downregulated. Similarly, LIMMA analysis revealed that a total of 645 DEPs significantly dysregulated in BKPyVN in comparison to STA biopsies (Supplementary Table S5), with the expression levels of 357 proteins upregulated and 288 downregulated. In addition, significant changes in expression levels of 467 proteins in TCMR occurred in comparison with BKPyVN biopsies (Supplementary Table S5).

Build protein signature panels for STA, TCMR and BKPyVN

To build specific protein signature panels for FFPE biopsies of different diseases, the cDEPs that were confidently quantified with the same trend (increase or decrease) in both label-free- (Supplementary Table S5) and TMT-based proteomics analyses (Supplementary Table S6) were extracted. The STA samples were applied as negative controls for the disease samples. As a result, 106, 40, and 154 proteins were identified as cDEPs in both quantitative proteomics methods for TCMR *vs.* STA, TCMR *vs.* BKPyVN, and BKPyVN *vs.* STA, respectively (Supplementary Tables S7and S8). As shown in the reference sections in Supplementary Tables S9 and S10, a number of these potential biomarkers were previously reported to be associated with kidney transplant injuries.

Comparison of different machine learning algorithms for construction of a prediction model for TCMR

To develop a prediction model that can diagnose TCMR, the DEPs commonly quantified from both label-free- and TMT-based quantitative proteomics (Supplementary Table S7) were used as the classifiers. After combining the above 106, 40 and 154 cDEPs and removing the overlapped proteins, a total of 247 proteins formed a panel of protein classifiers (Supplementary Table S11) for predictive model construction. The detailed procedures to construct the predictive model are outlined in Figure 3. Three different machine learning algorithms, *i.e.*, LDA, SVM and RF, were applied to the panel of protein classifiers, respectively. The performance of these machine learning algorithms was compared by using a leave-one-out cross-validation method. During this analysis, each algorithm was performed once for every instance, with the selected instance as a single-item test set and all the other instances as training data set. As shown in Figure 4, the disease and normal phenotypes could be obviously distinguished from each other using the three prediction models, with 100%, 100% and 93.3% accuracy achieved in pairwise cross-validation for SVM, RF and LDA, respectively. The receiver operating characteristic (ROC) curve, which has been widely used in clinical epidemiology, was also performed to evaluate the accuracy of our prediction model to discriminate between "diseased" and "non-diseased" (36, 37). For all three algorithms, the area under the curve (AUC) of 1 for the injury subtype provides 100% specificity and 100% sensitivity between each two disease types (Figure S1).

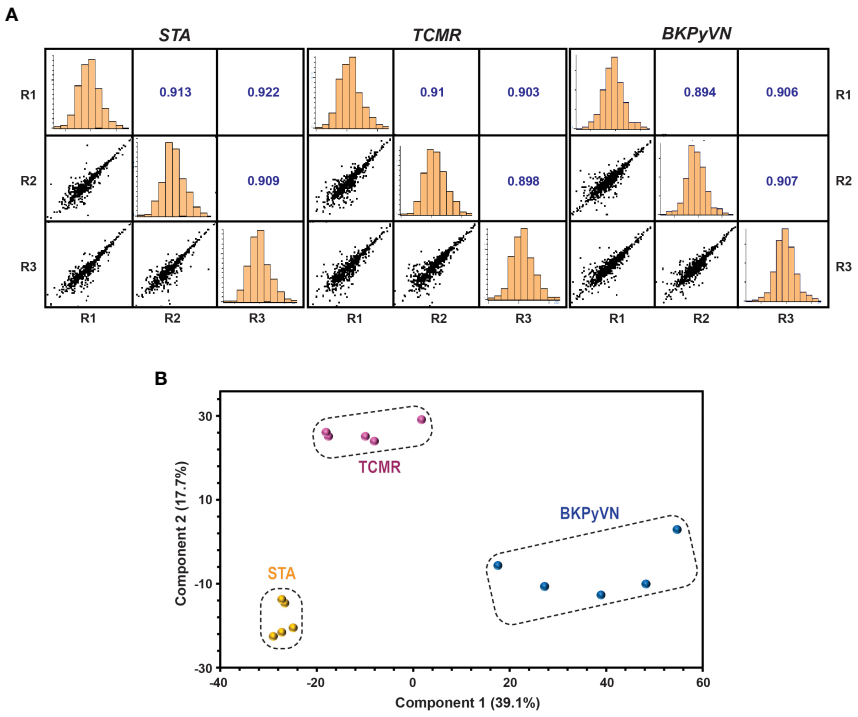

FIGURE 2
Quantitative proteomic profiling of FFPE biopsies segregates different kidney transplant injuries. **(A)** Repeatability of label-free quantitative analysis. Correlations among 3 replicates for each sample were shown. The correlation coefficient shown in the figure represents the statistical relationship between every two replicates. The larger the value, the higher repeatability between the two replicates. **(B)** A PCA plot obtained by Perseus software demonstrated that the quantified FFPE biopsy proteins were able to segregate TCMR, BKPyVN and STA samples. The PC1 axis is the first principal direction along which the samples show the largest variation. The PC2 axis is the second most important direction, and it is orthogonal to the PC1 axis.

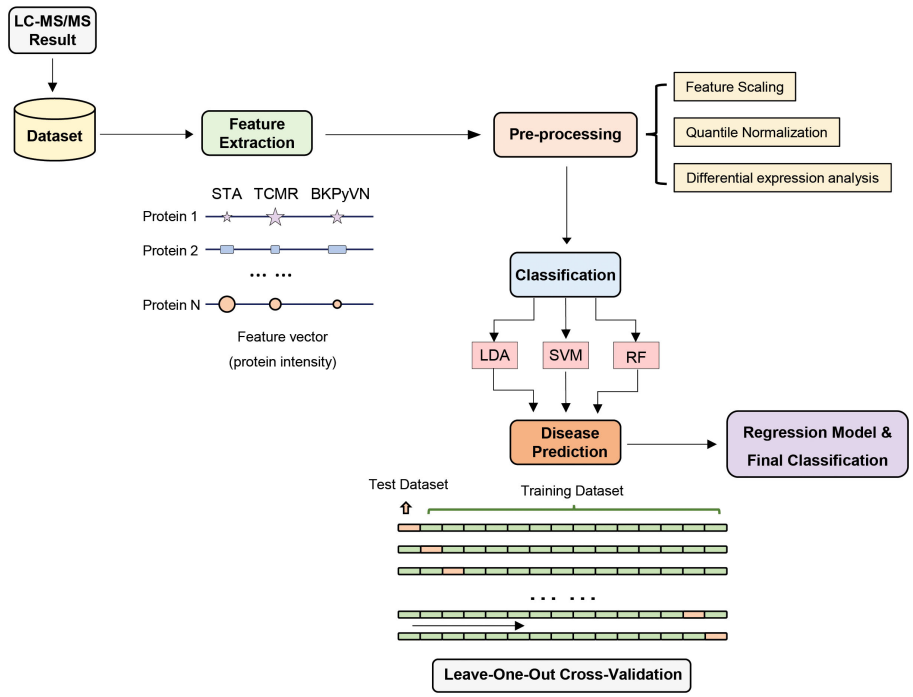

FIGURE 3
Development of machine learning derived disease prediction model for TCMR, BKPyVN and STA. With the LC-MS/MS data sets of the total of 15 kidney transplant FFPE samples collected, the protein names and corresponding intensities were obtained after database search. Feature selection process selects the critical features (e.g., intensity) for the prediction of kidney rejection disease. After feature selection, preprocessing procedures such as outlier removal, feature scaling (log transformation) and quantile normalization were performed. Various classification techniques were applied to the preprocessed data, with performance evaluated *via* leave-one-out cross-validation strategy. For a total of 15 samples (5 TCMR + 5 BKPyVN + 5 STA), 14 were used as training dataset and the other one as test dataset. Finally, the optimized biomarker panel and disease prediction model were obtained.

Validation of the TCMR prediction model with blindly tested biopsies

To verify the predictive power of the TCMR prediction models, an independent set of validation samples consisting of 5 TCMR and 5 STA biopsies was used for blind testing. The samples were subjected to label-free proteomics analysis, and the data obtained from each sample was quantile normalized based on the testing data one by one (Supplementary Tables S12 and S13). With the RF-based model, all (100%) the 5 STA and 4 (80%) out of 5 TCMR samples were correctly predicted (80% sensitivity and 100% specificity). With the SVM-based model, 3 (60%) out 5 STA and 4 (80%) out of 5 TCMR samples were correctly predicted (80% sensitivity and 60% specificity). Meanwhile, with the LDA-based model, all (100%) of the 5 STA and 3 (60%) out of the 5 TCMR samples were correctly predicted (60% sensitivity and 100% specificity).

Validation of the TCMR prediction model using published transcriptome data sets

To further validate the predictive power of the TCMR prediction models, published transcriptome data was used. The classifiers using the 247 proteins from proteomics analysis were applied to two microarray-based data sets [GSE48581 (38) and GSE36059 (39)] posted on the Gene Expression Omnibus website. Applying the three predictive models to GSE36059 achieves 26/35 = 74.3% (SVM), 29/35 = 82.9% (RF) and 25/35 = 71.4% (LDA) in sensitivity as well as 170/281 = 60.5% (SVM), 165/281 = 58.7% (RF) and 182/281 = 64.8% (LDA) in specificity, respectively. Meanwhile, when applied to GSE48581, the sensitivities of the three models are 24/32 = 75% (SVM), 25/32 = 78.1% (RF) and 24/32 = 75% (LDA) and the specificities are 142/222 = 64.0% (SVM), 143/222 = 64.4% (RF) and 136/222 = 61.3% (LDA), respectively.

Discussion

The FFPE specimen is an invaluable archive for the development of novel molecular diagnostic tests (40). Nucleic acid-based tests have been explored using material from fresh frozen specimens but have been hampered by the low quality and efficiency and high cost of DNA/RNA extraction, along with the scant amount of tissue generally available from needle biopsies (41). We have focused on developing proteomics-based molecular diagnostic tests using proteins extracted from FFPE biopsy specimens.

In comparison with urine and blood, which are also valuable sources in clinical proteomics for disease screening, diagnosis and management as they can be obtained non-invasively, FFPE specimens are advantageous in several aspects. For instance, the FFPE samples are stable at room temperature, and the storage time (up to 32 years) does not have a significant effect on protein identifications from FFPE kidney tissues (42). By contrast, the protein abundance would change significantly when urine was stored up to 3 days at 4°C or up to 6

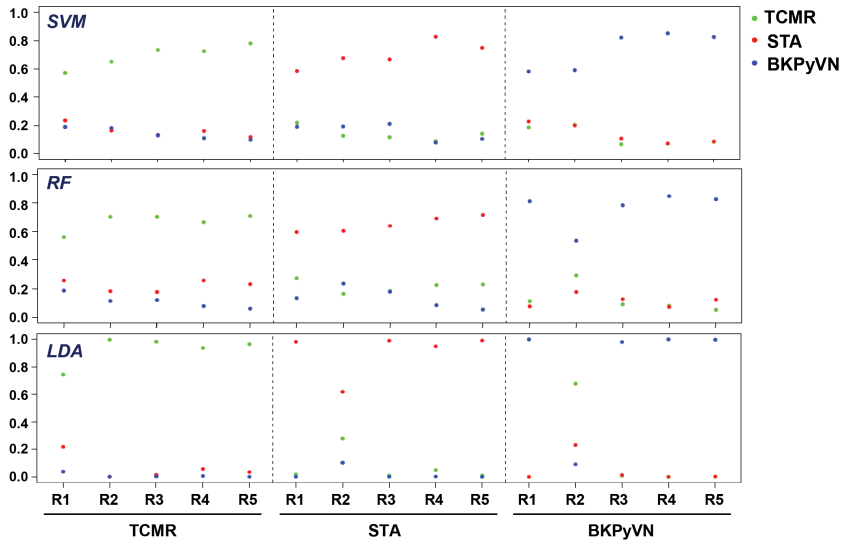

FIGURE 4
Diagnostic ability of the three different predictive models applied to disease and normal phenotypes. The probability calculated for the kidney transplant biopsy specimens using biomarker panel with the three different prediction models. LDA directly provides posterior probabilities. For random forest (RF), the probabilities are the proportions of votes among the ensembled trees. For SVM, we fit logistic distribution and obtain posterior probabilities by setting probabilities=TRUE in svm function of "e1071" package. R1-R5 are individual samples in each kidney pathology.

hours at room temperature (43). Similar changes in protein abundance were observed in blood samples when were stored for 1 month at temperatures above -20°C (44). In addition, the extremely wide concentration range, spanning at least nine orders of magnitude, raises a significant challenge for the discovery of blood biomarkers (45). Due to the differences in the daily intake of fluid, the protein and peptide concentrations widely vary with time of collection in urine samples (43), which limit the study of urine biomarkers. Therefore,

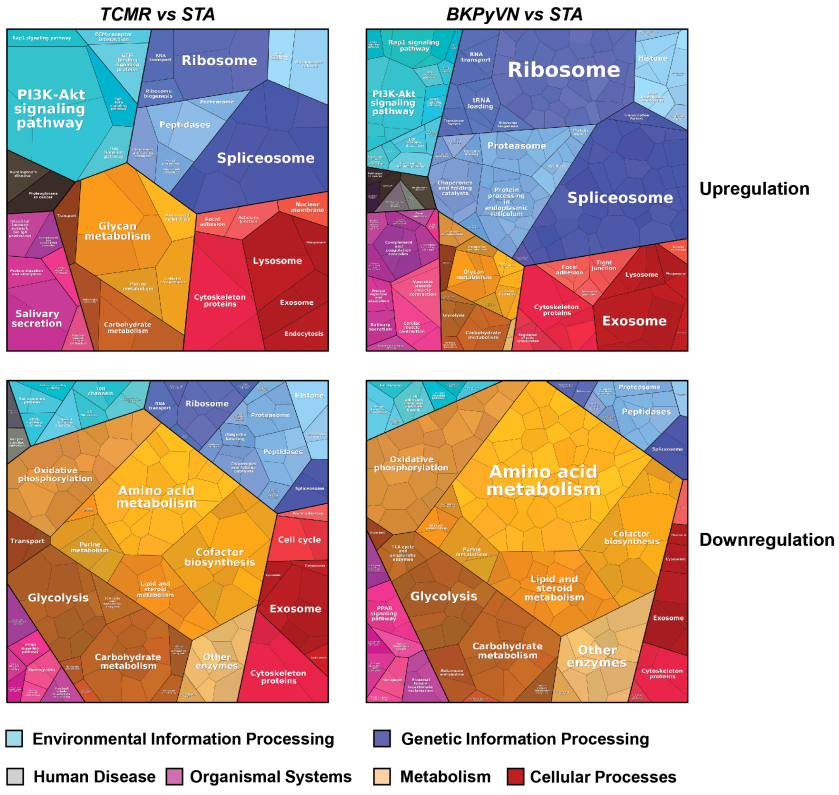

FIGURE 5
Biological classification of DEPs from label-free quantitative proteome data sets. Treemap of cellular categories altered in disease biopsies in comparison with STA sample illustrated by Proteomaps. The conditions of each disease are marked on the upper side.

FFPE specimens constitute a major part of most archival biobank and provide an invaluable resource for retrospective studies. As biopsy-based histopathologic examination remains essential for evaluating kidney allograft dysfunction, developing clinical proteomics assays using FFPE biopsy specimens is of great significance to assist the pathologists to enhance biopsy interpretation.

In our previous work, a TMT-based quantitative proteomic workflow was developed for molecular profiling of FFPE specimens (15). However, this workflow is not easily manageable in clinical practice for several reasons. First, TMT-labeling reagents are expensive and analyzing TMT-labeled samples requires high-end mass spectrometers with high resolution. Second, the TMT labeling procedures are labor-intensive, and quantitative accuracy is hampered by low labeling efficiency if the experiments are not performed under optimal conditions. Therefore, in this work, we developed a label-free quantitative proteomic workflow for FFPE biopsies as a widely applicable, user-friendly clinical tool, combining the advantages of a simplified sample preparation process with the possibility to perform comparative quantification across many samples. In addition, the cost for reagents can be as low as a few dollars per test.

As a proof-of-principle study, we applied this label-free quantitative proteomic workflow to a small discovery cohort of 15 FFPE biopsies including 5 TCMR, 5 BKPyVN and 5 STA. The high Pearson's correlation coefficient between the replicate experiments demonstrated that a good reproducibility can be achieved. Although only about one third of proteins (800-1350 proteins) were identified and quantified in the label-free proteomics workflow compared to those (2,798 proteins) in the TMT-based workflow, the PCA clustering result revealed that the obtained label-free proteomic data sets is capable of differentiation among different graft pathologies.

To gain insight into disease mechanism, the 329 DEPs between TCMR *vs*. STA and the 645 DEPs between BKPyVN *vs*. STA obtained by label-free proteomics were subjected to bioinformatic analysis. The Proteomap analysis revealed that these two pools of DEPs shared many enriched biological functions and pathways (46). As shown in Figure 5, proteins involved in splicing (spliceosome), protein synthesis (ribosome), and PI3K-AKT signaling pathway were enriched in the DEPs upregulated in both TCMR and BKPyVN. Proteins involved in metabolism pathways (*e.g.*, amino acid metabolism, carbohydrate metabolism, lipid and steroid metabolism) and energy production (*e.g.*, oxidative phosphorylation and glycolysis) are mostly downregulated in both disease phenotypes. It is worth mentioning that a number of proteins in the mitochondrial electron transfer chain, responsible for oxidative phosphorylation and ATP synthesis, were downregulated in both TCMR and BKPyVN. Whether the downregulation of the mitochondrial electron transfer chain proteins is one of the causes or the results of the kidney allograft rejection needs to be further investigated.

A similar observation was noted when the 329 DEPs between TCMR *vs*. STA were subjected to STRING analysis (Figure S2A). Many proteins involved in electron transfer chain and energy production, for example, oxidoreductases and proteins for glycolysis and oxidative phosphorylation, were expressed at lower levels in TCMR biopsies in comparison with STA specimens. To get more clues to disease mechanism for TCMR, the 329 DEPs between TCMR *vs*. STA were subjected to DAVID analysis; and several groups of proteins stood out (Supplementary Table S14 and Figures S2B–E). Most of these proteins are involved in innate immune system and inflammation response. The first group is collagens (Figure S2B). Compared with STA specimens, the expression of the many collagens, including COL1A2, COL6A1, COL6A3, COL1A1, COL4A2, COL6A2 AND COL18A1, was upregulated in TCMR. It is interesting that a recent genome study on the adaptive immune landscape of kidney allograft biopsies showed a significant increase in both formation and degradation of collagens in TCMR compared with STA biopsies (47). The second group of proteins that stood out in the 329 DEPs between TCMR *vs*. STA is the ion channel proteins and transporters. Abnormal ion transport is known to be associated with local or systemic inflammatory response (48). In this study, most of the ion channel proteins and transporters were downregulated in TCMR in comparison with STA (Figure S2C). For example, chloride intracellular channel protein CLIC1, which was reported to participate in the regulation of the NLRP3 inflammasome (49), was found to be decreased in its expression in TCMR in comparison with STA. The third group of proteins is protein kinases (Figure S2D). As an important class of intracellular enzymes that play a crucial role in most signal transduction cascades, from controlling cell growth and proliferation to the initiation and regulation of immunological responses (50), many protein kinases were found to be decreased in TCMR in comparison with STA biopsies. For example, creatine kinase (CK), which is associated with reduced inflammation (51), decreased 7-fold in TCMR biopsies. The fourth group of proteins that significantly changed in their expression levels between the TCMR and STA biopsies is translation and transcription regulators (Figure S2E). Among them, HNRNPK, which could promote the activation of NLRP3 inflammasome (52), increased 2-fold in TCMR biopsies. The bioinformatic analysis demonstrated that the developed label-free-based proteomics method in this study not only could facilitate the understanding of the molecular mechanisms associated with TCMR, but also provide the potential biomarkers for disease diagnosis.

To obtain a panel of protein classifiers/biomarkers to diagnose TCMR with high accuracy, we chose the DEPs confidently quantified with the same trend (increase or decrease) in protein expression in both label-free-based- and TMT-based proteomics analyses. As a result, 106, 40, and 154 proteins were identified as potential classifiers for TCMR *vs*. STA, TCMR *vs*. BKPyVN, and BKPyVN *vs*. STA, respectively (Supplementary Table S7). The 106 potential classifiers/biomarkers between TCMR *vs*. STA were subjected to Ingenuity Pathway Analysis (IPA). The analysis revealed that the 106 potential classifiers/biomarkers were mainly located in extracellular exosome, nucleus, plasma membrane, ER-golgi and mitochondrion (Figure 6A), while more than 60% of them were enzymes (Figure 6B). In addition, these proteins were enriched in various signaling pathways associated with the inflammatory response, including iron homeostasis signaling pathway (53), energy production pathways (*e.g.*, galactose and sucrose degradation) (54), apoptosis pathways (*e.g.*, LXR/RXR and FXR/RXR activation) (55), and atherosclerosis signaling (56) (Figure 6C and Supplementary Table S15). In addition, these 106 potential classifiers/biomarkers between TCMR *vs*. STA are associated with kidney damage (e.g., ATP1B1, CST3, FAH, GSS, HPX and LYZ), tubule injury (e.g., CRYM, GSS, HAGH, HPX and LYZ) and kidney inflammation (e.g., DCN) (Supplementary Table S15). For

example, CST3 (cystatin C), an extracellular space protein, was used as a biomarker to evaluate kidney function (glomerular filtration rate, GFR) (NCT00300066 in ClinicalTrials.gov database) and to predict the risk of ischemic stroke (NCT00479518). CST3 was also used as a potential biomarker to measure the efficacy of valsartan in the treatment of hypertension for patients with kidney dysfunction (NCT00140790). In addition to CST3, other proteins such as VIM (vimentin), LCP1 (lymphocyte cytosolic protein 1), and FTL (ferritin light chain) are also potential biomarkers for clinical diagnosis (Table S9). The above analysis showed that many proteins in the potential classifier panel were reported not only influences innate immunity but also determine T-cell-mediated immune response, demonstrating the feasibility of using this potential classifier panel in building TMCR disease prediction model.

We further evaluated whether a workflow integrating label-free quantitative proteomics technology with machine learning could be developed into a disease prediction tool for TCMR diagnosis. The protein intensity data (the summarized intensities of all identified peptides for each protein) in the FFPE biopsies of TCMR, BKPyVN and STA obtained from the label-free-based experiments was used as the classifiers for machine learning prediction model. As the core component of the developed prediction model, the selection of an optimal machine learning algorithm is prerequisite. LDA, Logistic Regression, Decision Tree, k-Nearest Neighbors, RF, SVM, Naive Bayes and Artificial Neural Network are among the commonly used machine learning techniques (57–59). In this study, three machine learning algorithms, LDA, SVM, and RF, were applied to the quantitative proteomics data collected from kidney FFPE biopsies. cDEPs identified in common from both TMT and label-free proteomic workflows were used as classifiers. With leave-one-out cross-validation, all three algorithms were found to achieve preliminary predictive performance for rejection with 100% sensitivity and specificity when applied to the discovery sample set. In addition, using an independent validation sample set of 5 TCMR and 5 STA biopsies, the TCMR prediction models also achieved satisfactory predictive power. A good prediction result was also achieved when the models were applied to transcriptome data published by others. Among the three models constructed in this study, RF-based TCMR prediction model outperformed the two other models. These results demonstrated the diagnostic potential of RF-based prediction model for kidney transplant injuries.

Although we applied stringent histopathologic criteria to define TCMR, rejection is a heterogenous process, and a larger sample size will be necessary to cover the broad spectrum of TCMR. Since no simple rule of thumb is available to determine the necessary sample size for omics studies seeking to find novel biomarkers, our study has limitations. The potential classifiers/biomarkers identified in this

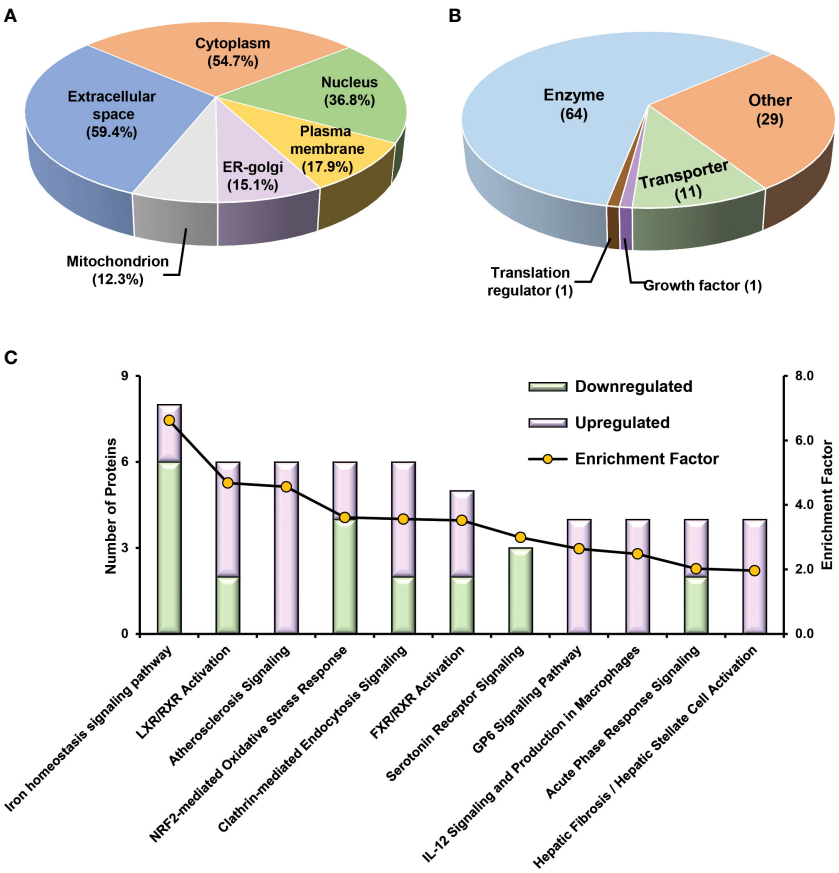

FIGURE 6
Bioinformatics analysis of 106 potential classifiers between TCMR and STA commonly quantified from two methods. Ingenuity Pathways Analysis of cDEPs commonly identified from both TMT- and label-free quantitative proteome analysis revealed cellular component **(A)**, molecular function **(B)**, and canonical pathways **(C)** enriched in the 106 potential classifiers between TCMR *vs.* STA samples. The orange and green labeled bars respectively represented the up-regulated and down-regulated proteins in TCMR in comparison with STA.

study will need to be optimized and validated using larger kidney rejection biopsy cohorts. The potential classifiers/biomarkers identified by mass spectrometry-based proteomic technology also need to be verified using other biomedical methods before being used to develop molecular tests. More accurate and specific molecular testing can lead to more effective treatment, prolong graft life, and improve the quality of life for patients with chronic kidney failure.

Conclusion

Taken together, we have successfully developed an integrative pipeline by combining label-free quantitative proteomics and machine learning prediction models for TCMR diagnosis. Instead of relying on a single biomarker for disease diagnosis, we used a multi-biomarker panel to enhance diagnostic accuracy, sensitivity, and specificity. Because of the small sample size in this pilot study, the biomarker panel identified here will require further optimization and validation in larger biopsy data sets. As a proof-of-principle study, however, this report demonstrates the feasibility of clinical implementation of molecular diagnostics tests integrating label-free quantitative proteomics and machine learning predictive models.

Data availability statement

The data presented in the study are deposited in the PRIDE repository, accession number PXD038601.

Ethics statement

The studies involving human participants were reviewed and approved by University of Pittsburgh IRB (protocol 10110393). The ethics committee waived the requirement of written informed consent for participation.

Author contributions

FF, PR, and KX designed the study. FF, PL, LS, PR, and KX conducted the study. FF, PL, LS, LM, XL, MR, GT, and KX performed data analyses. FF, PL, LS, PW, DB, PR, and KX interpreted the data. FF and KX wrote the manuscript with the support of PW, DB, LS, LM, XL, MR, and PR. All authors contributed to the article and approved the submitted version.

Funding

This study is partially supported by NIH 1R21AI148776 (to KX and PR).

Acknowledgments

The authors would like to thank Drs. Jacalyn Newman (Publication office at the Allegheny Health Network) and David Millington (Duke University) for carefully reading the manuscript and for providing comments and suggestions.

Conflict of interest

The authors declare that the research was conducted in the absence of any commercial or financial relationships that could be construed as a potential conflict of interest.

Publisher's note

Supplementary material

The Supplementary Material for this article can be found online at: https://www.frontiersin.org/articles/10.3389/fimmu.2023.1090373/full#supplementary-material

References

1. Collins AJ, Foley RN, Chavers B, Gilbertson D, Herzog C, Ishani A, et al. US Renal data system 2013 annual data report. *Am J Kidney Dis* (2014) 63(1):A7. doi: 10.1053/j.ajkd.2013.11.001

2. Loupy A, Aubert O, Orandi BJ, Naesens M, Bouatou Y, Raynaud M, et al. Prediction system for risk of allograft loss in patients receiving kidney transplants: International derivation and validation study. *BMJ* (2019) 366:l4923. doi: 10.1136/bmj.l4923

3. Ghelichi-Ghojogh M, Mohammadizadeh F, Jafari F, Vali M, Jahanian S, Mohammadi M, et al. The global survival rate of graft and patient in kidney transplantation of children: A systematic review and meta-analysis. *BMC Pediatr* (2022) 22(1):503. doi: 10.1186/s12887-022-03545-2

4. Halloran PF. T Cell-mediated rejection of kidney transplants: A personal viewpoint. *Am J Transplant* (2010) 10(5):1126–34. doi: 10.1111/j.1600-6143.2010.03053.x

5. Roufosse C, Simmonds N, Clahsen-van Groningen M, Haas M, Henriksen KJ, Horsfield C, et al. A 2018 reference guide to the banff classification of renal allograft pathology. *Transplantation* (2018) 102(11):1795–814. doi: 10.1097/TP.0000000000002366

6. Bobka S, Ebert N, Koertvely E, Jacobi J, Wiesener M, Buttner-Herold M, et al. Is early complement activation in renal transplantation associated with later graft outcome? *Kidney Blood Press Res* (2018) 43(5):1488–504. doi: 10.1159/000494014

7. Randhawa P. The molecular microscope (MMDX(R)) interpretation of thoracic and abdominal allograft biopsies: Putting things in perspective for the clinician. *Clin Transpl* (2021) 35(4):e14223. doi: 10.1111/ctr.14223

8. Randhawa P. The MMDx((R)) diagnostic system: A critical re-appraisal of its knowledge gaps and a call for rigorous validation studies. *Clin Transplant* (2022) 36(11): e14747. doi: 10.1111/ctr.14747

9. Pan L, Lyu Z, Adam B, Zeng G, Wang Z, Huang Y, et al. Polyomavirus BK nephropathy-associated transcriptomic signatures: A critical reevaluation. *Transplant Direct* (2018) 4(2):e339. doi: 10.1097/TXD.0000000000000752

10. Drachenberg CB, Papadimitriou JC, Hirsch HH, Wali R, Crowder C, Nogueira J, et al. Histological patterns of polyomavirus nephropathy: Correlation with graft outcome and viral load. *Am J Transpl* (2004) 4(12):2082–92. doi: 10.1046/j.1600-6143.2004.00603.x

11. Wynants L, Van Calster B, Collins GS, Riley RD, Heinze G, Schuit E, et al. Prediction models for diagnosis and prognosis of covid-19: Systematic review and critical appraisal. *BMJ* (2020) 369:m1328. doi: 10.1136/bmj.m1328

12. Park DJ, Park MW, Lee H, Kim YJ, Kim Y, Park YH. Development of machine learning model for diagnostic disease prediction based on laboratory tests. *Sci Rep* (2021) 11(1):7567. doi: 10.1038/s41598-021-87171-5

13. Cruz JA, Wishart DS. Applications of machine learning in cancer prediction and prognosis. *Cancer Inform* (2007) 2:59–77.

14. Liu P, Tseng G, Wang Z, Huang Y, Randhawa P. Diagnosis of T-cell-mediated kidney rejection in formalin-fixed, paraffin-embedded tissues using RNA-seq-based machine learning algorithms. *Hum Pathol* (2019) 84:283–90. doi: 10.1016/j.humpath.2018.09.013

15. Song L, Fang F, Liu P, Zeng G, Liu H, Zhao Y, et al. Quantitative proteomics for monitoring renal transplant injury. *Proteomics Clin Appl* (2020) 14(4):e1900036. doi: 10.1002/prca.201900036

16. Zeng G, Huang Y, Huang Y, Lyu Z, Lesniak D, Randhawa P. Antigen-specificity of T cell infiltrates in biopsies with T cell-mediated rejection and BK polyomavirus viremia: Analysis by next generation sequencing. *Am J Transpl* (2016) 16(11):3131–8. doi: 10.1111/ajt.13911

17. Loupy A, Haas M, Roufosse C, Naesens M, Adam B, Afrouzian M, et al. The banff 2019 kidney meeting report (I): Updates on and clarification of criteria for T cell- and antibody-mediated rejection. *Am J Transpl* (2020) 20(9):2318–31. doi: 10.1111/ajt.15898

18. Xiao K, Zhao Y, Choi M, Liu H, Blanc A, Qian J, et al. Revealing the architecture of protein complexes by an orthogonal approach combining HDXMS, CXMS, and disulfide trapping. *Nat Protoc* (2018) 13(6):1403–28. doi: 10.1038/nprot.2018.037

19. Zhao Y, Xiao K. Proteomic analysis of the beta-arrestin interactomes. *Methods Mol Biol* (2019) 1957:217–32. doi: 10.1007/978-1-4939-9158-7_14

20. Rappsilber J, Ishihama Y, Mann M. Stop and go extraction tips for matrix-assisted laser desorption/ionization, nanoelectrospray, and LC/MS sample pretreatment in proteomics. *Anal Chem* (2003) 75(3):663–70. doi: 10.1021/ac026117i

21. Wisniewski JR, Zougman A, Nagaraj N, Mann M. Universal sample preparation method for proteome analysis. *Nat Methods* (2009) 6(5):359–62. doi: 10.1038/nmeth.1322

22. Chawade A, Alexandersson E, Levander F. Normalyzer: a tool for rapid evaluation of normalization methods for omics data sets. *J Proteome Res* (2014) 13(6):3114–20. doi: 10.1021/pr401264n

23. Tyanova S, Temu T, Sinitcyn P, Carlson A, Hein MY, Geiger T, et al. The Perseus computational platform for comprehensive analysis of (prote)omics data. *Nat Methods* (2016) 13(9):731–40. doi: 10.1038/nmeth.3901

24. Alter O, Brown PO, Botstein D. Singular value decomposition for genome-wide expression data processing and modeling. *Proc Natl Acad Sci USA* (2000) 97(18):10101–6. doi: 10.1073/pnas.97.18.10101

25. Ritchie ME, Phipson B, Wu D, Hu Y, Law CW, Shi W, et al. Limma powers differential expression analyses for RNA-sequencing and microarray studies. *Nucleic Acids Res* (2015) 43(7):e47. doi: 10.1093/nar/gkv007

26. Pineda S, Sigdel TK, Chen J, Jackson AM, Sirota M, Sarwal MM. Corrigendum: Novel non-histocompatibility antigen mismatched variants improve the ability to predict antibody-mediated rejection risk in kidney transplant. *Front Immunol* (2018) 9:107. doi: 10.3389/fimmu.2018.00107

27. Huang da W, Sherman BT, Lempicki RA. Systematic and integrative analysis of large gene lists using DAVID bioinformatics resources. *Nat Protoc* (2009) 4(1):44–57. doi: 10.1038/nprot.2008.211

28. Huang da W, Sherman BT, Lempicki RA. Bioinformatics enrichment tools: paths toward the comprehensive functional analysis of large gene lists. *Nucleic Acids Res* (2009) 37(1):1–13. doi: 10.1093/nar/gkn923

29. Shashoa NAA, Salem NA, Jleta IN, Abusaeeda O. Classification depend on linear discriminant analysis using desired outputs, in: Proceedings in the 2016 17th International Conference on Sciences and Techniques of Automatic Control and Computer Engineering (STA), (Sousse, Tunisia: New York: IEEE) (2016). 19–21 p.

30. Tang YC. Deep learning using linear support vector machines. *Challenges in Representation Learning Workshop* (Atlanta, GA, USA: ICML) (2013).

31. Saffari A, Leistner C, Santner J, Godec M, Bischof H. On-line random forests, in: *2009 IEEE 12th International Conference on Computer Vision Workshops, ICCV Workshops*, (Koyoto, Japan: IEEE) (2009). 1393-1400 p.

32. Shao Z, Er MJ. Efficient leave-One-Out cross-validation-based regularized extreme learning machine. *Neurocomputing* (2016) 194:260–70. doi: 10.1016/j.neucom.2016.02.058

33. Cawley GC, Talbot NL. Fast exact leave-one-out cross-validation of sparse least-squares support vector machines. *Neural Netw* (2004) 17(10):1467–75. doi: 10.1016/j.neunet.2004.07.002

34. Kearns M, Ron D. Algorithmic stability and sanity-check bounds for leave-one-out cross-validation. *Neural Comput* (1999) 11(6):1427–53. doi: 10.1162/089976699300016304

35. Wu J, Mei J, Wen S, Liao S, Chen J, Shen Y. A self-adaptive genetic algorithm-artificial neural network algorithm with leave-one-out cross validation for descriptor selection in QSAR study. *J Comput Chem* (2010) 31(10):1956–68. doi: 10.1002/jcc.21471

36. Hajian-Tilaki K. Receiver operating characteristic (ROC) curve analysis for medical diagnostic test evaluation. *Caspian J Intern Med* (2013) 4(2):627–35.

37. Hanley JA, McNeil BJ. The meaning and use of the area under a receiver operating characteristic (ROC) curve. *Radiology* (1982) 143(1):29–36. doi: 10.1148/radiology.143.1.7063747

38. Halloran PF, Pereira AB, Chang J, Matas A, Picton M, De Freitas D, et al. Potential impact of microarray diagnosis of T cell-mediated rejection in kidney transplants: The INTERCOM study. *Am J Transpl* (2013) 13(9):2352–63. doi: 10.1111/ajt.12387

39. Reeve J, Sellares J, Mengel M, Sis B, Skene A, Hidalgo L, et al. Molecular diagnosis of T cell-mediated rejection in human kidney transplant biopsies. *Am J Transpl* (2013) 13(3):645–55. doi: 10.1111/ajt.12079

40. Zhang P, Lehmann BD, Shyr Y, Guo Y. The utilization of formalin fixed-Paraffin-Embedded specimens in high throughput genomic studies. *Int J Genomics* (2017) 2017:1926304. doi: 10.1155/2017/1926304

41. Vonbrunn E, Ries T, Sollner S, Muller-Deile J, Buttner-Herold M, Amann K, et al. Multiplex gene analysis reveals T-cell and antibody-mediated rejection-specific upregulation of complement in renal transplants. *Sci Rep* (2021) 11(1):15464. doi: 10.1038/s41598-021-94954-3

42. Piehowski PD, Petyuk VA, Sontag RL, Gritsenko MA, Weitz KK, Fillmore TL, et al. Residual tissue repositories as a resource for population-based cancer proteomic studies. *Clin Proteomics* (2018) 15:26. doi: 10.1186/s12014-018-9202-4

43. Decramer S, Gonzalez de Peredo A, Breuil B, Mischak H, Monsarrat B, Bascands JL, et al. Urine in clinical proteomics. *Mol Cell Proteomics* (2008) 7(10):1850–62. doi: 10.1074/mcp.R800001-MCP200

44. Rai AJ, Gelfand CA, Haywood BC, Warunek DJ, Yi J, Schuchard MD, et al. HUPO plasma proteome project specimen collection and handling: towards the standardization of parameters for plasma proteome samples. *Proteomics* (2005) 5(13):3262–77. doi: 10.1002/pmic.200401245

45. Anderson NL, Anderson NG. The human plasma proteome: history, character, and diagnostic prospects. *Mol Cell Proteomics* (2002) 1(11):845–67. doi: 10.1074/mcp.R200007-MCP200

46. Liebermeister W, Noor E, Flamholz A, Davidi D, Bernhardt J, Milo R. Visual account of protein investment in cellular functions. *Proc Natl Acad Sci USA* (2014) 111(23):8488–93. doi: 10.1073/pnas.1314810111

47. Franco B, Mueller HY, Li C, Snopkowski C, Dadhania DM, Xiang JZ, et al. Adaptive immune landscape of T-cell mediated rejection of human kidney allografts. *bioRxiv* (2022). doi: 10.1101/2022.05.15.492021

48. Eisenhut M. Changes in ion transport in inflammatory disease. *J Inflamm (Lond)* (2006) 3:5. doi: 10.1186/1476-9255-3-5

49. Domingo-Fernandez R, Coll RC, Kearney J, Breit S, O'Neill LAJ. The intracellular chloride channel proteins CLIC1 and CLIC4 induce IL-1beta transcription and activate the NLRP3 inflammasome. *J Biol Chem* (2017) 292(29):12077–87. doi: 10.1074/jbc.M117.797126

50. Karin M. Inflammation-activated protein kinases as targets for drug development. *Proc Am Thorac Soc* (2005) 2(4):386–90; discussion 94-5. doi: 10.1513/pats.200504-034SR

51. Bekkelund SI, Johnsen SH. Creatine kinase is associated with reduced inflammation in a general population: The tromso study. *PloS One* (2018) 13(5):e0198133. doi: 10.1371/journal.pone.0198133

52. Feng J, Li H, Li J, Meng P, Wang L, Liu C, et al. hnRNPK knockdown alleviates NLRP3 inflammasome priming by repressing FLIP expression in Raw264.7 Macrophages. *Redox Rep* (2020) 25(1):104–11. doi: 10.1080/13510002.2020.1857157

53. Bonaccorsi-Riani E, Danger R, Lozano JJ, Martinez-Picola M, Kodela E, Mas-Malavila R, et al. Iron deficiency impairs intra-hepatic lymphocyte mediated immune response. *PloS One* (2015) 10(8):e0136106. doi: 10.1371/journal.pone.0136106

54. Delmastro-Greenwood MM, Piganelli JD. Changing the energy of an immune response. *Am J Clin Exp Immunol* (2013) 2(1):30–54.

55. Ekert PG, Vaux DL. Apoptosis and the immune system. *Br Med Bull* (1997) 53(3):591–603. doi: 10.1093/oxfordjournals.bmb.a011632

56. Lei ZN, Teng QX, Tian Q, Chen W, Xie Y, Wu K, et al. Signaling pathways and therapeutic interventions in gastric cancer. *Signal Transduct Target Ther* (2022) 7(1):358. doi: 10.1038/s41392-022-01190-w

57. Hassan M, Butt A, Baba M. *Logistic regression versus neural networks: The best accuracy in prediction of diabetes disease*. (Coimbatore, India: The Research Publication) (2017). 33-42 p.

58. Khanna D, Sahu R, Baths V, Deshpande B. Comparative study of classification techniques (SVM, logistic regression and neural networks) to predict the prevalence of heart disease. *Int J Mach Learn Computing* (2015) 5:414–9. doi: 10.7763/IJMLC.2015.V5.544

59. Muthuvel M, Sivaraju D, Ramamoorthy G. *Analysis of heart disease prediction using various machine learning techniques*. (Coimbatore, India: Springer Cham) (2019).

frontiers | Frontiers in Immunology

TYPE Perspective
PUBLISHED 23 February 2023
DOI 10.3389/fimmu.2023.1124249

OPEN ACCESS

EDITED BY
Long Zheng,
The second Affiliated Hospital of Zhejiang University School of Medicine, China

REVIEWED BY
Fei Fang,
Michigan State University, United States
Wei Wang,
Tongji University, China

*CORRESPONDENCE
Ibrahim Batal
ib2349@cumc.columbia.edu

SPECIALTY SECTION
This article was submitted to Alloimmunity and Transplantation, a section of the journal Frontiers in Immunology

RECEIVED 14 December 2022
ACCEPTED 06 February 2023
PUBLISHED 23 February 2023

CITATION
Batal I, Khairallah P, Weins A, Andeen NK and Stokes MB (2023) The role of HLA antigens in recurrent primary focal segmental glomerulosclerosis. *Front. Immunol.* 14:1124249. doi: 10.3389/fimmu.2023.1124249

The role of HLA antigens in recurrent primary focal segmental glomerulosclerosis

Ibrahim Batal[1]*, Pascale Khairallah[2], Astrid Weins[3], Nicole K. Andeen[4] and Michael B. Stokes[1]

[1]Pathology and Cell Biology, Columbia University Irving Medical Center, New York, NY, United States, [2]Medicine, Division of Nephrology, Columbia University Irving Medical Center, New York, NY, United States, [3]Pathology, Brigham and Women's Hospital and Harvard Medical School, Boston, MA, United States, [4]Pathology, Oregon Health & Science University, Portland, OR, United States

Primary focal segmental glomerulosclerosis (FSGS), typically characterized by diffuse podocyte foot process effacement and nephrotic syndrome (diffuse podocytopathy), is generally attributed to a circulating permeability factor. Primary FSGS can recur after transplantation where it manifests as diffuse foot process effacement in the early stages, with subsequent evolution of segmental sclerotic lesions. Previous published literature has been limited by the lack of stringent selection criteria to define primary FSGS. Although immunogenetic factors play an important role in many glomerular diseases, their role in recurrent primary FSGS post-transplantation has not been systematically investigated. To address this, we retrospectively studied a multicenter cohort of 74 kidney allograft recipients with end stage kidney disease due to primary FSGS, confirmed by clinical and histologic parameters. After adjusting for race/ethnicity, there was a numeric higher frequency of HLA-A30 antigen in primary FSGS (19%) compared to each of 22,490 healthy controls (7%, adjusted OR=2.0, P=0.04) and 296 deceased kidney donors (10%, OR=2.1, P=0.03). Within the group of transplant patients with end stage kidney disease due to primary FSGS, donor HLA-A30 was associated with recurrent disease (OR=9.1, P=0.02). Multivariable time-to-event analyses revealed that recipients who self-identified as Black people had lower risk of recurrent disease, probably reflecting enrichment of these recipients with *APOL1* high-risk genotypes. These findings suggest a role for recipient and donor immunogenetic makeup in recurrent primary FSGS post-transplantation. Further larger studies in well-defined cohorts of primary FSGS that include high-resolution HLA typing and genome-wide association are necessary to refine these hereditary signals.

KEYWORDS

recurrent focal segmental glomerular sclerosis, kidney allograft, HLA, diffuse podocytopathy, focal segment glomerulosclerosis

Abbreviations: BMI, body mass index; BWH, Brigham and Women's Hospital; CUIMC, Columbia University Irving Medical Center; DP, diffuse podocytopathy; ESKD, end stage kidney disease; FSGS, focal segmental glomerulosclerosis; GWAS, genome-wide association studies; KDIGO, Kidney Disease Improving Global Outcomes; OHSU, Oregon Health & Science University.

Introduction

Focal segmental glomerulosclerosis (FSGS) is a histologic pattern of glomerular scarring associated with diverse forms of kidney damage (1). Primary FSGS is characterized by diffuse foot process effacement with nephrotic syndrome (diffuse podocytopathy; DP). The pathogenesis of primary FSGS remain unknown but clinical and experimental evidence support the existence of circulating permeability factor(s) that causes primary diffuse podocyte injury (1), which, lead to podocyte loss, segmental adhesion of the injured tuft to Bowman's capsule (segmental glomerulosclerosis) and eventually to global glomerulosclerosis (2). Since these putative permeability factors remain poorly characterized, the diagnosis of primary FSGS currently relies on clinical and pathologic findings, and exclusion of known secondary causes.

Primary FSGS can recur following kidney transplantation and has a negative impact on graft survival. Recurrent primary FSGS manifests initially as nephrotic syndrome and diffuse foot process effacement, identical to minimal change disease (MCD), while segmental sclerotic lesions develop later (3, 4), probably reflecting cumulative podocyte depletion in susceptible individuals (5).

In addition to primary FSGS, the 2021 Kidney Disease Improving Global Outcomes (KDIGO) classification of FSGS includes three other categories (1) Secondary FSGS, caused by viruses, drugs, or, more commonly, adaptive responses to reduction of functioning nephrons and compensatory glomerular hyperfiltration, usually associated with focal foot process effacement and subnephrotic proteinuria (2) Genetic FSGS, which is most commonly monogenic in nature, and include familial, syndromic, and sporadic cases, and (3) Undetermined FSGS, characterized by focal foot process effacement, proteinuria without the nephrotic syndrome, and no identified secondary or genetic causes (6).

However, the current classification of FSGS is not ideal. The diagnosis of secondary FSGS can be difficult as, depending on the time of presentation, viral and drug-induced causes may go unnoticed. Diagnosing genetic FSGS is also challenging. While the most common monogenic causes of FSGS can now be efficiently identified using targeted gene panels, the list of genetic causes is continually expanding (7). Furthermore, it is increasingly apparent that common inherited variants, such as HLA polymorphisms, may also contribute to the risk of primary FSGS (8), which complicates the current definition of genetic FSGS. Equally important, classifying FSGS in patients with Apolipoprotein L1 (*APOL1*) kidney risk variants is particularly problematic (9). Nephropathic *APOL1* variants occur with high frequency but low penetrance in populations with recent African ancestry, and may contribute to a higher incidence of kidney diseases from diverse etiologies (e.g., HIV-associated nephropathy, COVID-19 associated nephropathy, lupus nephritis, and hypertensive nephrosclerosis) (10, 11). That said, investigators from Mayo Clinic have shown that defining primary FSGS based on the presence of nephrotic syndrome and >80% foot process effacement is effective in excluding adaptive and monogenic forms of FSGS (12).

Despite the negative impact of recurrent DP on allograft survival (13), our knowledge of the immunologic and inherited factors associated with disease recurrence is extremely limited. This reflects the small sample size of published studies, the difficulty of completely excluding non-primary forms of FSGS, and the fact that FSGS in the allograft may arise from etiologies other than recurrent disease (e.g., adaptive FSGS from reduced nephron number and drug toxicity). In this report, we use the more expansive term DP to include cases of early recurrent primary FSGS that are characterized by nephrotic syndrome with complete or near-complete foot process effacement (≥ 80% of glomerular capillary surface area) but lack segmental sclerosis on light microscopy (14, 15).

Previous studies by us and others showed an association between donor inherited factors and recurrence of both membranous nephropathy (16, 17) and IgA nephropathy (18). We hypothesized that immunogenetic background in the donors and/or the recipients contributes to the development of recurrent DP/primary FSGS. In this report, we examined the frequency of HLA antigens in a large multicenter cohort of kidney transplant patients with end stage kidney disease (ESKD) attributed to DP/primary FSGS. Here for the first time we show that patients with ESKD due to primary FSGS tend to be enriched with HLA-A30 antigen while donor HLA-A30 is associated with increased risk of recurrent disease after transplantation.

Material and methods

This study was a retrospective multicenter study that included the pathology archives of three North American medical centers: Columbia University Irving Medical Center (CUIMC, New York, NY), Brigham and Women's Hospital (BWH, Boston, MA), and Oregon Health & Science University (OHSU, Portland, OR). Each center collected data under approval by their Institutional Review Boards.

In this report, strict inclusion criteria were used to select our cohort:

(1) Recurrent DP (n=47) was defined as recurrence of nephrotic syndrome (proteinuria ≥ 3.5 g and serum albumin ≤ 3.5 g/dL) in kidney allograft recipients with ESKD attributed to DP/FSGS, accompanied by allograft biopsies (performed in all but one recipient) showing foot process effacement involving ≥ 80% of glomerular capillary surface area. The remaining patient had a biopsy-proven MCD in the native kidney followed by FSGS, and presented 8 days after transplantation with nephrotic syndrome (urine protein/creatinine: 10 g/g and serum albumin 1.6 g/dL) and serum creatinine of 1.1 mg/dL. Native kidney biopsies and/or pathology reports were available for 29 of these subjects and showed FSGS (n=21) and MCD (n=8, including 7 patients with subsequent native kidney biopsies that showed FSGS). The remaining 18 cases had a clinical diagnosis of FSGS but pathologic materials were not available for re-review.

(2) Non-recurrent DP (n=27) was defined as absence of nephrotic syndrome post-transplantation in kidney transplant recipients who developed nephrotic syndrome in their native

kidney (≥ 3.5 g of proteinuria and ≤ 3.5 g/dL of serum albumin) with a concurrent native kidney biopsy showing near complete foot process effacement (involving ≥ 80% of the glomerular capillary surface area). Of these, 24 subjects had native kidney biopsy showing FSGS and 3 demonstrated MCD (including 2 patients with subsequent native biopsies showing development of FSGS).

Serologic and/or molecular typing for HLA-A, -B, -DR, and -DQ was performed for both donors and recipients. The outcome was recurrence of DP in the kidney allograft and the subjects were censored at loss of follow-up or allograft failure. Studied variables including recipient demographics (age, sex, and race), donor demographics, allograft source, HLA-mismatch (A, B, and DR: scale 0-6), prior kidney transplant, and induction immunotherapy, were extracted from the medical record.

To test which HLA antigens that are potentially associated with DP, the most frequent HLA antigens in our transplant cohort were compared to two group of controls:

(1) External controls of healthy US residents (n=22,490) from National Bone Marrow Donor Program (19), providing HLA allelic frequencies for reference comparisons.

(2) Internal controls of deceased kidney donors whose kidneys were transplanted at CUIMC in 2010 onwards that were matched with our cohort of DP patients with regard to self-reported ancestry (n=296; for each patient with DP, four deceased donors were matched by ancestry).

Statistical analyses were performed using Prism 9 (Graphpad Inc, San Diego, CA) and SPSS Statistics, 26.0 (IBM, Armonk, NY). Categorical data were compared using Fisher Exact test while continuous data were compared using the Mann-Whitney test. With the except of discovery study, P less than 0.05 with two-sided hypothesis testing were considered statistically significant.

Results

Basic characteristics of transplant patients with ESKD attributed to DP/primary FSGS

We identified 74 kidney allograft recipients who had ESKD due to DP/primary FSGS [CUIMC (n=60), OHSU (n=9), and BWH (n=5)]. Subjects were followed-up for a median of 68 (IQRs: 17, 107) months after transplantation. During follow-up, 47 (64%) patients developed recurrent disease [median 34 (IQRs: 12, 210) days post-transplantation] and 40 (54%) developed allograft failure [median 26 (IQRs: 14, 70) months after transplantation].

The median age at transplantation was 35 years (Supplemental Table 1). The cohort included 51% women, 27% Black recipients, 9% with prior kidney transplant, 40% recipients of living-related allografts, and a median donor-recipient HLA mismatch of 4. Donors had a median age of 35 years and included 57% women and 27% Black subjects. Most of the patients received induction therapy with a depleting agent (83%; including 76% with Thymoglobulin and 7% with Alemtuzumab) (Supplemental Table 1).

DP/Primary FSGS in the native kidney is associated with high frequency of HLA-A30 antigen

We initially identified the most frequent HLA antigens in all 74 recipients in this cohort [A2: 45%, A1: 20%, and A30: 19% in the A region; B44: 19%, B51: 18%, and B35: 16% in the B region; DR15: 28%, DR4: 27%, and DR7: 24% in the DR region; and DQ6: 47%, DQ7: 41%, and DQ2: 29% in the DQ region] (Supplemental Table 2).

We compared the frequency of these antigens to external healthy controls (n=22,490) (19). Since 12 HLA antigens have been compared, a Bonferroni-corrected significance cutoff of 0.05/12 = 0.004 was utilized to define statistical significance. HLA-A30 was the only antigen that was more prevalent in recipients with DP (OR=3.0, P=0.0008). However, this particular antigen, which is typically more prevalent in Black people (Supplemental Table 2), did not reach Bonferroni-threshold for statistical significance after adjusting for race/ethnicity using Cochran–Mantel–Haenszel test (adjusted OR=2.0, P=0.04) (Figure 1A). Using conditional logistic regression conditioned on self-reported race/ethnicity matching, HLA-A30 was more common in DP compared to a second set of controls composed of 296 deceased kidney donors matched by race/ethnicity [14/74 (19%) vs. 29/296 (10%), OR=2.1, P=0.03] (Figure 1A).

HLA-A30 antigen in the donor is associated with recurrent DP/primary FSGS

To test whether HLA-A30 is associated with recurrent DP, we compared the frequencies of this antigen in both recipients and donors with recurrent and non-recurrent disease. While the proportion of recipient HLA-A30 was not significantly different [6/47 (13%) recurrent vs. 8/27 (30%) non-recurrent, P=0.12], the frequency of donor HLA-A30 was higher in recurrent disease [12/45 (27%) recurrent DP vs. 1/26 (4%) non-recurrent DP, OR=9.1, P=0.02)] (Figure 1B). Despite the small sample size, the results for the association between HLA-A30 and recurrent disease remained significant even after adjustment for donor age and donor Black race (binary logistic regression: OR=11.0, P=0.03). The frequency of other HLA antigens did not differ between recurrent and non-recurrent diseases (Supplemental Table 3). Overall, donor HLA-A30 had 96% specificity, 27% sensitivity, 92% positive predictive value, and 43% negative predictive value for predicting recurrence of DP (Supplemental Table 4). The breakdown for the association of HLA-A30 in the recipients and donors with recurrent disease is also presented in Supplemental Table 5.

Black recipients have lower risk of developing recurrent DP/primary FSGS

To identify independent predictors for recurrent DP, all transplant patients with ESKD due to DP (n=74) were studied in a time-to event model, where DP recurrence was considered as the outcome of interest (Table 1). Univariable and multivariable

10.3389/fimmu.2023.1124249

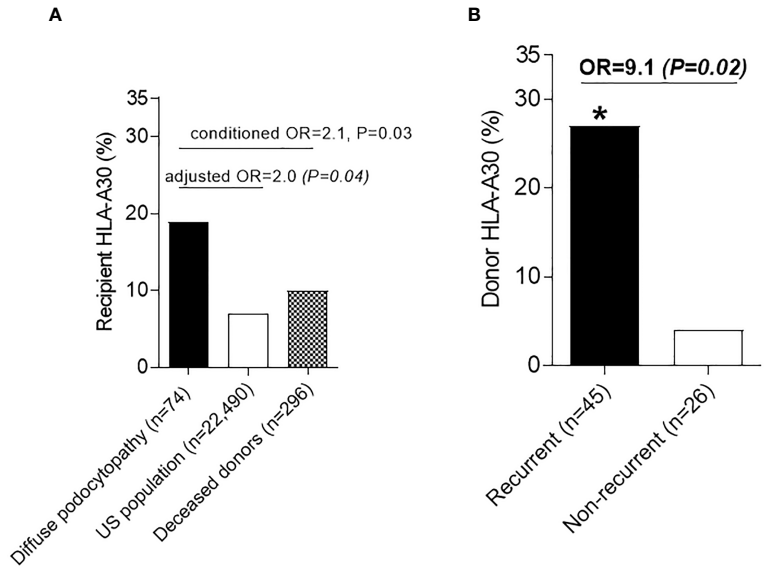

FIGURE 1
Human Leukocyte antigens in diffuse podocytopathy **(A)** Prevalence of HLA-A30 antigen in cases with diffuse podocytopathy (patients with end stage kidney disease due to diffuse podocytopathy, n=74) compared to US population (n=22,490) and deceased kidney donors matched to cases with regard to race/ethnicity (n=296). **(B)** Prevalence of HLA-A30 in the kidney donors of patients with recurrent (n=42) vs. non-recurrent (n=22) diffuse podocytopathy. Donor typing for class-I was not available for 2 donors with recurrent diseases and 1 without recurrent disease. * (significant P value).

analyses showed that Black recipient race was the only independent variable associated with the outcome, where it was protective against recurrent disease [(aHR)=0.31, P=0.008] (Table 1). When the relation between recipient Black recipients and recurrent DP was explored further, we found that 4/5 (80%) of self-identified Black recipients with non-recurrent disease that were genotyped for *APOL1* had high-risk genotypes (3 G1/G1 and 1 G1/G2).

Discussion and perspectives

Primary FSGS and MCD are DP, characterized by diffuse foot process effacement and nephrotic syndrome (6). In the native kidney, there is growing recognition that abnormalities of T and B cell immunity are common in DP and may play a pathogenic role (20). This includes the association with allergy, immunization, and

TABLE 1 Univariable and multivariable analyses of the associations with recurrent disease in patients with end stage kidney disease due to diffuse podocytopathy.

Variables	Univariable (n=74)			Multivariable (n=71), events=45	
	N events	HR (95% CI)	P value	aHR (95% CI)	P value
Recipient age at transplant (per each year)	47	0.99 (0.97 – 1.01)	0.49		
Recipient female gender	47	1.21 (0.68 – 2.16)	0.51		
Black recipient	47	0.26 (0.11 – 0.62)	0.002	0.31 (0.13 – 0.74)	0.008
Black donor	45	0.68 (0.34 – 1.38)	0.28		
Allograft source (living-related)	47	1.44 (0.81 – 2.56)	0.21		
Number of HLA mismatches (per antigen: 0-6)	45	0.81 (0.64 – 1.01)	0.07	0.86 (0.67 – 1.10)	0.22
Recipient HLA-A30	47	0.52 (0.22 – 1.23)	0.14		
Donor HLA-A30	45	1.90 (0.97 – 3.71)	0.06	1.66 (0.85 – 3.24)	0.14
Prior kidney transplantation	47	1.06 (0.42 – 2.69)	0.90		
Induction therapy with depletion agent	36	0.55 (0.25 – 1.21)	0.14		

Cox proportional hazards models were constructed to account for confounders. All factors that demonstrated a suggestive association with the outcome (P value <0.1) at the univariable analysis were included in the multivariable cox proportional hazards models. Individuals with missing information on a tested predictor were excluded from the corresponding univariable time-to-event analysis; individuals with missing data in one or more predictors at the multivariable analyses were also excluded from the latter analyses.

B cell neoplasms, as well as responsiveness to immunomodulatory therapies, including corticosteroid therapy and B cell depletion (21, 22). With regard to inherited factors, genome-wide association studies (GWAS) have shown that steroid-sensitive nephrotic syndrome, including MCD and primary FSGS, is associated with genomic susceptibility loci in HLA regions (23–25) and non-HLA regions (23, 26), most of which are linked to the immune system. Lastly, in addition to other associations, nephropathic *APOL1* genotypes have also been linked to FSGS (27), sometimes with diffuse foot process effacement. Together, these findings suggest that DP/primary FSGS is a polygenic disease associated with immune dysregulation and immunogenetic susceptibility.

Although the pathogenesis of recurrent DP post-transplantation is unknown, the existence of a circulating glomerular permeability factor is supported by several observations, including rapid recurrence of the nephrotic syndrome following transplantation, induction of proteinuria in the rat using serum from a patient with recurrent FSGS (28), and resolution of recurrent nephrotic syndrome following re-transplantation of the kidney into a different recipient (29).

Uffing et al. published the largest study to date of recurrent FSGS in the kidney allograft, which included 176 kidney transplant recipients who developed ESKD from FSGS (13). In addition to the association with White recipient race, older recipient age, and history of bilateral nephrectomy, this study showed a significant association between recurrent FSGS and lower recipient body mass index (BMI) (13). The latter finding may reflect the association between higher BMI and adaptive FSGS secondary to obesity in the native kidney, which is unlikely to recur early after transplantation in the form of nephrotic syndrome. Interestingly, a few prior studies have shown that young recipient age, rather than old recipient age as shown by Uffing et al., was a risk factor for FSGS recurrence (30, 31). Furthermore, depending on the study, recurrence rate for primary FSGS in the kidney allograft varies from 20% to 52% of cases (32, 33). These contradicting results suggest contamination of the previously studied cohorts by secondary forms of FSGS and support the crucial need for using rigorous criteria to exclude non-primary cases of FSGS when studying disease recurrence after transplantation.

Although HLA antigens have emerged as important immunogenetic risk factors in many immune-mediated kidney diseases (34–37), their role in recurrent disease has not been systematically examined in a pure cohort of DP/primary FSGS. One study attempted to assess this issue in a pediatric transplant population with ESKD attributed to FSGS and found an association between recurrent FSGS and a few HLA class-II antigens, including DQ2, DR7, and DR53 (38). However, that study was registry-based and lacked data on clinical and histologic parameters at time of diagnosis of FSGS in the native kidney, which further increases the possibility of selection bias and contamination by non-primary forms of FSGS, which in our experience comprise the bulk of cases labeled as FSGS-induced ESKD.

In this report, we used stringent inclusion criteria requiring the presence of both nephrotic syndrome (≥ 3.5 g of proteinuria, ≤ 3.5 g/dL serum albumin) and ≥ 80% of foot process effacement to assemble a relatively pure cohort of DP/primary FSGS (15). Despite the contribution of three major transplant centers, we only could identify 74 transplant patients fulfilling our rigorous selection criteria. Notably, our study showed that several patients with ESKD due to primary FSGS had prior native kidney biopsies that demonstrated MCD. These findings further support the intimate association between these two morphologic manifestations of DP.

Although not reaching statistical significance by Bonferroni criteria in this relatively small sample, our data suggested an association between primary FSGS in the native kidney and HLA-A30 antigen. Prior studies have shown an association between HLA-A30 and several autoimmune diseases, including type 1 diabetes mellitus, vitiligo, and systemic sclerosis (39–41), which suggest that HLA-A30 may contribute to immune dysregulation. Our study also demonstrated an association between HLA-A30 in the donor and recurrent primary FSGS. It is conceivable that donor HLA antigens may influence antigen presentation by donor immune cells or podocytes, which can function as antigen-presenting cells (42), cross reactivity/molecular mimicry, or acceleration of podocyte death in immunologically susceptible patients.

Despite the high positive predictive value (92%) of HLA-A30 in predicting recurrent disease, it was not surprising that this relatively low frequency HLA antigen, which has a prevalence of 7% in the general population and 19% in patients with ESKD secondary to primary FSGS, did not reach statistical significance as an independent predictor for recurrent disease in this small cohort.

With regard to recipient inherited factors, a few prior studies have shown that White recipient race is a risk factor for developing recurrent FSGS (13, 43, 44). We propose that White recipient race may not be a real risk factor but rather may be confounded by the genetic make-up in Black recipients, in whom FSGS may be less likely to recur after receiving a kidney from a donor with a different genomic constitution. Indeed, multivariable analyses in the current study showed lower risk of recurrence in Black subjects with FSGS/DP. This might reflect the increased prevalence of high-risk *APOL1* genotypes (80%) in Black recipients with non-recurrent DP. It is now well accepted that donor *APOL1* kidney risk variants may be a risk factor for podocyte damage in the kidney allograft (45, 46) while *APOL1* status in the recipient is less likely to influence recurrent disease. Importantly, while it is still unclear how to classify FSGS in patients with *APOL1* high-risk genotypes, it would be interesting in the future to systematically assess *APOL1* genotypes in recipients with vs. without recurrent DP/primary FSGS.

Our findings should be interpreted in light of several limitations, including small sample size, low resolution of HLA typing, lack of HLA-DQ typing in several recipients and donors, lack of *APOL1* genotyping in most Black recipients, and the lack of detailed clinical history (e.g., recipient BMI and whether native kidney nephrectomies were performed or not).

In conclusion, a strict definition of recurrent DP/primary FSGS is an initial step to advance our understanding of recurrent disease after transplantation. Our pilot study represents the first attempt to systematically assess immunogenetic predictors of recurrent disease

in a well-defined cohort of transplant patients with ESKD attributed to DP/primary FSGS. Our results suggest that donor HLA-A30 is a potential risk factors for recurrent DP/primary FSGS while Black recipient race may be a potential protective factor. However, it is still possible that the observed association between HLA-A30 and primary FSGS is affected by the differential distribution of HLA-A30 across worldwide populations. Therefore, future larger GWAS studies that properly control for genetic ancestry are crucial to examine the effects of HLA-A30 in a more comprehensive manner, to refine the donor and recipient genomic signals contributing to recurrent primary FSGS, and to obtain better insights into the pathobiology of recurrent DP (47). The ultimate goals of such efforts would be to guide the clinician towards improving donor-recipient matching and develop targeted approaches to prevent recurrence and improve allograft survival.

Data availability statement

The original contributions presented in the study are included in the article/Supplementary Material. Further inquiries can be directed to the corresponding author.

Ethics statement

The studies involving human participants were reviewed and approved by Columbia University Institutional Review Board. Written informed consent from the participants' legal guardian/next of kin was not required to participate in this study in accordance with the national legislation and the institutional requirements.

Author contributions

IB participated in research design, performance of research, data analyses, and in the writing of the manuscript. PK participated in performance of research and writing of the manuscript. AW participated in research design, performance of research, and writing the manuscript. NA participated in research design, performance of research, and writing the manuscript. MBS participated in research design and writing of manuscript. PK is currently at the Baylor College of Medicine Houston, TX. All authors contributed to the article and approved the submitted version.

Funding

IB is supported by the 2022 Nelson Faculty Development Award. AW is supported by a NephCure Kidney International – NephCure-Neptune Ancillary Study Award.

Acknowledgments

We thank Carley Shaut (Medicine, Division of Nephrology, Oregon Health & Science University), Melissa Yeung (Medicine, Division of Nephrology, Brigham and Women's Hospital and Harvard Medical School), Xiaoyi Ye (Medicine, Division of Nephrology, Hartford Hospital), Emily Daniel, Hilda Fernandez, and Francesca Zanoni (Medicine, Division of Nephrology, Columbia University Irving Medical Center), and Geo Serban and Elena-Rodica Vasilescu (Pathology and Cell Biology, Columbia University Irving Medical Center) for providing missing clinical and laboratory data. We thank Krzysztof Kiryluk for his advices regarding statistical analyses.

Conflict of interest

The authors declare that the research was conducted in the absence of any commercial or financial relationships that could be constructed as a potential conflict of interest.

Publisher's note

Supplementary material

The Supplementary Material for this article can be found online at: https://www.frontiersin.org/articles/10.3389/fimmu.2023.1124249/full#supplementary-material

References

1. D'Agati VD, Kaskel FJ, Falk RJ. Focal segmental glomerulosclerosis. *N Engl J Med* (2011) 365(25):2398–411. doi: 10.1056/NEJMra1106556

2. Lim BJ, Yang JW, Do WS, Fogo AB. Pathogenesis of focal segmental glomerulosclerosis. *J Pathol Transl Med* (2016) 50(6):405–10. doi: 10.4132/jptm.2016.09.21

3. Nadasdy T, Ivanyi B, Marofka F, Orvos H, Mohacsi G, Ormos J. Two cases of recurrent focal and segmental glomerulosclerosis in renal allografts. *Nephrol Dial Transplant.* (1991) 6(5):375–6. doi: 10.1093/ndt/6.5.375

4. Schachter ME, Monahan M, Radhakrishnan J, Crew J, Pollak M, Ratner L, et al. Recurrent focal segmental glomerulosclerosis in the renal allograft: Single center experience in the era of modern immunosuppression. *Clin Nephrol.* (2010) 74 (3):173–81. doi: 10.5414/CNP74173

5. Maas RJ, Deegens JK, Smeets B, Moeller MJ, Wetzels JF. Minimal change disease and idiopathic FSGS: manifestations of the same disease. *Nat Rev Nephrol.* (2016) 12 (12):768–76. doi: 10.1038/nrneph.2016.147

6. Rovin BH, Adler SG, Barratt J, Bridoux F, Burdge KA, Chan TM. Kidney disease: Improving global outcomes glomerular diseases work g. KDIGO 2021 clinical practice guideline for the management of glomerular diseases. *Kidney Int* (2021) 100(4S):S1–S276. doi: 10.1016/j.kint.2021.05.021

7. Sambharia M, Rastogi P, Thomas CP. Monogenic focal segmental glomerulosclerosis: A conceptual framework for identification and management of a heterogeneous disease. *Am J Med Genet C Semin Med Genet* (2022) 190(3):377–98. doi: 10.1002/ajmg.c.31990

8. Gerbase-DeLima M, Pereira-Santos A, Sesso R, Temin J, Aragao ES, Ajzen H. Idiopathic focal segmental glomerulosclerosis and HLA antigens. *Braz J Med Biol Res* (1998) 31(3):387–9. doi: 10.1590/S0100-879X1998000300010

9. Dummer PD, Limou S, Rosenberg AZ, Heymann J, Nelson G, Winkler CA, et al. APOL1 kidney disease risk variants: An evolving landscape. *Semin Nephrol.* (2015) 35 (3):222–36. doi: 10.1016/j.semnephrol.2015.04.008

10. Daneshpajouhnejad P, Kopp JB, Winkler CA, Rosenberg AZ. The evolving story of apolipoprotein L1 nephropathy: The end of the beginning. *Nat Rev Nephrol.* (2022) 18(5):307–20. doi: 10.1038/s41581-022-00538-3

11. Larsen CP, Beggs ML, Saeed M, Ambruzs JM, Cossey LN, Messias NC, et al. Histopathologic findings associated with APOL1 risk variants in chronic kidney disease. *Mod Pathol* (2015) 28(1):95–102. doi: 10.1038/modpathol.2014.92

12. Miao J, Pinto EVF, Hogan MC, Erickson SB, El Ters M, Bentall AJ, et al. Identification of genetic causes of focal segmental glomerulosclerosis increases with proper patient selection. *Mayo Clin Proc* (2021) 96(9):2342–53. doi: 10.1016/j.mayocp.2021.01.037

13. Uffing A, Perez-Saez MJ, Mazzali M, Manfro RC, Bauer AC, de Sottomaior Drumond F, et al. Recurrence of FSGS after kidney transplantation in adults. *Clin J Am Soc Nephrol.* (2020) 15(2):247–56. doi: 10.2215/CJN.08970719

14. Jacobs-Cacha C, Vergara A, Garcia-Carro C, Agraz I, Toapanta-Gaibor N, Ariceta G, et al. Challenges in primary focal segmental glomerulosclerosis diagnosis: from the diagnostic algorithm to novel biomarkers. *Clin Kidney J* (2021) 14(2):482–91. doi: 10.1093/ckj/sfaa110

15. De Vriese AS, Sethi S, Nath KA, Glassock RJ, Fervenza FC. Differentiating primary, genetic, and secondary FSGS in adults: A clinicopathologic approach. *J Am Soc Nephrol.* (2018) 29(3):759–74. doi: 10.1681/ASN.2017090958

16. Batal I, Vasilescu ER, Dadhania DM, Adel AA, Husain SA, Avasare R, et al. Association of HLA typing and alloimmunity with posttransplantation membranous nephropathy: A multicenter case series. *Am J Kidney Dis* (2020) 76(3):374–83. doi: 10.1053/j.ajkd.2020.01.009

17. Berchtold L, Letouze E, Alexander MP, Canaud G, Logt AV, Hamilton P, et al. HLA-d and PLA2R1 risk alleles associate with recurrent primary membranous nephropathy in kidney transplant recipients. *Kidney Int* (2021) 99(3):671–85. doi: 10.1016/j.kint.2020.08.007

18. Kavanagh CR, Zanoni F, Leal R, Jain NG, Stack MN, Vasilescu ER, et al. Clinical predictors and prognosis of recurrent IgA nephropathy in the kidney allograft. *Glomerular Dis* (2022) 2(1):42–53. doi: 10.1159/000519834

19. Maiers M, Gragert L, Klitz W. High-resolution HLA alleles and haplotypes in the united states population. *Hum Immunol* (2007) 68(9):779–88. doi: 10.1016/j.humimm.2007.04.005

20. Campbell RE, Thurman JM. The immune system and idiopathic nephrotic syndrome. *Clin J Am Soc Nephrol* (2022) 17(12):1823–34. doi: 10.2215/CJN.07180622

21. Caster DJ, Magalhaes B, Pennese N, Zaffalon A, Faiella M, Campbell KN, et al. Efficacy and safety of immunosuppressive therapy in primary focal segmental glomerulosclerosis: A systematic review and meta-analysis. *Kidney Med* (2022) 4 (8):100501. doi: 10.1016/j.xkme.2022.100501

22. Tedesco M, Mescia F, Pisani I, Allinovi M, Casazza G, Del Vecchio L, et al. The role of rituximab in primary focal segmental glomerular sclerosis of the adult. *Kidney Int Rep* (2022) 7(8):1878–86. doi: 10.1016/j.ekir.2022.05.024

23. Dufek S, Cheshire C, Levine AP, Trompeter RS, Issler N, Stubbs M, et al. Genetic identification of two novel loci associated with steroid-sensitive nephrotic syndrome. *J Am Soc Nephrol.* (2019) 30(8):1375–84. doi: 10.1681/ASN.2018101054

24. Debiec H, Dossier C, Letouze E, Gillies CE, Vivarelli M, Putler RK, et al. Transethnic, genome-wide analysis reveals immune-related risk alleles and phenotypic correlates in pediatric steroid-sensitive nephrotic syndrome. *J Am Soc Nephrol.* (2018) 29(7):2000–13. doi: 10.1681/ASN.2017111185

25. Jia X, Horinouchi T, Hitomi Y, Shono A, Khor SS, Omae Y, et al. Strong association of the HLA-DR/DQ locus with childhood steroid-sensitive nephrotic syndrome in the Japanese population. *J Am Soc Nephrol.* (2018) 29(8):2189–99. doi: 10.1681/ASN.2017080859

26. Jia X, Yamamura T, Gbadegesin R, McNulty MT, Song K, Nagano C, et al. Common risk variants in NPHS1 and TNFSF15 are associated with childhood steroid-sensitive nephrotic syndrome. *Kidney Int* (2020) 98(5):1308–22. doi: 10.1016/j.kint.2020.05.029

27. Friedman DJ, Pollak MR. APOL1 nephropathy: From genetics to clinical applications. *Clin J Am Soc Nephrol.* (2021) 16(2):294–303. doi: 10.2215/CJN.15161219

28. Zimmerman SW. Increased urinary protein excretion in the rat produced by serum from a patient with recurrent focal glomerular sclerosis after renal transplantation. *Clin Nephrol.* (1984) 22(1):32–8.

29. Gallon L, Leventhal J, Skaro A, Kanwar Y, Alvarado A. Resolution of recurrent focal segmental glomerulosclerosis after retransplantation. *N Engl J Med* (2012) 366 (17):1648–9. doi: 10.1056/NEJMc1202500

30. Francis A, Trnka P, McTaggart SJ. Long-term outcome of kidney transplantation in recipients with focal segmental glomerulosclerosis. *Clin J Am Soc Nephrol.* (2016) 11(11):2041–6. doi: 10.2215/CJN.03060316

31. Hickson LJ, Gera M, Amer H, Iqbal CW, Moore TB, Milliner DS, et al. Kidney transplantation for primary focal segmental glomerulosclerosis: Outcomes and response to therapy for recurrence. *Transplantation* (2009) 87(8):1232–9. doi: 10.1097/TP.0b013e31819f12be

32. Dall'Amico R, Ghiggeri G, Carraro M, Artero M, Ghio L, Zamorani E, et al. Prediction and treatment of recurrent focal segmental glomerulosclerosis after renal transplantation in children. *Am J Kidney Dis* (1999) 34(6):1048–55. doi: 10.1016/S0272-6386(99)70010-7

33. Tejani A, Stablein DH. Recurrence of focal segmental glomerulosclerosis posttransplantation: A special report of the north American pediatric renal transplant cooperative study. *J Am Soc Nephrol.* (1992) 2(12 Suppl):S258–63. doi: 10.1681/ASN.V212s258

34. Doxiadis II, De Lange P, De Vries E, Persijn GG, Claas FH. Protective and susceptible HLA polymorphisms in IgA nephropathy patients with end-stage renal failure. *Tissue Antigens* (2001) 57(4):344–7. doi: 10.1034/j.1399-0039.2001.057004344.x

35. Klouda PT, Manos J, Acheson EJ, Dyer PA, Goldby FS, Harris R, et al. Strong association between idiopathic membranous nephropathy and HLA-DRW3. *Lancet* (1979) 2(8146):770–1. doi: 10.1016/S0140-6736(79)92118-4

36. Phelps RG, Rees AJ. The HLA complex in goodpasture's disease: a model for analyzing susceptibility to autoimmunity. *Kidney Int* (1999) 56(5):1638–53. doi: 10.1046/j.1523-1755.1999.00720.x

37. Andeen NK, Smith KD, Vasilescu ER, Batal I. Fibrillary glomerulonephritis is associated with HLA-DR7 and HLA-B35 antigens. *Kidney Int Rep* (2020) 5(8):1325–7. doi: 10.1016/j.ekir.2020.05.010

38. Shaw BI, Ochoa A, Chan C, Nobuhara C, Gbadegesin R, Jackson AM, et al. HLA loci and recurrence of focal segmental glomerulosclerosis in pediatric kidney transplantation. *Transplant Direct.* (2021) 7(10):e748. doi: 10.1097/TXD.0000000000001201

39. Deng C, Tong N, Li X. [Association of HLA-A0205 and HLA-A30 with latent autoimmune diabetes in adults]. *Sheng Wu Yi Xue Gong Cheng Xue Za Zhi.* (2010) 27 (5):1089–94.

40. Finco O, Cuccia M, Martinetti M, Ruberto G, Orecchia G, Rabbiosi G. Age of onset in vitiligo: relationship with HLA supratypes. *Clin Genet* (1991) 39(1):48–54. doi: 10.1111/j.1399-0004.1991.tb02984.x

41. Del Rio AP, Sachetto Z, Sampaio-Barros PD, Marques-Neto JF, Londe AC, Bertolo MB. HLA markers for poor prognosis in systemic sclerosis Brazilian patients. *Dis Markers.* (2013) 35(2):73–8. doi: 10.1155/2013/301415

42. Goldwich A, Burkard M, Olke M, Daniel C, Amann K, Hugo C, et al. Podocytes are nonhematopoietic professional antigen-presenting cells. *J Am Soc Nephrol.* (2013) 24(6):906–16. doi: 10.1681/ASN.2012020133

43. Abbott KC, Sawyers ES, Oliver JD3rd, Ko CW, Kirk AD, Welch PG, et al. Graft loss due to recurrent focal segmental glomerulosclerosis in renal transplant recipients in the united states. *Am J Kidney Dis* (2001) 37(2):366–73. doi: 10.1053/ajkd.2001.21311

44. Nehus EJ, Goebel JW, Succop PS, Abraham EC. Focal segmental glomerulosclerosis in children: multivariate analysis indicates that donor type does not alter recurrence risk. *Transplantation* (2013) 96(6):550–4. doi: 10.1097/TP.0b013e31829c2431

45. Santoriello D, Husain SA, De Serres SA, Bomback AS, Crew RJ, Vasilescu ER, et al. Donor APOL1 high-risk genotypes are associated with increased risk and inferior prognosis of *de novo* collapsing glomerulopathy in renal allografts. *Kidney Int* (2018) 94 (6):1189–98. doi: 10.1016/j.kint.2018.06.024

46. Oniszczuk J, Moktefi A, Mausoleo A, Pallet N, Malard-Castagnet S, Fourati S, et al. *De novo* focal and segmental glomerulosclerosis after COVID-19 in a patient with a transplanted kidney from a donor with a high-risk APOL1 variant. *Transplantation* (2021) 105(1):206–11. doi: 10.1097/TP.0000000000003432

47. Zanoni F, Khairallah P, Kiryluk K, Batal I. Glomerular diseases of the kidney allograft: Toward a precision medicine approach. *Semin Nephrol.* (2022) 42(1):29–43. doi: 10.1016/j.semnephrol.2022.01.005

frontiers | Frontiers in Immunology

TYPE Original Research
PUBLISHED 24 April 2023
DOI 10.3389/fimmu.2023.1151127

OPEN ACCESS

EDITED BY
Long Zheng,
The second Affiliated Hospital of Zhejiang University School of Medicine, China

REVIEWED BY
Lauren Higdon,
Immune Tolerance Network, United States
Bo Peng,
Central South University, China

*CORRESPONDENCE
Magali Giral
magali.giral@chu-nantes.fr
Sophie Brouard
sophie.brouard@univ-nantes.fr

†These authors have contributed equally to this work and share last authorship

SPECIALTY SECTION
This article was submitted to Alloimmunity and Transplantation, a section of the journal Frontiers in Immunology

RECEIVED 25 January 2023
ACCEPTED 06 April 2023
PUBLISHED 24 April 2023

CITATION
Mai HL, Degauque N, Lorent M, Rimbert M, Renaudin K, Danger R, Kerleau C, Tilly G, Vivet A, Le Bot S, Delbos F, Walencik A, Giral M and Brouard S (2023) Kidney allograft rejection is associated with an imbalance of B cells, regulatory T cells and differentiated CD28-CD8+ T cells: analysis of a cohort of 1095 graft biopsies. *Front. Immunol.* 14:1151127. doi: 10.3389/fimmu.2023.1151127

Kidney allograft rejection is associated with an imbalance of B cells, regulatory T cells and differentiated CD28-CD8+ T cells: analysis of a cohort of 1095 graft biopsies

Hoa Le Mai[1], Nicolas Degauque[1], Marine Lorent[1], Marie Rimbert[1,2], Karine Renaudin[1,3], Richard Danger[1], Clarisse Kerleau[1], Gaelle Tilly[1], Anaïs Vivet[1], Sabine Le Bot[1,4], Florent Delbos[5], Alexandre Walencik[5], Magali Giral[1,4,6*†] and Sophie Brouard[1,6*†] on behalf of DIVAT Consortium

[1]Centre Hospitalier Universitaire (CHU) Nantes, Nantes Université, Institut National de la Santé et de la Recherche Médicale (INSERM), Center for Research in Transplantation and Translational Immunology, Unité mixte de recherche (UMR) 1064, Institut de Transplantation Urologie-Néphrologie (ITUN), Nantes, France, [2]Laboratoire d'Immunologie, Centre d'ImmunoMonitorage Nantes-Atlantique (CIMNA), CHU Nantes, Nantes, France, [3]Service d'Anatomie et Cytologie Pathologiques, CHU Nantes, Nantes, France, [4]Service de Néphrologie et Immunologie Clinique, CHU Nantes, Nantes, France, [5]Etablissement Français du Sang (EFS), Nantes, France, [6]Fondation Centaure (RTRS), Nantes, France

Introduction: The human immune system contains cells with either effector/memory or regulatory functions. Besides the well-established CD4+CD25hiCD127lo regulatory T cells (Tregs), we and others have shown that B cells can also have regulatory functions since their frequency and number are increased in kidney graft tolerance and B cell depletion as induction therapy may lead to acute rejection. On the other hand, we have shown that CD28-CD8+ T cells represent a subpopulation with potent effector/memory functions. In the current study, we tested the hypothesis that kidney allograft rejection may be linked to an imbalance of effector/memory and regulatory immune cells.

Methods: Based on a large cohort of more than 1000 kidney graft biopsies with concomitant peripheral blood lymphocyte phenotyping, we investigated the association between kidney graft rejection and the percentage and absolute number of circulating B cells, Tregs, as well as the ratio of B cells to CD28-CD8+ T cells and the ratio of CD28-CD8+ T cells to Tregs. Kidney graft biopsies were interpreted according to the Banff classification and divided into 5 biopsies groups: 1) normal/subnormal, 2) interstitial fibrosis and tubular atrophy grade 2/3 (IFTA), 3) antibody-mediated rejection (ABMR), 4) T cell mediated-rejection (TCMR), and 5) borderline rejection. We compared group 1 with the other groups as well as with a combined group 3, 4, and 5 (rejection of all types) using multivariable linear mixed models.

Results and discussion: We found that compared to normal/subnormal biopsies, rejection of all types was marginally associated with a decrease in the percentage

of circulating B cells (p=0.06) and significantly associated with an increase in the ratio of CD28-CD8+ T cells to Tregs (p=0.01). Moreover, ABMR, TCMR (p=0.007), and rejection of all types (p=0.0003) were significantly associated with a decrease in the ratio of B cells to CD28-CD8+ T cells compared to normal/subnormal biopsies. Taken together, our results show that kidney allograft rejection is associated with an imbalance between immune cells with effector/memory functions and those with regulatory properties.

KEYWORDS

kidney transplantation, rejection, B lymphocytes, Treg, CD28-CD8+ T cells

Introduction

In kidney transplantation, T cells and B cells participate in the alloimmune responses underlying the two main forms of graft rejection, T cell-mediated rejection (TCMR) and antibody-mediated rejection (ABMR), respectively. Although B cells are known for their effector functions, namely antibody production and antigen presentation, a randomized clinical trial in 2009 studying rituximab as B cell depleting-induction therapy was prematurely terminated because acute cellular rejection occurred in 6 of 8 treated kidney graft recipients, suggesting that B cells also have regulatory functions (1). In concordance with that observation, we (2–4) and others (5) independently reported that patients with drug-free kidney transplant tolerance have increased absolute number and relative frequency of circulating B lymphocytes compared to patients with stable graft function under immunosuppression, suggesting that B cells with regulatory functions may contribute to graft tolerance. Several studies have shown that human regulatory B cells (Bregs) are contained in the plasmablast (6) and transitional B cell (7) subsets defined as CD19 +CD27+CD38+ and CD19+CD24hiCD38hi, respectively. IL-10 secretion has been shown to be an important mechanism of action of Bregs (IL-10+ Bregs) (8). Besides IL-10+ Bregs, we (9) and others (10) have identified another Breg subset that exerts their functions through the production of granzyme B (GZMB+ Bregs). Concordantly, kidney graft tolerance has been shown to be associated with an increase in circulating granzyme B-expressing B cells (9) and IL-10-expressing transitional B cells (5). In parallel, we (11, 12) and others (13) have reported that CD4 + CD25 +CD127loFoxP3+ Tregs were increased in tolerant patients compared to patients with stable renal function under immunosuppression. Therefore, it is likely that both Tregs and Bregs act in favor of immune tolerance in kidney transplantation (14, 15).

At the other end, among immune cells with effector/memory properties, CD28-CD8+ T cells are an intriguing T cell population. The interaction between CD28 on T cells and B7 on antigen-presenting cells provides the costimulatory signals necessary for T cell activation. However, chronic immune activation may down-regulate CD28 expression on CD8+ T cells. As a result, CD28-CD8 + T cells are increased in conditions or diseases associated with chronic antigenic exposure such as aging, autoimmune diseases, cancer, chronic infection, and transplantation (16, 17). Although some early studies in autoimmune disease models argued for a regulatory role of this T cell population (18, 19), we (20) and others (21) have demonstrated that human CD28-CD8+ T cells have strong cytotoxic effector function in response to alloantigen stimulation. Moreover, we also reported that CD28-CD8+ T cells are increased in kidney recipients with chronic rejection (20). To confirm those findings, we have established from 2008 to 2016 a large cohort of nearly 1500 kidney graft biopsies performed at Nantes University Hospital concomitant with a lymphocyte phenotyping by flow cytometry focusing on the CD28-CD8+ T cell population. By analyzing this cohort, we have shown that ABMR was associated with an increase in the percentage and absolute number of CD28-CD8+ T cells and those cells responded more vigorously to stimulations through T cell receptor (TCR) or FcγRIIIA (CD16) compared to their CD28+ counterparts, confirming their potent effector functions (22).

Having recognized the potential importance of B lymphocytes in transplant tolerance, from 2011 afterwards, we added B cells to the flow cytometry panel so that the later part of the aforementioned cohort contained 1095 kidney graft biopsies from 737 patients for whom the lymphocyte phenotyping included B cells in addition to CD28-CD8+ T cells and Tregs. In the current study, we analyzed this subcohort in order to explore whether there was an association between kidney graft rejection and the absolute number and relative frequency of B cells, Tregs, the ratio of B cells to CD28-CD8+ T cells, and the ratio of CD28-CD8+ T cells to Tregs. We found that kidney graft rejection was significantly associated with a decrease in the ratio of B cells to CD28-CD8+ T cells and an increase in the ratio of CD28-CD8+ T cells to Tregs. Taken together, our findings suggest that the imbalance between effector/memory and regulatory immune cells contributes to allograft rejection.

Materials and methods

Study design

As aforementioned, from 2008 to 2016, we established at Nantes University Hospital (Centre Hospitalier Universitaire or CHU de Nantes) a cohort of nearly 1500 kidney graft biopsies (protocol

"Peribiopsy N° RC13_0251") for which a peripheral lymphocyte phenotyping focusing on CD28-CD8+ T cells was performed at the time of biopsy (22). From 2011 afterward, we added B cells and Tregs to the panel so that the subcohort from 2011 to 2016 contained 1195 biopsies in which the frequency and absolute number of B cells, CD28-CD8+ T cells, and Tregs were available for analysis. Renal biopsies were interpreted by our renal pathologist (K.R.) based on the Banff 2017 Kidney Meeting Report (23) except for the diagnosis of chronic active TCMR which was based exclusively on the presence of chronic allograft arteriopathy as described in the Banff 2015 Kidney Meeting Report (24). More details on renal biopsy interpretation were described in our previous report (22). After having taken into account the clinical decision, the histological diagnoses were organized into 6 biopsy groups:

- -Group 1 (n=802): normal/subnormal or interstitial fibrosis and tubular atrophy (IFTA) grade 1.
- -Group 2 (n=56): IFTA grade 2 or 3.
- -Group 3 (n=148): ABMR or borderline rejection treated as ABMR with plasma exchanges and intravenous immunoglobulins (IVIg), with or without rituximab.
- -Group 4 (n=33): TCMR or borderline rejection treated as TMCR with corticosteroids.
- -Group 5 (n=56): borderline rejection without treatment.
- -Group 6 (n=100): other changes not considered to be caused by rejection.

Since our study focused on the association between lymphocyte phenotypes and rejection, 100 biopsies from group 6 (other changes) were excluded, leaving 1095 biopsies for the analysis, including 313 for cause biopsies and 414 and 368 three-month and 1-year surveillance biopsies, respectively. We investigated whether there was an association between the relative frequency and the absolute number of B cells, Tregs, the ratio of B cells to CD28-CD8+ T cells, and the ratio of CD28-CD8+ T cells to Tregs and the five biopsy groups. We also combined group 3 (ABMR), 4 (TCMR), and 5 (borderline rejection) into one group (hereinafter referred to as rejection of all types) and compared it with group 1 (normal/subnormal biopsy).

Lymphocyte phenotyping of fresh blood

Each time a patient underwent a kidney graft biopsy at CHU de Nantes, a blood sample was drawn for laboratory analyses and an EDTA tube containing about 5 ml of blood was sent to the center for immunomonitoring (Centre d'Immunomonitorage Nantes-Atlantique or CIMNA) at CHU de Nantes for lymphocyte phenotyping. Flow cytometry was performed on fresh whole blood within 24 h after sampling and cells were analyzed on a BD FACS Canto II flow cytometer. To determine lymphocyte subset numbers, whole blood was stained in BD Trucount™ Tubes with the four-color monoclonal antibody reagents BD Multitest™ CD3/CD8/CD45/CD4 and BD Multitest™ CD3/CD19/CD16 + 56/CD45 according to the manufacturer's instruction (BD Biosciences). To determine the percentage of Tregs and CD8+CD28- T cells, whole blood was incubated with the following fluorescence-conjugated monoclonal antibodies: anti-CD45-PerCP Cy5.5 (clone 2D1), anti-CD3-FITC (clone SK7), anti-CD4-APC (clone 13B8), anti-CD25-PE-Cy7 (clone 2A3), anti-CD127-PE (clone R34.34) anti-CD8-PE (clone B9.11), and anti-CD28-APC (clone CD28.2) (all from BD Biosciences except anti-CD4, anti-CD8, and anti-CD127 from Beckman Coulter) and then lyzed with FACS lyzing solution (BD Biosciences) (see Supplementary Figure 1 for Treg gating strategy). B cells, Tregs, and CD28-CD8+ T cells were defined as CD3-CD19 +, CD3+CD4+CD25hiCD127lo, and CD3+CD8+CD28-, respectively and their percentages in total lymphocytes were reported. The absolute number of CD28-CD8+ T cells and Tregs were calculated by multiplying the absolute number of CD8+ T cells by the percentage of CD28-CD8+ T cells in CD8+ T cells and multiplying the absolute number of CD4+ T cells by the percentage of Tregs in CD4+ T cells, respectively. Absolute numbers of lymphocyte subsets were expressed as thousand per µl of blood.

Phenotypic analysis of B cells using frozen PBMCs

Frozen PBMCs were thawed using CTL anti-aggregate buffer (Immunospot). $2x10^6$ PBMCs were stained with fixable viability stain 440UV (BD Biosciences), followed by fluorescence conjugated antibodies for cell surface markers including anti-CD3-BUV737 (clone UCHT1), anti-CD19-BV510 (clone HIB19), anti-CD24-BV711 (clone ML5), anti-CD38-BV785 (clone HIT2), anti-CD27-AF488 (clone QA17A18), anti-IgD-BV421 (clone IA6-2), anti-CD25-PE (clone BC96), and anti-CD9-PerCP Cy5.5 (clone H19a). Next, cells were permeabilized with Intracellular Fixation & Permeabilization Buffer Set (Thermo Fisher), stained with anti-granzyme B- PE Cy7 (clone QA18A28) (all antibodies from BioLegend except anti-CD3 from BD Biosciences), and acquired on a Celesta flow cytometer (BD Biosciences). Data were analyzed with Flowjo software version 10.8.0 (BD). The percentages of each B cell subset were compared among the 5 biopsy groups and between the normal/subnormal biopsy group and rejection of all types with the Kruskal-Wallis test and the Mann-Whitney test, respectively using the GraphPad Prism software version 5. All tests were 2-sided and $p<0.05$ was considered as statistical significant.

Clinical data

Clinical data required for the analysis were extracted from the DIVAT (for "Données Informatisées et Validées en Transplantation") database which was carried out prospectively, exhaustively, and independently by clinical research associates on key dates during post-operative follow-up of clinical and biological data of all incident transplanted patients at our institutes. The data are subject to an annual audit to warrant quality and completeness. Recipient characteristics include age, gender, transplantation rank (first transplantation or retransplantation), type of transplantation

(renal or combined kidney/pancreas transplantation), year of transplantation, the initial kidney disease (possibly recurrent or not), the cytomegalovirus (CMV) serology, history of diabetes, history of arterial hypertension, history of cardiovascular disease, CMV serology, number of HLA-A-B-DR incompatibilities, ABO mismatch, donor-specific antibodies (DSA), and anti-HLA class I and II immunization. Donor characteristics include age, gender, and donor type (living or deceased). Baseline transplantation parameters were cold ischemia time, delayed graft function (DGF), induction therapy, and maintenance treatments [including cyclosporine A (CSA), tacrolimus, mammalian target of rapamycin (mTOR) inhibitors, mycophenolate mofetil (MMF), and corticosteroids]. Parameters collected at the time of biopsy were the reason for biopsy – for cause or surveillance biopsy (at 3 months or 1 year post-transplantation), serum creatinine, the rank of biopsy, post-transplantation time, histological diagnosis according to Banff 2017 classification and the whole details of the Banff elementary lesions, DSA, and type of treatment for each rejection episode, and the percentage and absolute number of total B cells, CD28-CD8+ T cells, and Tregs. The follow-up and the collection of data were stopped upon graft failure (defined as return to dialysis or retransplantation) or death.

Statistical analyses using multivariable models

The characteristics at the time of biopsy between the five biopsy groups were described using median and interquartile range for continuous variables and frequency and proportion for categorical data. Six features were studied: the percentage and the absolute number of B cells and Tregs, the ratio between the absolute number of B cells and CD28-CD8+ T cells, and the ratio between the absolute number of CD28-CD8+ T cells and Tregs (only data from the lymphocyte phenotyping of fresh blood were included in the multivariate models). Since those features were non-Gaussian, we performed square root and logarithm transformation for each of those 6 features, plotted transformed data on histograms, and then selected the type of transformation that more closely resembled a normal distribution. In this way, square root transformation was used for the percentage and absolute number of B cells and Tregs whereas natural logarithm transformation was used for the ratio between the absolute number of B cells and CD28-CD8+ T cells and the ratio between the absolute number of CD28-CD8+ T cells and Tregs. We first performed linear mixed-effects models (random intercept per transplantation) to analyze the unadjusted effects of covariates on the studied feature (25). Covariates having p value less than 0.2 were then included into the multivariable models. We also forced into the multivariable models the following clinically important covariates (regardless of p value): recipient and donor age, recipient and donor sex, re-transplantation, recipient and donor CMV serology, cold ischemia time, time from transplantation to biopsy, reason for biopsy (for cause vs surveillance biopsy), induction therapy at transplantation, creatinine at biopsy, HLA-A, -B and-DR incompatibilities and anti-HLA class I and II immunization. We did not consider interaction. The residuals' analyses were performed to check the models' validities. In each model, we first tested if the outcome was significantly different in at least one of the biopsy groups using a likelihood ratio test. If significant, we explored which groups differed by performing the following comparisons: group 2 versus 1, group 3 versus 1, group 4 versus 1, and group 5 versus 1. We also compared rejection of all types (combination of group 1, 3, and 5) to group 1. Corrected p-values were determined using the Holm-Bonferroni method to control for the inflation of the type I error rate associated with multiple testing. Analyses were performed with R 4.0.3.

Results

Patient characteristics

Our analysis included 1095 kidney graft biopsies performed on 747 kidney or combined kidney/pancreas allograft from 737 patients. 73.2 percent (n=802) of biopsies were normal/subnormal (group 1), 5.1% (n=56) were grade 2/3 IFTA (group 2), 13.5% (n=148) were ABMR (group 3), 3% (n=33) were TCMR (group 4), and 5.1% (n=56) were untreated borderline rejection (group 5). The characteristics of the whole sample (1095 biopsies) as well as of each histological group from 1 to 5 were presented in Table 1.

Rejection of all types is marginally associated with a decrease in the percentage of B cells in the peripheral blood

We first analyzed the unadjusted effects of covariates on the square root of B cell percentage using linear mixed models (Supplementary Table 1). Biopsy groups were not associated with the square root of B cell percentage (p=0.21) whereas compared to group 1, rejection of all types (combination of group 3, 4, and 5) was associated with a decrease in the square root of B cell percentage (p=0.04). The following covariates with p value of less than 0.2 were included into the multivariable model (in addition to clinically important covariates already forced into the model regardless of p value – see Materials and Methods): history of hypertension, ABO blood group mismatch, depleting induction, cyclosporine, tacrolimus, corticosteroids, and biopsy rank. We then performed multivariable linear mixed model analyses of the square root of B cell percentage and confirmed that biopsy groups were not associated with B cell percentage (p=0.22) (Table 2). Nevertheless, compared to group 1, rejection of all types was marginally associated with a decrease in the square root of B cell percentage, the adjusted mean difference was -0.18, 95% CI [-0.38, 0.01] (p=0.06) (Table 3). Next, we performed the same statistical analyses of the square root of B cell absolute number and found no association between biopsy groups and B cell absolute number (Supplementary Table 2, 3). The combined group (rejection of all types) also showed no difference in the square root of B cell absolute number compared to the normal/subnormal group, the adjusted mean difference was -0.01, 95% CI [-0.03, 0.02] (p=0.63) (Supplementary Table 4).

TABLE 1 Characteristics of 1095 renal biopsies included in the analysis according their biopsy groups.

	Whole sample (n=1095)			Biopsy group 1 (n=802)			Biopsy group 2 (n=56)			Biopsy group 3 (n=148)			Biopsy group 4 (n=33)			Biopsy group 5 (n=56)		
	NA	n	%	NA	n	%	NA	n	%	NA	n	%	NA	n	%	NA	n	%
Transplantation after 2008	0	990	90.4	0	770	96.0	0	44	78.6	0	96	64.9	0	26	78.9	0	54	96.4
Male recipient	0	679	62.0	0	499	62.2	0	34	60.7	0	93	62.8	0	17	51.5	0	36	64.3
Retransplantation	0	191	17.4	0	139	17.3	0	7	12.5	0	38	25.7	0	3	9.1	0	4	7.1
Renal transplantation	0	992	90.6	0	724	90.3	0	53	94.6	0	139	93.9	0	27	81.8	0	49	87.5
Recurrent initial disease	0	248	22.7	0	179	22.3	0	11	19.6	0	41	27.7	0	3	9.1	0	14	25.0
Delayed graft function	13	345	31.9	8	240	30.2	2	23	42.6	3	46	31.7	0	14	42.4	0	22	39.3
History of diabetes	0	262	23.9	0	196	24.4	0	7	12.5	0	29	19.6	0	12	36.4	0	18	32.1
History of hypertension	0	961	87.8	0	706	88.0	0	48	85.7	0	128	86.5	0	30	90.9	0	49	87.5
History of cardiovascular disease	0	391	35.7	0	272	33.9	0	24	42.9	0	59	39.9	0	16	48.5	0	20	35.7
Recipient/Donor CMV serology	5			0			2			2			0			1		
0		379	34.8		284	35.4		12	22.2		53	36.3		13	39.4		17	30.9
1		224	20.6		155	19.3		20	37.0		30	20.6		7	21.2		12	21.8
2		245	22.5		190	23.7		6	11.1		34	23.3		6	18.2		9	16.4
3		242	22.2		173	21.6		16	29.6		29	19.9		7	21.2		17	30.9
Male donor	0	626	52.2	0	465	58.0	0	37	66.1	0	79	53.4	0	19	57.6	0	26	46.4
Deceased donor	0	967	88.3	0	704	87.8	0	52	92.9	0	130	87.8	0	29	87.9	0	52	92.9
HLA-A-B-DR mismatches > 4	0	255	23.3	0	187	23.3	0	10	17.9	0	36	24.3	0	10	30.3	0	12	21.4
ABO mismatch	0	22	2.0	0	18	2.2	0	0	0.0	0	3	2.0	0	0	0.0	0	1	1.8
Depleting induction	0	447	40.8	0	331	41.3	0	17	30.4	0	75	50.7	0	11	33.3	0	13	23.2
Cyclosporine	0	89	8.1	0	37	4.6	0	6	10.7	0	31	21.0	0	5	15.2	0	10	17.9
Tacrolimus	0	1004	91.7	0	764	95.3	0	50	89.3	0	116	78.4	0	28	84.9	0	46	82.1
mTOR	0	16	1.5	0	10	1.3	0	0	0.0	0	3	2.0	0	0	0.0	0	3	5.4
Calcineurin inhibitors	0	1090	99.5	0	799	99.6	0	56	100.0	0	147	99.3	0	33	100.0	0	55	98.2
Corticosteroids	0	948	86.6	0	696	86.8	0	45	80.4	0	130	87.8	0	26	78.8	0	51	91.1

(Continued)

10.3389/fimmu.2023.1151127

TABLE 1 Continued

	Whole sample (n=1095)			Biopsy group 1 (n=802)			Biopsy group 2 (n=56)			Biopsy group 3 (n=148)			Biopsy group 4 (n=33)			Biopsy group 5 (n=56)		
	NA	n	%	NA	n	%	NA	n	%	NA	n	%	NA	n	%	NA	n	%
Positive anticlass I immunization	1	339	31.0	0	247	30.8	1	13	23.6	0	66	44.6	0	6	18.2	0	7	12.5
Positive anticlass II immunization	1	310	28.3	0	219	27.3	1	9	16.4	0	65	43.9	0	8	24.2	0	9	16.1
Positive DSA	0	85	7.8	0	53	6.6	0	2	3.6	0	28	18.9	0	1	3.0	0	1	1.8
Biopsy rank	0			0			0			0			0			0		
1		644	58.8		494	61.6		20	35.7		75	50.7		22	66.7		33	58.9
2		372	34.0		274	34.2		29	51.8		42	28.4		7	21.2		20	35.7
3		71	6.5		32	4.0		7	12.5		26	17.6		3	9.1		3	5.4
4		7	0.6		2	0.3		0	0.0		4	2.7		1	3.0		0	0.0
5		1	0.1		0	0.0		0	0.0		1	0.7		0	0.0		0	0.0
For causes biopsy	0	313	28.6	0	158	19.7	0	26	46.4	0	102	68.9	0	21	63.6	0	6	10.7
	NA	Median	Q1-Q3	NA	Median	Q1-Q3	NA	Median	Q1-Q3	NA	Median	Q1-Q3	NA	Median	Q1-Q3	NA	Median	Q1-Q3
B cells (%)	0	10.8	6.5-17.6	0	10.8	6.5-18.4	0	9.3	5.4-16.5	0	11.7	7.0-16.2	0	10.9	8.0-12.5	0	9.3	5.2-14.9
B cells (absolute number)	0	0.10	0.06-0.19	0	0.10	0.06-0.18	0	0.11	0.07-0.18	0	0.14	0.07-0.18	0	0.10	0.06-0.17	0	0.10	0.05-0.17
Tregs (%)	27	2.3	1.5-3.0	21	2.3	1.6-3.0	2	1.9	1.2-2.6	2	2.1	1.4-2.9	2	2.8	2.2-3.6	0	2.4	1.8-3.4
Tregs (absolute number)	28	0.02	0.01-0.04	21	0.02	0.01-0.04	2	0.02	0.01-0.03	2	0.02	0.01-0.04	2	0.03	0.02-0.04	0	0.03	0.02-0.04
CD28-CD8+ T cells (%)	11	6.6	3.0-15.4	8	5.9	2.7-13.4	1	12.7	4.6-20.9	2	9.4	3.6-23.8	0	7.7	3.6-16.8	0	7.6	3.2-16.2
CD28-CD8+ T cells (absolute num)	11	0.06	0.03-0.17	8	0.05	0.02-0.14	1	0.16	0.04-0.25	2	0.12	0.04-0.29	0	0.08	0.04-0.18	0	0.08	0.03-0.16
Recipient age (years)	0	51.0	40.0-63.0	0	51.0	41.0-63.0	0	53.5	38.8-63.3	0	50.0	34.0-61.0	0	52.0	36.0-63.0	0	52	25.0-64.0
Cold ischemia time (hours)	0	14.8	11.2-19.0	0	14.4	10.9-18.3	0	15.2	11.5-22.6	0	16.6	13.1-23.2	0	15.5	12.7-18.8	0	15.3	12.7-17.8
Donor age (years)	0	53.0	41.0-64.0	0	54.0	42.0-64.0	0	57	45.3-67.0	0	52.0	34.0-63.0	0	50.0	34.0-64.0	0	54.0	41.8-65.0
Creatininemia at biopsy (µmol/l)	12	139.0	110.0-179.0	9	133.0	106.0-169.0	2	175.0	141.3-247.0	0	163.5	132.8-214.5	0	199.0	141.0-291.0	1	125.0	105.0-160.0
Post-transplantation time of the biopsy (years)	0	0.97	0.26-1.03	0	0.36	0.26-1.01	0	1.03	1.00-5.21	0	1.87	0.99-7.00	0	0.55	0.25-2.29	0	0.28	0.26-1.01

CMV, Cytomegalovirus; Recipient/Donor CMV serology definition, 0, negative donor and recipient; 1, negative donor and positive recipient; 2, positive donor and negative recipient; 3, positive donor and recipient; DSA, donor-specific antibodies; HLA, human leukocyte antigens; Q, quartile; Q1, 25th percentile; Q3, 75th percentile; NA, not available (missing). %, percent of total lymphocytes; absolute number: thousand per µl. Biopsy group 1: normal/subnormal, group 2: interstitial fibrosis/tubular atrophy (IFTA) grade 2 or 3, group 3: ABMR, group 4, TCMR; group 5, borderline rejection.

10.3389/fimmu.2023.1151127

10.3389/fimmu.2023.1151127

TABLE 2 Results of the multivariable linear mixed model of square root of B lymphocytes in percentage measured at the time of biopsy (5 biopsy groups).

	Adjusted mean difference	95% CI	p-value
Biopsy group			0.2224
2 (vs. 1)	-0.03	[-0.37; 0.31]	
3 (vs. 1)	-0.14	[-0.44; 0.11]	
4 (vs. 1)	-0.45	[-0.85; -0.05]	
5 (vs. 1)	-0.14	[-0.45; 0.18]	
Recipient age (years)	0.00	[-0.01; 0.01]	0.7448
Male recipient	-0.12	[-0.31; 0.06]	0.1979
Retransplantation	0.10	[-0.20; 0.40]	0.5070
Cold ischemia time (hours)	0.00	[-0.01; 0.01]	0.6806
History of hypertension	-0.20	[-0.48; 0.08]	0.1699
Recipient/Donor CMV serology			<0.0001
1 (vs. 0)	-0.45	[-0.69; -0.20]	
2 (vs. 0)	-0.16	[-0.40; 0.08]	
3 (vs. 0)	-0.33	[-0.57; -0.08]	
Donor age (years)	0.00	[-0.01; 0.01]	0.5639
Male donor	-0.09	[-0.27; 0.09]	0.3401
HLA-A-B-DR mismatches > 4	0.21	[-0.01; 0.42]	0.0610
ABO mismatch	-0.34	[-0.96; 0.28]	0.2781
Depleting induction	0.79	[0.56; 1.01]	<0.0001
Cyclosporine	-0.75	[-1.82; 0.32]	0.1710
Tacrolimus	0.04	[-1.04; 1.13]	0.9356
Corticosteroids	0.19	[-0.08; 0.46]	0.1687
Positive anti-class I immunization	-0.07	[-0.28; 0.14]	0.5199
Positive anti-class II immunization	-0.08	[-0.31; 0.15]	0.4923
Biopsy rank			0.1805
2 (vs. 1)	0.02	[-0.11; 0.16]	
3 (vs. 1)	-0.25	[-0.52; 0.02]	
4 (vs. 1)	-0.61	[-1.37; 0.14]	
5 (vs. 1)	-0.70	[-2.61; 1.20]	
For causes biopsy	0.17	[-0.02; 0.36]	0.0802
Creatininemia at biopsy (µmol/l)	0.00	[0.00; 0.00]	<0.0001
Post-transplantation time of the biopsy (years)	-0.01	[-0.04; 0.03]	0.6800

CI, confidence interval; CMV, cytomegalovirus; Recipient/Donor CMV serology definition. 0, negative donor and recipient; 1, negative donor and positive recipient; 2, positive donor and negative recipient; 3, positive donor and recipient; HLA ,human leucocyte antigens; Biopsy group 1, normal/subnormal; group 2, interstitial fibrosis/tubular atrophy (IFTA) grade 2 or 3; group 3, ABMR; group 4, TCMR; group 5, borderline rejection.

10.3389/fimmu.2023.1151127

TABLE 3 Results of the multivariable linear mixed model of square root of B lymphocytes in percentage measured at the time of biopsy (Rejection of all types versus normal/subnormal).

	Adjusted mean difference	95% CI	p-value
Rejection of all types vs. normal/subnormal	-0.18	[-0.38; 0.01]	0.0623
Recipient age (years)	0.00	[-0.01; 0.01]	0.9417
Male recipient	-0.11	[-0.31; 0.08]	0.2409
Retransplantation	0.08	[-0.23; 0.38]	0.6220
Cold ischemia time (hours)	0.00	[-0.02; 0.01]	0.6222
History of hypertension	-0.16	[-0.45; 0.13]	0.2730
Recipient/Donor CMV serology			<0.0001
1 (vs. 0)	-0.47	[-0.72; -0.22]	
2 (vs. 0)	-0.16	[-0.40; 0.08]	
3 (vs. 0)	-0.28	[-0.53; -0.03]	
Donor age (years)	0.00	[-0.01; 0.01]	0.7714
Male donor	-0.07	[-0.26; 0.12]	0.4562
HLA-A-B-DR mismatches > 4	0.21	[-0.01; 0.43]	0.0581
ABO mismatch	-0.34	[-0.96; 0.28]	0.2839
Depleting induction	0.81	[0.58; 1.04]	<0.0001
Cyclosporine	-0.73	[-1.81; 0.34]	0.1820
Tacrolimus	0.07	[-1.08; 1.10]	0.9893
Corticosteroids	0.10	[-0.10; 0.46]	0.1976
Positive anti-class I immunization	-0.08	[-0.30; 0.13]	0.4424
Positive anti-class II immunization	-0.10	[-0.34; 0.14]	0.4099
Biopsy rank			0.2436
2 (vs. 1)	0.04	[-0.09; 0.17]	
3 (vs. 1)	-0.21	[-0.49; 0.07]	
4 (vs. 1)	-0.61	[-1.36; 0.14]	
5 (vs. 1)	-0.57	[-2.47; 1.32]	
For causes biopsy	0.17	[-0.03; 0.37]	0.0886
Creatininemia at biopsy (µmol/l)	0.00	[0.00; 0.00]	<0.0001
Post-transplantation time of the biopsy (years)	-0.01	[-0.04; 0.02]	0.5666

CI, confidence interval; CMV, cytomegalovirus; Recipient/Donor CMV serology definition. 0, negative donor and recipient; 1, negative donor and positive recipient; 2, positive donor and negative recipient; 3, positive donor and recipient; HLA, human leucocyte antigens.

B cell subset relative frequencies were not significantly different between biopsy groups

In order to perform an in-depth study into B cell subpopulations, we searched in our biocollection for cryopreserved PBMCs from the whole cohort and were able to retrieve a total of 334 frozen samples from 334 patients, including 279, 7, 23, 6, and 19 patients with normal/subnormal biopsy, IFTA grade 2 or 3, ABMR, TCMR, and borderline rejection, respectively. We determined the percentage of principal B cell subsets among total B cells (CD3-CD19+), including naïve (CD27-IgD+), switched memory (CD27+IgD-), non-switched memory (CD27+IgD+), non-conventional (CD27-IgD-), transitional B cells (CD24hiCD38hi), and plasmablasts (CD24loCD38hi), as well as of other B cells subsets shown to have regulatory properties such as CD25+ (26), CD9+ (27), and granzyme B+ (9, 10) B cells (see Supplementary Figure 2 for the gating strategy). We first compared the percentages of each B cell subset among the 5 biopsy groups and found no statistically significant differences between those groups (data not shown). Next, we compared the B cell subset percentages between rejection of all types and normal/subnormal biopsies and did not

find significant differences between the 2 groups. Only rejection of all types tended to be associated with an increase in switched memory B cells, but the difference did not reach statistical significance (p=0.08, Mann-Whitney test) (Supplementary Table 5).

ABMR, TCMR, and rejection of all types are associated with a decrease in the ratio of B cells to CD28-CD8+ T cells

We recently demonstrated that ABMR was associated with an increase in the percentage and absolute number of the differentiated CD28-CD8+ T cells in the peripheral blood. We also showed that and CD28-CD8+ T cells contained higher percentage of effector/memory CD8+ T cells expressing CD45RA (TEMRA) defined as CCR7-CD45RA+ and had stronger effector functions compared to their CD28+ counterpart (22). In the current study, we asked whether the balance between B cells and CD28-CD8+ T cells had an impact on the occurrence of kidney graft rejection. For this purpose, we first analyzed the unadjusted effects of covariates on the natural logarithm of the ratio between the absolute number of peripheral B cells and CD28-CD8+ T cells (Supplementary Table 6). Next, we performed multivariable linear mixed model analyses and observed a significant association between the natural logarithm of the ratio between the absolute number of peripheral B cells and CD28-CD8+ T cells and biopsy groups (p=0.007) (Table 4). The adjusted mean difference between group 3 and group 1 and between group 4 and group 1 were -0.44, 95% CI [-0.69, -0.19] and -0.33, 95%CI [-0.73, -0.06], respectively. Similar results were obtained when we compared rejection of all types with normal/subnormal biopsy (group 1). The adjusted mean difference between rejection of all types and group 1 was -0.36, 95% CI [-0.55, -0.16] (p=0.0003) (Table 5). In other words, the ratio of B cells to CD28-CD8+ T cells was 43 percent higher in the normal/subnormal biopsy group compared to rejection of all types. Taken together, ABMR, TCMR, as well as rejection of all types were associated with a decrease in the ratio of B cells to CD28-CD8+ T cells measured in the peripheral blood at the time of biopsy compared normal/subnormal biopsies.

Rejection of all types is associated with an increase in the ratio of CD28-CD8+ T cells to Tregs

Since we have previously shown that kidney tolerant patients had increased circulating Tregs (11, 12), in this study, we investigated the association between the 5 biopsy groups and Tregs, both in relative frequency and in absolute number. We first analyzed the unadjusted effects of covariates on the square root of Tregs in percentage and observed that biopsy groups were associated with the square root of Treg percentage (p=0.03) (Supplementary Table 7), however the association did not reach statistical significance when analyzed by multivariable linear mixed models (p=0.08) (Supplementary Table 8). We also found that biopsy groups were not associated with the square root of Treg absolute number (p=0.23 by multivariable analyses) (Supplementary Tables 9, 10). Similarly, multivariable analyses did not show statistically significant differences in Treg percentage and Treg absolute number between rejection of all types and normal/subnormal biopsy. The adjusted mean difference in the square root of Treg percentage and Treg absolute number between rejection of all types and normal/subnormal biopsy were 0.06, 95% CI [-0.02, 0.13], p=0.10 and 0.01, 95% CI [0.00, 0.02], p=0.089, respectively (Supplementary Tables 11, 12).

Next, we asked whether the balance between CD28-CD8+ T cells and Tregs was associated with kidney graft rejection. To this end, we first analyzed the unadjusted effects of covariates on the natural logarithm of the ratio between CD28-CD8+ T cells and Tregs and observed an association between this ratio and biopsy groups (p<0.0001) or rejection of all types (p=0.0002) (Supplementary Table 13). Next we performed multivariable linear mixed model analyses of the natural logarithm of the ratio between CD28-CD8+ T cells and Tregs and found a marginal association between this ratio and biopsy groups (p=0.06), especially the adjusted mean difference between group 3 and group 1 was 0.34, 95% CI [0.11, 0.58] (Table 6). More interestingly, multivariable analyses confirmed that rejection of all types was significantly associated with an increase in the ratio of CD28-CD8+ T cells to Tregs compared to normal/subnormal biopsy, the adjusted mean difference in the log of the ratio of CD28-CD8+ T cells/Tregs was 0.23, 95% CI [0.05, 0.41], p=0.01 (Table 7). In other words, the ratio of CD28-CD8+ T cells to Tregs was 26 percent higher in rejection of all types compared to the normal/subnormal biopsy group.

Besides biopsy groups, as observed in the aforementioned tables (Tables 2–7), some other covariates, especially depleting induction and recipient/donor CMV serology, were also found to be statistically significant. Indeed, depleting induction has an impact on lymphocyte numbers and frequencies, especially when half of the biopsies were performed within the first post-transplantation year (Table 1). In this cohort, depleting induction therapy was mainly based on anti-thymocyte globulin (ATG), which profoundly depletes T cells but reduces other lymphocyte subsets in a much lesser extent. This may explain the finding that depleting induction was associated with a significant increase in B cell percentage (Tables 2, 3) and in the ratio of B cells to CD28-CD8+ T cells (Tables 4, 5). On the contrary, the ratio of CD28-CD8+ T cells to Tregs was not affected by depleting induction (Tables 6, 7) since ATG depletes all T cell subpopulations.

Interestingly, the covariate recipient/donor CMV serology was also found to be statistically significant. In our multivariable linear mixed models, we compared transplant recipients having positive CMV serology (group 1: positive recipient/negative donor and group 3: positive recipient/positive donor) or having high risk to become CMV positive (group 2: negative recipient/positive donor) with the group of recipients having negative CMV serology and at low risk to become CMV positive (group 0: negative recipient/negative donor). We found that compared to the CMV group 0, the other groups had a significant decrease in B cell percentage (Tables 2, 3), a significant decrease in the ratio of B cells to CD28-

10.3389/fimmu.2023.1151127

TABLE 4 Results of the multivariable linear mixed model of log of the ratio between B lymphocytes in absolute number and CD28-CD8+ T cells in absolute number measured at the time of biopsy (5 biopsy groups).

	Adjusted mean difference	95% CI	p-value
Biopsy group			0.0073
2 (vs. 1)	-0.13	[-0.47; 0.21]	
3 (vs. 1)	-0.44	[-0.69; -0.19]	
4 (vs. 1)	-0.33	[-0.73; -0.06]	
5 (vs. 1)	-0.21	[-0.51; 0.10]	
Recipient age (years)	0.00	[-0.01; 0.01]	0.9204
Male recipient	-0.03	[-0.22; 0.16]	0.7536
Renal transplantation	0.46	[0.10; 0.81]	0.0115
Delayed graft function	-0.09	[-0.29; 0.11]	0.3839
Retransplantation	-0.42	[-0.73; -0.11]	0.0072
Cold ischemia time (hours)	-0.02	[-0.03; 0.00]	0.0375
Recipient/Donor CMV serology			<0.0001
1 (vs. 0)	-1.38	[-1.62; -1.14]	
2 (vs. 0)	-0.69	[-0.93; -0.46]	
3 (vs. 0)	-1.33	[-1.57; -1.09]	
Donor age (years)	-0.01	[-0.02; 0.00]	0.0098
Male donor	-0.13	[-0.32; 0.05]	0.1516
Deceased donor	0.13	[-0.25; 0.48]	0.5388
HLA-A-B-DR mismatches > 4	0.13	[-0.09; 0.34]	0.2511
Depleting induction	0.54	[0.31; 0.78]	<0.0001
Cyclosporine	-2.34	[-4.07; -0.60]	0.0085
Tacrolimus	-1.50	[-3.27; 0.28]	0.0980
mTOR inhibitors	0.44	[-0.35; 1.22]	0.2735
Calcineurin inhibitors	3.69	[1.42; 5.95]	0.0015
Positive anti-class I immunization	-0.04	[-0.25; 0.17]	0.7208
Positive anti-class II immunization	0.09	[-0.14; 0.32]	0.4491
Biopsy rank			<0.0001
2 (vs. 1)	-0.30	[-0.43; -0.17]	
3 (vs. 1)	-0.47	[-0.73; -0.21]	
4 (vs. 1)	-1.16	[-1.89; -0.44]	
5 (vs. 1)	-0.74	[-2.55; 1.08]	
For causes biopsy	0.13	[-0.06; 0.32]	0.1867
Creatininemia at biopsy (100 µmol/l)	0.08	[-0.01; 0.18]	0.0957
Post-transplantation time of the biopsy (years)	-0.01	[0.04; 0.03]	0.7013

CI, confidence interval; CMV, cytomegalovirus; HLA, human leucocyte antigens; mTOR, mammalian target of rapamycin; Recipient/Donor CMV serology definition. 0, negative donor and recipient; 1, negative donor and positive recipient; 2, positive donor and negative recipient; 3, positive donor and recipient; Log, natural logarithm; Biopsy group 1, normal/subnormal; group 2, interstitial fibrosis/tubular atrophy (IFTA) grade 2 or 3; group 3, ABMR; group 4, TCMR; group 5, borderline rejection.

10.3389/fimmu.2023.1151127

TABLE 5 Results of the multivariable linear mixed model of log of the ratio between B lymphocytes in absolute number and CD28-CD8+ T cells in absolute number measured at the time of biopsy (Rejection of all types versus normal/subnormal).

	Adjusted mean difference	95% CI	p-value
Rejection of all types vs. normal/subnormal	-0.36	[-0.55; -0.16]	0.0003
Recipient age (years)	0.00	[-0.01; 0.01]	0.7902
Male recipient	-0.05	[-0.22; 0.15]	0.5821
Renal transplantation	0.44	[0.10; 0.81]	0.0162
Delayed graft function	-0.07	[-0.28; 0.12]	0.4845
Retransplantation	-0.42	[-0.72; -0.11]	0.0084
Cold ischemia time (hours)	-0.02	[-0.03; 0.00]	0.0499
Recipient/Donor CMV serology			<0.0001
1 (vs. 0)	-1.37	[-1.61; -1.13]	
2 (vs. 0)	-0.68	[-0.93; -0.46]	
3 (vs. 0)	-1.28	[-1.56; -1.08]	
Donor age (10 years)	-0.01	[-0.02; 0.00]	0.0167
Male donor	-0.13	[-0.31; 0.06]	0.1636
Deceased donor	0.10	[-0.24; 0.49]	0.6097
HLA-A-B-DR mismatches > 4	0.12	[-0.10; 0.34]	0.2887
Depleting induction	0.56	[0.30; 0.77]	<0.0001
Cyclosporine	-2.35	[-4.09; -0.61]	0.0085
Tacrolimus	-1.52	[-3.27; 0.28]	0.0939
mTOR inhibitors	0.43	[-0.36; 1.20]	0.2867
Calcineurin inhibitors	3.63	[1.39; 5.92]	0.0018
Positive anti-class I immunization	-0.08	[-0.26; 0.16]	0.4445
Positive anti-class II immunization	0.07	[-0.15; 0.30]	0.5346
Biopsy rank			<0.0001
2 (vs. 1)	-0.31	[-0.42; -0.16]	
3 (vs. 1)	-0.50	[-0.74; -0.22]	
4 (vs. 1)	-1.22	[-1.95; -0.51]	
5 (vs. 1)	-0.83	[-2.65; 0.97]	
For causes biopsy	0.13	[-0.08; 0.29]	0.2085
Creatininemia at biopsy (100 µmol/l)	0.08	[-0.02; 0.18]	0.1030
Post-transplantation time of the biopsy (years)	-0.01	[0.04; 0.03]	0.5394

CI, confidence interval; CMV, cytomegalovirus; Recipient/Donor CMV serology definition. 0, negative donor and recipient; 1, negative donor and positive recipient; 2, positive donor and negative recipient; 3, positive donor and recipient. HLA, human leucocyte antigens; mTOR, mammalian target of rapamycin; Log, natural logarithm.

CD8+ T cells (Tables 4, 5), and a significant increase in the ratio of CD28-CD8+ T cells to Tregs (Tables 6, 7). Several recent studies have shown that kidney transplant patients with positive CMV serology have higher frequency of CD28-CD8+ T cells compared to those with negative CMV serology (28–30). Therefore, the decrease in the ratio of B cells to CD28-CD8+ T cells and the increase in the ratio of CD28-CD8+ T cells to Tregs can be explained at least in part by the increase in CD28-CD8+ T cells. On the other hand, the association between B cell frequency and CMV status is less well-documented (29, 31). The effect of CMV on lymphocyte phenotypes in transplant recipients is an interesting issue necessitating further research but is beyond the scope of this paper. In summary, the presence of covariates with statistical significance such as CMV serology and depleting induction does not affect our conclusion that certain blood lymphocyte phenotypes are significantly associated with kidney graft rejections because these covariates have been adjusted in the multivariable linear mixed models.

10.3389/fimmu.2023.1151127

TABLE 6 Results of the multivariable linear mixed model of log of the ratio between CD28-CD8+ T cells in absolute number and Tregs in absolute number measured at the time of biopsy (5 biopsy groups).

	Adjusted mean difference	95% CI	p-value
Biopsy group			0.0673
2 (vs. 1)	0.13	[-0.19; 0.44]	
3 (vs. 1)	0.34	[0.11; 0.58]	
4 (vs. 1)	0.09	[-0.29; 0.46]	
5 (vs. 1)	0.10	[-0.19; 0.38]	
Transplantation after 2008	0.29	[-0.22; 0.79]	0.2695
Recipient age (years)	0.00	[-0.01; 0.01]	0.6200
Male recipient	-0.08	[-0.26; 0.09]	0.3576
Retransplantation	0.48	[0.19; 0.76]	0.0013
Renal transplantation	0.09	[-0.25; 0.42]	0.6064
Recurrent initial disease	0.07	[-0.13; 0.27]	0.5058
Delayed graft function	0.10	[-0.08; 0.29]	0.2799
Cold ischemia time (hours)	0.00	[-0.01; 0.02]	0.5476
Recipient/Donor CMV serology			<0.0001
1 (vs. 0)	1.31	[1.08; 1.54]	
2 (vs. 0)	0.67	[0.45; 0.89]	
3 (vs. 0)	1.30	[1.07; 1.52]	
Donor age (years)	0.01	[0.00; 0.02]	0.0061
Male donor	0.13	[-0.04; 0.30]	0.1383
Deceased donor	0.19	[-0.15; 0.53]	0.2667
HLA-A-B-DR mismatches > 4	0.03	[-0.18; 0.23]	0.7951
Depleting induction	-0.03	[-0.26; 0.19]	0.7607
Cyclosporine	0.06	[-0.92; 1.04]	0.9023
Tacrolimus	-0.30	[-1.30; 0.69]	0.5518
Corticosteroids	0.19	[-0.06; 0.43]	0.1354
Positive anti-class I immunization	-0.05	[-0.25; 0.15]	0.6170
Positive anti-class II immunization	-0.13	[-0.34; 0.09]	0.2522
Biopsy rank			<0.0001
2 (vs. 1)	0.50	[0.37; 0.62]	
3 (vs. 1)	0.59	[0.35; 0.84]	
4 (vs. 1)	0.73	[0.04; 1.42]	
5 (vs. 1)	0.65	[-1.03; 2.34]	
For causes biopsy	0.14	[-0.04; 0.33]	0.1212
Creatininemia at biopsy (100 µmol/l)	0.00	[-0.10; 0.10]	0.9868
Post-transplantation time of the biopsy (years)	0.04	[-0.01; 0.09]	0.1101

CI, confidence interval; CMV, cytomegalovirus; HLA, human leucocyte antigens; Recipient/Donor CMV serology definition. 0, negative donor and recipient; 1, negative donor and positive recipient; 2, positive donor and negative recipient; 3, positive donor and recipient; Log, natural logarithm; Biopsy group 1, normal/subnormal; group 2, interstitial fibrosis/tubular atrophy (IFTA) grade 2 or 3; group 3, ABMR; group 4, TCMR; group 5, borderline rejection.

10.3389/fimmu.2023.1151127

TABLE 7 Results of the multivariable linear mixed model of log of the ratio between CD28-CD8+ T cells in absolute number and Tregs in absolute number measured at the time of biopsy (Rejection of all types versus normal).

	Adjusted mean difference	95% CI	p-value
Rejection of all types vs. normal/subnormal	0.23	[0.05; 0.41]	0.0126
Transplantation after 2008	0.35	[-0.18; 0.88]	0.1976
Recipient age (years)	0.00	[-0.01; 0.01]	0.7945
Male recipient	-0.06	[-0.24; 0.12]	0.5383
Retransplantation	0.46	[0.16; 0.75]	0.0023
Renal transplantation	0.09	[-0.25; 0.43]	0.5986
Recurrent initial disease	0.08	[-0.12; 0.29]	0.3972
Delayed graft function	0.10	[-0.09; 0.29]	0.3008
Cold ischemia time (hours)	0.01	[-0.01; 0.02]	0.5023
Recipient/Donor CMV serology			<0.0001
1 (vs. 0)	1.30	[1.07; 1.53]	
2 (vs. 0)	0.64	[0.42; 0.87]	
3 (vs. 0)	1.24	[1.01; 1.47]	
Donor age (years)	0.01	[0.00; 0.02]	0.0110
Male donor	0.13	[-0.04; 0.30]	0.1452
Deceased donor	0.18	[-0.17; 0.53]	0.3132
HLA-A-B-DR mismatches > 4	0.03	[-0.18; 0.23]	0.8057
Depleting induction	-0.03	[-0.26; 0.20]	0.7838
Cyclosporine	0.09	[-0.89; 1.06]	0.8641
Tacrolimus	-0.30	[-1.30; 0.69]	0.5489
Corticosteroids	0.15	[-0.11; 0.40]	0.2534
Positive anti-class I immunization	0.00	[-0.19; 0.20]	0.9683
Positive anti-class II immunization	-0.12	[-0.34; 0.10]	0.2796
Biopsy rank			<0.0001
2 (vs. 1)	0.52	[0.39; 0.64]	
3 (vs. 1)	0.65	[0.39; 0.91]	
4 (vs. 1)	0.80	[0.10; 1.50]	
5 (vs. 1)	0.80	[-0.91; 2.51]	
For causes biopsy	0.15	[-0.04; 0.34]	0.1192
Creatininemia at biopsy (100 µmol/l)	0.00	[-0.10; 0.11]	0.9830
Post-transplantation time of the biopsy (years)	0.04	[-0.01; 0.09]	0.0903

CI, confidence interval; CMV, cytomegalovirus; HLA, human leucocyte antigens; Recipient/Donor CMV serology definition. 0, negative donor and recipient; 1, negative donor and positive recipient; 2, positive donor and negative recipient; 3, positive donor and recipient; Log, natural logarithm.

Discussion

The association between peripheral blood lymphocyte phenotypes and kidney graft rejection has been a subject of many studies. However, most of the previous reports, including ours, were based on relatively small numbers of patients and univariate analyses. In the current study, we prospectively established a large cohort of 1095 kidney graft biopsies with concomitant lymphocyte phenotyping and data were analyzed using multivariable linear mixed models. We first compared each type of rejection to the normal/subnormal biopsy group. We next performed an additional analysis comparing the combined group, rejection of all types, to the normal/subnormal biopsy group to obtain additional results. The combined group with higher number of cases helps to increase statistical power. Moreover,

from an immunological point of view, graft rejection usually requires the mobilization of different components of the immune system (32). For example, the principal mechanism of ABMR involves B cells and antibodies, but T cell help is indispensable for B cell differentiation and antibody production. It has been shown that kidney graft biopsies with ABMR also contain abundant T cells and a third of patients diagnosed with TCMR also have positive DSA (33).

First of all, our multivariable analysis showed a marginal association (p=0.06) between a decrease in the percentage of total B cell and rejection of all types (Table 3), in concordance with previous reports showing that preservation of the B-cell compartment favored kidney graft tolerance (2–5, 34). However, this finding is not conclusive and the changes in total B cells may not represent changes in Bregs. In order to perform a more detailed B cell phenotype analysis, we searched for cryopreserved PBMCs in our biocollection and were able to retrieve frozen samples in about one-third of the studied cohort. In kidney transplant patients, the most studied B cell subset with regulatory properties is CD4hiCD38hi transitional B cells. Several studies reported that patients with kidney graft rejections, especially ABMR, have a reduction in circulating transitional B cells compared to those with stable graft function (35–40). In this study, we performed univariate analyses of B cell phenotyping data from more than 300 patients and did not find any significant association between kidney graft rejections and the relative frequency of Breg subsets, including transitional, CD25+, CD9+, Granzyme B+ B cells, and plasmablasts. We found that rejection of all types tend to be associated with an increase in the percentage of CD27+IgD- switched memory B cells, but the difference was not statistically significant (p=0.08). Switched memory B cells have been reported to be increased in patients with chronic ABMR compared to stable kidney recipients (35). Future studies should provide a more comprehensive phenotyping of B cells with emphasize on Bregs. Since Bregs have been shown to exert their suppressive effects through different signaling pathways, including IL-10, IL-35, TGF-β, granzyme B, and PD-L1 [reviewed in (41–43)], there is no unique marker for Breg. Therefore, carefully designed B cell panels including many surface markers together with intracellular cytokine staining should better study the association between distinct Breg subsets and graft rejection.

We next investigated the relationship between peripheral blood CD4+CD25hiCD127lo Tregs and graft rejections. We and others previously reported that compared to patients with stable renal function, patients with acute rejection (44), chronic rejection (45, 46) or ABMR (40) had lower frequency and/or number of circulating Tregs. However, as aforementioned, those studies were based on small numbers of patients and univariate analyses. The current study based on multivariable analyses of more than 1000 graft biopsies did not show any significant association between circulating Treg relative frequency or absolute number and biopsy groups, either separately or combined (rejection of all types). Despite the important role of Tregs in modulating alloimmune responses in transplantation, attempts to investigate the potential of circulating Tregs as biomarkers in kidney transplantation have not been successful so far (47). Because CD4+CD25hiCD127lo Tregs are likely a heterogeneous population, detailed Treg phenotyping should provide more knowledge on the mechanisms of action of different Treg subsets in the transplant setting. For example, we have recently shown that memory Tregs defined as CD45RA-FoxP3hi have a central role in kidney transplant tolerance. Memory Tregs in tolerant patients have increased FoxP3 Treg-specific demethylated region (TSDR) demethylation and express high levels of the ectonucleotidase CD39 which can degrade adenosine triphosphate (ATP), a key factor in inflammation (11, 12). Therefore, lymphocyte phenotyping using additional markers to further define Treg subpopulations such as CD45RA, CD45RO, CD39, or methylation status (11, 12, 48, 49) might help to unveil a better correlation between circulating Treg subsets and graft rejections.

Since allograft rejections may occur when immune cells with effector/memory functions overbalance those with regulatory functions, we next investigate the association between the ratio of circulating B cells to CD28-CD8+ T cells as well as the ratio of CD28-CD8+ T cells to Tregs and kidney graft rejections. CD28-CD8+ T cells represent an important T cell population with effector/memory function since they are enriched in TEMRA and display potent cytotoxic properties (22, 50), whereas B cells have been shown to have regulatory function [reviewed in (14)]. Here we showed that ABMR, TMCR, and rejection of all types were significantly associated with a decrease in the ratio of B cells to CD28-CD8+ T cells. We also found that ABMR and rejection of all types were marginally and significantly associated with an increase in the ratio of CD28-CD8+ T cells to Tregs, respectively. Since we have previously shown that CD28-CD8+ T cells are significantly increased in ABMR and TCMR (22), it is likely that the increase in CD28-CD8+ T cells itself contributes to the increase in the ratio of CD28-CD8+ T cells to Tregs and the decrease in the ratio of B cells to CD28-CD8+ T cells in graft rejection. On the other hand, the differences in and B cells and Tregs between different biopsy groups did not reach statistical significance. Thus, the possible explanation for the changes in these two ratios is an increase in CD28-CD8+ T cells coupled with an absence of statistically significant changes in the other two populations. In other words, the increase in memory/effector T cells is not counterbalanced by a significant increase in other cell populations with potential regulatory properties. Taken together, the novel finding here is that graft rejection is associated not only with an increase in memory/effector T cells but also with an overbalance of memory/effector T cells over regulatory cells.

Relatively few studies have explored the impact of the balance between various circulating effector and regulatory cells on kidney graft outcome. For example, increased circulating follicular helper T cells (Tfh) to follicular regulatory T cells (Tfr) has been shown to be an independent risk factor for chronic allograft dysfunction (51). Another study found that a reduction in the ratio of IL-10-secreting (anti-inflammatory) to TNF-α-secreting (pro-inflammatory) transitional B cells was associated with subsequent deterioration of graft function (52). The results of our current study reemphasized the importance of the balance between effector/memory and regulatory immune cells in the maintenance of allograft acceptance.

Our study has some limitations. Based upon our publication in 2006, we selected only a few markers so that lymphocyte phenotyping on fresh blood could be carried out rapidly at our hospital laboratories at the same time as graft biopsy. Today, we know that more markers are necessary to define naïve/memory T cells, Treg, and Breg subsets. With the advent of modern flow cytometry allowing the label of up to

40 markers at the same time, carefully designed multicenter study using comprehensive antibody panels covering all Breg and Treg subsets should help to better study the association between kidney graft rejections and peripheral blood lymphocyte phenotypes. Finally, the exact relationship between circulating immune cell phenotypes and graft rejection is not clear. For example, the decrease of a subpopulation in the blood may result from either a real reduction or migration into the graft (53). Concomitant analysis of graft infiltrates may help to better understand the role of different leukocyte subpopulations in graft rejection.

Taken together, despite some limitations, our current study analyzing a large transplant biopsy cohort using multivariable linear mixed models sheds new insight into the underlying mechanisms of graft rejection, further supports the notion that rejection may be linked to the imbalance between effector/memory and regulatory immune cells, and paves the way for future research to discover new biomarkers for graft rejection and graft outcome.

Data availability statement

The original contributions presented in the study are included in the article/Supplementary Material. Further inquiries can be directed to the corresponding authors.

Ethics statement

The studies involving human participants were reviewed and approved by Commission nationale de l'informatique et des libertés (CNIL). The patients/participants provided their written informed consent to participate in this study.

Author contributions

HM, ND, MR, KR, SB, and MG participate in the writing and revision of the manuscript. SB, MG, HM, ND, ML, and RD participate in the conceptualization and methodology. MR provides and verifies lymphocyte phenotyping data. KR interpretes kidney graft biopsies. FD and AW provide and verify patients' laboratory data. ML perform statistical analyses. ND, GT, and AV design and perform detailed B cell phenotyping. CK perform data extraction from the DIVAT database. SL, RD, CK, HM, SB, and MG verify the extracted data. SB and MG acquire funding and supervise the study. All authors approved the final version of the manuscript. All authors contributed to the article and approved the submitted version.

DIVAT Cohort Collaborators

(Medical Doctors, Surgeons, HLA Biologists) in Nantes: Gilles Blancho, Julien Branchereau, Diego Cantarovich, Agnès Chapelet, Jacques Dantal, Clément Deltombe, Lucile Figueres, Claire Garandeau, Magali Giral, Caroline Gourraud-Vercel, Maryvonne Hourmant, Georges Karam, Clarisse Kerleau, Christophe Masset, Delphine Kervela, Sabine Lebot, Aurélie Meurette, Simon Ville, Christine Kandell, Anne Moreau, Karine Renaudin, Anne Cesbron, Florent Delbos, Alexandre Walencik, and Anne Devis.

Funding

Agence Nationale de la Recherche (KTD Innov: ANR-17-RHUS-0010, LabEx IGO: LABX-0016-01, Biket: ANR-17-CE17-0008).

Conflict of interest

The authors declare that the research was conducted in the absence of any commercial or financial relationships that could be construed as a potential conflict of interest.

Publisher's note

Supplementary material

The Supplementary Material for this article can be found online at: https://www.frontiersin.org/articles/10.3389/fimmu.2023.1151127/full#supplementary-material

References

1. Clatworthy MR, Watson CJ, Plotnek G, Bardsley V, Chaudhry AN, Bradley JA, et al. B-cell-depleting induction therapy and acute cellular rejection. *N Engl J Med* (2009) 360(25):2683–5. doi: 10.1056/NEJMc0808481

2. Pallier A, Hillion S, Danger R, Giral M, Racapé M, Degauque N, et al. Patients with drug-free long-term graft function display increased numbers of peripheral b cells with a memory and inhibitory phenotype. *Kidney Int* (2010) 78(5):503–13. doi: 10.1038/ki.2010.162

3. Sagoo P, Perucha E, Sawitzki B, Tomiuk S, Stephens DA, Miqueu P, et al. Development of a cross-platform biomarker signature to detect renal transplant tolerance in humans. *J Clin Invest.* (2010) 120(6):1848–61. doi: 10.1172/JCI39922

4. Louis S, Braudeau C, Giral M, Dupont A, Moizant F, Robillard N, et al. Contrasting CD25hiCD4+T cells/FOXP3 patterns in chronic rejection and operational drug-free tolerance. *Transplantation* (2006) 81(3):398–407. doi: 10.1097/01.tp.0000203166.44968.86

5. Newell KA, Asare A, Kirk AD, Gisler TD, Bourcier K, Suthanthiran M, et al. Identification of a b cell signature associated with renal transplant tolerance in humans. *J Clin Invest.* (2010) 120(6):1836–47. doi: 10.1172/JCI39933

6. Matsumoto M, Baba A, Yokota T, Nishikawa H, Ohkawa Y, Kayama H, et al. Interleukin-10-producing plasmablasts exert regulatory function in autoimmune inflammation. *Immunity* (2014) 41(6):1040–51. doi: 10.1016/j.immuni.2014.10.016

7. Blair PA, Noreña LY, Flores-Borja F, Rawlings DJ, Isenberg DA, Ehrenstein MR, et al. CD19(+)CD24(hi)CD38(hi) b cells exhibit regulatory capacity in healthy individuals but are functionally impaired in systemic lupus erythematosus patients. *Immunity* (2010) 32(1):129–40. doi: 10.1016/j.immuni.2009.11.009

8. Fillatreau S, Sweenie CH, McGeachy MJ, Gray D, Anderton SM. B cells regulate autoimmunity by provision of IL-10. *Nat Immunol* (2002) 3(10):944–50. doi: 10.1038/ni833

9. Chesneau M, Michel L, Dugast E, Chenouard A, Baron D, Pallier A, et al. Tolerant kidney transplant patients produce b cells with regulatory properties. *J Am Soc Nephrol* (2015) 26(10):2588–98. doi: 10.1681/ASN.2014040404

10. Lindner S, Dahlke K, Sontheimer K, Hagn M, Kaltenmeier C, Barth TF, et al. Interleukin 21-induced granzyme b-expressing b cells infiltrate tumors and regulate T cells. *Cancer Res* (2013) 73(8):2468–79. doi: 10.1158/0008-5472.CAN-12-3450

11. Braza F, Dugast E, Panov I, Paul C, Vogt K, Pallier A, et al. Central role of CD45RA- Foxp3hi memory regulatory T cells in clinical kidney transplantation tolerance. *J Am Soc Nephrol* (2015) 26(8):1795–805. doi: 10.1681/ASN.2014050480

12. Durand M, Dubois F, Dejou C, Durand E, Danger R, Chesneau M, et al. Increased degradation of ATP is driven by memory regulatory T cells in kidney transplantation tolerance. *Kidney Int* (2018) 93(5):1154–64. doi: 10.1016/j.kint.2017.12.004

13. Moraes-Vieira PM, Silva HM, Takenaka MC, Monteiro SM, Lemos F, Saitovitch D, et al. Differential monocyte STAT6 activation and CD4(+)CD25(+)Foxp3(+) T cells in kidney operational tolerance transplanted individuals. *Hum Immunol* (2010) 71(5):442–50. doi: 10.1016/j.humimm.2010.01.022

14. Stolp J, Turka LA, Wood KJ. B cells with immune-regulating function in transplantation. *Nat Rev Nephrology.* (2014) 10(7):389–97. doi: 10.1038/nrneph.2014.80

15. Braza F, Durand M, Degauque N, Brouard S. Regulatory T cells in kidney transplantation: new directions? *Am J Transplant.* (2015) 15(9):2288–300. doi: 10.1111/ajt.13395

16. Strioga M, Pasukoniene V, Characiejus D. CD8+ CD28- and CD8+ CD57+ T cells and their role in health and disease. *Immunology* (2011) 134(1):17–32. doi: 10.1111/j.1365-2567.2011.03470.x

17. Mou D, Espinosa J, Lo DJ, Kirk AD. CD28 negative T cells: is their loss our gain? *Am J Transplant.* (2014) 14(11):2460–6. doi: 10.1111/ajt.12937

18. Najafian N, Chitnis T, Salama AD, Zhu B, Benou C, Yuan X, et al. Regulatory functions of CD8+CD28- T cells in an autoimmune disease model. *J Clin Invest.* (2003) 112(7):1037–48. doi: 10.1172/JCI17935

19. Davila E, Kang YM, Park YW, Sawai H, He X, Pryshchep S, et al. Cell-based immunotherapy with suppressor CD8+ T cells in rheumatoid arthritis. *J Immunol* (2005) 174(11):7292–301. doi: 10.4049/jimmunol.174.11.7292

20. Baeten D, Louis S, Braud C, Braudeau C, Ballet C, Moizant F, et al. Phenotypically and functionally distinct CD8+ lymphocyte populations in long-term drug-free tolerance and chronic rejection in human kidney graft recipients. *J Am Soc Nephrol* (2006) 17(1):294–304. doi: 10.1681/ASN.2005020178

21. Lo DJ, Weaver TA, Stempora L, Mehta AK, Ford ML, Larsen CP, et al. Selective targeting of human alloresponsive CD8+ effector memory T cells based on CD2 expression. *Am J Transplant.* (2011) 11(1):22–33. doi: 10.1111/j.1600-6143.2010.03317.x

22. Mai HL, Degauque N, Le Bot S, Rimbert M, Renaudin K, Danger R, et al. Antibody-mediated allograft rejection is associated with an increase in peripheral differentiated CD28-CD8+ T cells - analyses of a cohort of 1032 kidney transplant recipients. *EBioMedicine* (2022) 83(104226). doi: 10.1016/j.ebiom.2022.104226

23. Haas M, Loupy A, Lefaucheur C, Roufosse C, Glotz D, Seron D, et al. The banff 2017 kidney meeting report: revised diagnostic criteria for chronic active T cell–mediated rejection, antibody-mediated rejection, and prospects for integrative endpoints for next-generation clinical trials. *Am J Transplantation.* (2018) 18(2):293–307. doi: 10.1111/ajt.14625

24. Loupy A, Haas M, Solez K, Racusen L, Glotz D, Seron D, et al. The banff 2015 kidney meeting report: current challenges in rejection classification and prospects for adopting molecular pathology. *Am J Transplantation.* (2017) 17(1):28–41. doi: 10.1111/ajt.14107

25. Laird NM, Ware JH. Random-effects models for longitudinal data. *Biometrics* (1982) 38(4):963–74. doi: 10.2307/2529876

26. Ibrahim EH, Aly MG, Opelz G, Morath C, Zeier M, Süsal C, et al. Higher CD19+CD25(+) bregs are independently associated with better graft function in renal transplant recipients. *BMC Nephrol.* (2021) 22(1):180. doi: 10.1186/s12882-021-02374-2

27. Brosseau C, Durand M, Colas L, Durand E, Foureau A, Cheminant MA, et al. CD9(+) regulatory b cells induce T cell apoptosis via IL-10 and are reduced in severe asthmatic patients. *Front Immunol* (2018) 9(3034). doi: 10.3389/fimmu.2018.03034

28. Daniel L, Tassery M, Lateur C, Thierry A, Herbelin A, Gombert JM, et al. Allotransplantation is associated with exacerbation of CD8 T-cell senescence: the particular place of the innate CD8 T-cell component. *Front Immunol* (2021) 12(674016). doi: 10.3389/fimmu.2021.674016

29. Wang L, Rondaan C, de Joode AAE, Raveling-Eelsing E, Bos NA, Westra J. Changes in T and b cell subsets in end stage renal disease patients before and after kidney transplantation. *Immun Aging* (2021) 18(1):43. doi: 10.1186/s12979-021-00254-9

30. Pickering H, Sen S, Arakawa-Hoyt J, Ishiyama K, Sun Y, Parmar R, et al. NK and CD8+ T cell phenotypes predict onset and control of CMV viremia after kidney transplant. *JCI Insight* (2021) 6(21):e153175. doi: 10.1172/jci.insight.153175

31. Besançon-Watelet C, De March AK, Renoult E, Kessler M, Béné MC, Faure GC, et al. Early increase of peripheral b cell levels in kidney transplant recipients with CMV infection or reactivation. *Transplantation* (2000) 69(3):366–71. doi: 10.1097/00007890-200002150-00010

32. Nankivell BJ, Alexander SI. Rejection of the kidney allograft. *N Engl J Med* (2010) 363(15):1451–62. doi: 10.1056/NEJMra0902927

33. Calvani J, Terada M, Lesaffre C, Eloudzeri M, Lamarthée B, Burger C, et al. *In situ* Multiplex immunofluorescence analysis of the inflammatory burden in kidney allograft rejection: a new tool to characterize the alloimmune response. *Am J Transpl* (2020) 20(4):942–53. doi: 10.1111/ajt.15699

34. Silva HM, Takenaka MC, Moraes-Vieira PM, Monteiro SM, Hernandez MO, Chaara W, et al. Preserving the b-cell compartment favors operational tolerance in human renal transplantation. *Mol Med (Cambridge Mass).* (2012) 18(1):733–43. doi: 10.2119/molmed.2011.00281

35. Nouël A, Ségalen I, Jamin C, Doucet L, Caillard S, Renaudineau Y, et al. B cells display an abnormal distribution and an impaired suppressive function in patients with chronic antibody-mediated rejection. *Kidney Int* (2014) 85(3):590–9. doi: 10.1038/ki.2013.457

36. Cherukuri A, Rothstein DM, Clark B, Carter CR, Davison A, Hernandez-Fuentes M, et al. Immunologic human renal allograft injury associates with an altered IL-10/TNF-α expression ratio in regulatory b cells. *J Am Soc Nephrol* (2014) 25(7):1575–85. doi: 10.1681/ASN.2013080837

37. Shabir S, Girdlestone J, Briggs D, Kaul B, Smith H, Daga S, et al. Transitional b lymphocytes are associated with protection from kidney allograft rejection: a prospective study. *Am J Transplant.* (2015) 15(5):1384–91. doi: 10.1111/ajt.13122

38. Svachova V, Sekerkova A, Hruba P, Tycova I, Rodova M, Cecrdlova E, et al. Dynamic changes of b-cell compartments in kidney transplantation: lack of transitional b cells is associated with allograft rejection. *Transpl Int* (2016) 29(5):540–8. doi: 10.1111/tri.12751

39. Salehi S, Shahi A, Afzali S, Keshtkar AA, Farashi Bonab S, Soleymanian T, et al. Transitional immature regulatory b cells and regulatory cytokines can discriminate chronic antibody-mediated rejection from stable graft function. *Int immunopharmacology.* (2020) 86(106750). doi: 10.1016/j.intimp.2020.106750

40. Louis K, Fadakar P, Macedo C, Yamada M, Lucas M, Gu X, et al. Concomitant loss of regulatory T and b cells is a distinguishing immune feature of antibody-mediated rejection in kidney transplantation. *Kidney Int* (2022) 101(5):1003–16. doi: 10.1016/j.kint.2021.12.027

41. Long W, Zhang H, Yuan W, Lan G, Lin Z, Peng L, et al. The role of regulatory b cells in kidney diseases. *Front Immunol* (2021) 12(683926). doi: 10.3389/fimmu.2021.683926

42. Catalán D, Mansilla MA, Ferrier A, Soto L, Oleinika K, Aguillón JC, et al. Immunosuppressive mechanisms of regulatory b cells. *Front Immunol* (2021) 12(611795). doi: 10.3389/fimmu.2021.683926

43. Jansen K, Cevhertas L, Ma S, Satitsuksanoa P, Akdis M, van de Veen W. Regulatory b cells, a to z. *Allergy* (2021) 76(9):2699–715. doi: 10.1111/all.14763

44. Mirzakhani M, Shahbazi M, Akbari R, Oliaei F, Asgharpour M, Nikoueinejad H, et al. Reduced CD4(+) CD25(++) CD45RA(-) Foxp3(hi) activated regulatory T cells and its association with acute rejection in patients with kidney transplantation. *Transpl Immunol* (2020) 60(101290). doi: 10.1016/j.trim.2020.101290

45. Braudeau C, Racape M, Giral M, Louis S, Moreau A, Berthelot L, et al. Variation in numbers of CD4+CD25highFOXP3+ T cells with normal immuno-regulatory properties in long-term graft outcome. *Transpl Int* (2007) 20(10):845–55. doi: 10.1111/j.1432-2277.2007.00537.x

46. Akl A, Jones ND, Rogers N, Bakr MA, Mostafa A, El Shehawy el M, et al. An investigation to assess the potential of CD25highCD4+ T cells to regulate responses to donor alloantigens in clinically stable renal transplant recipients. *Transpl Int* (2008) 21(1):65–73. doi: 10.1111/j.1432-2277.2007.00560.x

47. López-Hoyos M, San Segundo D, Brunet M. Regulatory T cells as biomarkers for rejection and immunosuppression tailoring in solid organ transplantation. *Ther Drug monitoring.* (2016) 38(Suppl 1):S36–42. doi: 10.1097/FTD.0000000000000265

48. San Segundo D, Millán O, Muñoz-Cacho P, Boix F, Paz-Artal E, Talayero P, et al. High proportion of pretransplantation activated regulatory T cells (CD4+CD25highCD62L+CD45RO+) predicts acute rejection in kidney transplantation: results of a multicenter study. *Transplantation* (2014) 98(11):1213–8. doi: 10.1097/TP.0000000000000202

49. McRae JL, Chia JS, Pommey SA, Dwyer KM. Evaluation of CD4(+) CD25(+/-) CD39(+) T-cell populations in peripheral blood of patients following kidney transplantation and during acute allograft rejection. *Nephrol (Carlton Vic).* (2017) 22(7):505–12. doi: 10.1111/nep.12894

50. Jacquemont L, Tilly G, Yap M, Doan-Ngoc TM, Danger R. Terminally differentiated effector memory CD8(+) T cells identify kidney transplant recipients at high risk of graft failure. *J Am Soc Nephrol* (2020) 31(4):876–91. doi: 10.1681/ASN.2019080847

51. Yan L, Li Y, Li Y, Wu X, Wang X, Wang L, et al. Increased circulating tfh to tfr ratio in chronic renal allograft dysfunction: a pilot study. *BMC Immunol* (2019) 20 (1):26. doi: 10.1186/s12865-019-0308-x

52. Cherukuri A, Salama AD, Carter CR, Landsittel D, Arumugakani G, Clark B, et al. Reduced human transitional b cell T1/T2 ratio is associated with subsequent deterioration in renal allograft function. *Kidney Int* (2017) 91(1):183–95. doi: 10.1016/j.kint.2016.08.028

53. Heidt S, Vergunst M, Anholts JDH, Swings G, Gielis EMJ, Groeneweg KE, et al. Presence of intragraft b cells during acute renal allograft rejection is accompanied by changes in peripheral blood b cell subsets. *Clin Exp Immunol* (2019) 196(3):403–14. doi: 10.1111/cei.13269

frontiers | Frontiers in Immunology

TYPE Original Research
PUBLISHED 03 May 2023
DOI 10.3389/fimmu.2023.1183768

OPEN ACCESS

EDITED BY
Xuanchuan Wang,
Fudan University, China

REVIEWED BY
Katrin Scionti,
Gamanity Health and Cosmetics,
United Kingdom
Ali Akbar Pourfathollah,
Tarbiat Modares University, Iran

*CORRESPONDENCE
Bin Yang
by5@le.ac.uk

†These authors have contributed equally to this work and share first authorship

RECEIVED 10 March 2023
ACCEPTED 13 April 2023
PUBLISHED 03 May 2023

CITATION
Wu Y, Huang L, Sai W, Chen F, Liu Y, Han C, Barker JM, Zwaini ZD, Lowe MP, Brunskill NJ and Yang B (2023) HBSP improves kidney ischemia-reperfusion injury and promotes repair in properdin deficient mice *via* enhancing phagocytosis of tubular epithelial cells. *Front. Immunol.* 14:1183768. doi: 10.3389/fimmu.2023.1183768

HBSP improves kidney ischemia-reperfusion injury and promotes repair in properdin deficient mice *via* enhancing phagocytosis of tubular epithelial cells

Yuanyuan Wu[1,2†], Lili Huang[3†], Wenli Sai[4†], Fei Chen[3], Yu Liu[3], Cheng Han[3], Joanna M. Barker[5], Zinah D. Zwaini[6], Mark P. Lowe[5], Nigel J. Brunskill[2,3] and Bin Yang[2,3*]

[1]Department of Pathology, Medical School of Nantong University, Nantong, China, [2]Department of Cardiovascular Sciences, College of Life Sciences, University of Leicester, University Hospitals of Leicester NHS Trust, Leicester, United Kingdom, [3]Nantong-Leicester Joint Institute of Kidney Science, Nephrology, Affiliated Hospital of Nantong University, Nantong, China, [4]Research Center of Clinical Medicine, Affiliated Hospital of Nantong University, Nantong, China, [5]School of Chemistry, University of Leicester, Leicester, United Kingdom, [6]Department of Respiratory Sciences, College of Life Sciences, University of Leicester, Leicester, United Kingdom

Phagocytosis plays vital roles in injury and repair, while its regulation by properdin and innate repair receptor, a heterodimer receptor of erythropoietin receptor (EPOR)/β common receptor (βcR), in renal ischaemia-reperfusion (IR) remains unclear. Properdin, a pattern recognition molecule, facilitates phagocytosis by opsonizing damaged cells. Our previous study showed that the phagocytic function of tubular epithelial cells isolated from properdin knockout (P^{KO}) mouse kidneys was compromised, with upregulated EPOR in IR kidneys that was further raised by P^{KO} at repair phase. Here, helix B surface peptide (HBSP), derived from EPO only recognizing EPOR/βcR, ameliorated IR-induced functional and structural damage in both P^{KO} and wild-type (WT) mice. In particular, HBSP treatment led to less cell apoptosis and F4/80+ macrophage infiltration in the interstitium of P^{KO} IR kidneys compared to the WT control. In addition, the expression of EPOR/βcR was increased by IR in WT kidneys, and furthered increased in IR P^{KO} kidneys, but greatly reduced by HBSP in the IR kidneys of P^{KO} mice. HBSP also increased PCNA expression in IR kidneys of both genotypes. Moreover, iridium-labelled HBSP (HBSP-Ir) was localized mainly in the tubular epithelia after 17-h renal IR in WT mice. HBSP-Ir also anchored to mouse kidney epithelial (TCMK-1) cells treated by H_2O_2. Both EPOR and EPOR/βcR were significantly increased by H_2O_2 treatment, while further increased EPOR was showed in cells transfected with small interfering RNA (siRNA) targeting properdin, but a lower level of EPOR was seen in EPOR siRNA and HBSP-treated cells. The number of early apoptotic cells was increased by EPOR siRNA in H_2O_2-treated TCMK-1, but markedly reversed by HBSP. The phagocytic function of TCMK-1 cells assessed by uptake fluorescence-labelled *E.coli* was

enhanced by HBSP dose-dependently. Our data demonstrate for the first time that HBSP improves the phagocytic function of tubular epithelial cells and kidney repair post IR injury, *via* upregulated EPOR/βcR triggered by both IR and properdin deficiency.

KEYWORDS

HBSP, innate repair receptor, ischaemia-reperfusion injury, phagocytosis, properdin, repair, tubular epithelial cells

Introduction

Acute kidney injury (AKI), characterized by a sudden decline of kidney filtration function, is a common health problem associated with high mortality and chronic transformation (1, 2). Ischemia/reperfusion (IR)-related injury is one of important causes of AKI in clinical settings (3). However, due to limited understanding of its underlying mechanism modulating AKI progression, effective and timely intervention is currently unavailable (4).

Erythropoietin (EPO) receptors include the homodimer $(EPOR)_2$ initiating erythropoiesis and the heterodimer EPOR/βcR that delivers tissue protection only, thus also known as the innate repair receptor, without role in erythropoiesis (5). The function of EPOR/βcR was mainly discovered *via* its specific ligand EPO-derived helix B surface peptide (HBSP) (6). HBSP attenuated cell death, inflammation and prevented progression of chronic fibrosis after kidney IR injury through multiple signaling pathways, including caspase 9/3, HSP70 and PI3K/Akt/FoxO3a signaling (7–9). It was also reported that EPOR maintains tissue homeostasis (10) by inhibiting the pro-inflammatory functions of macrophages, whilst enhancing their phagocytic functions through activating JAK2/ERK/PPARγ (11). We previously reported that EPOR expression was upregulated by IR at the repair phase of 72 h post injury in mice and further elevated by properdin knockout (P^{KO}) that also led to more severe damage than wild type (WT) controls (12).

Phagocytosis is a critical process to limit injury and initiate repair after renal IR *via* clearance of damaged cells and inflammation (13). The recognition and uptake of dead cells by a phagocyte usually relies on 'find-me signals', opsonization and 'eat-me signals' through phagocytic receptors (14). Recently, the complement regulator properdin was found to function as a pattern recognition molecule (PRM) aside from being the sole positive regulator of the alternative pathway activation. Kemper and colleagues reported that neutrophil-released but not serum-derived properdin recognized and bound to apoptotic T cells and facilitated their uptake by macrophages (15). It was also found that properdin binds to the glycosaminoglycan chains of cell surface proteoglycans in apoptotic T cells and is recognized by phagocytic macrophages through heparin receptors. In addition, properdin can also bind to carbon nanotubes and enhance their uptake by macrophages, acting as a PRM and participating in the process of opsonization during phagocytosis (16). Usually produced by inflammatory cells (17, 18), properdin was also expressed on renal tubular epithelial cells (TECs) (12, 19). We revealed *in vitro* that viable TECs produced properdin anchored on damaged TECs subjected to IR-related injury, facilitated the phagocytic clearance of damaged cells and also were directly involved in the phagocytic function of TECs, as semi-professional phagocytes (12).

Investigations whether raised EPOR could function as a compensatory mechanism of phagocytosis in P^{KO} condition and thus would contribute to the clearance of damaged cells and inflammation after IR injury warranted as proof of principle. Here, based on our previous 72-h renal IR injury model using both P^{KO} and WT mice, the effect of HBSP treatment was further studied in mice of both genotypes at the same time point. Furthermore, the mechanism of HBSP protection in properdin deficiency mice was explored in particular with focuses on regulating EPO receptors and phagocytosis in TECs.

Materials and methods

Mouse kidney IR model

Previously, adult male C57BL/6 WT and P^{KO} mice aged 8-12 week were subjected to bilateral renal ischaemia 30 min and reperfusion for 72 h, as well as sham surgery (WT sham: n = 4; P^{KO} sham: n = 5; WT IR: n = 9; P^{KO} IR: n = 8.) (12). Here, under equal standard of animal maintenance and anesthetic practice, the same IR surgical procedure was performed to additional P^{KO} and their littermates WT mice with treatment of HBSP (Figure 1A).

HBSP (Science Peptide, Shanghai, China), dissolved in saline and warmed to 37°C, was given to animals at a total dose of 24 nmol/kg body weight through injecting at the onset of occlusion and 15 minutes after reperfusion (half/half) intraperitoneally. There were 6 or 5 mice in WT IR + HBSP group and P^{KO} IR + HBSP group, respectively. Reperfusion was confirmed by the color of the renal surface changing from dark to patched blanching and then back to normal pink. All mice studies were performed in accordance with institutional guidelines approved by the United Kingdom Home Office. At 72 h of reperfusion, the animals were humanely killed and whole blood as well as bilateral kidneys were then obtained for further analysis.

10.3389/fimmu.2023.1183768

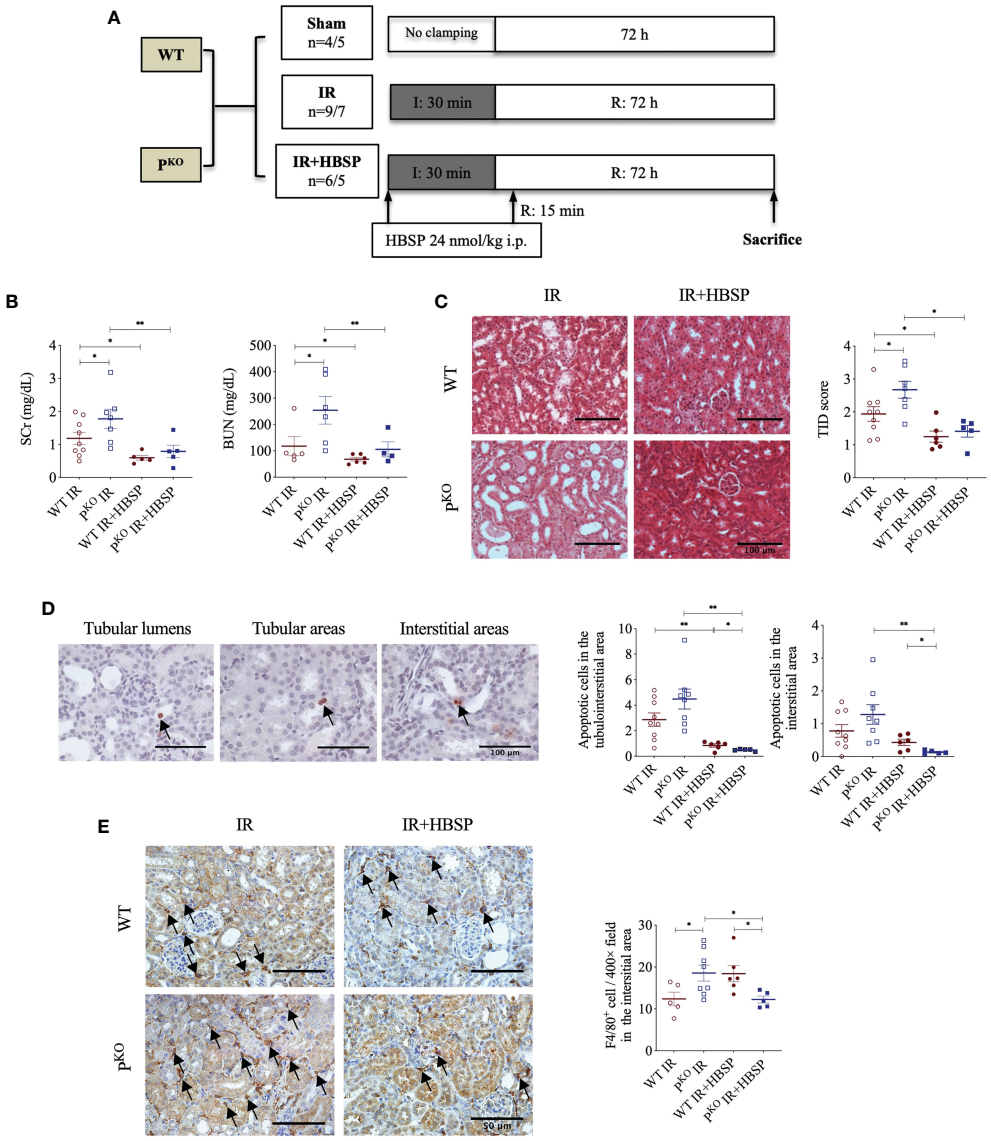

FIGURE 1
At 72 h, HBSP effectively reduced kidney IR damage in both WT and P^{KO} mice. **(A)** Animal study design. WT: wildtype; P^{KO}: properdin knockout; I: ischemia; R: reperfusion; IR: ischemia/reperfusion. **(B)** HBSP significantly decreased the SCr and BUN levels in both WT and P^{KO} IR mice. **(C)** Representative images of renal cortex with H&E staining shows that HBSP greatly reduced the tubulointerstitial damage (TID) score of the renal cortex in both genotypes. Scale bar, 100 μm; magnification, 20x. **(D)** Representative images of TUNEL staining shows apoptotic cells in tubular lumina, tubular areas and interstitial areas. Scale bar, 100 μm; magnification, 40x. Semi-quantitative analysis illustrated that HBSP significantly attenuated total and interstitial apoptosis in both IR mice of genotypes, and further on P^{KO}. **(E)** Representative images of F4/80 staining show macrophages in interstitial areas. Scale bar, 50 μm; magnification, 40x. Semi-quantitative analysis demonstrated that IR kidneys of P^{KO} mice with HBSP treatment showed a lower level of macrophage infiltration than the P^{KO} IR group and the WT control modified by HBSP. One-way ANOVA, Least significance difference (LSD) test. IR: n = 5-9; IR + HBSP: n = 4-6. Plots depict means ± SEM. *, $P<0.05$, **, $P<0.01$.

Biochemical detection

Serum Creatinine (SCr) and Blood urea nitrogen (BUN) levels were determined using a QuantiChromTM Creatinine Assay Kit and a Bioassay System urea assay kit (BioAssay System, Hayward, CA) according to the manufacturer's instruction.

Histological assessment

Four μm sections of paraffin-embedded kidney tissue were stained using hematoxylin & eosin. The score of tubulointerstitial damage (TID) in cortical areas was evaluated by two researchers blinded to the groups and treatment, using a previously described method (20). The sections were viewed at 400x magnification and 15 randomly selected cortical fields were scored for each kidney. The final TID for each animal was determined by dividing average scores from the left and right kidneys of each animal.

Labeling apoptotic cells

In situ labeling of DNA strand breaks in apoptotic cells in paraffin-embedded kidney sections was done with the ApopTag®

Peroxidase kit (Merck, Watford, UK). The positively stained cells were revealed by AEC (3-amino-9-ethylcarbazole, bright red color) substrate (Vectorlabs, Newark, CA) and hematoxylin was used for counter staining. Apoptotic cells were separately examined in the tubular area, tubular lumen, and interstitial area of the renal cortex in 15 randomly selected fields at 400x magnification for each tissue. The final number of apoptotic cells in each animal was calculated by averaging the cell numbers from all fields of the left and right kidneys.

Labeling macrophages

Interstitial infiltration of macrophages was analyzed by F4/80 staining. The paraffin-embedded kidney sections were dewaxed and treated with the EDTA Antigen Retrieval Solution (E673003, BBI, Shanghai, China) for 10 min in a high-pressure steam cooker. The sections were then processed to the QuickBlock blocking buffer (P0260, Beyotime, Shanghai, China) for 30 min at room temperature, followed by incubation with the primary rabbit–anti mouse F4/80 antibody (1:1000, 28463-1-AP, Proteintech, Chicago, USA) or normal rabbit IgG for negative control (2729S, CST, Danvers, USA) at 4°C overnight. The next day, the secondary antibody (PV-6000, ZSGB-BIO, Beijing, China) was applied to the sections for 20 min at 37°C. The 3,3′-diaminobenzidine (DAB, Beyotime) was used to reveal the antibody binding and then the sections were counterstained with hematoxylin. Positively stained cells were counted at 400× magnification for 15 randomly selected fields per section. The average of counts per field from both left and right kidneys in each animal was used for statistical analysis.

Cell culture and treatment

TCMK-1, a mouse kidney epithelial cell line (ATCC, CCL-139), was maintained in the complete medium containing DMEM/F12 1:1 medium (Gibco, Paisley, UK), 10% fetal bovine serum (FBS, Sigma, Dorset, UK), 2 mM L-glutamine (Gibco), 100 U/ml penicillin G and 100 mg/ml streptomycin (Sigma), at 37°C in a 5% CO_2 humidified atmosphere.

Cells at a density of 1×10^5 cells/well were seeded into six-well plates and cultured in complete medium but without antibodies. The next day, the cells were changed culture medium to DMEM/F12 1:1 only and then transfected with siRNA (Thermo Fisher Scientific, Rockford, USA) targeting mouse properdin (PsiRNA, s71507), EPOR (EPORsiRNA, s65611) or negative control siRNA (NCsiRNA, 4390843, not targeting any known mammalian genes) at 20 nM with assistant of Lipofectamine™ RNAiMAX (Invitrogen, Carlsbad, USA).

Six hours after transfection, the cells were then changed culture medium to complete medium and stimulated with hydrogen peroxide (H_2O_2) at 100 μM to mimic oxidative stress during renal IR. At the same time, HBSP (Science Peptide) at 20 ng/ml was added to the cell culture medium for treatment. After another 18 hours, whole protein was extracted for detecting EPOR and EPOR/βcR by western blotting and co-immunoprecipitation. In addition, the percentage of early and later apoptotic cells was examined by Annexin V/PI staining (Roche, Mannheim, Germany) and determined by a flow cytometer (FACSCanto, BD, Bergen, USA). In each experiment, two replicates per group were used, while the individual experiment was repeated at least three times.

Immunoblotting

The mice kidney and tubular cells were harvested and homogenized in RIPA lysis buffer (89900, Thermo Fisher Scientific). Twenty-five μg proteins were separated in SDS-PAGE gel and then transferred onto PVDF membrane (Merck, Watford, UK) at constant current of 300 mA for 1 h. The membrane was then blocked with 5% non-fat milk (Bio-Rad, Berkeley, USA) and incubated with Rabbit polyclonal primary antibody to EPOR (1:1,000, PAB18350, Abnova, Taiwan), PCNA (1:1,000, M0879, DAKO, Glostrup, Denmark) or β-actin (1:5,000, A5441, Sigma, Dorset, UK) overnight at 4°C. The secondary antibody (Goat–anti-Rabbit/Mouse, K4063, DAKO) was peroxidase-conjugated and incubated with the membrane for 2 h at room temperature. The membrane was developed using ECL substrate (Thermo Fisher Scientific) and a Molecular Imager ChemiDoc XRS+ system (Bio-Rad). Blots were semi-quantitatively analyzed by scanning volume density using Bio-Rad Image Lab Software 5.2.1 (Bio-Rad). Optical volume density values for target proteins were corrected by β-actin.

Co-immunoprecipitation

The EPOR protein was immunoprecipitated from 200 μg tissue/cell homogenates through incubation with 1 μg of anti-EPOR antibody (PAB18350, Abnova) for overnight at 4 °C on a rotator. Then, 40 μl protein A sepharose beads (17-0469-01, GE healthcare, Pittsburgh, USA) was added to each sample and incubated for another 2 h at 4 °C on the rotator. Afterwards, the beads were collected by spinning at 500 g for 30 s and washed 3 times with RIPA buffer. The supernatant was discarded and 25 μl of 4×loading buffer (Bio-Rad) was added to each sample and boiled for 10 min at 100 °C on a heat block. The samples were separated by SDS-PAGE gels, transferred onto PVDF membranes and probed with anti-βcR antibody (sc-93281, Santa Cruz, Dallas, USA). The final detected βcR bands represent the level of EPOR/βcR heterodimer.

HBSP localization in mice organs and tubular cells

For location tracking, HBSP was conjugated with iridium (Ir), which was produced by our collaborators in the Chemistry Department of University of Leicester.

In vivo, adult male C57BL/6 mice between 8-12 weeks, were subjected to bilateral renal ischaemia for 0 min (sham surgery) or 30 min followed by reperfusion for 17 h. Afterwards, HBSP-Ir conjugate (dissolved in sterile 0.9% saline) at 48 nmol/kg body

weight was injected *via* the tail vein. Thirty minutes later, the mice were sacrificed and the kidneys, heart, liver and lungs were embedded in OCT and snap frozen in liquid nitrogen. Cryopreserved tissues from different organs were then cut into sections at 5 μm thickness using Leica freezing microtome (CM1950, Wetzlar, Germany), and mounted in Anti-Fade Fluorescence Mounting Medium (ab104135, abcam). The florescence signal (green) of Ir was excited at 405 nm and emission was collected between 500 +/- 20 nm using a confocal microscope (TCS SP8, Leica).

In vitro, TCMK-1 cells were seeded onto glass coverslips pre-coated with Poly-D-lysine (0.1 mg/ml; P1149, sigma). The density of seeding was 1.0×10^5 cells/ml. After 24 h, the cells were stimulated with 200 μM of H_2O_2 for another 24 h. Then, HBSP, Ir or HBSP-Ir was added to the culture medium at a concentration of 50 μM. One hour later, the cells were labeled with Rhodamine Phalloidin (PHDR1, Cytoskeleton, Denver, USA) in order to visualize the cellular skeletal protein F-actin. The specimens were then mounted and observed using the confocal microscope (TCS SP8, Leica). Ir fluorescence was measured at the parameter same with the *in vivo* tracking. Rhodamine fluorescence was measured between 585 +/- 20 nm following excitation at 555 nm.

Phagocytic assay

The phagocytic ability of TCMK-1 cells was evaluated *via* uptaking *E.coli* Bioparticles (FITC-labelled pHrodo *E.coli* Bioparticles® Conjugate, P35366, Thermo Fisher Scientific) using flow cytometry. The fluorogenic dye conjugated to *E.coli* was pH sensitive that greatly increases in fluorescence when the surroundings becomes more acidic after phagocytosis occurs. TCMK-1 was seeded to 24-well plates at 1.0×10^5 cells/ml and treated with HBSP at 20, 40 and 80 ng/ml next day for 24 h. *E.coli* Bioparticles (0.5 mg/ml, suspended in DMEM/F12 medium) was then added at 500 μl/well for 2 h. Afterwards, the cells were washed to remove non-phagocytosed *E.coli* Bioparticles and resuspended after tripsinizing. For each sample, a total of 10,000 gated cells were analysed for the fluorescent intensity of FITC on a flow cytometer (FACSCanto, BD). The average FITC intensity of total cells and positive cells were defined by a selected threshold; a percentage of positive cells was then analyzed.

Statistical analysis

Data is expressed as mean ± standard error of the mean (SEM). One-way ANOVA and LSD (Least significance difference) tests were carried out by SPSS Statistics Standard V26.0 software (IBM, New York, USA) to assess differences between data means as appropriate. A P value of < 0.05 was considered statistically significant.

Results

HBSP protected 72-h IR kidneys in both genotype mice

The experimental design of a 72-h kidney IR injury model, illustrated in Figure 1A, used WT and P^{KO} C57BL/6 mice with or without HBSP treatment. Our previous publication has included the data from sham and IR groups of both genotypes (12), of which values on the renal function, structural, apoptosis and PCNA have also been included in the Table 1. Here, we demonstrated the therapeutic effect of HBSP on kidneys from the two genotypes. At IR 72 h, the elevated SCr was significantly decreased by HBSP in both WT (1.2 0.2 vs. 0.6 0.1, $P < 0.01$) and P^{KO} (1.8 0.3 vs. 0.8 0.2, $P < 0.01$) mice, with similar effects on BUN (Figure 1B). Structurally, the level of TID was increased by P^{KO} in contrast to WT kidneys after IR injury, while HBSP treatment greatly reduced the TID score in both WT and P^{KO} genotypes (Figure 1C). The number of apoptotic cells in the tubulointerstitial area of kidneys after IR was significantly reduced by HBSP, which was further decreased in P^{KO} mice (WT IR + HBSP vs. P^{KO} + IR + HBSP, 0.8 0.1 vs. 0.5 0.0, $P<0.05$, Figure 1D). Notably, the number of apoptotic cells was significantly lower in the interstitial area of IR kidneys from P^{KO} mice than that in the WT control

TABLE 1 Values of Sham vs. IR groups at IR 72 h.

Genotypes	Detections	Sham	IR	Statistics
WT	SCr	0.4 ± 0.1	1.2 ± 0.2	$P < 0.05$
	BUN	52.6 ± 2.9	82.3 ± 22.3	$P < 0.05$
	TID	1.2 ± 0.1	1.9 ± 0.2	$P < 0.05$
	Apoptosis	0.7 ± 0.1	2.9 ± 0.5	$P < 0.05$
	PCNA	1.0 ± 0.2	5.2 ± 1.1	$P < 0.05$
P^{KO}	SCr	0.3 ± 0.1	1.8 ± 0.3	$P < 0.01$
	BUN	40.3 ± 2.3	246.4 ± 44.9	$P < 0.01$
	TID	1.4 ± 0.0	2.7 ± 0.3	$P < 0.01$
	Apoptosis	0.5 ± 0.2	4.5 ± 0.8	$P < 0.01$
	PCNA	2.9 ± 0.9	8.2 ± 1.5	$P < 0.05$

modified by HBSP. These results demonstrated that HBSP greatly ameliorated IR-induced kidney functional and structural injury at 72 h in both WT and P^{KO} mice, and further decreased renal apoptotic level in P^{KO} mice than in the WT control.

HBSP further decreased macrophage infiltration in kidneys of P^{KO} at IR 72 h

The immunostaining of F4/80 in the kidney revealed macrophage infiltration modified by IR and HBSP in both genotypes. There was no staining found in the negative control sections (results not shown). In the positively stained sections, the F4/80+ cells in the interstitial area were not significantly changed by HBSP in kidneys of WT mice, but were greatly reduced in P^{KO} kidneys at IR 72 h (Figure 1E). Moreover, the P^{KO} kidneys showed fewer positive cells than the WT control after treatment significantly (12.2 0.8 vs. 18.4 1.9, $P<0.05$). Thus, HBSP treatment decreased the number of interstitial F4/80+ cells in IR kidneys of P^{KO} mice only, which also showed a considerable reduction of F4/80 + cells than in the WT control after treatment.

EPOR, EPOR/βcR and PCNA expression were regulated by IR, P^{KO} and HBSP

EPOR was previously found upregulated by IR and enhanced by P^{KO} at IR 72 h (12), thus, the expressional change of EPOR, especially EPOR/βcR, in IR kidneys regulated by HBSP was further explored. The highly expressed EPOR in IR kidneys was greatly downregulated by HBSP in WT mice, but not in P^{KO} mice (Figure 2A). In fact, the level of EPOR in P^{KO} IR kidneys was still significantly higher than that in the WT control (1.7 0.8 vs. 0.1 0.0, $P<0.05$) after HBSP treatment. In addition, the expression of the heterodimer EPOR/βcR was greatly increased by IR injury in both genotypes and furthered by P^{KO} (7.6×10^6 1.8×10^6 vs. 3.2×10^6 8.0×10^5, $P<0.05$, Figure 2B). HBSP treatment significantly decreased the level of EPOR/βcR in the kidneys of P^{KO} mice, but not in WT mice after IR. The expression of PCNA protein was significantly upregulated by HBSP in both genotypes (Figure 2C). HBSP increased the PCNA in IR kidneys of both genotypes but modified the tissue protective receptors EPOR and EPOR/βcR differentially in WT and P^{KO} mice kidneys.

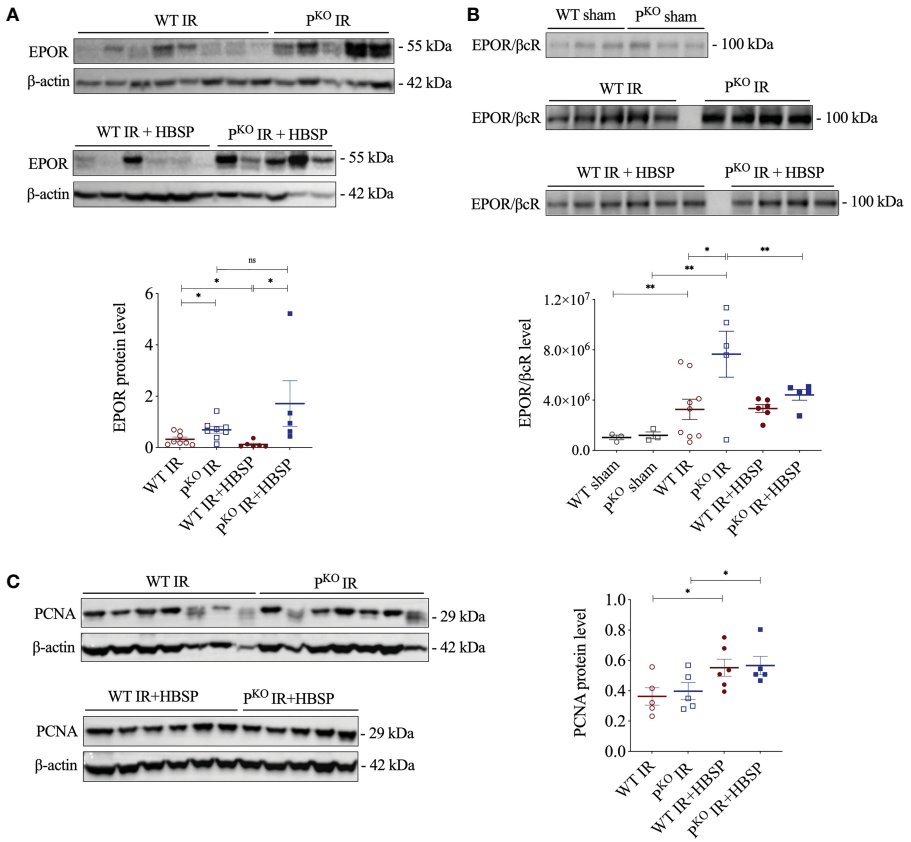

FIGURE 2
At 72 h, HBSP significantly reduced the high of EPOR proteins in WT IR mice and the heterodimer EPOR/βcR in P^{KO} IR mice. **(A)** HBSP decreased the high levels of EPOR in WT IR mice but not in P^{KO} IR mice by western blotting corrected with β-actin. **(B)** Co-immunoprecipitation demonstrated that the expression of EPOR/βcR protein complex was IR significantly increased in both WT and P^{KO} kidneys after IR, but reduced by HBSP only in P^{KO} kidneys. **(C)** HBSP increased the level of PCNA in IR mice of both WT and P^{KO} mice by western blotting corrected with β-actin. One-way ANOVA, LSD test. Sham: n = 3; IR: n = 5-8; IR + HBSP: n = 4-6. Plots depict means ± SEM. *, $P<0.05$, **, $P<0.01$, ns, no significance.

HBSP located in tubular epithelial cells post IR and IR-related injury

The structure and chemical formulas of Ir, HBSP and HBSP-Ir are shown in Figures 3A–C respectively. The excitation and emission wavelengths of Ir were 300-450 nm and 400-600 nm (shown as green signals), respectively (Figure 3D). HBSP-Ir was used to track the localization of HBSP in major organs and cells in the context of renal IR injury (Figure 4A). As shown in Figure 4B, there was no recognizable green signal (seen as Ir) in the kidney of sham animals, nor in the heart and liver (left panel). However, at IR 17 h, the green signal was greatly distributed in the kidney and mainly localized at tubules (right panel). High magnification pictures demonstrated that the green signal was localized on the apical surface of tubules (Figure 4C). Green signals were also found in the lungs of both sham animals and IR animals, but much weaker than that in IR kidneys.

In vitro, HBSP, Ir or HBSP-Ir was used to treat H_2O_2-stimulated TCMK-1 cells for tracking HBSP-Ir in contrast to the Rhodamine-labelled F-actin (Red, Figure 4D). TCMK-1 cells treated with both HBSP-Ir and H_2O_2 demonstrated marked green signals (Figure 4E), which was around or overlapped with F-actin (Orange, Figure 4F). However, cells treated with H_2O_2 only, H_2O_2 + HBSP or H_2O_2 + Ir, and even HBSP-Ir only, did not show visible green signals. Both *in vivo* and *in vitro* tracking of HBSP-Ir demonstrated that renal tubular epithelial cells are the main target during IR and related injury.

Properdin knockdown increased EPOR expression and affected apoptosis in tubules

The relationship between properdin and EPOR or EPOR/βcR expression, as well as the association between EPOR expression and tubular apoptosis, was further explored by using relevant siRNA *in vitro*. Western blotting results showed that H_2O_2 stimulation significantly increased the expression of EPOR and EPOR/βcR in TCMK-1 cells (Figures 5A, B). Moreover, PsiRNA further upregulated the EPOR level, but not EPOR/βcR, in comparison with NCsiRNA (Figure 5A). The knockdown efficacy of PsiRNA used here was evaluated previously (12). Using EPORsiRNA or HBSP, the EPOR expression was greatly reduced in TCMK-1 cells after H_2O_2 treatment (Figure 5C). However, Flow cytometry analysis showed that EPORsiRNA significantly increased the level of early and late apoptosis in H_2O_2-stimulated TCMK-1 cells, of which the

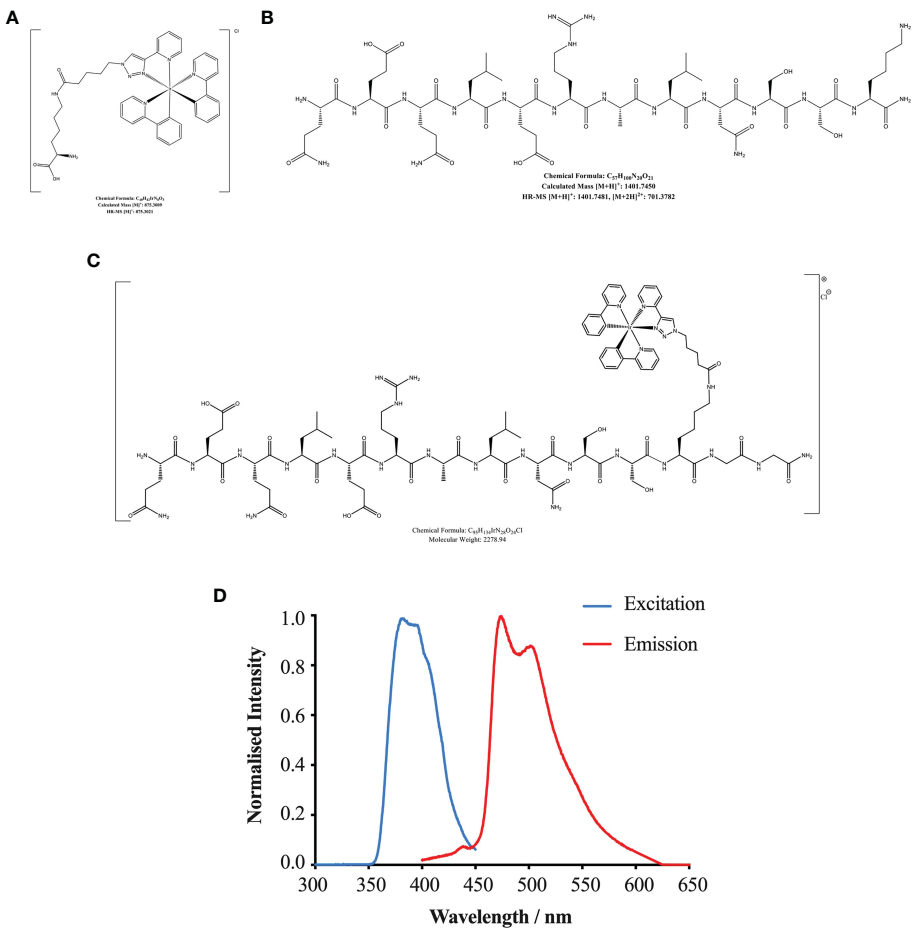

FIGURE 3
Chemical formulas of Iridium **(A)**, HBSP **(B)** and iridium (Ir)-labelled HBSP (HBSP-Ir, **C**). **(D)** Normalized excitation and emission profile of complex HBSP-Ir.

10.3389/fimmu.2023.1183768

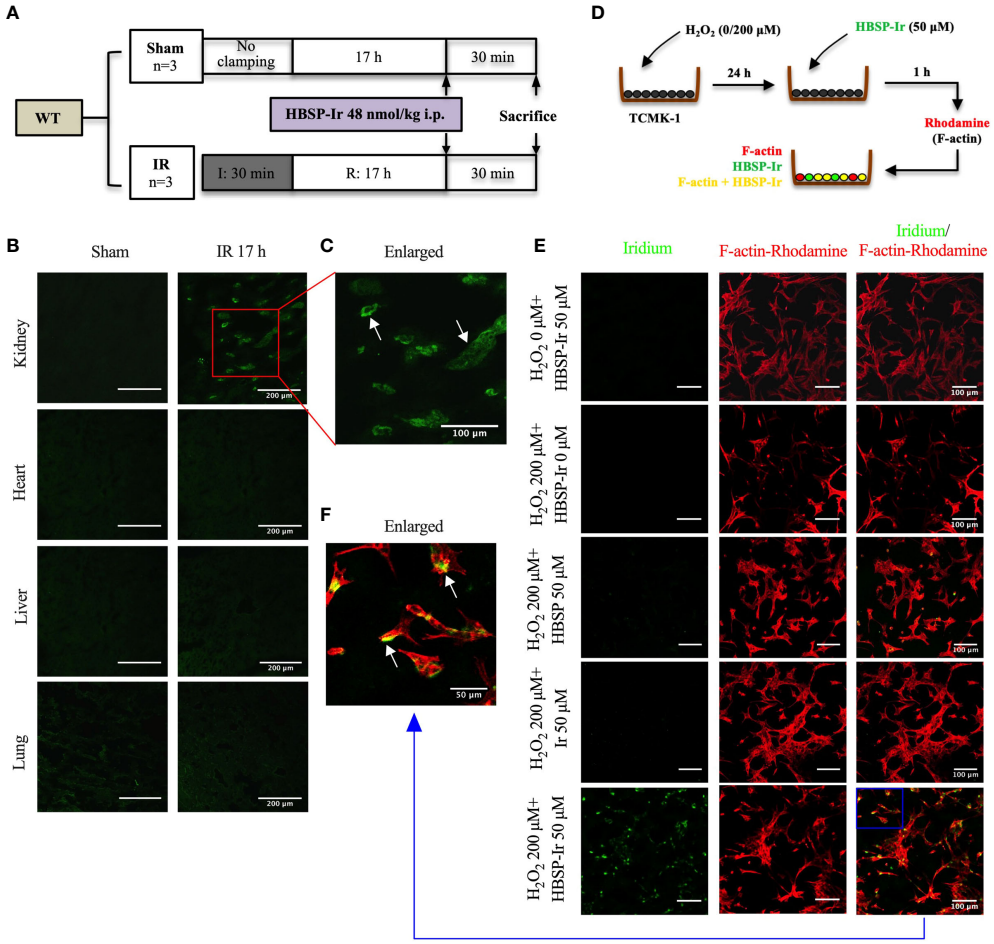

FIGURE 4
HBSP anchors on tubular epithelial cells under IR or IR-related stimulation both *in vivo and in vitro*. **(A)** The experimental design of mouse kidney IR models treated with HBSP-Ir at 17 h. **(B, C)** Representative micrographs from the kidney, heart, liver and lung of sham or IR mice show HBSP-Ir mainly locates on renal TECs, with some weak signals in lung alveolus. The boxed area is enlarged. Scale bar, 200 μm/100 μm (the enlarged image); magnification: 40×. **(D)** The *in vitro* study design of HBSP-Ir localization in tubular epithelial cell (TCMK-1) treated with H_2O_2. **(E, F)** TCMK-1 cells treated with both H_2O_2 and HBSP-Ir showed significant co-localization of HBSP-Ir (green) and F-actin (Rhodamine, red). Scale bar, 100 μm/50 μm (the enlarged image); magnification: 40×.

percentage of raised late apoptosis was attenuated by HBSP (Figure 5D). These results showed that knocking down of properdin further elevated the EPOR expression in TCMK-1 cells upon H_2O_2 stimulation, and the maintenance of the high EPOR expression controls the apoptotic level in TCMK-1 cells.

HBSP enhanced the phagocytic function of kidney tubular epithelia

The role of HBSP on the phagocytic function of kidney tubular epithelia was assessed by the uptake of FITC fluorescent-labeled *E.coli* and detected by flow cytometry (Figure 6A). In contrast to the control cells, there were no significant differences in TCMK-1 cells treated with gradient doses of HBSP, demonstrated by fold changes in the average fluorescent intensity of total cells and positive cells (Figures 6B, C). However, the fold change in average fluorescent intensity of positive cells was significantly increased by HBSP dose-dependently compared to the control (Figure 6D). Thus, HBSP treatment enhanced the phagocytic function of TCMK-1 cells.

Discussion

It has been widely reported, including our previous studies that HBSP, a non-erythropoietic peptide derived from EPO, remarkably ameliorated IR-induced kidney damage with notable improvement in cell death (7, 21–23). However, the mechanism of HBSP renoprotection has not been fully defined, in particular its effect on phagocytosis associated with properdin. In the present study, HBSP significantly improved IR kidney injury in P^{KO} mice in terms of reducing cell apoptosis and macrophage infiltration, while P^{KO} IR kidneys had more severe damage than WT controls. Properdin was shown to be an essential opsonizing molecule of phagocytic process, and also involved in the phagocytic function of renal TECs (12, 24). The protective effect of HBSP against IR injury in P^{KO} kidneys might

10.3389/fimmu.2023.1183768

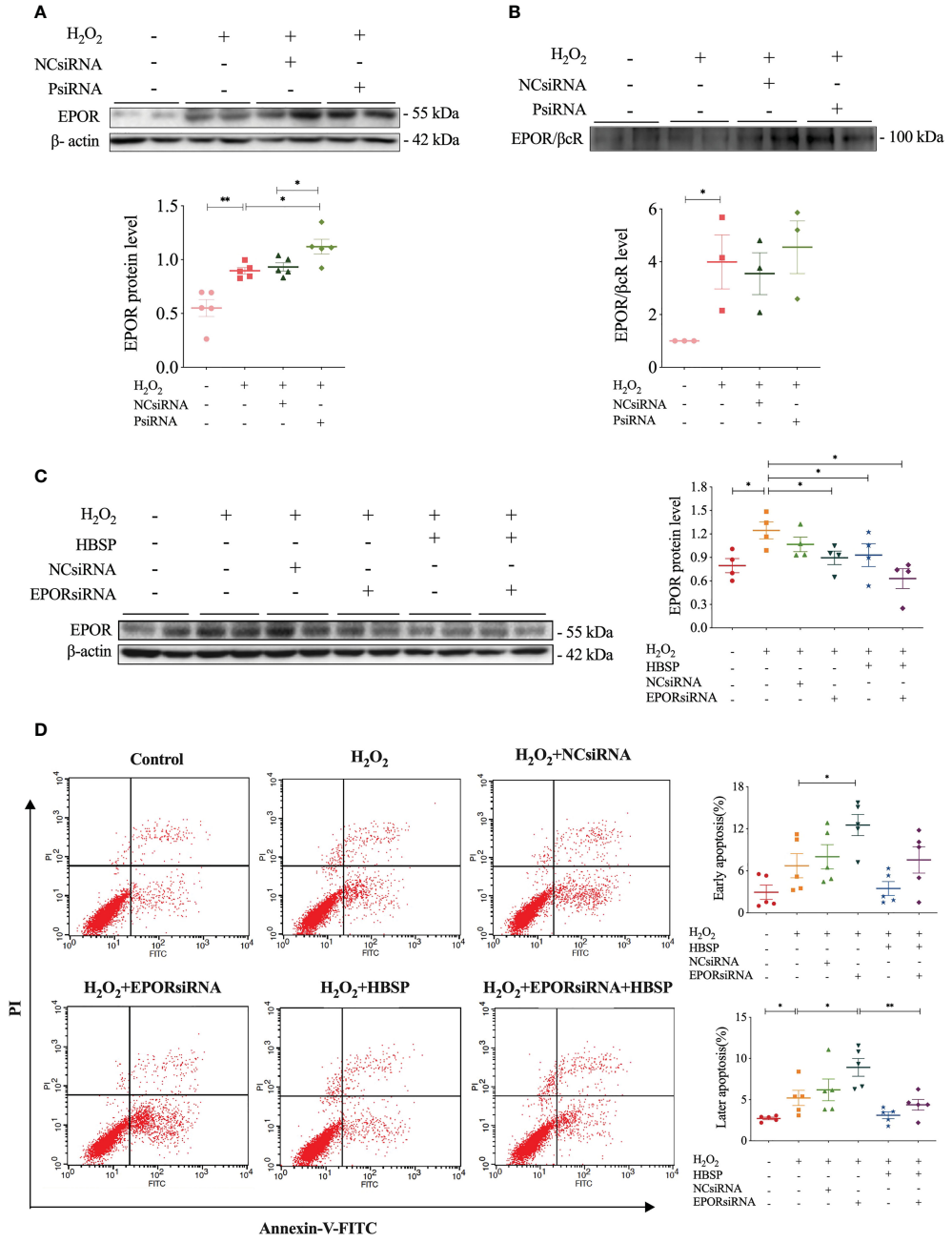

FIGURE 5
Properdin silencing increased EPOR expression that mediated cell apoptosis revealed in kidney tubular epithelial cells. **(A)** Small interfering RNA targeting mouse properdin (PsiRNA) significantly increased the EPOR level in TCMK-1 cells stimulated with H_2O_2 by western blotting, corrected with β-actin. Five independent experiments with 2 replicates each time. **(B)** Co-immunoprecipitation shows that H_2O_2 greatly increased EPOR/βcR protein complex in TCMK-1, but remained a similar level under PsiRNA interfering. Three independent experiments with 2 replicates each time. **(C)** Western blot shows that the level of EPOR protein in TCMK-1 cells was decreased by small interfering RNA targeting mouse EPOR (EPORsiRNA), HBSP or EPORsiRNA + HBSP significantly under stimulation with H_2O_2. Four independent experiments with 2 replicates each time. **(D)** Flow cytometry data demonstrates that H_2O_2 treatment significantly increases % late apoptosis (upper right quadrant), furthered by EPORsiRNA, but decreased by HBSP. EPORsiRNA also increased % early apoptosis (lower right quadrant) under H_2O_2 treatment. Five independent experiments with 2 replicates each time. One-way ANOVA, LSD test. Plots depict means ± SEM. *, $P<0.05$, **, $P<0.01$.

attribute to the higher expression of EPOR/βcR in TECs, by which HBSP might boost the phagocytic function of TECs as a compensation mechanism for the impact of properdin deficiency on phagocytosis.

HBSP, a specific ligand of the tissue protective receptor EPOR/βcR, reversed renal IR-induced functional and structural damage and promoted proliferation, not only in the kidneys of WT mice, but also more effective in severe damaged kidneys of properdin deficient mice. We demonstrated that the expression of EPOR/βcR in kidneys was greatly increased by the absence of properdin after IR injury, which was also reliant upon the level of elevated EPOR. The upregulated expression of these receptors would facilitate renoprotection of HBSP treatment in terms of compensating the absence of properdin

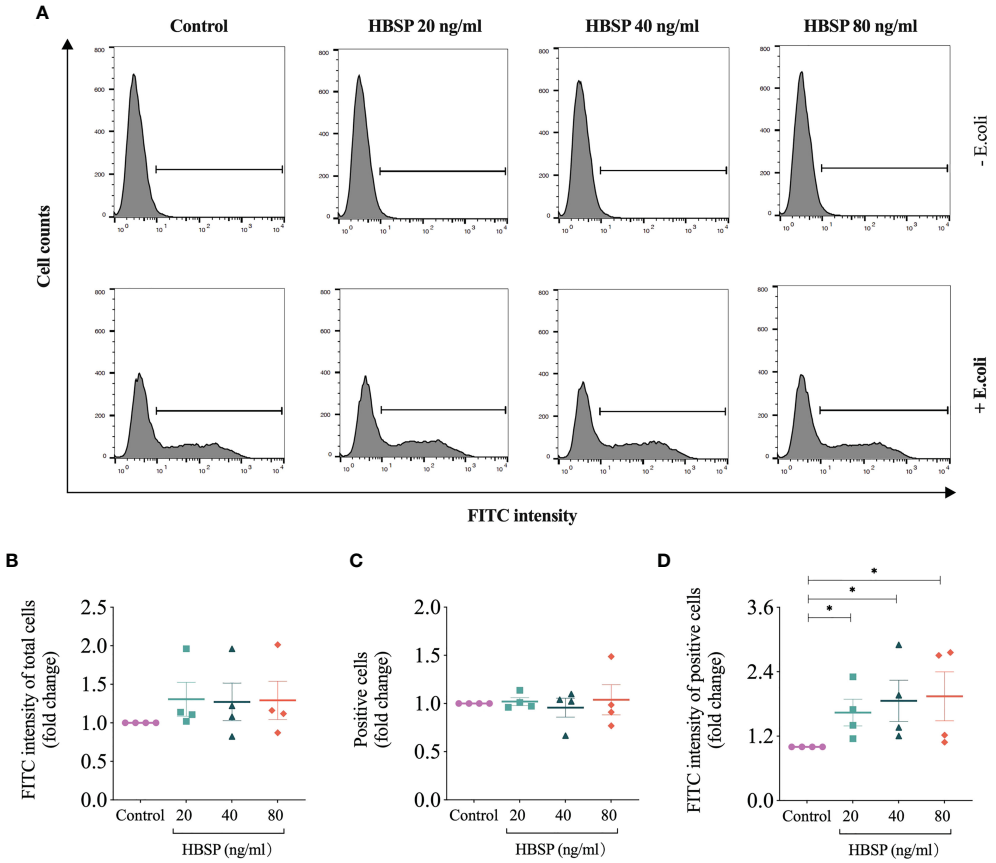

FIGURE 6
HBSP treatment enhances the phagocytic function of tubular epithelial cell *in vitro*. **(A)** Flow cytometry analyses TCMK-1 cells uptaking FITC-labeled *E.coli*. Cells under the threshold line were seen as positive. **(B-D)** The fold change of the average intensity of FITC fluorescence among total analyzed cells, positive cell counts and the average intensity of FITC fluorescence among positive cells are shown against the corresponding group without *E.coli* treatment. Four independent experiments with 2 replicates each time. One-way ANOVA, LSD test. Plots depict means ± SEM.*, $P<0.05$.

opsonized phagocytosis. In addition, it was worth to note that HBSP treatment led to fewer interstitial apoptotic cells as well as F4/80+ macrophages in P^{KO} mouse kidneys compared with the WT control. Apoptotic cells in interstitial areas are often regarded as remnants of dead infiltrated inflammatory cells after they finished the mission of clearing acute inflammation. Thus, the fewer apoptosis in the interstitial area would result from the less macrophage infiltration in the P^{KO} IR kidneys. The location of heterodimer EPOR/βcR was found in the tubules of WT and P^{KO} mouse kidneys after IR (7, 12). The highly expressed EPOR/βcR in P^{KO} mouse kidneys could contribute to the better preservation of renal parenchymal cells including TECs, thus reduce tissue injury and macrophage infiltration. In addition, it has been reported that HBSP could reduce the secretion of pro-inflammatory cytokines from macrophages, as well as the transformation of macrophages towards pro-inflammatory M1 genotype, but promote their survival by upregulating the expression of caspase activation inhibitors including survivin and Bag1 (10, 25). These evidences indicated the direct effect of HBSP on inflammation including not only infiltration, but also releasing cytokines and genotype transformation. Thus, HBSP *via* the highly expressed EPOR/βcR, in particular in P^{KO} mouse kidneys, modulated the biological function and fate of both inflammatory cells and tubular cells including the proportion of apoptotic cells and F4/80+ macrophages in interstitial areas, subsequently balanced immune responses in the acute stage of AKI.

The location and type of EPOR/βcR expressing cells were further verified in kidneys and other organs by conjugating HBSP with iridium that emits green florescence upon excitation. Tracking HBSP-Ir using confocal microscope showed that strong green signals were mainly in the apical surface of tubular lumen in the kidneys after IR for 17 h, but not in the sham controls. Weak signals were seen in the heart and liver, as well as both sham and IR groups. Although the lung showed weaker signals than in the kidney, it had stronger signal than in the heart and liver in the IR group would attribute to the auto-fluorescent from the lung as shown in the sham group. *In vitro*, TCMK-1 cells were further used to confirm the binding of HBSP-Ir with EPOR/βcR upon IR-related oxidative stress at 24 h. Intriguingly, HBSP treatment modulated EPOR and EPOR/βcR expression in both genotype mouse kidneys, but in a different manner. The level of EPOR protein was significantly decreased by HBSP in WT mouse kidneys, but still remained high in P^{KO} mouse kidneys after IR. However, EPOR/βcR in the IR kidneys was significantly reduced by HBSP in the P^{KO} mice only. It was reported that the high level of EPOR in the kidney leads to renal

tubulointerstitial fibrosis 2 weeks after IR (26). Therapeutic EPO stimulated profibrotic factors and promoted fibrosis and myofibroblast proliferation 4 weeks post IR, which might be due to its higher affinity to $(EPOR)_2$ than EPOR/βcR (27). Properdin deficiency further upregulated the expression of EPOR/βcR in IR kidneys associated with more severe injury, but also initiated stronger repair and better responses to the treatment of its ligand HBSP. However, the constant highly expressed EPOR in the kidney of P^{KO} mice before and after HBSP treatment might indicate potential negative impact of EPOR towards late stage of renal IR (26).

To further explore the association between properdin and EPO receptors, as well as their biological significance in IR kidneys, siRNA target both genes were applied in cultured TCMK-1 cells. Silencing properdin in TCMK-1 cells significantly upregulated the expression of EPOR protein under oxidative stress, indicating a complementary regulation between properdin and EPOR expression or an intrinsic balance *via* EPOR against properdin deficiency-mediated damage (12). However, in the above cell model, the expression of EPOR/βcR was not significantly upregulated by silencing properdin, which may be resulted from the limited observation period of 24 h *in vitro* compared to 72 h *in vivo*. We also demonstrated that the basic level of EPOR expression is essential for maintaining cell survival as silencing EPOR increased the number of apoptotic TCMK-1 cells. It has been found that EPO/EPOR signaling could enhance the uptake of apoptotic cells by macrophages and improve immune tolerance (11). It has also been reported that macrophage EPO signaling is temporally induced during infections, which increases engulfing bacteria, promotes infection resolution, and lowers antibiotic requirements (28). Here, it is the first time to show that HBSP greatly increased the phagocytic function of TCMK-1 cells assessed by uptaking *E.coli* Bioparticles. This implies that the protective role of EPOR/βcR signaling in TECs is associated with the phagocytic efficacy of TECs. As a result, renal parenchymal cells were then preserved and tissue injury was reduced by the timely clearance of dead cells. Thereby, the further increased EPOR/βcR in P^{KO} mouse kidneys could subsequently promote the phagocytic function of TECs to limit the damage level of IR kidneys caused by properdin deficiency and compromised phagocytosis, and also enhanced the therapeutic effect of HBSP.

There are limitations in this study. The relationship between properdin, EPOR and EPOR/βcR could be further explored *in vivo* and *in vitro* in a time-course model by modifying gene expression during renal IR-related injury. The significance of high level of EPOR in IR kidneys of P^{KO} mice with or without HBSP treatment would be further studied, as well as the long-term biological role of EPOR and EPOR/βcR would be differentiated. In addition, the phagocytic function demonstrated by HBSP would be further verified in TECs subjected to IR-related injury.

Conclusion

HBSP protected kidneys against IR not only in WT mice, but also with enhanced renoprotection in P^{KO} mice. The elevated EPOR and EPOR/βcR by P^{KO} in IR kidneys might initiate repair, sensitizing them to HBSP treatment, subsequently leading to less cell apoptosis and inflammation, and kidney restoration. The relationship between HBSP, properdin, EPOR and EPOR/βcR and its related biological functions are worthy of further study.

Data availability statement

The raw data supporting the conclusions of this article will be made available by the authors, without undue reservation.

Ethics statement

The animal study was reviewed and approved by United Kingdom Home Office.

Author contributions

BY and YW designed the study. YW and ZZ carried out animal experiments. LH, WS, FC conducted analysis of animal specimens. YL and CH performed cell experiments. JB and ML synthesized HBSP-Ir. YW, LH and WS analyzed the data and made the figures. YW, BY and NB drafted and revised the paper. All authors contributed to the article and approved the submitted version.

Funding

This study was supported by project grants (81873622 and 82200765) from the National Natural Science Foundation of China; a project grant (BK20210842) from Jiangsu Provincial Department of Science and Technology; and a project grant (MS22022092) from Nantong Science and Technology Foundation. the University of Leicester and the Research & Development Directorate of the University Hospitals of Leicester NHS Trust.

Acknowledgments

The authors acknowledge the Division of Biomedical Services, Preclinical Research Facility, University of Leicester, for technical support and the care of experimental animals. Particular thanks are expressed to our long-term collaborator Dr Cordula Stover (Department of Respiratory Sciences, University of Leicester) for her continued support, provision of mice and fruitful discussions.

Conflict of interest

The authors declare that the research was conducted in the absence of any commercial or financial relationships that could be construed as a potential conflict of interest.

Publisher's note

References

1. Ronco C, Bellomo R, Kellum JA. Acute kidney injury. *Lancet* (2019) 394 (10212):1949–64. doi: 10.1016/S0140-6736(19)32563-2

2. Coca SG, Singanamala S, Parikh CR. Chronic kidney disease after acute kidney injury: a systematic review and meta-analysis. *Kidney Int* (2012) 81(5):442–8. doi: 10.1038/ki.2011.379

3. Mehta RL, Burdmann EA, Cerda J, Feehally J, Finkelstein F, Garcia-Garcia G, et al. Recognition and management of acute kidney injury in the international society of nephrology 0by25 global snapshot: a multinational cross-sectional study. *Lancet* (2016) 387(10032):2017–25. doi: 10.1016/S0140-6736(16)30240-9

4. Kaushal GP, Shah SV. Challenges and advances in the treatment of AKI. *J Am Soc Nephrol* (2014) 25(5):877–83. doi: 10.1681/ASN.2013070780

5. Brines M, Cerami A. The receptor that tames the innate immune response. *Mol Med* (2012) 18:486–96. doi: 10.2119/molmed.2011.00414

6. Dennhardt S, Pirschel W, Wissuwa B, Imhof D, Daniel C, Kielstein JT, et al. Targeting the innate repair receptor axis. *Front Immunol* (2022) 13:1010882(1010882). doi: 10.3389/fimmu.2022.1010882

7. Yang C, Zhao T, Lin M, Zhao Z, Hu L, Jia Y, et al. Helix b surface peptide administered after insult of ischemia reperfusion improved renal function, structure and apoptosis through beta common receptor/erythropoietin receptor and PI3K/Akt pathway in a murine model. *Exp Biol Med (Maywood).* (2013) 238(1):111–9. doi: 10.1258/ebm.2012.012185

8. Yang C, Hosgood SA, Meeta P, Long Y, Zhu T, Nicholson ML, et al. Cyclic helix b peptide in preservation solution and autologous blood perfusate ameliorates ischemia-reperfusion injury in isolated porcine kidneys. *Transplant Direct* (2015) 1(2):e6. doi: 10.1097/TXD.0000000000000515

9. Yang C, Cao Y, Zhang Y, Li L, Xu M, Long Y, et al. Cyclic helix b peptide inhibits ischemia reperfusion-induced renal fibrosis *via* the PI3K/Akt/FoxO3a pathway. *J Transl Med* (2015) 13(355):1–10. doi: 10.1186/s12967-015-0699-2

10. Bohr S, Patel SJ, Vasko R, Shen K, Iracheta-Vellve A, Lee J, et al. Modulation of cellular stress response *via* the erythropoietin/CD131 heteroreceptor complex in mouse mesenchymal-derived cells. *J Mol Med* (2015) 93(2):199–210. doi: 10.1007/s00109-014-1218-2

11. Luo B, Gan W, Liu Z, Shen Z, Wang J, Shi R, et al. Erythropoeitin signaling in macrophages promotes dying cell clearance and immune tolerance. *Immunity* (2016) 44(2):287–302. doi: 10.1016/j.immuni.2016.01.002

12. Wu Y, Zwaini ZD, Brunskill NJ, Zhang X, Wang H, Chana R, et al. Properdin deficiency impairs phagocytosis and enhances injury at kidney repair phase post ischemia-reperfusion. *Front Immunol* (2021) 12:697760. doi: 10.3389/fimmu.2021.697760

13. Morioka S, Kajioka D, Yamaoka Y, Ellison RM, Tufan T, Werkman IL, et al. Chimeric efferocytic receptors improve apoptotic cell clearance and alleviate inflammation. *Cell* (2022) 185(26):4887–903.e17. doi: 10.1016/j.cell.2022.11.029

14. Cockram TOJ, Dundee JM, Popescu AS, Brown GC. The phagocytic code regulating phagocytosis of mammalian cells. *Front Immunol* (2021) 12:629979. doi: 10.3389/fimmu.2021.629979

15. Kemper C, Mitchell LM, Zhang L, Hourcade DE. The complement protein properdin binds apoptotic T cells and promotes complement activation and phagocytosis. *Proc Natl Acad Sci USA* (2008) 105(26):9023–8. doi: 10.1073/pnas.0801015105

16. Kouser L, Paudyal B, Kaur A, Stenbeck G, Jones LA, Abozaid SM, et al. Human properdin opsonizes nanoparticles and triggers a potent pro-inflammatory response by macrophages without involving complement activation. *Front Immunol* (2018) 9:131 (131). doi: 10.3389/fimmu.2018.00131

17. Schwaeble W, Huemer HP, Most J, Dierich MP, Strobel M, Claus C, et al. Expression of properdin in human monocytes. *Eur J Biochem* (1994) 219(3):759–64. doi: 10.1111/j.1432-1033.1994.tb18555.x

18. Schwaeble W, Dippold WG, Schafer MK, Pohla H, Jonas D, Luttig B, et al. Properdin, a positive regulator of complement activation, is expressed in human T cell lines and peripheral blood T cells. *J Immunol* (1993) 151(5):2521–8. doi: 10.4049/jimmunol.151.5.2521

19. Gaarkeuken H, Siezenga MA, Zuidwijk K, van Kooten C, Rabelink TJ, Daha MR, et al. Complement activation by tubular cells is mediated by properdin binding. *Am J Physiol Renal Physiol* (2008) 295(5):F1397–403. doi: 10.1152/ajprenal.90313.2008

20. Wu Y, Chen W, Zhang Y, Liu A, Yang C, Wang H, et al. Potent therapy and transcriptional profile of combined erythropoietin-derived peptide cyclic helix b surface peptide and caspase-3 siRNA against kidney Ischemia/Reperfusion injury in mice. *J Pharmacol Exp Ther* (2020) 375(1):92–103. doi: 10.1124/jpet.120.000092

21. Zhang Y, Chen W, Wu Y, Yang B. Renoprotection and mechanisms of erythropoietin and its derivatives helix b surface peptide in kidney injuries. *Curr Protein Pept Sci* (2017) 18(12):1183–90. doi: 10.2174/1389203717666160909144436

22. Wu Y, Zhang J, Liu F, Yang C, Zhang Y, Liu A, et al. Protective effects of HBSP on ischemia reperfusion and cyclosporine a induced renal injury. *Clin Dev Immunol* (2013) (758159):1–12. doi: 10.1155/2013/758159

23. Brines M, Patel NS, Villa P, Brines C, Mennini T, De Paola M, et al. Nonerythropoietic, tissue-protective peptides derived from the tertiary structure of erythropoietin. *Proc Natl Acad Sci United States America* (2008) 105(31):10925–30. doi: 10.1073/pnas.0805594105

24. Kemper C, Atkinson JP, Hourcade DE. Properdin: emerging roles of a pattern-recognition molecule. *Annu Rev Immunol* (2010) 28:131–55. doi: 10.1146/annurev-immunol-030409-101250

25. Ueba H, Shiomi M, Brines M, Yamin M, Kobayashi T, Ako J, et al. Suppression of coronary atherosclerosis by helix b surface peptide, a nonerythropoietic, tissue-protective compound derived from erythropoietin. *Mol Med* (2013) 19(195-202):195–202. doi: 10.2119/molmed.2013.00037

26. Shi M, Flores B, Li P, Gillings N, McMillan KL, Ye J, et al. Effects of erythropoietin receptor activity on angiogenesis, tubular injury, and fibrosis in acute kidney injury: a "U-shaped" relationship. *Am J Physiol Renal Physiol* (2018) 314(4): F501–F16. doi: 10.1152/ajprenal.00306.2017

27. Gobe GC, Bennett NC, West M, Colditz P, Brown L, Vesey DA, et al. Increased progression to kidney fibrosis after erythropoietin is used as a treatment for acute kidney injury. *Am J Physiol Renal Physiol* (2014) 306(6):F681–92. doi: 10.1152/ajprenal.00241.2013

28. Liang F, Guan H, Li W, Zhang X, Liu T, Liu Y, et al. Erythropoietin promotes infection resolution and lowers antibiotic requirements in e. coli- and s. aureus-initiated infections. *Front Immunol* (2021) 12:658715. doi: 10.3389/fimmu.2021.658715

frontiers | Frontiers in Immunology

TYPE Original Research
PUBLISHED 11 July 2023
DOI 10.3389/fimmu.2023.1192440

OPEN ACCESS

EDITED BY
Long Zheng,
The Second Affiliated Hospital of Zhejiang University School of Medicine, China

REVIEWED BY
Caroline Lamarche,
Montreal University, Canada
Wei Wang,
Tongji University, China

*CORRESPONDENCE
Didier Ducloux
dducloux@chu-besancon.fr

†These authors have contributed equally to this work

RECEIVED 23 March 2023
ACCEPTED 26 June 2023
PUBLISHED 11 July 2023

CITATION
Gaiffe E, Colladant M, Desmaret M, Bamoulid J, Leroux F, Laheurte C, Brouard S, Giral M, Saas P, Courivaud C, Degauque N and Ducloux D (2023) Pre-transplant immune profile defined by principal component analysis predicts acute rejection after kidney transplantation. *Front. Immunol.* 14:1192440. doi: 10.3389/fimmu.2023.1192440

Pre-transplant immune profile defined by principal component analysis predicts acute rejection after kidney transplantation

Emilie Gaiffe[1,2†], Mathilde Colladant[2,3†], Maxime Desmaret[1,2], Jamal Bamoulid[2,3], Franck Leroux[1], Caroline Laheurte[2], Sophie Brouard[4], Magali Giral[4], Philippe Saas[2], Cécile Courivaud[2,3], Nicolas Degauque[4] and Didier Ducloux[1,2,3*]

[1]Besançon University Hospital, INSERM CIC-1431, Besançon, France, [2]Univ. Franche-Comté, INSERM, Etablissement Français du Sang Bourgogne Franche-Comté, Unité Mixte de Recherche (UMR) 1098, RIGHT Interactions Hôte-Greffon-Tumeur/Ingénierie Cellulaire et Génique, Besançon, France, [3]Besançon University Hospital, Department of Nephrology, Besançon, France, [4]Centre Hospitalier Universitaire (CHU) Nantes, Nantes Université, INSERM, Center for Research in Transplantation and Translational Immunology, Unité Mixte de Recherche (UMR) 1064, Institut de Transplantation Université de Nantes (ITUN), Nantes, France

Background: Acute rejection persists as a frequent complication after kidney transplantation. Defining an at-risk immune profile would allow better preventive approaches.

Methods: We performed unsupervised hierarchical clustering analysis on pre-transplant immunological phenotype in 1113 renal transplant recipients from the ORLY-EST cohort.

Results: We identified three immune profiles correlated with clinical phenotypes. A memory immune cluster was defined by memory $CD4^+$T cell expansion and decreased naïve $CD4^+$T cell. An activated immune cluster was characterized by an increase in $CD8^+$T cells and a decreased CD4/CD8 ratio. A naïve immune cluster was mainly defined by increased naïve $CD4^+$T cells. Patients from the memory immune profile tend to be older and to have diabetes whereas those from the activated immune profile were younger and more likely to have pre-transplant exposure to CMV. Patients from the activated immune profile were more prone to experience acute rejection than those from other clusters [(HR=1.69, 95%IC[1.05-2.70], p=0.030) and (HR=1.85; 95%IC[1.16-3.00], p=0.011). In the activated immune profile, those without previous exposure to CMV (24%) were at very high risk of acute rejection (27 vs 16%, HR=1.85; 95%IC [1.04-3.33], p=0.039).

Conclusion: Immune profile determination based on principal component analysis defines clinically different sub-groups and discriminate a population at high-risk of acute rejection.

KEYWORDS

immune profile, biomarker, acute rejection, kidney transplantation, hierarchical clustering analysis

Introduction

With progress in immunosuppression, acute rejection became less frequent during the last decades. However, it still concerns 15 to 20% of kidney transplant recipients and affects long-term graft survival (1, 2). Pre-transplant risk factors explaining why only some patients developed acute rejection while they are all exposed to similar immunosuppression are imperfectly defined. Clinical factors (age, race), Human Leucocyte Antigen (HLA) typing and alloantibody screening are practically the only determinants that can be used for risk stratification.

In this context, it is tempting to search for immune biomarkers that could be predictive of acute rejection. Several candidates have been evaluated. Patients with positive donor-reactive or panel T cell reactive IFNγ ELISPOT assay are more likely to experience acute rejection (3, 4). Pre-transplant soluble CD30 (Cluster of Differentiation) has been suggested to be predictive of acute rejection (5). Our group reported that pre-transplant Recent Thymic Emigrant (RTE) were strongly associated with the occurrence of acute rejection in antithymocyte globulin (ATG)-treated kidney transplant recipients (6). Finally, the incidence of acute rejection has been reported to depend on specific genetic polymorphisms (7–9). Nevertheless, it should be emphasized that most of these studies have not or could not be replicated.

All these studies suffered from a major bias. Every immune parameter, cell or molecule, interacts with virtually all the immune system and should be interpreted in a general context, taking into account for positive and negative interactions. Thus, a more global approach is needed to consider the complexity of the system. Nevertheless, the number of information to collect is very important and often redundant. Thus, the data have to be summarized and reduced for better analysis.

Principal component analysis (PCA) is a method of comprehensive multivariate statistics and data analysis that allows to reduce the dimensionality of a dataset, enhancing interpretation while preserving information diversity (10). In the clinical setting of kidney transplantation, PCA should permit to merge patients with a similar biological profile. Thus, detection of specific immune profiles would be critical for detection of at-risk patients for acute rejection and subsequent targeted prevention.

In this study, we used individual determination of a panel of immune cells obtained from flow cytometry (including both frequency and total amount). Using hierarchical clustering, we separated different groups of patients based on immune profile. We first correlated these biological profiles with clinical profiles and second, determined whether biological profile may help to discriminate patients at risk for acute rejection.

Materials and methods

Patients

Research has been conducted in the 1113 kidney transplant recipients from the *Influence de l'Orientation de la Réponse LYmphocytaire* (ORLY-Est, NCT02843867) study. ORLY-Est is a prospective cohort study of incident renal transplant recipients in 7 French transplant centers (Besançon, Clermont-Ferrand, Dijon, Le Kremlin-Bicêtre, Nancy, Reims and Strasbourg) (6). The main objective of this study was to describe interactions between immune status and atherosclerosis after transplantation. For each patient, blood samples were collected at the time of transplantation and 1 year later. Clinical data were prospectively collected at the time of transplantation, 1 year, 3 years, 5 years and 10 years later. Sample collection was performed after regulatory approval by the French Ministry of Health (agreement number DC-2008-713, June 11, 2009). The ethics committee of the Franche-Comté study approved the study (2008). Patients enrolled in the ORLY-Est study gave their written informed consent.

To avoid the effects of previous immunosuppression on immune profile, we excluded patients having received a previous transplantation (n=126, 11.3%). Among the remaining 987 recipients of a first transplant, 205 patients (21%) had received T-cell depleting ATG therapy and 528 (63%) had received nondepleting aCD25 mAb therapy. One hundred and fifty five (15.7%) had missing data making inclusion in PCA impossible. Finally, eight hundred and thirty two were analyzed (Figure 1). Calcineurin inhibitors and mycophenolate mofetil were widely used as an immunosuppressive regimen. All the transplant procedures were performed with a negative cross match. Cytomegalovirus (CMV) prophylaxis was given according to each center's practice. All patients received Pneumocystis antimicrobial prophylaxis with trimethoprim sulfamethoxazole for at least 6 months.

Confounding factors

Age, gender, body mass index, diabetes, dyslipidemia, hypertension, past history of cardiovascular events, previous neoplastic history, and chronic lung disease were analyzed as covariates. Dialysis mode (none, hemodialysis, or peritoneal dialysis), and its duration prior to transplantation were also recorded. HLA mismatches were recorded for HLA-A, -B, and -DR loci. Other relevant immunological parameters such as, pre-transplant panel reactive antibodies (0 vs. positive at any level), and transplant type (living/deceased) were analyzed as covariates. Cold ischemia time, donor age, and presence of delayed graft function were also considered. Methods of assessment and definitions of these variables have been previously described in details (6).

Flow cytometry of whole blood

Peripheral blood mononuclear cells were isolated by density gradient centrifugation (Pancoll; Pan-Biotech GmBH, Aidenbach, Germany). Cells were stained with the following conjugated antibodies directed against CD3, CD4, CD8, CD31, CD45RA CD16, CD56, CD14 and CD45RO. The identification of lymphocyte subpopulations is carried out using four

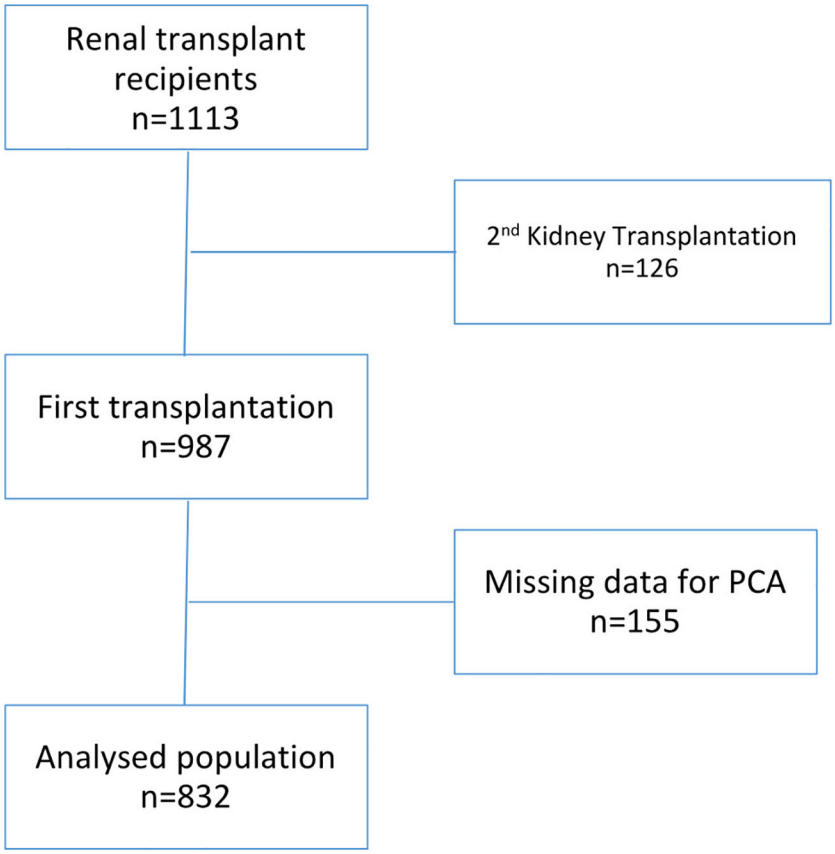

FIGURE 1
Patient flow chart.

combinations of cluster of differentiation. The source and clone of each antibody is specified in the Supplementary materials and methods. Immune markers used in PCA included lymphocytes, monocytes and Natural Killer (NK) cells identified by: T cells (CD3+), CD4+ T cells (CD3+CD4+CD8-), CD8+ T cells (CD3+CD8+CD4-), B cells (CD19+), NK cells (CD56+CD3-), naive CD4+ T cells (CD4+CD45RA+), memory CD4+ T cells (CD4+CD45RO+), RTE (CD4+CD45RA+CD31+), classical monocytes (CD14+CD16-) and intermediate monocytes (CD14+CD16+). Antibody clones and gating strategies are detailed in Supplementary materials and methods. For exploring the association between lymphocytes subsets and acute rejection, CD45RA and CCR7 serve as defining four T cell subsets (naïve, CD45RA+CCR7+; effector memory, CD45RA-CCR7-; central memory, CD45RA-CCR7+; effector memory expressing CD45RA, CD45RA+CCR7-) (11).

Cell debris and doublets were excluded on the basis of side versus forward scatter. Percentage of T cells, B cells, NK cells and monocytes were determined on fresh samples by flow cytometry with an FC500 cytometer (Beckman Coulter, Villepinte, France) according to the manufacturer's recommendations. Absolute numbers of different immune population, CD4+ and CD8+ T cells were determined on fresh samples by a single platform flow cytometry approach using the TetraCXP method, Flow-Count fluorospheres, and the same cytometer.

Outcomes

Acute rejection was considered in the presence of serum creatinine elevation. Only biopsy-proven acute rejections were considered. Acute rejection was defined according to the Banff classification (12). Only cellular acute rejections were considered.

Delayed Graft Function (DGF) was considered when dialysis is needed in the first week after transplantation.

Multiparameter analysis and hierarchical clustering

Pre-transplant immunological populations were used for the Principal Component Analysis (PCA) (CD3+, CD3+CD4+, CD45RO+CD4+, CD45RA+CD4+, CD31+CD45RA+CD4+, CD3+CD8+, CD19+, CD3+CD56+, CD45CD14+, CD45CD14+DR+ cell count and frequency as well as CD4/CD8 ratio). Only patients with all available analyses were included. We retained components with eigenvalues above 1. We then performed unsupervised hierarchical clustering based on the significant components using Ward's method with Euclidian distances. The number of clusters was selected based on the higher relative loss of inertia criteria [iclusters n+1/i(cluster n)]. Detailed analysis is

depicted in Supplementary materials and methodes. PCA and clustering were performed using the FactoMineR version 2.3 package with R version 4.0.2 (R Core Team, Vienna, Austria).

Statistical analyses

Clinical characteristics of the participants were described with mean expressed as +/- SD, median with the interquartile range (IQR) and numbers of events with percentage. After PCA and clustering, each cluster was described using the 18 quantitative immunologic parameters as well as clinical characteristics. Cluster comparisons were based on analysis of variance (ANOVA) for quantitative variables and chi-2 test for categorical variables (or Fischer test when appropriate).

Survival without acute rejection analysis was then performed for the clusters using Kaplan-Meier survival curves. As patient may die or return to dialysis before experiencing the outcome of interest, death from any cause as well as graft failure were considered as competing risks. Therefore, we used a competing-risk approach. The time-to-event was calculated from the date of transplantation to the outcome (acute rejection). Cumulative incidence function curves were also constructed for each cluster. The Fine-Gray model was used to analyze the prognostic effect of belonging to a specific cluster on the sub-distribution hazard function of the outcome (13). Unadjusted as well as age- and gender-adjusted sub-distribution relative hazards were estimated with the corresponding 95% confidence intervals (CI). Competing risk analysis was performed with R using the survival and prodlim version 2019.11.13 packages or using Prism, version 5.0 software (GraphPad Software, San Diego, CA) and SAS software (SAS institute Inc., Cary, NC).

Results

Study population

Characteristics of the study population were depicted in Table 1. Mean age was 53 ± 14 years and about two thirds of patients were male. Twenty percent had diabetes mellitus. All the patients had at least a one-year follow-up. The rate of missing data was < 5 percent for all studied parameters.

Identification of distinct patient groups using hierarchical clustering of immune profiles

A PCA was conducted on immune cells (frequency and total amount). PCA identified three clusters of individuals based on the distances between each branches of the dendogram (Figure 2A). Clusters, determined by the unsupervised hierarchical clustering analysis, were supposed to define immune profile and reflect groups of patients with similar immunophenotype. Three clusters were isolated (Figure 2B; Table 2).

TABLE 1 Clinical characteristics of the study population.

Characteristics	Overall patients (No. = 832)
Age, year, mean (SD)	53 (14)
Median (IQR)	54 (44-63)
Male gender, n (%)	515 (62%)
BMI, kg/m², mean ± SD	26 (5)
Median (IQR)	25 (22-29)
Missing	*19*
Hypertension, n (%)	
No	119 (15%)
Yes	694 (85%)
Missing	*19*
Diabetes, n (%)	
No	659 (80%)
Yes	161 (20%)
Missing	12
AntiHLA immunization, n (%)	232 (28%)
Dialysis antecedent, n (%)	740 (90%)
Missing	*11*
Hemodialysis, n (%)	601 (81%)
Peritoneal dialysis, n (%)	139 (19%)
Causal Nephropathy	
Glomerulopathy	170 (21%)
Vascular nephropathy	79 (10%)
Chronic interstitial nephropathy	48 (6%)
Congenital	12 (1%)
Polycystic	139 (17%)
Diabetes	99 (12%)
Other	258 (32%)
Missing	*27*
Anti-CMV antibodies, n (%)	
+	471 (57%)
-	352 (43%)
Missing	*9*
Induction therapy, n (%)	
No	76 (9%)
aCD25mAb	528 (65%)
ATG	205 (26%)
Missing	*23*

ATG, antithymocyte globulin; CMV, cytomegalovirus; aCD25mAb, anti CD25 monoclonal antibody; HLA, human leucocyte antigen.

10.3389/fimmu.2023.1192440

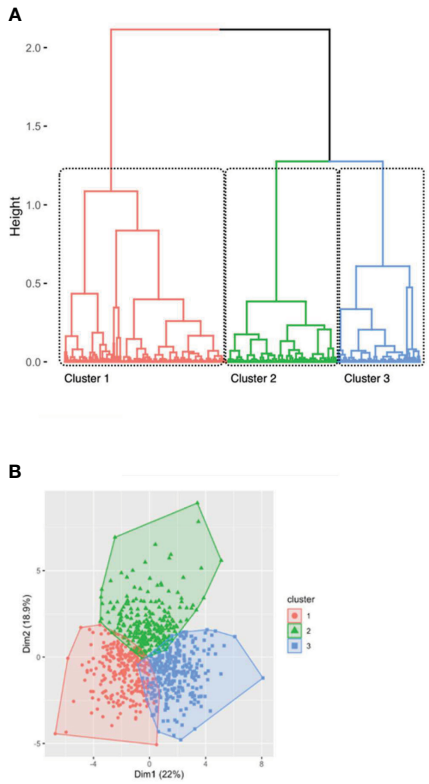

FIGURE 2
Hierarchical clustering of patients after principal component analysis **(A)** represented by the dendrogram of patients and **(B)** by a scatter view plot. **(A)** identification of 3 clusters among 832 first transplant recipients according to immunological data. Profiles were assigned based on the separation of the clustering trees. **(B)** Colors were based on clustering profile and mainly defined by dimension 2 and dimension 1 in our hierarchical clustering. Three clusters were identified: older immunity in red (cluster 1), activated immunity in green (cluster 2) and naïve immunity in blue (cluster 3).

A first cluster (n=271 patients) was characterized by an increase in memory CD4+ T cells and a decrease in naive CD4+ T cells (including central CD4+ T cells). However, the absolute number of immune cell (representing by T cell count) was low. This cluster was called "memory immune profile". A second cluster (n=270 patients) was characterized by an increased number of immune cells especially CD8+ T cells (in percentage and absolute number). The total rate of T cells was increased but the CD4/CD8 ratio was lower suggesting an "activated immune profile". A third cluster (n=291 patients) was characterized by increased naive immune cells, mostly naive CD4+ T cells and central CD4+ T cells defining a "naïve immune profile". Of note, all cell subsets counts and frequencies differed in all three groups (Table 2).

Immune cell profiles correlate with clinical phenotypes

We analyzed and compared demographics and clinical characteristics of the three immune profiles. The results are summarized in Table 3.

Patients classified as having a memory immune profile were older, had higher BMI, and were more prone to have type 2 diabetes. Patients assigned to the activated immune profile were younger and were more likely to have had pre-transplant CMV exposure. Patients allocated to the naïve immune profile were more frequently CMV-naïve. Other characteristics did not differ between the three immune profiles. Consequently, main demographic and clinical drivers of pre-transplant immune status were age, CMV status, and diabetes.

Immune profiles are associated with acute rejection

There was no difference in induction therapy or maintenance immunosuppressive treatments between the 3 immune profiles (Table 3). The proportion of patients with DGF was also similar in the 3 groups. One hundred and seven patients (13.6%) experienced acute rejection in the first year post-transplant. Mean time between transplantation and acute rejection was 105 +/- 88 days. Patients exhibiting an activated immune profile were more prone to develop acute rejection that both those with a naïve immune profile (HR=1.68, IC95% [1.06; 2.67], p=0.027) and those with a memory immune profile (HR 1.32, IC95% [0.95-1.88], p=0.096) (Figure 3). A competitive analysis taken death into account provided similar results (HR=1.606, 95%IC [1.00-2.58], p=0.0498) (Figure 4).

Because activated immune profile is mainly defined by CD8+ T cell expansion, we analyzed whether CD8+ T cell count and/or frequency may replicate previous results. Neither CD8+ T cell count nor frequency were associated with the occurrence of acute rejection (Supplementary data, Tables S1A, B). Patients were divided into three groups corresponding to tertiles of CD8+ T cells count: 39 - 217 CD8+/mm3, 217 - 374 CD8+/mm3, 374 - 1400 CD8+/mm3. Frequency of acute rejection was similar in the three tertiles of CD8+ T cells (Supplementary data, Figure S1A). There was also no difference according to the percentage of CD8+ T cells (Supplementary data, Figure S1B). No other T cell subset was associated with acute rejection. ATG profoundly affects lymphocyte counts and phenotype. We separately studied the association between clusters and acute rejection in patients having or not received ATG. The association between clusters and acute rejection was similar in both groups of patients.

Delayed graft function (HR=1.48, IC95% [1.01-2.18], p=0.046) was also associated with acute rejection and retained in the multivariate analysis. Age, CMV status, and diabetes, closely linked to cluster definitions, were forced into the model. After multivariate analysis, the activated immune profile was still associated with acute rejection (HR=1.69, IC95% [1.05-2.70], p=0.030 and HR=1.85, IC95% [1.16; 3.00], p=0.011, versus the "memory immune profile" and the "naïve immune profile", respectively). DGF (HR=1.50, IC95% [1.02-2.33], p=0.040) remained associated with acute rejection. Age, gender, and diabetes mellitus were not associated with acute rejection.

10.3389/fimmu.2023.1192440

TABLE 2 Immune population phenotype at the day of transplantation among the different clusters determined by hierarchical clustering.

	Memory immunity (cluster 1, n=271)	Activated immunity (cluster 2, n=270)	Naïve immunity (cluster 3, n=291)	*p* value
Tcell (CD3+) (n/mm3)	732 (± 285)	1337 (± 466)	939 (± 374)	<0.001
Tcell (CD3+) (%)	68.1 (± 9.4)	80.6 (± 5.8)	80.1 (± 6.3)	<0.001
CD4+ Tcell (CD3+CD4+) (n/mm3)	465 (± 202)	773 (± 320)	702 (± 302)	<0.001
CD4+ Tcell (CD3+CD4+) (%)	42.8 (± 8.2)	45.9 (± 7.6)	59.6 (± 6.9)	<0.001
CD8+ Tcell (CD3+CD8+) (n/mm3)	248 (± 123)	531 (± 205)	218 (± 97)	<0.001
CD8+ Tcell (CD3+CD8+) (%)	23.4 (± 7.9)	32.7 (± 8.1)	18.9 (± 6.0)	<0.001
CD4+/CD8+ ratio	2.1 (± 0.9)	1.5 (± 0.6)	3.6 (± 1.5)	<0.001
Bcell (CD19+) (n/mm3)	111 (± 93)	161 (± 199)	90 (± 64)	<0.001
Bcell (CD19+) (%)	10.1 (± 6.2)	8.9 (± 6.6)	7.4 (± 3.9)	<0.001
Naïve CD4+ Tcell (CD3+CD4+CD45RA+) (n/mm3)	29.5 (± 12.3)	36.6 (± 13.5)	50.2 (± 12.0)	<0.001
Memory CD4+ Tcell (CD3+CD4+CD45RO+) (n/mm3)	70.2 (± 12.5)	63.4 (± 13.5)	49.6 (± 12.2)	<0.001
RTE (CD3+CD4+CD45RA+CD31+) (n/mm3)	18.3 (± 9.0)	23.9 (± 11.5)	32.3 (± 10.7)	<0.001
NK cell (CD56+) (n/mm3)	223.1 (± 135.2)	167.3 (± 126.7)	130.5 (± 82.4)	<0.001
NK cell (CD56+) (%)	20 (± 9)	10 (± 4)	11 (± 6)	<0.001
Monocyte (CD14+) (n/mm3)	456 (± 277)	400 (± 162)	403 (± 210)	0.004
Monocyte (CD14+) (%)	7.9 (± 3.4)	6.2 (± 2.3)	7.0 (± 2.6)	<0.001
Infl. Monocyte (CD14+CD16+) (n/mm3)	62 (± 61)	45 (± 39)	46 (± 38)	<0.001
Infl. Monocyte (CD14+CD16+) (%)	1.2 (± 1.6)	0.7 (± 0.6)	0.8 (± 0.6)	<0.001

RTE, recent thymic emigrant - ANOVA for quantitative variable.

Subsequent analyses of the activated immune profile

The activated immune profile shares some similarities with the immune risk profile, which is mainly characterized by CD8+ T cell expansion and CMV seropositivity. Nevertheless, 24% of patients assigned to the activated immune profile were CMV-naïve (Table 3). CMV-exposed patients tended to be older (49+/-14 vs 45+/-15 years, p=0.087). Although CMV-exposed patients had moderately higher CD8 T cell count than CMV-naïve patients, they had similar CD8 frequency (37 + 11 vs 39 + 11, p=0.399). We observed that acute rejection was less frequent in CMV-exposed patients (16 vs 27%, HR=0.54, IC95% [0.30; 0.97], p=0.039) (Figure 5; Supplementary data, Table S2).

We therefore hypothesized that CD8 subset distribution could be different between CMV-naïve and CMV-exposed patients. Naïve CD8+ T cell (CD8+CD45RA+CCR7+) frequency was much higher (35 + 18 vs 27 + 18%, p=0.006) in CMV-naïve patients, whereas frequency of TEMRA CD8 T cells (CD8+CDRA+CCR7-) tended to be lower (42 + 18 vs 47 + 16%, p=0.059) (Supplementary data, Table S2). Nevertheless, none of these subsets was associated with acute rejection.

Discussion

We report in a large cohort of kidney transplant recipients that immune profile determination based on PCA defines clinically different sub-groups of population and may help to discriminate patients at-risk for acute rejection. The association between immune profiles and acute rejection was independent and observed in all sub-groups of patients. A specific category of patients with high CD8+ T cells level and no past exposure to CMV seems to be at the highest risk of acute rejection. Using a large panel of immune cellular subtypes, we isolated three immune profiles with distinct clinical phenotypes. Clinical phenotypes were concordant with expected immune profiles. Three main clinical characteristics seems to drive immune clustering, namely age, diabetes, and CMV exposure. Immune senescence is driven by ageing and some studies report increased senescence in patients with insulin resistance (14, 15). Persistent CMV infection leads to chronic stimulation of CD8 T cells, which expand clonally exhibiting an effector memory phenotype. Meijers et al. showed that TEMRA $CD8^+$ T cell expansion in end-stage renal disease patients were highly associated with CMV exposure (16). Clinical correlation may be considered as an internal validation for the relevance of the immune clusters defined by PCA.

The "activated immune profile" shares some similarities with the immune risk phenotype (IRP). IRP was first defined as the association of high CD8 and low CD4 numbers, and poor proliferative response to concanavalin A (17). Further studies suggested that IRP could be defined using only the inverted CD4/CD8 ratio (18). Further studies have extended these results (19, 20). CMV exposure and an increase in the number of lately

10.3389/fimmu.2023.1192440

TABLE 3 Clinical characteristics among the 3 immune profiles determined with hierarchical clustering.

Characteristics	Memory immunity (cluster 1, n=271)	Activated immunity (cluster 2, n=270)	Naïve immunity (cluster 3, n=291)	*p* value
Age, year, mean (SD)	56 (± 13)	48 (± 15)	54 (± 12)	<0.001
Median (IQR)	58 (48 - 67)	47 (36 - 60)	55 (47 - 63)	
Male gender, n (%)	183 (68%)	162 (60%)	170 (58%)	0.098
BMI, kg/m², mean ± SD	27 (± 5)	25 (± 5)	26 (± 5)	0.004
Median (IQR)	26 (23 - 30)	25 (22 - 28)	25 (22 - 29)	
Missing	8	4	7	
Hypertension, n (%)				0.110
No	29 (11%)	41 (15%)	49 (17%)	
Yes	234 (86%)	226 (84%)	234 (80%)	
Missing	8 (3%)	3 (1%)	8 (3%)	
Diabetes, n (%)				0.003
No	196 (72%)	219 (81%)	244 (84%)	
Yes	73 (27%)	49 (18%)	39 (13%)	
Missing	2 (1%)	2 (1%)	8 (3%)	
Anti-HLA immunization, n (%)				0.082
No	197 (73%)	176 (65%)	197 (68%)	
Yes	65 (24%)	89 (33%)	78 (27%)	
Dialysis antecedent, n (%)				0.005
No	15 (6%)	41 (15%)	25 (9%)	
Hemodialysis, n (%)	201 (74%)	168 (62%)	192 (66%)	
Peritoneal dialysis, n (%)	40 (15%)	46 (17%)	53 (18%)	
DP/HD	14 (5%)	13 (5%)	13 (4%)	
Missing	1 (0%)	1 (0%)	5 (2%)	
Causal Nephropathy				<0.001
Glomerulopathy	53 (20%)	61 (23%)	56 (19%)	
Vascular nephropathy	29 (11%)	23 (9%)	27 (9%)	
Chronic interstitial nephropathy	17 (6%)	16 (6%)	15 (5%)	
Congenital	4 (1%)	5 (2%)	3 (1%)	
Polycystic	35 (13%)	26 (10%)	78 (27%)	
Diabetes	52 (19%)	25 (9%)	22 (8%)	
Other	49 (18%)	68 (25%)	57 (20%)	
unspecified	23 (8%)	40 (15%)	21 (7%)	
Missing	9 (3%)	6 (2%)	12 (4%)	
Anti-CMV antibodies, n (%)				<0.001
+	152 (56%)	205 (76%)	114 (39%)	
-	116 (43%)	64 (24%)	172 (59%)	
Missing	3 (1%)	1 (0%)	5 (2%)	

Fisher test for binary variable, Chi2 for more than 2 modality variable, ANOVA for quantitative variable.

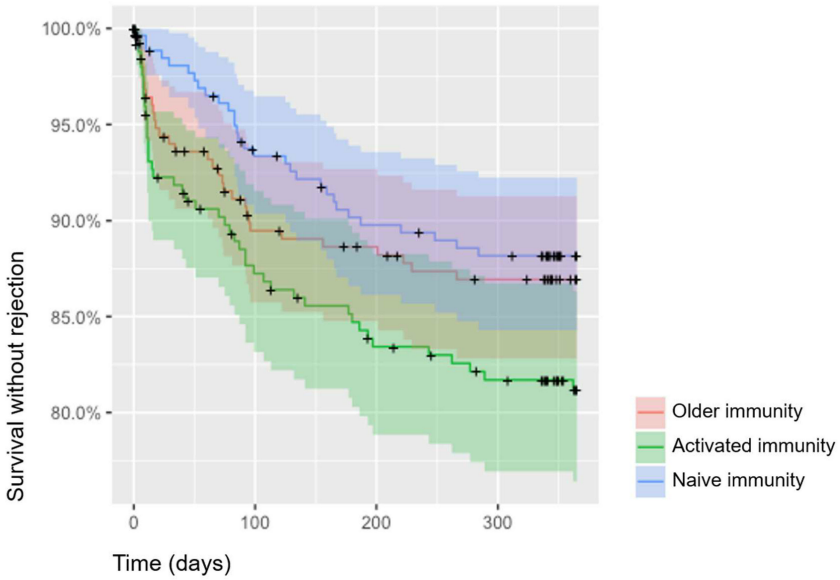

FIGURE 3
Kaplan Meier curves for survival without acute rejection according to cluster belinging. Three clusters were identified: memory immunity in red (cluster 1), activated immunity in green (cluster 2) and naïve immunity in blue (cluster 3).

differentiated CD8+ CD28 effector cells have been linked to IRP. More recently, IRP was also found to be more prevalent in younger CMV-exposed patients (21). The "activated immune profile" is mainly characterized by high CD8+ T cells count, lower CD4/CD8, and CMV seropositivity, which are predominant features of the IRP. Nevertheless, the "activated immune profile" is likely to be different from IRP. Patients with IRP have typically low CD4+ T cells whereas this subset is high in patients with "activated immune profile". Moreover, most patients do not have inverted CD4/CD8 ratio. Finally, one quarter of patients in the activated immune profile were CMV-naïve.

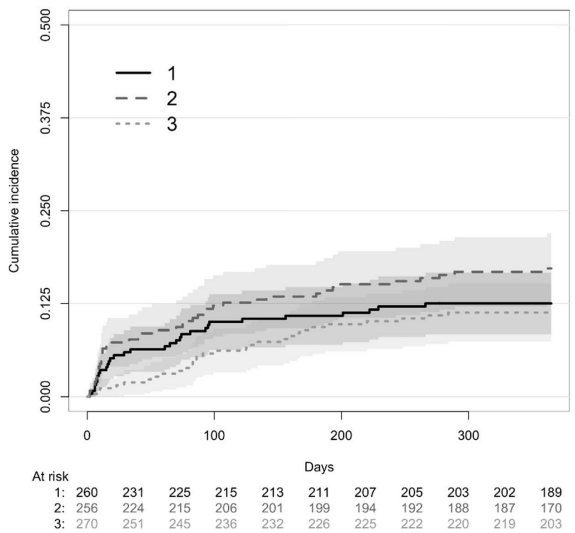

FIGURE 4
Competitive risk of death and acute rejection at 1 years post transplantation according to clusters determined with principal component analysis identified as older immunity (cluster 1), activated immunity (cluster 2) and naïve immunity (cluster 3). Three clusters were identified: memory immunity with full line (cluster 1), activated immunity with dashed line (cluster 2) and naïve immunity with dotted line (cluster 3).

Distributions of both CD4+ and CD8+ T cells profiles are largely different between CMV-naïve and CMV-exposed patients and suggest more pronounced T cell exhaustion in CMV-positive patients. However, CMV-naïve patients assigned to the activated immune profile appear to be at very high risk of acute rejection. Consistent with this result, Betjes et al. reported that expansion of terminally differentiated CD8+ TEMRA protects against acute rejection after kidney transplantation (22). Consistent with this result, we also showed a trend towards a lower incidence of acute rejection in patients with pre-transplant IRP (23). Nevertheless, the role of TEMRA in acute rejection is probably more complex as recent studies identified this population as being associated with both acute rejection and graft loss (24, 25).

However, in our study, no specific T cell subset was associated with acute rejection.

Indeed, despite subsequent phenotyping of T cells, we were unable to identify a specific subset explaining the association between having "an activated immune profile" and an increased incidence of acute rejection. We assume that this point reinforces our primary hypothesis. It suggests that a combination of different immune actors and multiple interactions rather than a unique factor contributes to acute rejection. We now have to integrate the complexity of immune interactions in our predicting models.

It is possible to plot supplementary individuals onto the principal axes. Using the formulae allowing principal components computations, we simply have to compute linear combinations of these supplementary point characteristics. Thus, a next patient may be included in a defined cluster before, subject to determination of immune parameters. This offers the opportunity of external

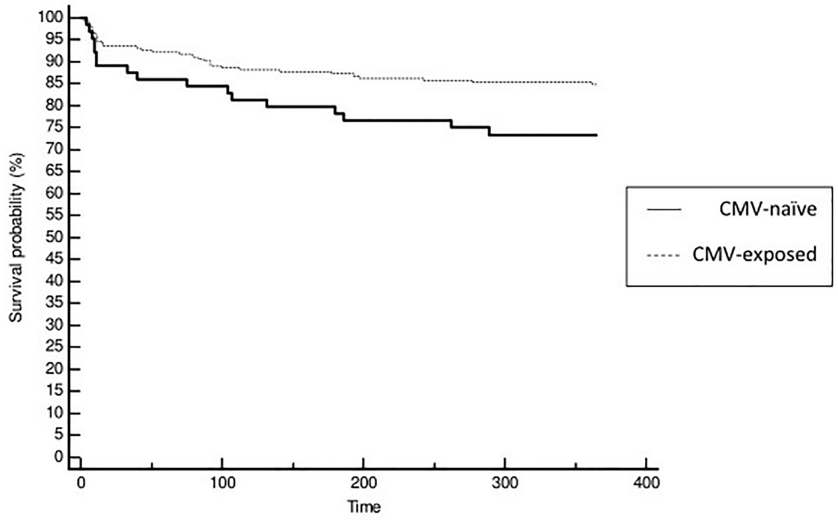

FIGURE 5
Kaplan Meier curves for survival without acute rejection according to patients CMV status of cluster 2 (activated immunity). Patients naïve to CMV exposure were identified with full line and patient exposed to CMV with dashed line.

validation of the PCA. Finally, clinical use may be generalized to classify patients and predict their risk category regarding acute rejection.

Our study has some limitations. Even when acute rejection was clearly defined, there was no centralized analysis of graft histology. Nevertheless, misclassification remains unlikely. The indication for biopsy may have varied from one center to another, but without any possible relationship with PCA. Importantly, systematic biopsies were not considered and only for cause-biopsies were analyzed. Due to the prospective design of the study, the rate of missing data was very low (<5%). Underreporting of events is unlikely in the early post-transplant period when all the patients are still followed in the transplant center.

Using PCA, we defined a subset of kidney transplant recipients carrying a high risk of acute rejection. These patients are characterized by an "activated immune profile" in the absence of previous exposure to CMV. Global approach of immune equilibrium may be more relevant to predict immune-related events than analysis of a single parameter.

Data availability statement

The raw data supporting the conclusions of this article will be made available by the authors, without undue reservation.

Ethics statement

The studies involving human participants were reviewed and approved by the ethics committee of the Franche-Comté study. The patients/participants provided their written informed consent to participate in this study.

Author contributions

EG and DD are the guarantors. DD, EG, MC, MD, and PS designed the study. CL, MG, ND, and SB carried out experiments. CC, CL, DD, EG, FL, JB, MC, ND, and PS supported (administrative, technical or material) the study. DD, EG, and PS supervised the study. CL, DD, EG, FL, MC, MD, MG, ND, and SB acquired, analyzed or interpreted the data. DD, EG, MC, and MD drafted the manuscript; DD, EG, MD, ND, and PS revised the paper; DD and PS obtained funding. All authors contributed to the article and approved the submitted version.

Funding

This study was supported by grants from the national "Programme Hospitalier de Recherche Clinique" (PHRC 2005), The Fondation de France (2007), The Fondation transplantation (2008), The "Direction générale de l'Offre de soins – Institut national de la santé et de la recherche médicale" grant (DHOS INSERM 2008) and the interregional "Programme Hospitalier de Recherche Clinique" (PHRC-Interreg 2011).

Acknowledgments

The ORLY-Est Cohort constitution is supported by the French Programme Hospitalier de Recherche clinique (2005), the Fondation de France funding (2007), the Fondation transplantation funding (2008), the "Direction de l'Hospitalisation et de l'Organisation des Soins/Institut national de la santé et de la recherche médicale" funding (2008), the French interregional Programme Hospitalier de Recherche clinique (2011) and Besançon hospital.

Conflict of interest

The authors declare that the research was conducted in the absence of any commercial or financial relationships that could be construed as a potential conflict of interest.

Publisher's note

All claims expressed in this article are solely those of the authors and do not necessarily represent those of their affiliated organizations, or those of the publisher, the editors and the reviewers. Any product that may be evaluated in this article, or claim that may be made by its manufacturer, is not guaranteed or endorsed by the publisher.

Supplementary material

The Supplementary Material for this article can be found online at: https://www.frontiersin.org/articles/10.3389/fimmu.2023.1192440/full#supplementary-material

References

1. Koo EH, Jang HR, Lee JE, Park JB, Kim SJ, Kim DJ, et al. The impact of early and late acute rejection on graft survival in renal transplantation. *Kidney Res Clin Pract* (2015) 34:160–4. doi: 10.1016/j.krcp.2015.06.003

2. Matas AJ, Smith JM, Skeans MA, Thompson B, Gustafson SK, Schnitzler MA, et al. OPTN/SRTR 2012 annual data report: kidney. *Am J Transplant* (2014) 14(Suppl 1):11–44. doi: 10.1111/ajt.12579

3. Augustine JJ, Siu DS, Clemente MJ, Schulak JA, Heeger PS, Hricik DE. Pre-transplant IFN-gamma ELISPOTs are associated with post-transplant renal function in African American renal transplant recipients. *Am J Transplant* (2005) 5:1971–5. doi: 10.1111/j.1600-6143.2005.00958.x

4. Poggio ED, Augustine JJ, Clemente M, Danzig JM, Volokh N, Zand MS, et al. Pretransplant cellular alloimmunity as assessed by a panel of reactive T cells assay correlates with acute renal graft rejection. *Transplantation* (2007) 83:847–52. doi: 10.1097/01.tp.0000258730.75137.39

5. Chen Y, Tai Q, Hong S, Kong S, Shang S, Liang S, et al. Pretransplantation soluble CD30 level as a predictor of acute rejection in kidney transplantation: a meta-analysis. *Transplantation* (2012) 94:911–8. doi: 10.1097/TP.0b013e31826784ad

6. Bamoulid J, Courivaud C, Crepin T, Carron C, Gaiffe E, Roubiou C, et al. Pretransplant thymic function predicts acute rejection in antithymocyte globulin-treated renal transplant recipients. *Kidney Int* (2016) 89:1136–43. doi: 10.1016/j.kint.2015.12.044

7. Ge YZ, Wu R, Lu TZ, Jia RP, Li MH, Gao XF, et al. Combined effects of TGFB1 +869 T/C and +915 G/C polymorphisms on acute rejection risk in solid organ transplant recipients: a systematic review and meta-analysis. *PloS One* (2014) 9: e93938. doi: 10.1371/journal.pone.0093938

8. Hu X, Bai Y, Li S, Zeng K, Xu L, Liu Z, et al. Donor or recipient TNF-a -308G/A polymorphism and acute rejection of renal allograft: a meta-analysis. *Transpl Immunol* (2011) 25:61–71. doi: 10.1016/j.trim.2011.04.004

9. Ducloux D, Deschamps M, Yannaraki M, Ferrand C, Bamoulid J, Saas P, et al. Relevance of toll-like receptor-4 polymorphisms in renal transplantation. *Kidney Int* (2005) 67:2454–61. doi: 10.1111/j.1523-1755.2005.00354.x

10. Joliffe IT, Morgan BJ. Principal component analysis and exploratory factor analysis. *Stat Methods Med Res* (1992) 1:69–95. doi: 10.1177/096228029200100105

11. Okada R, Kondo T, Matsuki F, Takata H, Takiguchi M. Phenotypic classification of human CD4+ T cell subsets and their differentiation. *Int Immunol* (2008) 20:1189–99. doi: 10.1093/intimm/dxn075

12. Colvin RB, Cohen AH, Saiontz C, Bonsib S, Buick M, Burke B, et al. Evaluation of pathologic criteria for acute renal allograft rejection: reproducibility, sensitivity, and clinical correlation. *J Am Soc Nephrol* (1997) 8(12):1930–41. doi: 10.1681/ASN.V8121930

13. Austin PC, Fine JP. Practical recommendations for reporting fine-Gray model analyses for competing risk data. *Stat Med* (2017) 36(27):4391–400. doi: 10.1002/sim.7501

14. Daryabor G, Atashzar MR, Kabelitz D, Meri S, Kalantar K. The effects of type 2 diabetes mellitus on organ metabolism and the immune system. *Front Immunol* (2020) 11:1582. doi: 10.3389/fimmu.2020.01582

15. Frasca D, Blomberg BB, Paganelli R. Aging, obesity, and inflammatory age-related diseases. *Front Immunol* (2017) 8:1745. doi: 10.3389/fimmu.2017.01745

16. Meijers RWJ, Litjens NHR, de Wit EA, Langerak AW, van der Spek A, Baan CC, et al. Cytomegalovirus contributes partly to uremia associated premature immunological ageing of the T-cell compartment. *Clin Exp Immunol* (2013) 174:424–32. doi: 10.1111/cei.12188

17. Ferguson FG, Wikby A, Maxson P, Olsson J, Johansson B. Immune parameters in a longitudinal study of a very old population of Swedish people: a comparison between survivors and nonsurvivors. *J Gerontol Biol Sci* (1995) 50A:B378–82. doi: 10.1093/gerona/50A.6.B378

18. Wikby A, Maxson P, Olsson J, Johansson B, Ferguson FG. Changes in CD8 and CD4 lymphocyte subsets, T cell proliferation responses and non-survival in the very old: the Swedish longitudinal OCTO-immune study. *Mech Ageing Dev* (1998) 102:187–98. doi: 10.1016/S0047-6374(97)00151-6

19. Olsson J, Wikby A, Johansson B, Lofgren S, Nilsson BO, Ferguson FG. Age-related change in peripheral blood T-lymphocyte subpopulations and cytomegalovirus infection in the very old: the Swedish longitudinal OCTO immune study. *Mech Ageing Dev* (2000) 121:187–201. doi: 10.1016/S0047-6374(00)00210-4

20. Wikby A, Johansson B, Olsson J, Lofgren S, Nilsson BO, Ferguson F. Expansions of peripheral blood CD8 T-lymphocyte subpopulations and an association with cytomegalovirus seropositivity in the elderly: the Swedish NONA immune study. *Exp Gerontol* (2002) 37:445–53. doi: 10.1016/S0531-5565(01)00212-1

21. Strindhall J, Skog M, Ernerudh J, Bengner M, Löfgren S, Matussek A, et al. The inverted CD4/CD8 ratio and associated parameters in 66-year-old individuals: the Swedish HEXA immune study. *Age* (2013) 35:985–91. doi: 10.1007/s11357-012-9400-3

22. Betjes MGH, Litjens NHR. High numbers of differentiated CD28null CD8+ T cells are associated with a lowered risk for late rejection and graft loss after kidney transplantation. *PloS One* (2020) 15:e0228096. doi: 10.1371/journal.pone.0228096

23. Crepin T, Gaiffe E, Courivaud C, Roubiou C, Laheurte C, Moulin B, et al. Pre-transplant end-stage renal disease-related immune risk profile in kidney transplant recipients predicts post-transplant infections. *Transpl Infect Dis* (2016) 18:415–22. doi: 10.1111/tid.12534

24. Yap M, Boeffard F, Clave E, Pallier A, Danger R, Giral M, et al. Expansion of highly differentiated cytotoxic terminally differentiated effector memory CD8+ T cells in a subset of clinically stable kidney transplant recipients: a potential marker for late graft dysfunction. *J Am Soc Nephrol* (2014) 25(8):1856–68. doi: 10.1681/ASN.2013080848

25. Jacquemont L, Tilly G, Yap M, Doan-Ngoc TM, Danger R, Guérif P, et al. Terminally differentiated effector memory CD8+ T cells identify kidney transplant recipients at high risk of graft failure. *J Am Soc Nephrol* (2020) 31(4):876–91. doi: 10.1681/ASN.2019080847

frontiers | Frontiers in Immunology

TYPE Review
PUBLISHED 17 August 2023
DOI 10.3389/fimmu.2023.1154650

OPEN ACCESS

EDITED BY
Long Zheng,
The Second Affiliated Hospital of Zhejiang University School of Medicine, China

REVIEWED BY
Vincenzo Cantaluppi,
University of Eastern Piedmont, Italy
Sandhya Bansal,
St. Joseph's Hospital and Medical Center, United States

*CORRESPONDENCE
David Cucchiari
cucchiari@clinic.cat

†These authors have contributed equally to this work

RECEIVED 30 January 2023
ACCEPTED 21 July 2023
PUBLISHED 17 August 2023

CITATION
Cuadrado-Payán E, Ramírez-Bajo MJ, Bañón-Maneus E, Rovira J, Diekmann F, Revuelta I and Cucchiari D (2023) Physiopathological role of extracellular vesicles in alloimmunity and kidney transplantation and their use as biomarkers. *Front. Immunol.* 14:1154650. doi: 10.3389/fimmu.2023.1154650

Physiopathological role of extracellular vesicles in alloimmunity and kidney transplantation and their use as biomarkers

Elena Cuadrado-Payán[1,2], María José Ramírez-Bajo[2,3], Elisenda Bañón-Maneus[2,3], Jordi Rovira[2,3], Fritz Diekmann[1,2,3], Ignacio Revuelta[1,2,3†] and David Cucchiari[1,2*†]

[1]Department of Nephrology and Kidney Transplantation, Hospital Clínic, Barcelona, Spain, [2]Laboratori Experimental de Nefrologia I Trasplantament (LENIT), Fundació de Recerca Clínic Barcelona-Institut d'Investigacions Biomèdiques August Pi I Sunyer (FRCB-IDIBAPS), Barcelona, Spain, [3]Red de Investigación Renal (REDINREN), Insituto de Salud Carlos III, Madrid, Spain

Antibody-mediated rejection is the leading cause of kidney graft dysfunction. The process of diagnosing it requires the performance of an invasive biopsy and subsequent histological examination. Early and sensitive biomarkers of graft damage and alloimmunity are needed to identify graft injury and eventually limit the need for a kidney biopsy. Moreover, other scenarios such as delayed graft function or interstitial fibrosis and tubular atrophy face the same problem. In recent years, interest has grown around extracellular vesicles, specifically exosomes actively secreted by immune cells, which are intercellular communicators and have shown biological significance. This review presents their potential as biomarkers in kidney transplantation and alloimmunity.

KEYWORDS

extracellular vesicles, exosomes, kidney, transplant, kidney transplant, biomarker

1 Introduction

In kidney transplantation, antibody-mediated rejection (ABMR) continues to represent the most significant challenge to be resolved in order to improve graft and patient survival (1, 2). Although acute ABRM is a potentially treatable disease, chronic ABMR has limited therapeutic options. It invariably progresses to end-stage chronic kidney disease (ESKD), representing over 50% of death-censored graft losses. Therefore, early detection of acute ABMR, timely treatment, and prevention of its progression to chronic ABMR are vital to guarantee satisfactory results for kidney transplant recipients, especially in the high immunological risk group. With this premise, some centers have developed a strategy based on protocol kidney graft biopsies. However, a biopsy is an invasive method with

potential risk of associated complications; moreover, it presents a high financial and resource cost (1, 2).

For this reason, many transplant centers choose to perform biopsies only "by indication" when some classical parameters are altered, such as creatinine, proteinuria, or the existence of specific anti-Human Leukocyte Antigen (HLA) donor antibodies (DSA) (3). However, these indicators need more sensitivity and change when rejection is established (3). This unmet clinical need led to a quest to discover early and sensitive biomarkers of graft damage, limiting renal graft biopsies' performance to only those patients with a high likelihood of rejection. Furthermore, beyond the rejection field, other scenarios in kidney transplantation, such as delayed graft function (DGF) or interstitial fibrosis and tubular atrophy (IFTA), run into the same problem without biomarkers that allow for early detection or differentiation from other pathologies.

Among these possible biomarkers, it is worth highlighting circulating extracellular vesicles (EVs), specifically, exosomes actively secreted by immune cells, which are intercellular communicators that carry microRNA, DNA, and proteins with biological significance as intercellular mediators (4).

This review summarizes the current EVs literature in kidney transplantation and their use as biomarkers.

2 Types of EVs

The discovery of EVs dates to the last century. Since then, several names have been attributed to them, and a sharp increase in scientific publications has been evidenced in the last decade (5). In 2014, the Minimal Information for Studies of Extracellular Vesicles ("MISEV") guidelines were released by the International Society for Extracellular Vesicles (ISEV). Subsequently, an update was proposed in 2018 by consensus of the largest group of EV experts, defining EVs as "the generic term for particles naturally released by cells that are delimited by a lipid bilayer and cannot replicate" (6). One year later, in 2019, another publication released by the corresponding authors of the MISEV guidelines asserted the accuracy and clarity of EV nomenclature to specialists and non-specialists and their use as a scaffold for progressively more detailed designation (7).

EVs are classified into three categories: exosomes, which are intraluminal vesicles contained in multivesicular bodies (MVBs) and released into the extracellular environment upon fusion of MVBs with the plasma membrane, microvesicles (also called microparticles) budded from the plasma membrane, and apoptotic bodies, the largest of the known vesicles and released during programmed cell death when the plasma membrane blebs (8–12) (Table 1).

Due to the internal origin of exosomes from MVBs, they represent the parental cell's internal activity and conditional state more closely than other types of EVs (5, 10, 11, 16, 17).

EVs seems that can be secreted by any cell type studied, including immune cells, are believed to play a central role in cell-to-cell communication (5, 6, 11). Their content is diverse and includes protein, lipids, nucleic acids, and other bioactive molecules that are determined according to the type of cell from which they arise (11, 16, 18). These content molecules provide EVs with different capabilities in terms of biogenesis and transport. Moreover, membrane curvature, which begins in the parent cell during membrane budding, determines the shape, composition, and size of each EV and therefore has a role in their physiological function (19–22).

Surface-exposed components and ligands determine EVs' biodistribution and their binding to target cells or binding to the extracellular matrix, allowing intracellular signaling pathways via simple interaction with the surface of the target cells or by internalization. For instance, proteins such as tetraspanins (CD81, CD82, CD63, or CD9) help penetrate exosomes inside cells, invasion, and fusion, whereas heat shock proteins such as HSP70 and HSP90 are involved in antigen binding and presentation. Other proteins such as Alix, annexins, Rab, or TSG101 are associated with exosome release, membrane transport, and function. Notably, some of these proteins, such as CD63, CD81, HSP70, and TSG101, which are enriched explicitly in exosomes, are generally used as their marker proteins (13, 17, 18)

Lipids such as cholesterol and sphingomyelin enrich EV membranes and, as well as their essential structural role, can also be transferred between cells (23).

The parent cell source and the properties of target cells determine EVs' biodistribution, and their quantity in circulation is determined by the balance between production and clearance. Clearance occurs via interactions with target cells through endocytosis, phagocytosis, pinocytosis, or membrane fusion (14), and also through the liver, spleen, and lungs (24, 25). Regarding the half-life, different studies have described a predominantly short one, ranging from 2–5 min to 5 h (24–27).

3 Isolation techniques

Up to now, there is no unique standardized protocol for EV isolation (28), and obtaining highly pure EVs is necessary to attribute them a specific function or property to be used as biomarkers (6). Their isolation and purification are decisive for most downstream applications due to their overlap with lipoproteins or protein aggregates; these can easily mistake EV

TABLE 1 Characteristics of the different types of EVs (13–15).

Exosomes	Microvesicles	Apoptotic bodies
Origin: multivesicular bodies	**Origin:** plasma membrane	**Origin:** apoptotic cell death
Size: 50–100 nm	**Size:** 100–1,000 nm	**Size:** 1,000–5,000 nm
Protein markers: CD9, CD81, CD63, TSG101, ALIX	**Protein markers:** CD40 ligands, integrins, selectins, annexin V	**Proteins markers:** Histones

detection due to their similar biophysical properties and act as contaminants (5, 15, 28).

EVs can be isolated from many sources, including biological fluids and cell culture supernatants (29, 30). Initial publications on blood-derived EVs prompted the recommendation to preferably conduct plasma studies due to platelet-derived EV released in the serum after blood collection during clot formation (30). In contrast, other studies have found EV isolation from serum to be more reproducible (29) and, in kidney transplantation, the serum content could reflect renal and endothelial recovery functions (31, 32)

According to MISEV 2018, differential ultracentrifugation was the most common isolation technique (6). It consists of consecutive centrifugation steps, each with an increase in centrifugation forces and durations, aiming to isolate smaller from larger particles based on differences in their densities (33). Other procedures, such as size exclusion chromatography (SEC), ultrafiltration, precipitation, or immunoisolation, were used by approximately 5–20% of researchers (6).

Since then, an assortment of techniques has been developed, such as field-flow fractionation (FFF), variations of size exclusion chromatography (SEC), ion exchange chromatography, microfiltration, fluorescence-activated sorting, novel immunoisolation techniques, and microfluidics or precipitation techniques using a plethora of commercial kits (5, 6).

Further information on EV isolation is beyond the scope of this review. All these methods, along with their strengths and weaknesses, are extensively discussed elsewhere (34, 35).

4 Biological function and role in immunology

EVs are involved in the regulation of physiological functions such as maintenance of homeostasis, enhanced coagulation (36–38), vessel integrity (39), tissue repair (40), or synaptic plasticity (41). They are also involved in inflammation, angiogenesis, or transmission of oncogenic molecules to neighboring cells, favoring neoplasia propagation and procoagulant capacity (4, 10, 11, 42–44).

Regarding their role in immunology, EVs act in innate and adaptative immune systems. In the innate, their major role has been described as pro-inflammatory mediators secreted by activated macrophages, neutrophilic granulocytes, NK cells, or mast cells in scenarios such as infection (45–47), sepsis (47–49), or chronic inflammation (50). In addition, an anti-inflammatory role also has been described through TGF-β secretion or regulation of endogenous lipid mediators (51).

Regarding adaptive immunity, EVs are a source of antigens for antigen-presenting cells (APC) such as macrophages, dendritic cells (DCs), and B cells. Depending on their cargo and parenting cells, they can induce immunogenic or tolerogenic responses (8, 42, 52). Recipient APCs can release EVs containing peptide-MHC I or II complexes and co-stimulatory molecules that contribute to antigen presentation (53, 54). This release is carried out constitutively, although this process can be increased after stimulation (55). Furthermore, graft-derived exosomes can initiate the immune response in a direct or semi-direct pathway that will end up causing graft rejection (56, 57). The direct pathway consists of exosomes from donor tissue behaving as donor APCs presenting MCH molecules or tissue-specific self-antigens to recipient T cells (58, 59). In contrast, in the semi-direct pathway, graft exosomes are taken up by recipient APCs, presenting intact MHC molecules from these graft exosomes on the surface of APCs, known as MHC cross-dressing (60).

Besides promoting intercellular information exchange via their surface molecules, their role as carriers of soluble mediators such as cytokines has been described. These cytokines include interleukin 1β (IL-1 β), interleukin 1α (IL-1 α), interleukin 18 (IL-18), macrophage migration inhibitory factor (MIF), interleukin 32, membrane-bound tumor necrosis factor (TNF), interleukin 6 (IL-6), vascular endothelial growth factor (VEGF), interleukin 8 (CXCL8), fractalkine (CX3CL1), CCL2, CCL3, CCL4, CCL5, and CCL20, and transforming growth factor β (TGF β) (27, 61).

5 Extracellular vesicles as biomarkers in kidney transplantation

Nowadays, biomarkers of the different EVs in circulation have been assessed in plenty of publications. The most developed field is oncology, where tumor mass has been linked to the amount of tumor-derived circulating exosomes. In the field of kidney disease, some studies demonstrate the participation of exosomes in different processes, which include acute kidney failure, autoimmune kidney disease, diabetic kidney disease, glomerulonephritis, vasculitis, or thrombotic microangiopathies (16).

Regarding transplantation, EVs in body fluids have been proposed as liquid biopsies. Mainly, publications focus on heart, lung, or pancreatic islet allografts. A profile of blood-derived EVs through multiplex flow cytometric assay using antibody-coated capture beads has been described in heart transplant recipients. A significant increase in the concentration of plasma-derived EVs in patients undergoing both acute cell and ABMR has been confirmed compared with subjects not undergoing them (62). In the lung, circulating exosomes with lung self-antigens can be a viable non-invasive biomarker for identifying patients at risk of developing chronic lung allograft dysfunction (63–65). Regarding pancreatic islet allografts, a human-into-mouse xenogeneic islet transplant model led to a marked decrease in the transplant islet exosome signal in early rejection, and changes in exosomal microRNA and proteomic profiles preceded hyperglycemia (66).

In kidney transplant, a decrease of circulating microparticle levels and their procoagulant activity after graft has been described in comparison to the prior hemodialysis status, hypothesizing that microparticles could be associated with cardiovascular risk improvement after transplant (67, 68). Studies have also been carried out on the urine and plasma of recipients, revealing their potential use as markers of cellular or humoral rejection, DGF, IFTA, mediated drug toxicity, and other non-specific graft injuries (18). Below, we expand the role of EVs in all of these settings (Figure 1). The methods of isolation for each study are summarized in Table 2.

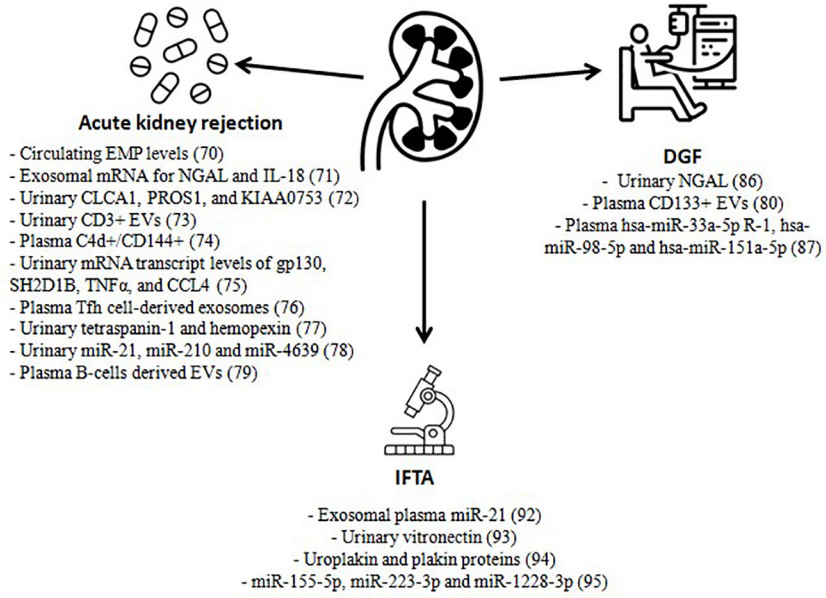

FIGURE 1
Extracellular vesicles as biomarkers in kidney transplantation. EMP, endothelial microparticles; NGAL, neutrophil gelatinase-associated lipocalin; IL-18, interleukin 18; EVs, extracellular vesicles; Tfh, T follicular helper; gp130, glycoprotein 130; SH2D1B SH2, domain containing 1B, TNFα, tumor necrosis factor alpha; CCL4, chemokine ligands 4; DGF, delayed graft function; IFTA, interstitial fibrosis and tubular atrophy.

TABLE 2 Methods of EV isolation in each study mentioned.

Study	EV isolation method
Qamri et al. (69)	Centrifugation
Peake et al. (70)	Centrifugation
Sigdel et al. (71)	Ultrafiltration
Park et al. (72)	Differential ultracentrifugation + immunoisolation
Tower et al. (73)	Centrifugation
Zhang et al. (74)	Precipitation - exoRNeasy serum/PlasmaMidi Kit
Yang et al. (75)	Precipitation - ExoQuickTM Kit (SBI Corporation)
Lim et al. (76)	Ultracentrifugation
Chen et al. (77)	Size-exclusion chromatography
Cucchiari et al. (78)	Size-exclusion chromatography
Alvarez et al. (79)	Ultracentrifugation
Dimuccio et al. (80)	Ultracentrifugation
Wang et al. (81)	Precipitation - exoEasy Maxi Kit (Qiagen)
Saejong et al. (82)	Precipitation - polyethylene glycol (PEG)
Carreras-Planella et al. (83)	Size-exclusion chromatography
Carreras-Planella et al. (84)	Size-exclusion chromatography
Costa de Freitas et al. (85)	Precipitation - miRCURY Exosome Kit (Qiagen)

5.1 Biomarkers for acute kidney rejection

In graft rejection, all the immune system components are involved in causing graft injury, including T and B lymphocytes, antibodies, endothelial cells, NK cells, macrophages, polymorphonuclear cells, or complement components (86).

Qamri et al. analyzed early post-transplant changes in circulating endothelial CD31+/CD42b− microparticle (EMP) levels after kidney transplant in 213 kidney recipients and 14 kidney + pancreas recipients. In the first cohort, no changes in circulating EMP levels were observed when graft dysfunction was unrelated to acute rejection. However, when this dysfunction was due to an episode of acute rejection (confirmed through a graft biopsy), an elevation in circulating EMP was detected. At the time of stratification according to PTC C4d staining, in patients with the negative one, a faster decrease in EMP levels was observed in comparison with patients with positive PTC C4d staining. This led the authors to suggest that circulating EMP levels could inform about ongoing endothelial cell injury. Moreover, when analyzing the different etiologies of end-stage kidney disease, a trend was found toward a decline in post-transplant EMP levels in causes due to diabetes mellitus, obstructive/inherited kidney disease, and autoimmune disease (69).

In another study by Peake et al., urinary exosomal mRNA from frequent kidney injury biomarkers such as neutrophil gelatinase-associated lipocalin (NGAL), interleukin-18 (IL-18) and kidney injury molecule-1 (KIM-1), together with the constitutively produced cystatin C, were compared with their corresponding

synthesized urinary protein levels as well as with the creatinine reduction ratio (CRR) on post-operatory day 7. The results showed that, although urinary NGAL and IL-18 protein levels did correlate with CRR on day 7, this was not the case for mRNA inside urinary exosomes. The explanation for these findings lay in the selectivity for exosome packaging and does not have to be representative of the parenting cell (70).

One year later, Sigdel et al. described 11 proteins to be enriched in the urinary exosomes of patients with biopsy-proven acute rejection; three of these proteins (CLCA1, PROS1, and KIAA0753) had not been previously identified in healthy urine exosomal proteins (71).

Park et al. reported a urine-based platform, iKEA (integrated kidney exosome analysis), to detect rejection of kidney transplants through T-cell-derived EVs. This platform, based on a magneto-electrochemical sensing system, revealed a higher level of CD3-positive EVs in kidney rejection recipients, with an accuracy of approximately 91.1% (72).

Tower et al. found a correlation between plasma C4d+, especially C4d+/CD144+ microvesicles, and the presence of ABMR and its severity and response to treatment in kidney recipients. Ninety-five kidney recipients with for-cause biopsies performed and twenty-three healthy volunteers were evaluated. After histopathologic examination of the graft biopsies, 28 patients with ABMR were found. In them, the density of C4d +/CD144+ microvesicles was 11-fold greater than in kidney transplant patients without ABMR and 24-fold greater than in healthy volunteers. The densities of C4d+ and C4d+/annexin V+ (C4d+/AVB+) microvesicles were also higher in ABMR recipients. Moreover, C4d+/AVB+ microvesicles correlated with ABMR biopsy severity. Lastly, in nine cases, treatment was associated with a reduction in the densities of C4d+/CD144+ and CD144+ microvesicles, which also showed them to be a treatment response monitoring tool (73).

Zhang et al. selected 21 genes (related to inflammatory and IL-6 signaling events or elevated in renal biopsies of patients with ABMR) whose mRNA transcript levels were increased in plasma exosomes of ABMR kidney recipients compared with cell-mediated rejection and/or no rejection. The authors also generated a gene score with the combination of the transcript levels of four of these genes (gp130, SH2D1B, TNFα, and CCL4), which was significantly higher in the ABMR group than the other groups (74).

Yang et al. suggested a correlation between ABMR and follicular helper T cell (Tfh cell)-derived exosomes through their increase in the circulation of such patients compared with non-ABMR patients. Moreover, Tfh cell-derived exosomes promoted B cell proliferation and differentiation. Moreover, their study reported a decline in CTLA-4 expression on the Tfh cell-derived exosome surface in kidney transplant patients with ABMR. CTLA-4 is a leukocyte differentiation antigen and a transmembrane receptor on T cells, with an established role in alloantigen-driven T cell activation and various autoimmune diseases. CTLA-4 on exosomes inhibited human T cell activation by directly interacting with the molecules CD80 or CD86. Furthermore, intracellular CTLA-4 can inhibit Tfh cell differentiation, reduce IL-21 secretion, and inhibit B cell proliferation and differentiation into plasma cells (75).

Regarding acute T cell-mediated rejection, Lim et al. identified several urinary exosomal biomarker candidates in an Asian population of kidney transplant patients using a proteomics approach. Validation of the findings by western blot assay proved that tetraspanin-1 and hemopexin were significantly higher in TCMR patients (76).

Chen et al. established a circulating exosomal miRNA panel by extracting plasma exosomes from 58 kidney transplant recipients and 27 healthy controls. Exosomal miR-21, miR-210, and miR-4639 could discriminate between subjects with chronic kidney dysfunction and those with normal graft function. At one year follow-up, patients with a low calculated score from this three-miRNA panel revealed a stable recovery of allograft function (77).

Lastly, our group has proposed using B-cells–derived EVs (BEVs) to check B cell proliferation in secondary lymphoid organs and bone marrow after desensitization. BEVs (CD19+ or HLA-II+) were associated with surviving B cells in lymph nodes retrieved upon surgery on patients who received desensitization with Rituximab, plasma exchanges, and immunoglobulins. After the administration of Rituximab, no B cells were circulating. CD19+ or HLA-II+ EVs may reflect the mass of surviving B cells in secondary lymphoid organs that may predispose them to subsequent rejection. This is suggested by the rebound of BEVs in patients who develop ABMR after desensitization (78).

5.2 Biomarkers for DGF

DGF leads to a higher risk of acute rejection and progression to chronic graft dysfunction (80, 87–89). The leading cause of DGF, ischemia-reperfusion injury (IRI), prompts a complex, alloantigen-independent immune response, which includes crosstalk between polymorphonuclear cells, macrophages, and donor cells as well as the release of EVs with pro-inflammatory and anti-inflammatory effects (80, 90, 91). Moreover, endothelial cells and renal tubular epithelial cells release EVs when exposed to oxidative stress, hypoxia, an acidic environment, or inflammation (8, 90, 91).

Among the first studies on exosomes and kidney dysfunction, Alvarez et al. evaluated if the different urine fractions (cellular or exosomal) have different NGAL expression in 15 kidney allograft recipients (eleven living donors and four deceased donors) soon after transplantation. Western blot analysis showed that the average NGAL expression in the exosomal fraction was significantly higher in deceased donor patients from the first post-operatory day and that its expression lasted increased in patients with DGF compared with non-DGF patients (79).

Dimuccio et al. showed lower levels of CD133-positive EVs in urine samples of transplanted patients. This decrease was evidenced from the first post-operatory day until day 7, when an increase was described. However, compared with patients with DGF, these last had a significant rise. Moreover, in patients with severe pre-transplant vascular injury of the allograft, CD133-positive EVs did not increase. The origin of CD133-positive EVs appeared restricted to glomeruli and proximal tubules. These data implicate CD133-positive cells in renal tissue regeneration after injury due to cold ischemia and IRI. Accordingly, no increase was

observed in recipients with severe pre-transplant vascular damage, implying an inefficient regeneration of the graft tissue in these recipients (80).

In another study, Wang et al. explored miRNA expression profiling in the DGF process. Fifty-two known and five conserved exosomal miRNAs expressed in kidney-transplanted patients with DGF were identified. Three co-expressed exosomal miRNAs: hsa-miR-33a-5p R-1, hsa-miR-98-5p, and hsa-miR-151a-5p, were further observed to be significantly upregulated in the peripheral blood of DGF patients. Moreover, hsa-miR-151a-5p was positively correlated with the patient's first-week serum creatinine levels, blood urea nitrogen, and uric acid after transplantation (81).

5.3 Biomarkers for interstitial fibrosis and tubular atrophy

In the field of kidney transplant, fibrosis serves as the final and irreversible stage of the pathogenic mechanisms that lead to the loss of allograft function (92). For this reason, beyond the invasiveness of renal biopsy, clinical data need to be more specific to allow for early detection (92–95).

Saejong et al. describe the potential use of microRNA (miR)-21 expression in plasma exosomes for non-invasive monitoring of high-grade IFTA in kidney transplant patients. There are already previous studies on the role of exosomal miR-21 as a fibrosis biomarker and its association with TGF-β, a cytokine known to be involved in fibrosis pathogenesis. In the study by Saejong, miR-21 from the plasma exosome fraction (but not from the whole plasma) could discriminate between low- versus high-grade IFTA. It is demonstrated that the released miR-21 decreases phosphatase and tensin homolog (PTEN), which causes the phosphorylation of Protein kinase B (AKT) signaling, in turn reducing the expression of E-cadherin and raising the expression of α-SMA and fibronectin in kidney tubules (82).

More recently, Carreras-Planella et al. describe the search for kidney allograft dysfunction protein biomarkers related to four biopsy-proven diagnoses: IFTA, acute T-cell rejection, calcineurin inhibitors toxicity, and normal kidney function. The authors carried out a proteomic analysis of the urinary EVs (uEVs), discovering some EV-associated proteins that show different expressions depending on whether they come from pathological or normal kidney function allografts. Moreover, a change in the expression of vitronectin (VTN) was also evidenced in recipients with chronic IFTA, suggesting urinary VTN levels as another possible biomarker for monitoring fibrotic changes in kidney transplant patients. For the fibrosis process to occur, VTN must join the potent profibrotic glycoprotein PAI-1, although the precise mechanisms are arguable. VTN has been reported to increase PAI-1 activity in the renal tissue, hindering fibrinolysis. However, other studies described the opposite, highlighting a protective role against fibrosis (83).

The same group also demonstrated the potential role of uEVs as biomarkers of chronic calcineurin inhibitor toxicity (CNIT). Their nephrotoxicity and role in kidney fibrosis are known and have been described in multiple studies and they are first-line agents in the immunosuppressive regimen of kidney transplantation. The problems we continue to face are CNIT diagnosis and management. In this study, the urine from kidney transplant recipients with CNIT diagnosis is compared with recipients with IFTA and without CNIT or normal allograft function (all of them under a similar immunosuppressive scheme that included CNI). After data analysis, members of the uroplakin (UPK1A, UPK1B, UPK2, and UPK3A) and plakin families (periplakin and envoplakin) were significantly upregulated in the CNIT group, suggesting a central role in CNIT development. The binding of uroplakin proteins covers the urothelium's surface to prevent urine influx from the lumen, also covering the renal pelvis, ureters, urinary bladder, and prostatic urethra. Periplakin and envoplakin function as cell-linker proteins. The upregulation of these proteins in the CNIT recipient's uEV suggests that the toxic effect of CNI on the urothelium may increase their citolinker activity (84).

Lastly, Costa de Freitas et al. also evaluated the expression of different urinary exosome-derived miRNAs (exo-miRs) in transplant patients on a tacrolimus regimen. As a result, a difference in the expression of 16 exo-miRs was observed. Among them, the marked upregulation of miR-155-5p and downregulation of miR-223-3p and miR-1228-3p stand out. Moreover, it was found that the tacrolimus dose correlated with the expression of miR-155-5p and miR-223-3p, serum creatinine with the expression of miR-223-3p, and the number of blood leukocytes with miR-223-3p and miR-1228-3p (85).

6 Discussion

EVs participate in intercellular communication in physiological and pathological processes, and in recent years, interest in them has grown as tools to monitor post-transplant evolution in a non-invasive way. Previous studies on diverse biological samples (blood or urine) include a wide range of pathologies such as kidney graft rejection (both cellular and humoral), DGF, IFTA, and drug toxicity. The limitations we have to consider are that the studies published and presented here do not often include multiple centers, the number of patients included is low, and the results have yet to be validated in larger cohorts. Appropriate method validation studies need to be improved, and the isolation protocol needs standardization to avoid the co-isolation of various vesicles or differences in contamination levels. The most modern technologies will likely offer new opportunities in this field; for instance, the Imaging Flow Cytometry (IFCM)-based methodology for the direct detection (without prior isolation) of donor-derived EVs (dd-EVs) in the plasma of kidney transplant patients based on Human Leukocyte Antigen (HLA) mismatch (96) or further investigation into the proteomic landscape and protein signature in urinary EVs (97).

Despite the promising published data, nowadays, we cannot use EVs as a definitive decision tool. Future studies are required before their analysis could facilitate the decision process in routine clinical practice. We still need basic parameters such as creatinine, proteinuria, or specific anti-HLA donor antibodies, and EV analysis may not replace the invasiveness of graft biopsy as the gold standard.

Future studies will extend our knowledge of the role of EVs as biomarkers in the kidney transplant field. A combination of biomarkers could help us decide whether a biopsy should be done and may have a supportive role when interpreting data provided by an allograft biopsy.

Author contributions

Conceptualization, EC-P, MR-B, EB-M, JR, and DC; resources, EC-P, MR-B, EB-M, JR, and FD; writing—original draft preparation, EC-P and DC; writing—review and editing, IR and DC; supervision, IR. All authors contributed to the article and approved the submitted version.

Conflict of interest

The authors declare that the research was conducted in the absence of any commercial or financial relationships that could be construed as a potential conflict of interest.

Publisher's note

References

1. Sellarés J, De Freitas DG, Mengel M, Reeve J, Einecke G, Sis B, et al. Understanding the causes of kidney transplant failure: The dominant role of antibody-mediated rejection and nonadherence. *Am J Transpl* (2012) 12(2):388–99. doi: 10.1111/j.1600-6143.2011.03840.x

2. Verhoeven JGHP, Boer K, Van Schaik RHN, Manintveld OC, Huibers MMH, Baan CC, et al. Liquid biopsies to monitor solid organ transplant function: A review of new biomarkers. *Ther Drug Monit* (2018) 40(5):515–25. doi: 10.1097/FTD.0000000000000549

3. Lo DJ, Kaplan B, Kirk AD. Biomarkers for kidney transplant rejection. *Nat Rev Nephrol* (2014) 10(4):215–25. doi: 10.1038/nrneph.2013.281

4. Van Niel G, D'Angelo G, Raposo G. Shedding light on the cell biology of extracellular vesicles. *Nat Rev Nephrol* (2014) 10(4):215–25. doi: 10.1038/nrneph.2013.281

5. Stam J, Bartel S, Bischoff R, Wolters JC. Isolation of extracellular vesicles with combined enrichment methods. *J Chromatogr B Analyt Technol BioMed Life Sci* (2021) 1169:122604. doi: 10.1016/j.jchromb.2021.122604

6. Théry C, Witwer KW, Aikawa E, Alcaraz MJ, Anderson JD, Andriantsitohaina R, et al. Minimal information for studies of extracellular vesicles 2018 (MISEV2018): a position statement of the International Society for Extracellular Vesicles and update of the MISEV2014 guidelines. *J Extracell Vesicles* (2018) 7(1):1535750. doi: 10.1080/20013078.2018.1535750

7. Witwer KW, Théry C. Extracellular vesicles or exosomes? On primacy, precision, and popularity influencing a choice of nomenclature. *J Extracell Vesicles* (2019) 8(1):1648167. doi: 10.1080/20013078.2019.1648167

8. Sailliet N, Ullah M, Dupuy A, Silva AKA, Gazeau F, Le Mai H, et al. Extracellular vesicles in transplantation. *Front Immunol* (2022) 13:800018. doi: 10.3389/fimmu.2022.800018

9. Gholizadeh S, Shehata Draz M, Zarghooni M, Sanati-Nezhad A, Ghavami S, Shafiee H, et al. Microfluidic approaches for isolation, detection, and characterization of extracellular vesicles: Current status and future directions. *Biosens Bioelectron* (2017) 91:588–605. doi: 10.1016/j.bios.2016.12.062

10. Karpman D, Ståhl AL, Arvidsson I. Extracellular vesicles in renal disease. *Nat Rev Nephrol* (2017) 13(9):545–62. doi: 10.1038/nrneph.2017.98

11. Colombo M, Raposo G, Théry C. Biogenesis, secretion, and intercellular interactions of exosomes and other extracellular vesicles. *Annu Rev Cell Dev Biol* (2014) 30:255–89. doi: 10.1146/annurev-cellbio-101512-122326

12. Sedgwick AE, D'Souza-Schorey C. The biology of extracellular microvesicles. *Traffic* (2018) 19(5):319–27. doi: 10.1111/tra.12558

13. Jadli AS, Ballasy N, Edalat P, Patel VB. Inside(sight) of tiny communicator: exosome biogenesis, secretion, and uptake. *Mol Cell Biochem* (2020) 467(1-2):77–94. doi: 10.1007/s11010-020-03703-z

14. Gurung S, Perocheau D, Touramanidou L, Baruteau J. The exosome journey: from biogenesis to uptake and intracellular signalling. *Cell Commun Signal* (2021) 19(1):47. doi: 10.1186/s12964-021-00730-1

15. György B, Módos K, Pállinger É, Pálóczi K, Pásztói M, Misják P, et al. Detection and isolation of cell-derived microparticles are compromised by protein complexes resulting from shared biophysical parameters. *Blood* (2011) 117(4):e39–48. doi: 10.1182/blood-2010-09-307595

16. Ashcroft J, Leighton P, Elliott TR, Hosgood SA, Nicholson ML, Kosmoliaptsis V. Extracellular vesicles in kidney transplantation: a state-of-the-art review. *Kidney Int* (2022) 101(3):485–97. doi: 10.1016/j.kint.2021.10.038

17. Colombo M, Moita C, Van Niel G, Kowal J, Vigneron J, Benaroch P, et al. Analysis of ESCRT functions in exosome biogenesis, composition and secretion highlights the heterogeneity of extracellular vesicles. *J Cell Sci* (2013) 126(24):5553–65. doi: 10.1242/jcs.128868

18. Gołębiewska JE, Wardowska A, Pietrowska M, Wojakowska A, Dębska-ślizień A. Small extracellular vesicles in transplant rejection. *Cells* (2021) 10(11):2989. doi: 10.3390/cells10112989

19. Kralj-Iglic VVP. Curvature-induced sorting of bilayer membrane constituents and formation of membrane rafts. *Adv Planar Lipid Bilayers Liposomes* (2006) 5:129–49. doi: 10.1016/S1554-4516(06)05005-8

20. Perez-Hernandez D, Gutiérrez-Vázquez C, Jorge I, López-Martín S, Ursa A, Sánchez-Madrid F, et al. The intracellular interactome of tetraspanin-enriched microdomains reveals their function as sorting machineries toward exosomes. *J Biol Chem* (2013) 288(17):11649–61. doi: 10.1074/jbc.M112.445304

21. Nazarenko I, Rana S, Baumann A, McAlear J, Hellwig A, Trendelenburg M, et al. Cell surface tetraspanin Tspan8 contributes to molecular pathways of exosome-induced endothelial cell activation. *Cancer Res* (2010) 70(4):1668–78. doi: 10.1158/0008-5472.CAN-09-2470

22. Batista BS, Eng WS, Pilobello KT, Hendricks-Muñoz KD, Mahal LK. Identification of a conserved glycan signature for microvesicles. *J Proteome Res* (2011) 10(10):4624–33. doi: 10.1021/pr200434y

23. Kooijmans SAA, Vader P, van Dommelen SM, van Solinge WW, Schiffelers RM. Exosome mimetics: A novel class of drug delivery systems. *Int J Nanomed* (2012) 7:1525–41. doi: 10.2147/IJN.S29661

24. Morishita M, Takahashi Y, Nishikawa M, Sano K, Kato K, Yamashita T, et al. Quantitative analysis of tissue distribution of the B16BL6-derived exosomes using a streptavidin-lactadherin fusion protein and Iodine-125-Labeled biotin derivative after intravenous injection in mice. *J Pharm Sci* (2015) 104(2):705–13. doi: 10.1002/jps.24251

25. Takahashi Y, Nishikawa M, Shinotsuka H, Matsui Y, Ohara S, Imai T, et al. Visualization and in *vivo* tracking of the exosomes of murine melanoma B16-BL6 cells in mice after intravenous injection. *J Biotechnol* (2013) 165(2):77–84. doi: 10.1016/j.jbiotec.2013.03.013

26. Rank A, Nieuwland R, Crispin A, Grützner S, Iberer M, Toth B, et al. Clearance of platelet microparticles in *vivo*. *Platelets* (2011) 22(2):111–6. doi: 10.3109/09537104.2010.520373

27. Yáñez-Mó M, Siljander PRM, Andreu Z, Zavec AB, Borràs FE, Buzas EI, et al. Biological properties of extracellular vesicles and their physiological functions. *J Extracell Vesicles J Extracell Vesicles* (2015) 4:27066. doi: 10.3402/jev.v4.27066

28. Erdbrügger U, Lannigan J. Analytical challenges of extracellular vesicle detection: A comparison of different techniques. *Cytometry A* (2016) 89(2):123–34. doi: 10.1002/cyto.a.22795

29. Hill AF, Pegtel DM, Lambertz U, Leonardi T, O'Driscoll L, Pluchino S, et al. ISEV position paper: extracellular vesicle RNA analysis and bioinformatics. *J Extracell Vesicles* (2013) 2(1):22859. doi: 10.3402/jev.v2i0.22859

30. Witwer KW, Buzás EI, Bemis LT, Bora A, Lässer C, Lötvall J, et al. Standardization of sample collection, isolation and analysis methods in extracellular vesicle research. *J Extracell Vesicles* (2013) 2(1). doi: 10.3402/jev.v2i0.20360

31. Burrello J, Bolis S, Balbi C, Burrello A, Provasi E, Caporali E, et al. An extracellular vesicle epitope profile is associated with acute myocardial infarction. *J Cell Mol Med* (2020) 24(17):9945–57. doi: 10.1111/jcmm.15594

32. Burrello J, Monticone S, Burrello A, Bolis S, Cristalli CP, Comai G, et al. Identification of a serum and urine extracellular vesicle signature predicting renal outcome after kidney transplant. *Nephrol Dial Transpl* (2023) 38(3):764–77. doi: 10.1093/ndt/gfac259

33. Théry C, Amigorena S, Raposo G, Clayton A. Isolation and characterization of exosomes from cell culture supernatants and biological fluids. *Curr Protoc Cell Biol* (2006). doi: 10.1002/0471143030.cb0322s30

34. Chen J, Li P, Zhang T, Xu Z, Huang X, Wang R, et al. Review on strategies and technologies for exosome isolation and purification. *Front Bioeng Biotechnol* (2022) 9:811971. doi: 10.3389/fbioe.2021.811971

35. Clos-Sansalvador M, Monguió-Tortajada M, Roura S, Franquesa M, Borràs FE. Commonly used methods for extracellular vesicles' enrichment: Implications in downstream analyses and use. *Eur J Cell Biol* (2022) 101(3):151227. doi: 10.1016/j.ejcb.2022.151227

36. Castaman G. A bleeding disorder characterised by isolated deficiency of platelet microvesicle generation. *Lancet* (1996) 347(9002):700–1. doi: 10.1016/s0140-6736(96)91259-3

37. Stormorken H. A new syndrome: thrombocytopathia, muscle fatigue, asplenia, miosis, migraine, dyslexia and ichthyosis. *Clin Genet* (1985) 28:367–74. doi: 10.1111/j.1399-0004.1985.tb02209.x

38. Weiss HJ, Vicic WJ, Lages BA, Rogers J. Isolated deficiency of platelet procoagulant activity. *Am J Med* (1979) 67(2):206–13. doi: 10.1016/0002-9343(79)90392-9

39. Abid Hussein MN, Böing AN, Sturk A, Hau CM, Nieuwland R. Inhibition of microparticle release triggers endothelial cell apoptosis and detachment. *Thromb Haemost* (2007) 98:1096–107. doi: 10.1160/th05-04-0231

40. Zhang B, Wang M, Gong A, Zhang X, Wu X, Zhu Y, et al. HucMSc-exosome mediated-Wnt4 signaling is required for cutaneous wound healing. *Stem Cells* (2015) 33(7):2158–68. doi: 10.1002/stem.1771

41. Cano A, Ettcheto M, Bernuz M, Puerta R, de Antonio EE, Sánchez-López E, et al. Extracellular vesicles, the emerging mirrors of brain physiopathology. *Int J Biol Sci* (2023) 19(3):721–43. doi: 10.7150/ijbs.79063

42. Burrello J, Monticone S, Gai C, Gomez Y, Kholia S, Camussi G. Stem cell-derived extracellular vesicles and immune-modulation. *Front Cell Dev Biol* (2016) 4:83. doi: 10.3389/fcell.2016.00083

43. Ramirez-Bajo MJ, Rovira J, Lazo-Rodriguez M, Banon-Maneus E, Tubita V, Moya-Rull D, et al. Impact of mesenchymal stromal cells and their extracellular vesicles in a rat model of kidney rejection. *Front Cell Dev Biol* (2020) 8:10. doi: 10.3389/fcell.2020.00010

44. Lugini L, Valtieri M, Federici C, Cecchetti S, Meschini S, Condello M, et al. Exosomes from human colorectal cancer induce a tumor-like behavior in colonic mesenchymal stromal cells. *Oncotarget* (2016) 7(31):50086–98. doi: 10.18632/oncotarget.10574

45. Oehmcke S, Mörgelin M, Malmström J, Linder A, Chew M, Thorlacius H, et al. Stimulation of blood mononuclear cells with bacterial virulence factors leads to the release of pro-coagulant and pro-inflammatory microparticles. *Cell Microbiol* (2012) 14(1):107–19. doi: 10.1111/j.1462-5822.2011.01705.x

46. Wang JG, Williams JC, Davis BK, Jacobson K, Doerschuk CM, Ting JPY, et al. Monocytic microparticles activate endothelial cells in an IL-1β-dependent manner. *Blood* (2011) 118(8):2366–74. doi: 10.1182/blood-2011-01-330878

47. Tian C, Wang K, Zhao M, Cong S, Di X, Li R. Extracellular vesicles participate in the pathogenesis of sepsis. *Front Cell Infect Microbiol* (2022) 12:1018692. doi: 10.3389/fcimb.2022.1018692

48. Mastronardi ML, Mostefai HA, Meziani F, Martínez MC, Asfar P, Andriantsitohaina R. Circulating microparticles from septic shock patients exert differential tissue expression of enzymes related to inflammation and oxidative stress. *Crit Care Med* (2011) 39(7):1739–48. doi: 10.1097/CCM.0b013e3182190b4b

49. Prakash PS, Caldwell CC, Lentsch AB, Pritts TA, Robinson BRH. Human microparticles generated during sepsis in patients with critical illness are neutrophil-derived and modulate the immune response. *J Trauma Acute Care Surg* (2012) 73(2):401–6. doi: 10.1097/TA.0b013e31825a776d

50. Boilard E, Nigrovic PA, Larabee K, Watts GFM, Coblyn JS, Weinblatt ME, et al. Platelets amplify inflammation in arthritis via collagen-dependent microparticle production. *Science* (2010) 327(5965):580–3. doi: 10.1126/science.1181928

51. Gasser O, Schifferli JA. Activated polymorphonuclear neutrophils disseminate anti-inflammatory microparticles by ectocytosis. *Blood* (2004) 104(8):2543–8. doi: 10.1182/blood-2004-01-0361

52. Ratajczak J, Wysoczynski M, Hayek F, Janowska-Wieczorek A, Ratajczak MZ. Membrane-derived microvesicles: Important and underappreciated mediators of cell-to-cell communication. *Leukemia* (2006) 20(9):1487–95. doi: 10.1038/sj.leu.2404296

53. Raposo G, Nijman HW, Stoorvogel W, Liejendekker R, Harding CV, Melief C, et al. B lymphocytes secrete antigen-presenting vesicles. *J Exp Med* (1996) 183(3):1161–72. doi: 10.1084/jem.183.3.1161

54. Giri PK, Schorey JS. Exosomes derived from M. bovis BCG infected macrophages activate antigen-specific CD4+ and CD8+ T cells in vitro and in *vivo*. *PloS One* (2008) 3(6):e2461. doi: 10.1371/journal.pone.0002461

55. Obregon C, Rothen-Rutishauser B, Gitahi SK, Gehr P, Nicod LP. Exovesicles from human activated dendritic cells fuse with resting dendritic cells, allowing them to present alloantigens. *Am J Pathol* (2006) 169(6):2127–36. doi: 10.2353/ajpath.2006.060453

56. Ramis JM. Extracellular vesicles in cell biology and medicine. *Sci Rep* (2020) 10(1):8667. doi: 10.1038/s41598-020-65826-z

57. Pêche H, Heslan M, Usal C, Amigorena S, Cuturi MC. Presentation of donor major histocompatibility complex antigens by bone marrow dendritic cell-derived exosomes modulates allograft rejection. *Transplantation* (2003) 76(10):1503–10. doi: 10.1097/01.TP.0000092494.75313.38

58. Segura E, Amigorena S, Théry C. Mature dendritic cells secrete exosomes with strong ability to induce antigen-specific effector immune responses. *Blood Cells Mol Dis* (2005) 35(2):89–93. doi: 10.1016/j.bcmd.2005.05.003

59. Pêche H, Renaudin K, Beriou G, Merieau E, Amigorena S, Cuturi MC. Induction of tolerance by exosomes and short-term immunosuppression in a fully MHC-mismatched rat cardiac allograft model. *Am J Transpl* (2006) 6(7):1541–50. doi: 10.1111/j.1600-6143.2006.01344.x

60. Mastoridis S, Londoño MC, Kurt A, Kodela E, Crespo E, Mason J, et al. Impact of donor extracellular vesicle release on recipient cell "cross-dressing" following clinical liver and kidney transplantation. *Am J Transpl* (2021) 21(7):2387–98. doi: 10.1111/ajt.16123

61. Gulinelli S, Salaro E, Vuerich M, Bozzato D, PizzIrani C, Bolognesi G, et al. IL-18 associates to microvesicles shed from human macrophages by a LPS/TLR-4 independent mechanism in response to P2X receptor stimulation. *Eur J Immunol* (2012) 42(12):3334–45. doi: 10.1002/eji.201142268

62. Castellani C, Burrello J, Fedrigo M, Burrello A, Bolis S, Di Silvestre D, et al. Circulating extracellular vesicles as non-invasive biomarker of rejection in heart transplant. *J Heart Lung Transpl* (2020) 39(10):1136–48. doi: 10.1016/j.healun.2020.06.011

63. Sharma M, Gunasekaran M, Ravichandran R, Fisher CE, Limaye AP, Hu C, et al. Circulating exosomes with lung self-antigens as a biomarker for chronic lung allograft dysfunction: A retrospective analysis. *J Heart Lung Transpl* (2020) 39(11):1210–9. doi: 10.1016/j.healun.2020.07.001

64. Gunasekaran M, Xu Z, Nayak DK, Sharma M, Hachem R, Walia R, et al. Donor-derived exosomes with lung self-antigens in human lung allograft rejection. *Am J Transpl* (2017) 17(2):474–84. doi: 10.1111/ajt.13915

65. Gunasekaran M, Sharma M, Hachem R, Bremner R, Smith MA, Mohanakumar T. Circulating exosomes with distinct properties during chronic lung allograft rejection. *J Immunol* (2018) 200(8):2535–41. doi: 10.4049/jimmunol.1701587

66. Vallabhajosyula P, Korutla L, Habertheuer A, Yu M, Rostami S, Yuan CX, et al. Tissue-specific exosome biomarkers for noninvasively monitoring immunologic rejection of transplanted tissue. *J Clin Invest* (2017) 127(4):1375–91. doi: 10.1172/JCI87993

67. Al-Massarani G, Vacher-Coponat H, Paul P, Arnaud L, Loundou A, Robert S, et al. Kidney transplantation decreases the level and procoagulant activity of circulating microparticles. *Am J Transpl* (2009) 9(3):550–7. doi: 10.1111/j.1600-6143.2008.02532.x

68. Al-Massarani G, Vacher-Coponat H, Paul P, Widemann A, Arnaud L, Loundou A, et al. Impact of immunosuppressive treatment on endothelial biomarkers after kidney transplantation. *Am J Transpl* (2008) 8(11):2360–7. doi: 10.1111/j.1600-6143.2008.02399.x

69. Qamri Z, Pelletier R, Foster J, Kumar S, MOmani H, Ware K, et al. Early posttransplant changes in circulating endothelial microparticles in patients with kidney transplantation. *Transpl Immunol* (2014) 31(2):60–4. doi: 10.1016/j.trim.2014.06.006

70. Peake PW, Pianta TJ, Succar L, Fernando M, Pugh DJ, McNamara K, et al. A comparison of the ability of levels of urinary biomarker proteins and exosomal mRNA to predict outcomes after renal transplantation. *PloS One* (2014) 9(6):e98644. doi: 10.1371/journal.pone.0098644

71. Sigdel KR, Cheng A, Wang Y, Duan L, Zhang YL. The emerging functions of long noncoding RNA in immune cells: autoimmune diseases. *J Immunol Res* (2015) 2015:848790. doi: 10.1155/2015/848790

72. Park J, Lin HY, Assaker JP, Jeong S, Huang CH, Kurdi A, et al. Integrated kidney exosome analysis for the detection of kidney transplant rejection. *ACS Nano* (2017) 11(11):11041–6. doi: 10.1021/acsnano.7b05083

73. Tower CM, Reyes M, Nelson K, Leca N, Kieran N, Muczynski K, et al. Plasma C4d+ endothelial microvesicles increase in acute antibody-mediated rejection. *Transplantation* (2017) 101(9):2235–43. doi: 10.1097/TP.0000000000001572

74. Zhang H, Huang E, Kahwaji J, Nast CC, Li P, Mirocha J, et al. Plasma exosomes from HLA-sensitized kidney transplant recipients contain mRNA transcripts which predict development of antibody-mediated rejection. *Transplantation* (2017) 101(10):2419–28. doi: 10.1097/TP.0000000000001834

75. Yang J, Bi L, He X, Wang Z, Qian Y, Xiao L, et al. Follicular helper T cell derived exosomes promote B cell proliferation and differentiation in antibody-mediated rejection after renal transplantation. *BioMed Res Int* (2019) 2019:6387924. doi: 10.1155/2019/6387924

76. Lim JH, Lee CH, Kim KY, Jung HY, Choi JY, Cho JH, et al. Novel urinary exosomal biomarkers of acute T cell-mediated rejection in kidney transplant recipients: A cross-sectional study. *PloS One* (2018) 13(9):e0204204. doi: 10.1371/journal.pone.0204204

77. Chen Y, Han X, Sun Y, He X, Xue D. A circulating exosomal microRNA panel as a novel biomarker for monitoring post-transplant renal graft function. *J Cell Mol Med* (2020) 24(20):12154–63. doi: 10.1111/jcmm.15861

78. Cucchiari D, Tubita V, Rovira J, Ramirez-Bajo MJ, Banon-Maneus E, Lazo-Rodriguez M, et al. B cell-derived extracellular vesicles reveal residual B cell activity in kidney graft recipients undergoing pre-transplant desensitization. *Front Med (Lausanne)* (2021) 8:781239. doi: 10.3389/fmed.2021.781239

79. Alvarez S, Suazo C, Boltansky A, Ursu M, Carvajal D, Innocenti G, et al. Urinary exosomes as a source of kidney dysfunction biomarker in renal transplantation. *Transplant Proc* (2013) 45(10):3719–23. doi: 10.1016/j.transproceed.2013.08.079

80. Dimuccio V, Ranghino A, Barbato LP, Fop F, Biancone L, Camussi G, et al. Urinary CD133+ extracellular vesicles are decreased in kidney transplanted patients with slow graft function and vascular damage. *PloS One* (2014) 9(8):e104490. doi: 10.1371/journal.pone.0104490

81. Wang J, Li X, Wu X, Wang Z, Zhang C, Cao G, et al. Expression profiling of exosomal miRNAs derived from the peripheral blood of kidney recipients with DGF using high-throughput sequencing. *BioMed Res Int* (2019) 2019:1759697. doi: 10.1155/2019/1759697

82. Saejong S, Townamchai N, Somparn P, Tangtanatakul P, Ondee T, HIrankarn N, et al. MicroRNA-21 in plasma exosome, but not from whole plasma, as a biomarker for the severe interstitial fibrosis and tubular atrophy (IF/TA) in post-renal transplantation. *Asian Pac J Allergy Immunol* (2022) 40(1):94–102. doi: 10.12932/AP-101019-0656

83. Carreras-Planella L, Cucchiari D, Cañas L, Juega J, Franquesa M, Bonet J, et al. Urinary vitronectin identifies patients with high levels of fibrosis in kidney grafts. *J Nephrol* (2021) 34(3):861–74. doi: 10.1007/s40620-020-00886-y

84. Carreras-Planella L, Juega J, Taco O, Cañas L, Franquesa M, Lauzurica R, et al. Proteomic characterization of urinary extracellular vesicles from kidney-transplanted patients treated with calcineurin inhibitors. *Int J Mol Sci* (2020) 21(20):1–14. doi: 10.3390/ijms21207569

85. Costa De Freitas RC, Bortolin RH, Vecchia Genvigir FD, Bonezi V, Crespo Hirata TD, Felipe CR, et al. Differentially expressed urinary exo-miRs and clinical outcomes in kidney recipients on short-term tacrolimus therapy: A pilot study. *Epigenomics* (2020) 12(22):2019–34. doi: 10.2217/epi-2020-0160

86. Monguió-Tortajada M, Lauzurica R, Borràs FE. Tolerance in organ transplantation: From conventional immunosuppression to extracellular vesicles. *Front Immunol* (2014) 5:416. doi: 10.3389/fimmu.2014.00416

87. Perico N, Cattaneo D, Sayegh M, Remuzzi G. Delayed graft function in kidney transplantation. *Lancet* (2004) 364(9447):1814–27. doi: 10.1016/S0140-6736(04)17406-0

88. Ponticelli C. Ischaemia-reperfusion injury: A major protagonist in kidney transplantation. *Nephrol Dial Transpl* (2014) 29(6):1134–40. doi: 10.1093/ndt/gft488

89. Eltzschig HK, Eckle T. Ischemia and reperfusion-from mechanism to translation. *Nat Med* (2011) 17(11):1391–401. doi: 10.1038/nm.2507

90. Quaglia M, Dellepiane S, Guglielmetti G, Merlotti G, Castellano G, Cantaluppi V. Extracellular vesicles as mediators of cellular crosstalk between immune system and kidney graft. *Front Immunol* (2020) 11:74. doi: 10.3389/fimmu.2020.00074

91. Duan P, Tan J, Miao Y, Zhang Q. Potential role of exosomes in the pathophysiology, diagnosis, and treatment of hypoxic diseases. *Am J Transl Res* (2019) 11(3):1184–201.

92. Boor P, Floege J. Renal allograft fibrosis: Biology and therapeutic targets. *Am J Transpl* (2015) 15(4):863–86. doi: 10.1111/ajt.13180

93. Eulalio A, Huntzinger E, Izaurralde E. Getting to the root of miRNA-mediated gene silencing. *Cell* (2008) 132(1):9–14. doi: 10.1016/j.cell.2007.12.024

94. Fabian MR, Sonenberg N, Filipowicz W. Regulation of mRNA translation and stability by microRNAs. *Annu Rev Biochem* (2010) 79:351–79. doi: 10.1146/annurev-biochem-060308-103103

95. Gallo A, Tandon M, Alevizos I, Illei GG. The majority of microRNAs detectable in serum and saliva is concentrated in exosomes. *PloS One* (2012) 7(3):e30679. doi: 10.1371/journal.pone.0030679

96. Woud WW, Hesselink DA, Hoogduijn MJ, Baan CC, Boer K. Direct detection of circulating donor-derived extracellular vesicles in kidney transplant recipients. *Sci Rep* (2022) 12(1):21973. doi: 10.1038/s41598-022-26580-6

97. Braun F, Rinschen M, Buchner D, Bohl K, Plagmann I, Bachurski D, et al. The proteomic landscape of small urinary extracellular vesicles during kidney transplantation. *J Extracell Vesicles* (2020) 10(1):e12026. doi: 10.1002/jev2.12026

frontiers | Frontiers in Immunology

TYPE Review
PUBLISHED 22 August 2023
DOI 10.3389/fimmu.2023.1206929

OPEN ACCESS

EDITED BY
Long Zheng,
The Second Affiliated Hospital of Zhejiang University School of Medicine, China

REVIEWED BY
Olga Millán,
Carlos III Health Institute (ISCIII), Spain
Enver Akalin,
Montefiore Medical Center, United States

*CORRESPONDENCE
Wiwat Chancharoenthana
wiwat.cha@mahidol.ac.th
Asada Leelahavanichkul
aleelahavanit@gmail.com

RECEIVED 16 April 2023
ACCEPTED 31 July 2023
PUBLISHED 22 August 2023

CITATION
Chancharoenthana W, Traitanon O, Leelahavanichkul A and Tasanarong A (2023) Molecular immune monitoring in kidney transplant rejection: a state-of-the-art review.
Front. Immunol. 14:1206929.
doi: 10.3389/fimmu.2023.1206929

Molecular immune monitoring in kidney transplant rejection: a state-of-the-art review

Wiwat Chancharoenthana[1,2,3]*, Opas Traitanon[3,4], Asada Leelahavanichkul[5,6]* and Adis Tasanarong[3,4]

[1]Department of Clinical Tropical Medicine, Faculty of Tropical Medicine, Mahidol University, Bangkok, Thailand, [2]Tropical Immunology and Translational Research Unit (TITRU), Department of Clinical Tropical Medicine, Faculty of Tropical Medicine, Mahidol University, Bangkok, Thailand, [3]Thammasat Multi-Organ Transplant Center, Thammasat University Hospital, Faculty of Medicine, Thammasat University, Pathumthani, Thailand, [4]Division of Nephrology, Department of Medicine, Faculty of Medicine, Thammasat University, Pathumthani, Thailand, [5]Center of Excellence on Translational Research in Inflammation and Immunology (CETRII), Department of Microbiology, Chulalongkorn University, Bangkok, Thailand, [6]Department of Microbiology, Faculty of Medicine, Chulalongkorn University, Bangkok, Thailand

Although current regimens of immunosuppressive drugs are effective in renal transplant recipients, long-term renal allograft outcomes remain suboptimal. For many years, the diagnosis of renal allograft rejection and of several causes of renal allograft dysfunction, such as chronic subclinical inflammation and infection, was mostly based on renal allograft biopsy, which is not only invasive but also possibly performed too late for proper management. In addition, certain allograft dysfunctions are difficult to differentiate from renal histology due to their similar pathogenesis and immune responses. As such, non-invasive assays and biomarkers may be more beneficial than conventional renal biopsy for enhancing graft survival and optimizing immunosuppressive drug regimens during long-term care. This paper discusses recent biomarker candidates, including donor-derived cell-free DNA, transcriptomics, microRNAs, exosomes (or other extracellular vesicles), urine chemokines, and nucleosomes, that show high potential for clinical use in determining the prognosis of long-term outcomes of kidney transplantation, along with their limitations.

KEYWORDS

chemokine, donor-derived cell-free DNA, exosomes, extracellular vesicles, MicroRNAs, molecular immune monitoring, nucleosome, transcriptomics

1 Introduction

A kidney transplant is typically the best option for patients with end-stage renal disease (ESRD). Kidney transplant (KT) recipients have a life expectancy that is more than double that of people on dialysis, and they also have a significant improvement in their quality of life (1). Furthermore, kidney transplantation is the most cost-effective long-term therapy for people with ESRD. Treatment developments have led to a steady decline in long-term

allograft failure over the past 15 years: the kidney allograft failure rates five years post-transplantation in recipients receiving kidneys from deceased donors (DD) and live donors (LD) dropped to 14% and 9%, respectively in the periods from 1996 to 2012. The long-term survival of DD recipients has increased from 8.2 years (between 1995 and 1999) to 11.7 years (between 2014 and 2017) (2). Data from the National Kidney Transplantation Registry of Thailand in 2019 revealed the renal allograft survival rates at one, five, and ten years for DD recipients were 95.9%, 78.5%, and 58.5%, respectively. Meanwhile LD recipients showed a better renal allograft outcome than that of DD recipients (renal allograft survival rates were 98.2%, 92.6%, and 77.8%, respectively) (3). Of note, the leading causes of early graft failure within five years were rejection (56%) and interstitial fibrosis and tubular atrophy (IF/TA) (22%) followed by vascular or urologic complications (11%). IF/TA were the leading causes of late allograft failure (46.3%), followed by rejection (33%) and recurrent glomerular diseases (9%) (3). Thus, the major etiology of returning to dialysis in KT recipients is still dialysis reinstitution due to the failure of the renal allograft (3, 4). Despite advances in immunosuppressants and the management of acute kidney allograft rejection, a better understanding of several aspects of kidney transplantation is still needed, especially to improve long-term renal allograft survival. As such, donor characteristics and recipient variables (age, gender, dialysis vintage, and comorbidity), immunosuppressive drug monitoring, and immunological aspects such as human leucocyte antigen (HLA) mismatch, delayed graft function (DGF), cold ischemia period, and acute rejection during the first year of transplantation, have all been linked to long-term graft survival (5–8). Currently, several noninvasive biomarkers, including molecules, proteins, and immune responses, in combination or as single factors, have been developed to identify the risk of allograft rejection (9–12).

In response to the growing use of minimally invasive biomarkers in clinical transplantation, the Banff Minimally Invasive Biomarkers Working Group was established in early 2021 to examine the application of biomarkers in the diagnosis and categorization of renal allograft rejection. In the Banff 2005 and 2017 classification, donor-specific antibody (DSA) was introduced as a criterion for antibody-mediated rejection (AMR) (13, 14), and the classification of AMR and T cell-mediated rejection (TCMR) was greatly modified in the Banff 2019 classification (15). Currently, non-DSA biomarkers are mentioned in the Banff classification as screening tests to: *i)* rule out rejection, *ii)* expedite a confirmatory renal biopsy, or *iii)* directly diagnose rejection, either alone or in conjunction with histology (15, 16). Hence, the ideal biomarkers for diagnosis of allograft rejection should be able to distinguish rejection from non-rejection, be specific to rejection, replace biopsies or add information to the biopsy, and lastly, demonstrate prognostic value. The biomarker should also be able to discriminate between AMR and TCMR, which are induced through different immunopathogenic mechanisms. Several biomarkers include donor-derived cell-free deoxyribonucleic acid (dd-cfDNA), transcriptomic patterns, micro ribonucleic acids (microRNAs), exosomes, extracellular vesicles, chemokines, and nucleosomes are mentioned.

Our aim in writing this review was to summarize the most current research regarding novel biomarkers in the kidney transplantation field in terms of allograft rejection and their relevance to outcomes. Currently, novel biomarker use can be classified into two categories as immunological biomarkers and non-immunological biomarkers. The immunological biomarkers identify immune dysfunctions ranging from subclinical to overt rejection, whereas the non-immunological biomarkers indicate adverse transplant outcomes, such as delayed graft function, cardiovascular events, infection, and cancer, in which immune dysfunction is not the primary abnormality. Accordingly, although the non-immunological testing is necessary for long-term renal allograft outcomes, these biomarkers are outside the scope of this review.

2 Pathophysiology of renal allograft rejection

2.1 T cell-mediated rejection

Both innate and adaptive immune response components contribute to T cell-mediated graft injury. As such, the damage-associated molecular patterns (DAMPs) that are released in response to the ischemia during the graft preparation are recognized by pattern recognition receptors (PRRs) of phagocytic cells of the innate immunity leading to the upregulation of costimulatory molecules and secretion of pro-inflammatory cytokines (17). Mismatched HLA epitopes on the graft are recognized subsequently by host T cell receptors via direct, indirect, and semi-direct pathways (Figure 1) and act in concert with innate immunity-derived stimuli to activate and expand recipient T cell clones with inflammatory or regulatory functions (17). The production and release of soluble mediators, including interleukin (IL)-15, IL-17, granzyme B, perforin, *Fas* ligand which is also known as tumor necrosis factor (TNF) ligand superfamily member 6, interferon (IFN)-γ, TNF, CXC-chemokine ligand (CXCL) 10, CC-chemokine ligand (CCL) 2, CCL3, CCL4, CCL5, and CX3CL1, potentiates the inflammatory injury that is the characteristics of acute allograft rejection (17). Then, the activated mononuclear cells accumulate in the renal interstitium, tubules, and, rarely, in the arteries of the graft (leading to endarteritis), whereas glomerulitis may occur in more severe cases of rejection and is accompanied by apoptosis of vascular endothelial cells and mesangiolysis.

Currently, the Banff classification (13) stratifies TCMR-induced graft injury into three classifications based on the presence of *i)* interstitial inflammation in the non-scarred area of the cortex, *ii)* tubulitis in cortical tubules within the non-scarred cortex, and *iii)* endarteritis (intimal and transmural arteritis with fibrinoid necrotic change) as well as medial smooth muscle necrosis with lymphocytic infiltration in the vessel (18). Despite the fact that TCMR normally responds rapidly to immunosuppressive drugs, persistent inflammation in the areas of IF/TA is frequently associated with sustained expression of gene transcripts characteristic of acute

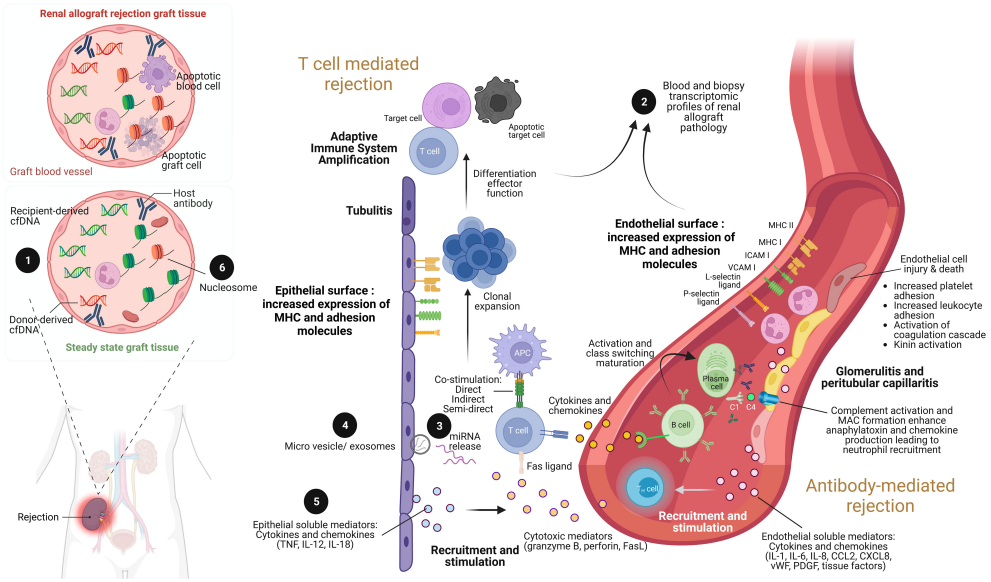

FIGURE 1
The illustration of renal allograft rejection and the application of biomolecular biomarkers from immunological pathogenesis. While the main pathogenesis of acute cellular mediated rejection (TCMR) is epithelial cell injury enhancement leading to adaptive immune system amplification, acute antibody-mediated rejection (AMR) is endothelial cell injury through antibody and complement enhancement. As a result, the culprit pathologic characteristic of TCMR is tubulitis compared to glomerulitis and peritubular capillaritis in AMR. Both patterns can be concurrently found in severe combined TCMR and AMR case. During renal allograft rejection process, both innate and adaptive immune system are activated from the imbalance differentiation between donor and recipient cell-free deoxyribonucleic acid (cfDNA) molecules ❶ (left panel). The final products of both T cell and B cell activation can be detected their signals and cellular origin of either peripheral blood or renal allograft tissue by transcriptomic profiles ❷. Indeed, plenty of mediators are produced during overwhelming inflammatory process from both TCMR and AMR, including the production of miRNAs ❸ within extracellular vesicles and exosomes ❹, and soluble mediators (cytokines and chemokines) ❺. Interestingly, the epigenetic control of gene expression by circulating cell-free nucleosome may play as a crucial step of renal allograft rejection activation ❻. Imbalance between donor- and recipient-derived nucleosomes with histone alteration is currently postulated as one of pathogenesis in renal allograft rejection. ICAM, intracellular adhesion molecule; IL, interleukin; MHC, major histocompatibility complex; VCAM, vascular cell adhesion molecule; TNF, tumor necrosis factor. Picture is created by BioRender.com.

kidney injury and predicts progression to chronic-active TCMR (19, 20).

2.2 Antibody-mediated rejection

Antibody-mediated rejection (AMR) is the most severe and destructive form of immune-mediated graft injury which is observed in approximately 30% of all patients with rejection (21). As such, AMR may occur with or without TCMR and can be detected early or late in the transplantation process, ranging from acute AMR with rapid and severe graft injury to chronic AMR with progressive graft destruction (21). Recipient $CD4^+$ T cells, which are activated by epitopes expressed on graft antigens, assist in the activation of graft-specific B cells, which is followed by class switching and affinity maturation; T cell assistance is mediated by costimulatory factors and receptors, including inducible T cell costimulator, CD40 ligand, CD80, and CD86 (22). These activated B cells generate plasmablasts and plasma cells that produce DSAs (Figure 1). It has been reported that 15% of KT recipients developed *de novo* DSAs over 4 years after transplantation, and graft survival at 10 years was diminished by 40% compared to patients without *de novo* DSAs due to chronically active AMR (23). Solid-phase assays can be used to detect DSAs and enable precise determination of alloreactivity, which is frequently directed against HLA class II epitopes but has also been observed against non-HLA targets such as type 1 angiotensin II receptor, perlecan, and collagen (24). The antibody against HLA is frequently initially circumscribed to mismatched epitopes expressed on the graft; however, repeated stimulation may enhance sensitization and broaden the epitope repertoire via intramolecular and intermolecular antigen spreading (epitope spreading) (25).

As highlighted by the Banff criteria, DSA binding to target epitopes expressed on the vascular endothelium led to acute microvascular injury that can be characterized by endothelial cell enlargement, vacuolization, loss of fenestrations, detachment from the basement membrane, and apoptosis (26). Mobilization of endothelial vesicles externalizes P-selectin, facilitates the binding of several cells at the site of injury, including platelets, neutrophils, macrophages, natural killer cells, and T cells, contributes to intimal arteritis which is a major characteristic of AMR injury (26). The formation of the membrane attack complex (C5b–C9), which exacerbates injury to the endothelium and other graft tissues (27), is triggered by the binding of the complement C1 complex to activate the classic complement pathway (Figure 1). Immunoglobulin subclasses 1 and 4 of the DSA are associated with enhanced C1 binding capacity and the degree of complement activation and may therefore determine the severity of the injury. Hence, C4d is frequently deposited at the site of complement activation, whereas C3a and C5a function as anaphylatoxins

enhancing infiltration in the kidney with innate immune cells (neutrophils and mononuclear inflammatory cells) that exacerbate the injury. Additionally, the complement-independent pathways may also be involved in AMR (21). As such, AMR is currently classified as active, smoldering, or chronic mechanisms and either the smoldering or chronic AMR is frequently resistant to treatment. Although none of the current therapeutic interventions has shown promising results in AMR, removal of circulating antibodies by plasmapheresis with the concurrent intravenous immunoglobulin administration to downregulate B cell activity is currently a standard of care (21) with inadequately supported evidence. Moreover, proteasome inhibitors, C1q or C5 inhibitors, anti-CD20 biologics, and cleaving endopeptidases have proven to be ineffective (28).

3 Immunological biomarkers

3.1 Donor-derived cell-free deoxyribonucleic acid

Donor-derived cell-free deoxyribonucleic acid (dd-cfDNA) has been proposed as a noninvasive marker for the early detection of rejection before clinical allograft dysfunction (an increase in serum creatinine). Cell-free DNA (cfDNA) is a DNA fragment released from cells with a fast turnover, making it a useful tool for real-time monitoring of allograft damage. In KT recipients, the total cf-DNA in blood can be derived from the cells of the host and donor (allograft), and the differentiation between the cf-DNA from the allograft (donor cells) or recipient cells (host cells) is essential for determining allograft dysfunction. Large quantities of donor cells are found in recipients with graft injury and/or rejection caused by cell death. Similar to the clearance of serum creatinine, the clearance of dd-cfDNA from an individual's body is comparable to that of cell-free DNA; however, additional study is required. In the circulation, cell-free DNA has a half-life of 16 minutes to 2.5 hours (29, 30). The DNase I enzyme present inside the liver and spleen can cause the entry of cell-free DNA and breakdown by the macrophages there (31). Cell-free DNA can also be excreted via the urine.

The blood level of dd-cfDNA is reported as the percentage of dd-cfDNA to the total cf-DNA, and its usefulness has been explored in several publications. In uncomplicated KT, high blood dd-cfDNA levels are encountered, with a median value of approximately 20% immediately (within hours) after renal engraftment and rapidly decreases on the first postoperative day to approximately 5% and then subsequently to below 1% (32). The level of dd-cfDNA depends on cell lysis (cell damage) (33) from any causes, including inflammation, infection, drug toxicity (calcineurin inhibitors), and disease recurrence. Due to its rapid change, dd-cfDNA can be used to obtain an immediate diagnosis of posttransplant rejection; however, the reported efficacy has varied among different studies (34–37). Sigdel et al. (35) demonstrate a new dd-cfDNA approach that employs a next generation sequencing (NGS) assay with single nucleotide polymorphisms (SNP)-based massively multiplex polymerase chain reaction (mmPCR) in a single-center retrospective analysis. The researchers examine 300 plasma samples acquired from 193 KT patients, including those with routine biopsies. The 217 biopsy-matched plasma samples from 193 KT patients, including 38 active rejection, 72 borderline TCMR rejection, 82 stable allografts, and 25 patients with other damages. Then, mmPCR is used to target 13,392 SNPs in dd-cfDNA. The test is able to distinguish acute allograft rejection (both AMR and TCMR) from non-rejection with an area under the curve (AUC) for the receiver-operator characteristic (ROC) curve (AUROC) curve of 0.87 with 88.7% sensitivity, 72.6% specificity, negative predictive value (NPV) 95.1%, and positive predictive value (PPV) of 51.9% and a stated cutoff of 1%. Unlike other dd-cfDNA technologies, the test is able to differentiate among TCMR, AMR and non-rejection causes (toxic damage or viral infection). Technical advancements enable a highly sophisticated mmPCR method allowing the use of over 13,000 SNP markers (35).

According to a meta-analysis, the sensitivity for AMR diagnosis is high at a fractional threshold of 1%, but less sensitive for TCMR, which generally needs a concentration higher than a 1% threshold, especially if the rejection is more severe than Banff 1B (38). With a cutoff of 0.69-1% for a positive test, most studies with commercially available dd-cfDNA assays demonstrate an AUC at 0.71-0.85, with a sensitivity and specificity of 45-89% and 69-85%, respectively, and a positive and negative predictive value of 52-77% and 66-95%, respectively, when compared with renal pathology, depending on the pretest probability of rejection (39).

Notably, most of the current studies on dd-cfDNA are *ad hoc* tests on patients who probably have a high pre-test risk of rejection. Categorization of blood dd-cfDNA into high (>1%) (35 cases), moderate (0.5-1%) (43 cases), and low (0.5%) (239 cases) among patients at 1-48 months post-transplantation revealed allograft rejection (biopsy within 2 months of dd-cfDNA measurement) in 24 of 62 cases (20%) among patients with moderate or high dd-cfDNA levels (40). The rejection was mostly demonstrated in patients with high (6 in 25 cases; 17%) and moderate dd-cfDNA (5 in 43 cases; 12%) when compared with the low level (13 in 239 cases; 5%) with no difference in the 1.6-year short-term graft outcomes using estimated glomerular filtration rate (eGFR) and *de novo* donor-specific antibodies (DSAs) (40). Most patients with high dd-cfDNA without allograft rejection remain stable without eGFR decline or graft loss (40). By contrast, a recent large multicenter study with approximately 1,100 kidney transplant patients indicated that patients with dd-cfDNA >0.5% had a greater risk of eGFR decline over 3 years and increased *de novo* DSA after follow-up (41).

A strong correlation is evident between high dd-cfDNA (>1%) and subclinical AMR using the Molecular Microscope Diagnostic System (MMDx; molecular tissue gene expression), but not by histopathology, among sensitized recipients (high risk of rejection), as indicated by DSAs, flow crossmatch at transplant, or documented non-adherence medication (42). These findings are also supported by the multicenter Trifecta trial (43). Likewise, Huang and colleagues (44) demonstrated that dd-cfDNA discriminated KT recipients with AMR (median 1.35%, interquartile range (IQR) 1.10% to 1.90%) from those without AMR (median 0.38%, IQR

0.26% to 1.10%), p <0.001. Interestingly, dd-cfDNA could not discriminate KT recipients with TCMR from those without rejection (44). A study by Whitlam et al. (45) provides further support, as 61 KT recipients with AMR showed receiver-operator characteristic AUC for graft-derived cfDNA concentration and graft fraction that were predictive of AMR (AUC = 0.91 (95% confidence interval (CI) 0.82 to 0.98) and 0.89 (95% CI 0.79 to 0.98). Again, both measures failed to diagnose borderline or type 1A TCMR (45).

High-normal dd-cfDNA (> 0.5%) can also identify individuals with borderline TCMR 1A histology who are likely to experience deteriorating kidney function (37). Indeed, the majority of patients with high dd-cfDNA and retained allograft function remained stable throughout the study without deterioration of function or graft loss (40). These publications support the preliminary use of dd-cfDNA as a screening test for renal biopsy and for categorizing rejection grading. Nevertheless, KT recipients with high DSA levels, BK poliomavirus (BKV) nephropathy, urinary traction infections, acute tubular necrosis, and post-renal allograft biopsy may also show increases in their dd-cfDNA levels (34, 46). Notably, absolute dd-cfDNA quantification in copies/mL might be more effective than the dd-cfDNA level as the percentage of total cf-DNA for discriminating allograft rejection (36). More studies would be interesting.

In summary, dd-cfDNA is a robust biomarker for the diagnosis of renal allograft rejection. Although dd-cfDNA alone cannot replace renal biopsy, it does provide a noninvasive way of identifying the potential causes of allograft failure in certain recipients, thereby enhancing the ability to predict long-term renal allograft outcomes. Increases in several regular biomarkers, including creatinine, proteinuria, and/or newly increased DSAs, are now indications for further dd-cfDNA tests (47). A routine cross-sectional dd-cfDNA testing of patients with a low pretest chance of rejection might be beneficial, and high dd-cfDNA levels are more common in DSA-positive recipients, highlighting the usefulness of dd-cfDNA in monitoring highly sensitized individuals (48). With the introduction of Allosure® and other comparable tests, dd-cfDNA is already being used as a supporting tool for diagnosis and therapy in clinical practice. The effects of repeated dd-cfDNA surveillance in kidney transplant recipients are currently being assessed in two prospective studies (The Ongoing Kidney Allograft Outcomes Registry (KOAR; NCT03984747), and The Prospera Kidney Transplant ACTIVE Rejection Assessment Registry (PROACTIVE; NCT03984747)

3.2 Transcriptomics

Several difficulties arise when attempting renal allograft rejection classification from kidney histology, including a lack of tissue, poor repeatability, and a dearth of well-trained pathologists. For this reason, transcriptome analysis has been the most highly feasible candidate technique for overcoming these limitations, as indicated by the use of C4d (49) and AMR-specific molecular panels (50, 51) for AMR diagnosis. Currently, the Molecular Microscope Diagnostic System (MMDx) is the gold standard for transcriptome analysis of kidney transplantation for AMR and TCMR (52, 53) with the identified key cellular pathways that contribute to rejection. However, many challenges remain in translating molecular diagnostics into clinical practice, including a large number of redundant gene sets that raise a need for standardization of various molecular diagnostic panels on gene analysis (e.g., microarrays and quantitative real-time polymerase chain reaction [qRT-PCR]), as well as an ongoing debate on rejection gene sets between AMR and TCMR (13).

Unlike the microarray gene-based MMDx platform, the NanoString nCounter platform needs only 100 ng of mRNA from formalin-fixed paraffin-embedded (FFPE) biopsies, without a requirement for a biopsy core, to detect mRNA target molecules within two days, allowing large-scale transcriptomic results from biopsy samples (54). The Banff Molecular Diagnostics Working Group developed molecular consensus gene sets for TCMR and AMR in 2015 (55) and proposed several molecular panels in 2017 (13). It subsequently launched the commercially available Banff-Human Organ Transplant (B-HOT) panel for transplantation in several organs (kidney, lung, heart, and liver) in 2019 without centralized molecular profiling (56). The incorporation of molecular pathology into clinical practice may use NanoString technology with the B-HOT panel for better diagnosis, categorization, and normalization, as demonstrated by the different gene expressions observed between no rejection versus AMR and TCMR (57).

Using the most predictive genes from the B-HOT and Element analysis, regression models based on the two least absolute shrinkage and selection operators are being developed to classify biopsies as AMR versus no AMR (57). These classifications include borderline rejection, TCMR, or no rejection, with a receiver-operating characteristic area under the curves (AUC) of 0.994 and 0.894, sensitivity of 0.821 and 0.480, and specificity of 1.00 and 0.979 during cross-validation compared with the gold standard renal biopsy (57). In addition, principal component analysis (PCA) of the microarray gene sets can identify the main categories of renal diagnosis and a comparable relationship between pathological diagnosis and molecular sets (58). As a result, non-chronic antibody-mediated rejection with high expression of endothelial genes can be detected by PC clustering with cell type analysis that is also able to reveal differences in genes from B-cells and plasma cells (58).

In addition, there are several tests that measure immunological activity by looking at the gene expression of circulating immune cells. A widely integrated gene expression profile (GEP) assay is AlloMap, which has been made available as a monitoring tool for heart transplant recipients since 2005 (59) with a high negative predictive value (NPV). However, immune system gene expression profiling in KT has been difficult to use as a consistently accurate and repeatable indicator of renal allograft rejection because the data remains controversial (9, 60–62). A most recent study from Akalin et al. (63) demonstrates the validation of a blood GEP developed to differentiate immune quiescence from both TCMR and AMR. On the basis of 56 peripheral blood samples, a five-gene classifier (DCAF12, MARCH8, FLT3, IL1R2, and PDCD1) is created and validated on two separate sample sets outside of the training cohort.

The main validation set includes 18 rejection examples—7 TCMR, 10 AMR, and one mixed rejection—and 98 quiescence samples. The second validation set has 11 rejection samples—7 TCMR, 2 AMR, and 2 mixed rejection—and eight quiescence samples. Interestingly, quiescence and rejection are distinguished significantly by AlloMap Kidney classifier scores in the primary validation set (median, 9.49; IQR, 7.68-11.53 and 11.25-15.28, respectively). The medians in the second validation set are similar to those in the first validation set, although the cohorts are significantly different (p =0.03). The primary validation's AUC for separating rejection from quiescence is 0.786, and the secondary validation's AUC is 0.800 (63). Thus, blood GEP and dd-cfDNA contribute independent signals and inform on different aspects of allograft rejection.

On the other hand, the Kidney Solid Organ Response Test (kSORT) is a microarray-based assay designed to identify recipients at high risk for acute rejection (64) using quantitative polymerase chain reaction (PCR) to measure the relative mRNA expression levels of 17 genes that are associated with acute renal allograft rejection or leukocyte trafficking in peripheral blood. An algorithm based on correlation is then used to generate risk scores and classify patients as having a high, medium, or uncertain risk of acute rejection. The kSORT assay is initially evaluated in a large multicenter study of 436 adult and pediatric kidney transplant recipients (Assessment of Acute Rejection in Renal Transplantation [AART]) with paired peripheral blood samples and kidney allograft biopsies (performed for allograft dysfunction or as part of a clinical protocol) using a case-control study design of selected recipients (64). With a sensitivity and specificity of 92% and 93%, respectively, the kSORT assay is able to identify patients at high risk of either TCMR or AMR. In addition, kSORT is able to identify subclinical rejection in 75% of biopsies and clinical rejection in over 60% of samples collected within three months prior to the diagnosis of biopsy-confirmed acute renal allograft rejection. Nonetheless, the test fails to differentiate between acute TCMR and AMR.

Moreover, the TruGraf® v1 assay is a DNA microarray-based gene expression blood test that is developed as an alternative to surveillance biopsies to rule out subclinical rejection in recipients with sustained graft function (65). Blood samples coupled with protocol biopsies from prevalent cohorts are utilized for the entirety of the discovery and external validation of the TruGraf® test. However, the performance of the test in recipients with renal allograft dysfunction has not been evaluated and must be studied further. Interestingly, combining the TruGraf® assay with dd-cfDNA enhances the detection of subclinical renal allograft rejection (66). Of note, by using multivariable logistic regression, the AUC is 0.81, which is substantially greater than the gene expression profile (p <0.001) or dd-cfDNA alone (p =0.006). Notably, when cases are divided according to rejection type, the gene expression profile is significantly better at detecting TCMR (AUC 0.80 versus 0.62; p =0.001), whereas the dd-cfDNA is significantly better at detecting AMR (AUC 0.84 versus 0.71; p =0.003) (66).

To sum up, at present, transcriptomic analysis is revealing the possible molecular mechanisms that might improve outcomes and be useful as precision diagnostic indicators in renal transplantation.

3.3 MicroRNAs

MicroRNAs (miRs) are a class of short, noncoding RNAs that can regulate gene expression (57). They can be detected by several different methods, including qRT-PCR, microarray, and next-generation sequencing analysis (global miR profiling) (67) in the blood (cells), serum/plasma, and urine (68, 69). Ischemic reperfusion injury during KT increases urine miR-146a content to higher levels in renal transplant recipients implanted from deceased donors than from living donors (70). Acute TCMR increases miR-223 and miR-142–3p in allografts and in peripheral blood mononuclear cells (PBMCs) of recipients (71). Patients with TCMR demonstrate higher miR-223, miR-10a (72), miR-99a, and miR-100 levels in blood samples (73), but lower levels of miR-99a expression in kidney allografts (74, 75), implying a possible difference in miR levels between renal tissue and blood samples. Interestingly, multivariable logistic regression analysis of a panel of blood miRs (miR-15b, miR-16, miR103a, miR106a, and miR-107) was able to differentiate acute vascular rejection (Banff II–III) from stable graft function (76). In acute TCMR, urinary miR-10a is upregulated, while miR-10b and miR-210 are downregulated. The urinary level of miR-210 (a cellular aging biomarker) is correlated with the severity of biopsy-proven rejection, but with low specificity and sensitivity, unfortunately (69). Increased levels of miR-142–5p are reported in the PBMCs of recipients with chronic, but not acute, AMR (77) and with acute TCMR (71, 74). Interestingly, alteration of miR levels between pre- and post-renal allograft rejection has been reported by Millán and colleague study group (78). As such, urinary levels of miR-142-3p and miR-155-5p significantly increase, while miR-210-3p decrease in allograft rejection. The miR-155-5p at the threshold values of 0.51 demonstrates sensitivity and specificity at 85% and 86%, respectively, and the analyses of receiver operating characteristic (AUC) effectively differentiate the recipients with versus without allograft rejection (AUC = 0.875; p =0.046) (78). Also, there is a good correlation between miR-155-5p and glomerular filtration rate or renal allograft restoration (78).

Additionally, the content of miR-211, miR-204, and miR-142–3p in the urine exosomes of patients with biopsy-proven IF/TA show a correlation between miRs in urine and renal tissue (79). Downregulation of miR-200b, miR-375, and miR-193b and upregulation of miR-423–5p and miR-345 are also detected in the urine of patients with IF/TA (one-year follow-up) without the association between miR-200b expression and proteinuria (68). Downregulation of miR-200b (80) and downregulation of miR-21 are observed in plasma from patients with IF/TA (81).

In summary, many miRs have been proposed as biomarkers for renal allograft dysfunction due to miR stability; however, assessment using receiver-operator characteristic areas under the curves (sensitivity and specificity) is limited. Nevertheless, a five-miR panel is able to distinguish T cell–mediated vascular rejection from stable graft function following kidney transplantation (76), implying possible benefits of combined miR (panels). MiRs from allograft biopsy tissue provide greater accuracy for rejection diagnosis, suggesting that tissue-derived miRs may have the potential to substitute for histology. More studies are warranted.

3.4 Extracellular vesicles (EVs) and exosomes

Extracellular vesicles (EVs) are bilayer lipid membranes released by all cells in the body and can include exosomes, microvesicles (MVs), ectosomes, oncosomes, and apoptotic bodies. In general, the term "EV" seems to be a generic label for a "secreted vesicle" (82). The EVs in body fluids operate as carriers in signal transmission between cells for the regulation of immunological responses, inflammation, and other cell activities (83, 84). Because all cells can generate EVs, the EVs in urine should be correlated with the cells with direct urine contact (e.g., the urinary epithelium, endothelium, and immune cells). By contrast, the source of cells that produce EVs in blood could be more difficult to determine. The determination of EVs from urine requires strict normalization, and normalization by the duration of urine collection (time normalization), especially 24-hour urine, seems to be mostly appropriate; however, unfortunately, the correlation observed between EVs in urine and other normalization biomarkers (creatinine, total proteins, number of EVs) remains inconclusive (85). The duration of urine in the bladder before urine collection might also alter the EVs in the urine sample, because bladder cells can also produce EVs, and those EVs could be altered by urine characteristics (pH, concentration, and excreted substances) (85). Nevertheless, EVs from both blood and urine are being extensively studied for biomarkers.

Among all the EV types, exosomes were observed for the first time in a multivesicular endocytic compartment in 1983 by Harding et al. (86). Since then, these EVs have undergone the most extensive exploration. Exosomes are 40-100 nm in diameter (82) and are formed as lipid bilayers that can protect several molecules inside. For example, several RNA types, including miRs, long noncoding RNAs (lncRNAs), small nuclear RNAs (snRNAs), and circular RNAs (circRNAs), are found in EVs and can be used as biomarkers (87). Current omics technology, including transcriptomics, proteomics, and metabolomics, is now used for the genetic association analysis of expression quantitative trait loci (eQTL), protein quantitative trait loci (pQTL), and methylation quantitative trait loci (mQTL) (88). This has made possible the expanded use of exosomes and EVs for locating potential sites in allografts that produce EVs (89). Despite the large number of EVs in the plasma (roughly 10^2–1.0^{13} vesicles per mL) (90), the tiny size, limited contents, and possible difference in contents inside each particle (referred to as "liquid biopsy") are limitations for the use of EVs as biomarkers. However, next-generation sequencing (NGS) and mass spectrometry can now amplify and detect the molecules within the vesicles or the intra-vesicular contents of EVs and have revealed several interesting aspects of EVs.

One example is the profile of urinary EVs from living-donor renal transplantation, which demonstrates that the EVs are derived from the nephron (glomeruli and other parts; descending limb of Henle's loop, the collecting tubules, etc.), epithelium, and endothelium (91). This categorization is established by the detection of several molecules, such as megalin, aquaporin (AQP), podocalyxin (PODXL), ion cotransporters, synaptotagmin 17 (SYT17), CD3, and CD133, which are expressed only at specific sites and might therefore be useful as biomarkers (92–94). Increases in these molecules in EVs from urine or blood mostly indicate that some damage has occurred to renal allografts.

Interestingly, the EV molecules related to epithelial cell differentiation seem to be upregulated in TCMR, while proteins of acute inflammation or antigen presentation are more related to AMR (95). Likewise, the levels of the sodium-chloride cotransporter (NCC) and Na-K-Cl cotransporter (NKCC2), the transporters commonly found in renal tubular cells, are higher in the EVs (exosomes) from patients treated with calcineurin inhibitors (CNIs; drugs with tubular toxicity) than with non-CNI regimens (96, 97). Similarly, miRNA-enriched EVs are reported in patients who experience long ischemic times during transplantation (98), implying that EVs might be directly related to ischemic mechanisms through the delivery of miRs and other molecules from one cell to others (99, 100).

In 2017, a landmark study by Park and colleagues reports the use of EVs in renal allograft rejection as T cell-derived EVs in urine might indicate renal tubular T cells infiltration during TCMR (101). Thus, an EVs-based diagnostic platform recognizing T cell-derived urinary EVs (uEVs), refer to as iKEA (integrated kidney exosome assay), is mentioned as TCMR biomarker. As such, CD3 is used to identify T cell-derived uEVs and the CD3-based iKEA demonstrates diagnostic accuracy of 91.1% in a discovery group of 30 recipients and 83.7% in a validation cohort of 14 recipients in subsequent clinical trials (101). Accordingly, iKEA might be a powerful noninvasive serial monitoring in kidney transplant recipients for better long-term renal allograft function. A subsequent well-design, large cohort study from El Fekih et al. established the rejection signatures using approximately 200 samples of the matched urinary exosomal mRNAs with the tissue of renal allograft biopsy for a powerful noninvasive liquid biopsy to identify renal allograft rejection (102). For the diagnosis of all-cause renal allograft rejection, the AUC of renal biopsy is 0.93 (95% CI, 0.87 to 0.98), while the AUCof eGFR is 0.57 (95% CI, 0.49 to 0.65). In parallel, the AUC of urinary exosome-based signature is 0.87 (95% CI 0.76 to 0.97) with positive and negative predictive values at 86.2% and 93.3%, respectively. Additionally, the exosome-based signature distinguishes recipients with TCMR from those with AMR with positive and negative predictive values at 77.8% and 90.6%, respectively (102). Despite a lower AUC than the gold standard renal allograft biopsy, the urine-based exosome measurement is noninvasive and can be frequently measured.

On the other hand, an elevation of EV numbers containing CD31 (glycosylated immunoglobulin-like membrane receptor of leucocytes, platelets, and endothelial cells) or CD81 (Tetraspanin; expressed in several cells except for erythrocytes, platelets, and neutrophils) is correlated with the length of cold ischemia, increased donor age, and reduced renal allograft blood flow (103). This suggests that the removal of EVs in KT recipients who experience long cold ischemic times before renal engraftment might be beneficial (104). The EVs may also transmit viruses through *en bloc* transmission of several viral genomes, which could modulate viral fitness and protect viruses within the lipid membrane (105). Viral particles in EVs might also dilute the physiologic contents and interfere with normal cell–cell communication (106). One virus, the BK polyomavirus (BKV), is

an important cause of renal allograft failure (107). Its presence in exosomes could encode the host's miRs and downregulate some host genes required for viral evasion processes (108), as elevated levels of miR-B1-5p and miR-B1-3p in urinary exosomes indicate possible BKV infection (109, 110).

Several challenges remain for the use of exosomes or EVs as biomarkers. These include methods for the purification and isolation of EVs (or exosomes) that preserve their integrity (111), the normalization, and the time-consuming procedure for 24-hour urine collection. Regarding the therapeutic aspects, EVs also represent possible vehicles for delivering therapeutic molecules to specific target cells (112), while the removal of EV-mediated ischemic responses might improve the long-term outcomes of KT (104). More clinical trials involving several candidates undergoing pre-clinical studies will be very interesting.

3.5 Urine and circulating chemokines

Inflammation is a response to cell damage, and detection of inflammation in renal allografts, especially with other biomarkers or clinical characteristics, possibly indicates allograft rejection. For example, urinary CXCL9 and CXCL10 are both increased in AMR and TCMR compared with patients with no rejection (113–115), elevated urinary CXCL10 predicts rejection (78), and treatment of allograft rejection reduces CXCL10 (78, 113, 116). However, combining CXCL9 with CXCL10 does not enhance the prediction ability compared with each molecule alone (114, 117). As an indicator of allograft rejection, urinary CXCL9 demonstrates sensitivity and specificity of 58-86% and 64-80%, respectively, while the values for CXCL10 are 59-84% and 76-90%, respectively (78, 113–115, 117). However, urinary CXCL10 seems to be associated with tubulointerstitial inflammation and peritubular capillaritis, rather than glomerulitis or isolated vascular inflammation (118) and urinary CXCL10, but not CXCL9, correlates with subclinical rejection (AUC 0.64; 95% CI, 0.55-0.73) (116). Both urinary CXCL9 and CXCL10 distinguish rejection from other non-rejection causes of graft dysfunction, with AUCs of 0.72 and 0.74, respectively (116). The urine CXCL10/creatinine ratio, together with the mean fluorescence intensity (MFI) of DSAs, predicts AMR and graft loss better than the DSA MFI alone, with a net reclassification increase of 73% (119). Nevertheless, urinary CXCL10 is not specific for rejection, although it is a good indicator of renal inflammation, as urinary CXCL10 is also elevated to similar levels in patients with BK viremia and in patients with tubulitis from rejection (113, 114). Interestingly, urinary CXCL10 is not increased in cytomegalovirus (CMV)-infected subjects (118), perhaps because of the greater genitourinary specificity of the BK virus compared with CMV. Urine CXCL9 and CXCL10 are also increased in patients with isolated leukocyturia and urinary tract infections (120) and leukocyturia with increased CXCL10 demonstrates more severe inflammation than leukocyturia alone (113). Notably, the levels of urinary CXCL9 and CXCL10 in both absolute terms and after adjustment to urine creatinine (urine creatinine normalization) are useful.

Urinary chemokines are enhanced before rejection becomes clinically apparent, implying that they are good candidates for screening tests (116, 121). Recipients with high urine CXCL10 levels have been divided into renal biopsy or regular surveillance in an ongoing multicenter trial (NCT 03206801). This trial could provide an opportunity to determine whether urinary chemokine levels, when considered alongside histologic variables, can improve the prediction of renal allograft outcomes. A test using urinary chemokines as KT biomarkers will be interesting. Recently, the Barcelona Consensus on Biomarker-Based Immunosuppressive Drugs Management in Solid Organ Transplantation has a preliminary proposal for using urinary chemokine CXCL9 and CXCL10 to guide and individualize immunosuppressive regimens, predict acute and chronic TCMR and AMR, and may be a useful tool for risk stratifying recipients. However, the standard immunoassay platforms are needed (122).

Circulating or plasmatic chemokines, CXCL10 is also a promising biomarker for renal allograft rejection determination. Due to the prevalence of clinical confounding factors, the utility of serum CXCL10 as a potential biomarker for assessing the risk of rejection remains controversial (123, 124). High serum CXCL10 during the pre-transplantation period is associated with long-term graft loss after kidney transplantation (123). As such, Xu et al. (125) demonstrate that serum CXCL10 measured on the fourth and seventh days after kidney transplantation are substantially higher in recipients with acute renal allograft rejection than those without rejection. The most recent study conducted in 28 recipients experienced rejection (14 TCMR cases and 14 recipients with AMR), 8 cases of subclinical rejection, 13 BKV infection, and 16 cases of CMV. Accordingly, in comparison with non-rejection, pre-transplantation circulating CXCL10 is significantly higher in TCMR and AMR. In post-transplantation, increased circulating CXCL10 is demonstrated in TCMR, AMR, and subclinical rejection. All CMV infected recipients show elevated circulating CXCL10 above the rejection threshold, whereas 80% of BKV infected recipients have CXCL10 concentration approximately at 100 pg/mL (126). Indeed, circulating CXCL10 can be used for pre-transplanted stratification and the selection of immunosuppressive regimens following the risk of rejection according to CXCL10 levels. However, BKV and CMV infection must be firstly excluded when using CXCL10 as a rejection biomarker (126).

On the other hand, urinary concentrations of neutrophil gelatinase-associated lipocalin (NGAL), during the early post-transplantation period, have been extensively examined as a predictor of delayed graft function in kidney transplantation (127, 128). Likewise, urine NGAL is demonstrated as a predictor of acute kidney injury in the later period after transplantation (129, 130) and an indicator of allograft loss after acute kidney injury (131). However, the diagnostic utility of NGAL in kidney transplant patients after the first year of transplantation with chronic processes of injury (a steadily deteriorated renal function) is demonstrated by only a few studies (132, 133). Additionally, the difference in urine NGAL assays in various studies makes it difficult for comparison and to propose the cut-off values using data from different studies. A recent study by Kielar et al. (134) demonstrates 2 folds higher urinary NGAL after 1-year post-transplantation in

recipients with at least a 10% reduction in eGFR compared to those with stable or improved function of the transplanted kidney. Independent of baseline eGFR and albuminuria, baseline NGAL strongly predicts the relative and absolute changes in eGFR as well as the mean eGFR during the follow-up. Furthermore, high urine NGAL levels in clinically stable kidney transplant recipients after the first year may be interpreted as a warning sign, prompting a search for transitory or chronic causes of graft failure or urinary tract infection (134).

While urinary NGAL might be associated with delayed graft function (127), the relationship between urinary kidney injury molecular-1 (uKIM-1) and renal allograft is not clear (135). As such, recipients with lower KIM-1 in the first week post-transplantation take a longer time to stabilize their renal function compared to the cases with normal uKIM-1. In addition, a prospective cohort study by Zhu et al. (136), in 160 recipients scheduled for kidney transplantation, is conducted to evaluate the predictive power of uKIM-1 for renal allograft prognosis. They discover that recipients with higher uKIM-1 levels on the first day after transplantation had a 23.5% higher risk of developing functioning delayed graft function and a 27.3% higher chance of having a longer renal allograft survival. Hence, it is possible that KIM-1 has a potential role in post-transplant renoprotection (137, 138).

3.6 Nucleosomes

The smallest structural component of chromatin is called a nucleosome and usually consists of 8 histone proteins and 146 DNA base pairs (139). The histone-encased DNA plays a crucial role in the epigenetic control of gene expression by modifying the "tail" regions of histones by methylation, acetylation, ubiquitination, and phosphorylation (140). After cell death, nucleosomes are released into the blood, modified by some enzymes, and are then referred to as "circulating cell-free nucleosomes" (CCFN) (141). The epigenetic signature of histones (histone alterations) in CCFNs might be able to differentiate between regular versus pathological cell deaths, as mentioned in cancer studies (142). For example, the addition of DNA modification (5-methylcytosine) and histone modifications (H2AZ, H2A1.1, and H3K4Me2) increased the diagnostic values of carbohydrate antigen (CA) 19-9, a conventional cancer biomarker, in pancreatic malignancy (143). Likewise, increases in nucleosomes with histone alterations are observed in acute renal allograft rejection (144). Indeed, the levels of CCFNs containing citrullinated histone H3 (Cit-H3), a biomarker of neutrophil extracellular traps (NETs) (145–147) important in AMR (118), are increased within several hours after AMR and can be detected using a modest quantity of sample (10 µL) (143). However, serial readings of histone-modified CCFN might be necessary, as the levels may fluctuate in the setting of acute renal allograft rejection. Notably, total nucleosome concentrations (absolute total CCFNs, regardless of histone modification) are only an indicator of cell damage, while CCFNs with specific nucleosome modifications can determine the cause of cell damage and possibly serve as useful markers for renal allograft rejection. More studies on this topic will be interesting.

4 The utility of molecular immune monitoring for renal allograft rejection in clinical practice

4.1 PROS and CONS

The most advantage of molecular immune monitoring for renal allograft rejection is the superior sensitivity and specificity to the conventional markers (serum creatinine, eGFR, proteinuria, and DSAs) which can reduce unnecessary invasive renal allograft biopsy (148). With conventional markers, detection of subclinical changes is difficult due to the lower sensitivity. Although serum creatinine at one-year post-transplantation reflects long-term renal allograft outcome (149), an individual serum creatinine level is neither sensitive nor specific for early renal allograft injury, particularly compared to urine chemokines (114). Likewise, both albuminuria and proteinuria are nonspecific markers of renal allograft injury without a demonstrable association with renal allograft pathology (150, 151). Although current data support the use of *de novo* DSAs post-transplantation which is associated with decreased renal allograft survival (23, 152), the utilization of DSAs as a noninvasive diagnosis of AMR or a predictor for the long-term renal allograft outcomes has not been clearly elucidated (23). As such, innovative strategies (molecular immune monitoring methods) have been developed to overcome these limitations of the existing biomarkers. Most noninvasive molecular immune monitoring tools, including miR, gene expression, or protein level detection of molecular markers, have been proposed using the easily accessible biologic fluids (blood, serum, plasma, or urine) through a wide spectrum of platforms, mostly for frequent assessment of recipient's immune status. However, the translation and validation of these discoveries and their implementation into standard transplantation clinical practice remain challenging. More large, prospective, interventional clinical trials are robustly needed to demonstrate the use of these molecular immune monitoring biomarkers for the improvement of renal allograft outcomes. In general, significant limitations of using these novel noninvasive molecular markers in clinical practice are regulatory issues, reimbursement from the Centers for Medicare and Medicaid Service, generalizability, cost, interpretation of the test, and, most importantly, the identification of beneficial populations compared with the conventional standard-of-care surveillance (153).

4.2 Combined molecular immune monitoring and the clinical parameters as a predictive score for renal allograft rejection

Due to the complexity and variability of immune responses, a panel of biomarkers (such as chemokines, DSAs, dd-cfDNA, and several miRs) might be more powerful than a single indicator for the

prediction and diagnosis of renal allograft rejection and the differentiation between TCMR and AMR. For example, the Common Rejection Module that consists of 11 genes might be overexpressed in the biopsy samples from various solid organ transplants, including renal allograft rejection (154). Additionally, the urinary gene expression-based score (mRNA of these 11 genes) using urine from 150 renal transplant recipients with concurrent renal biopsies, including 43 stable biopsies, 45 acute rejections (TCMR or AMR or mixed), 19 ambiguous rejections, and 43 BKV, demonstrates 95% and 98% sensitivity and specificity, respectively, for the diagnosis of acute rejection (155). The sensitivity of the urinary gene expression-based score for diagnosis of acute renal rejection is reduced to 87.1% with an addition of the cases with ambiguous renal rejection into the stable biopsy and is decreased to 77% sensitivity with an addition of BKV nephropathy cases, with an unchanged specificity (155). Then, the urinary gene expression-based score may be useful for the non-invasive monitoring of acute renal allograft rejection.

Indeed, the addition of potential confounding cases (such as urinary tract infection and BK virus reactivation) in the stable biopsy as "a diagnostic multi-parametric model" improves the performance of the biomarkers (120). As such, a model with the combination of eight parameters (recipient age, gender, eGFR, DSA, signs of urinary tract infection, blood BKV viral load, urine CXCL9, and CXCL10) is able to diagnose acute renal allograft rejection with high accuracy (AUC: 0.85, 0.80–0.89). These results are paving the way for future studies using the combining urinary biomarkers with clinical characteristics to achieve the highest clinical relevance and provide targeted therapy for KT recipients (120). Recently, a research group from the University of California San Francisco demonstrates another comprehensive noninvasive tool for diagnosing and predicting renal allograft rejection (156). They explore the performance of target markers in a Kidney Injury Test assay for chronic kidney disease (CKD) staging in the native and non-transplanted kidney (157) and develop a Q-Score from these data for the detection of acute renal allograft rejection. Based on measurements of six urinary DNA, protein, and metabolic biomarkers, a noninvasive, spot urine-based diagnostic assay is proposed. On a cohort of 601 distinct urine samples with kidney injury (both native kidneys and renal allografts), the urinary composite score enables the diagnosis of acute renal allograft rejection, with an AUC of 0.99 for the receiver-operator characteristic (ROC) curve. Interestingly, the clinical utility of the assay can predict acute renal allograft rejection better than an increased serum creatinine resulting in an earlier rejection diagnosis than the current standard-of-care tests (156).

In summary, the use of a combination of multiple variables with mathematical approaches to calculating rejection probability, but not using only biomarkers of "graft functional impairment" alone might be very useful for an early diagnosis of rejection and might also be helpful for the selection of immunosuppressive protocols. Additionally, the rapid and routine monitoring of renal allografts is possibly enabled by the noninvasive assays, especially with sensitive and quantitative methods.

5 Future directions

While the establishment of a worldwide consensus framework (i.e., the Banff criteria) is still ongoing, a great deal of progress has been made in the field of the diagnostic evaluations of allograft pathology. In the foreseeable future, a molecular diagnostic model for renal allograft pathology should show significant steps toward the final development of a decentralized multi-platform compatible system. This could significantly impact clinical practice and outcomes by placing particular emphasis on the complex normalization pipelines required to compare gene expression data generated by different technologies. The creation of this system must integrate the efforts of the whole transplantation community for its validation to ensure that these molecular technologies provide optimal performance. In addition, the continuous updating of diagnostic criteria for renal allograft rejection and related lesions has improved diagnostic accuracy and clinicopathologic correlations, while also helping to clarify the

TABLE 1 Summary of the novel biomarker studies of immunologic monitoring in kidney transplant rejection.

Biomarkers (Commercial Assay)	Sample	N	Primary outcome(s)	Sensitivity (%)	Specificity (%)	PPV (%)	NPV (%)	Study outcomes	Author, Year [References]
Donor-derived cell-free deoxyribonucleic acid (GRADE certainty rating [a]: MODERATE)									
dd-cfDNA (Allosure)	Plasma	102	Rejection	59	85	61	84	➢ Differentiation between rejection (TCMR and AMR) versus non-rejection and between AMR versus non-AMR recipients (AUC = 0.74)	Bloom et al, 2017 (34)
dd-cfDNA (Allosure)	Plasma	63	AMR	68	72	74	65	➢ dd-cfDNA discriminates AMR, but not TCMR, from non-rejection (AUC = 0.71)	Huang et al, 2019 (44)

(Continued)

TABLE 1 Continued

Biomarkers (Commercial Assay)	Sample	N	Primary outcome(s)	Sensitivity (%)	Specificity (%)	PPV (%)	NPV (%)	Study outcomes	Author, Year [References]
dd-cfDNA (Prospera)	Plasma	217	AMR	88.7	72.6	52	95	➢ dd-cfDNA discriminates AMR, and TCMR from non-rejection (AUC = 0.87)	Sigdel et al, 2018 (35)
dd-cfDNA (noncommercial)	Plasma	61	Acute AMR, chronic AMR	AMR: 0.90	AMR: 0.88	60	98	➢ dd-cfDNA and fraction are predictive of acute AMR (AUC = 0.92, 0.85) and composite diagnosis of AMR (AUC = 0.91, 0.89)	Whitlam et al, 2019 (45)
dd-cfDNA (noncommercial)	Plasma	189	Rejection	73	73			➢ Recipients with biopsy-proven rejection demonstrate 3.3-folds higher dd-cf-DNA (copies/mL) and 2.0-folds higher dd-cf-DNA (%) than those without rejection. ➢ dd-cfDNA absolute number is higher than dd-cfDNA in % (AUC = 0.73), OR = 7.31 for dd-cfDNA (copies/mL)	Oellerich et al, 2019 (36)
dd-cfDNA	Plasma	19	Rejection, BK polyoma virus nephropathy (BKPyVAN)					➢ BKPyVAN is associated with a slight increase in dd-cfDNA (median; IQR: 0.38% [0.27%-1.2%] vs. 0.21% [0.12%-0.34%] in non-rejection control recipients. ➢ dd-cfDNA levels are far lower than AMR (1.2% [0.82%-2.5%], but not different from TCMR.	Mayer et al, 2019 (158)
dd-cfDNA	Plasma	79	eGFR, rejection prediction, *de novo* DSA					➢ Increased dd-cfDNA predicts adverse outcomes as following: a) Recipients with increased dd-cfDNA have decreased eGFR by 8.5% compared with 0% in those with decreased dd-cfDNA b) *de novo* DSA is demonstrated in 40% vs 2.7% of recipients with increased or decreased dd-cfDNA, respectively c) Persistent rejection is developed in 21.4% of cases	Stites et al, 2020 (37)

(Continued)

TABLE 1 Continued

Biomarkers (Commercial Assay)	Sample	N	Primary outcome(s)	Sensitivity (%)	Specificity (%)	PPV (%)	NPV (%)	Study outcomes	Author, Year [References]
dd-cfDNA (noncommercial)	Plasma	29	Acute rejection	88	81	64	94	➢ dd-cfDNA levels discriminate between recipients with biopsy-proven acute rejection (median 5.24%; range 1.00–9.03), recipients without acute rejection (1.50%; 0.41–6.50), and recipients with borderline acute rejection (1.91%; 0.58–5.38). ➢ dd-cfDNA is significantly differences between recipients with versus without acute rejection (AUC = 0.84)	Dauber et al, 2020 (159)
Transcriptome (GRADE certainty rating [a]: MODERATE)									
Gene expression profile	Plasma	308	Subclinical acute rejection	64	87	61	88	➢ Gene expression profile of acute rejection predicts subclinical rejection	Friedewald et al, 2019 (160)
Targeted expression assay (TREx)	Plasma	113	Acute rejection at 3 months, renal allograft failure			79%	98%	➢ TREx predicts subclinical rejection at 3 months in 113 recipients (AUC = 0.830)	Zhang et al, 2019 (61)
Kidney Solid Organ Response Test (kSORT™) and enzyme-linked immune absorbent spot (ELISpot)	Plasma	75	Surveillance of recipients with stable renal allograft function					➢ kSORT™ and ELISpot predict subclinical TCMR and subclinical AMR (AUC > 0.85)	Crespo et al, 2017 (161)
TruGraf® gene expression profile	Plasma	Retrospective 192 recipients in 7 transplant centers with a prospective observational study in 45 recipients at 5 transplant centers.	Acute rejection					➢ TruGraf® affects to physician's clinical decision in 87.5% of cases ➢ 45 recipients' TruGraf® supported 87% of clinical decisions with 93% of investigators stating that they will use TruGraf® for their clinical practice	First et al, 2019 (162)
11 Common rejection genes	Urine	150 (43 stable renal allograft, 45 acute rejection, 19 borderline pathology, and 42 BK virus nephropathy)	Acute rejection	93.6	97.6			➢ 10 from 11 genes are elevated in acute rejection compared with stable renal allograft function. Of note, Psmb9 and CXCL10 could classify acute rejection from stable renal allograft function as accurately as the 11-gene model ➢ Urinary	Sigdel et al, 2019 (155)

(Continued)

TABLE 1 Continued

Biomarkers (Commercial Assay)	Sample	N	Primary outcome(s)	Sensitivity (%)	Specificity (%)	PPV (%)	NPV (%)	Study outcomes	Author, Year [References]
								common rejection model (uCRM) score differentiates AMR from stable renal allograft function (AUC = 0.9886)	
MicroRNAs (GRADE certainty rating [a]: LOW)									
miR-15B, miR-103A, miR-106A	Plasma	160	TCMR					➢ miR-15B, miR-103A, and miR-106A discriminate recipients with stable renal allograft function from the recipients with TCMR and urinary tract infection.	Matz et al, 2016 (163)
miR-223-3p, miR-424-3p, miR-145-5p	Plasma	111	TCMR, AMR					➢ miR-145-5p, miR-223-3p, and miR-424-3p discriminate recipients with stable renal allograft function from TCMR and AMR.	Matz et al, 2018 (164)
miR-142-3p, miR-155-5p, miR-210-3p, CXCL10	Urine	80	Acute rejection	85% 84%	86% 80%			➢ Increased miR-142-3p, miR-155-5p, CXCL10 and decreased miR-210-3p discriminate recipients with rejection and nonrejection	Millán et al, 2017 (78)
Molecular Microscpoic® Diagnostic System (MMDx™)/ microRNA	Renal allograft tissue	519	TCMR, AMR					➢ The agreement rates between MMDx™ and renal allograft tissue pathology are 76%-77% for TCMR, AMR, and non-rejection ➢ The MMDx™ is correlated with clinical judgment (87%) more than histology (80%).	Halloran et al, 2017 (53)
microRNA	Renal allograft tissue	11 studies	TCMR, AMR, and chronic AMR					➢ Increased miR-142, miR-155, miR-223 and decreased miR-30, miR-125, miR-204 predict the primary outcomes	Ledeganck et al, 2019 (165)
Extracellular vesicles and exosomes (GRADE certainty rating [a]: MODERATE)									
Exosomes	Serum	213 kidney transplant alone recipients, and 14 kidney-pancreas transplant recipients	Acute rejection is identified as $CD31^+$/ $CD42b^-$ microparticles and quantified by fluorescence-activated cell scanning					➢ Increased circulating exosomes levels is associated with acute rejection. ➢ Circulating exosomes are rapidly decreased after treatment for rejection in recipients with	Qamri et al, 2014 (166)

(Continued)

TABLE 1 Continued

Biomarkers (Commercial Assay)	Sample	N	Primary outcome(s)	Sensitivity (%)	Specificity (%)	PPV (%)	NPV (%)	Study outcomes	Author, Year [References]
								negative peritubular capillaritis C4d, but the decrease is slower in those with positive peritubular capillaritis C4d.	
	Urine (using LC-MS/MS method)	30	Acute rejection					➢ Eleven urine exosomal proteins are more abundant in urine samples from recipients with acute rejection. ➢ 3 out 11 of urine exosomal proteins are exclusive for the exosomal fraction. ➢ Exosomal acute rejection-specific biomarkers are also detected in unfractionated whole urine.	Sigdel et al, 2015 (167)
	Urine	Discovery phase (n = 30): 15 non-rejection recipients, 15 acute rejection, 3 chronic AMR, and 3 BK polyoma virus nephropathy. Validation cohort (n = 14): 7 acute rejection and 7 non-rejection recipients)	Acute rejection by using urine-based platform to detect iKEA					➢ Significantly higher level of $CD3^+$ exosomes among recipients undergoing TCMR, very low $CD3^+$ extracellular vesicle levels in BK poliomavirus nephropathy and chronic AMR recipients, supporting the specificity of iKEA for TCMR.	Park et al, 2017 (101)
		64 (18 AMR, 8 TCMR, and 38 non-rejection recipients)	TCMR and AMR by identified as mRNA expression					➢ Among 21 candidate genes, multiple genes are identified (gp130, CCL4, TNFα, SH2D1B, CAV1, atypical chemokine receptor 1 [Duffy blood group]) whose mRNA transcript levels in plasma exosomes significantly increased among AMR compared with TCMR and/or control recipients. ➢ A gene combination score calculated from 4 genes of gp130, SH2D1B, TNFα, and CCL4 is significantly higher in AMR than	Zhang et al, 2017 (168)

(Continued)

TABLE 1 Continued

Biomarkers (Commercial Assay)	Sample	N	Primary outcome(s)	Sensitivity (%)	Specificity (%)	PPV (%)	NPV (%)	Study outcomes	Author, Year [References]
								TCMR and non-rejection recipients.	
	Urine	47 (22 stable renal allograft function, 25 TCMR)	TCMR					➢ 17 proteins are increased in TCMR patients. ➢ Of all candidate biomarkers, tetraspanin-1 and hemopexin are two most significantly higher proteins in TCMR recipients.	Lim et al, 2018 (169)
	Urine and renal allograft tissue	78 (20 normal histology, 19 IF/TA, 17 calcineurin inhibitors toxicity, and 22 chronic active AMR)	Detection of exosomes-Western blot with antibody against SYT17 biopsies -immunohistochemistry with anti-SYT17, anti-STAT3 pY705, and anti-phospho NFκB p65 Ser276 antibodies					➢ No SYT17 protein is detected in whole-urine samples. ➢ SYT17 proteins are detectable in urinary exosomal fractions and high enrichment of SYT17 in exosomes from urine of chronic active AMR recipients compared to healthy volunteers and individuals in the normal renal allograft histology. ➢ SYT17 protein is expressed strongly in the chronic active AMR recipients compared to other recipient groups.	Takada et al, 2020 (94)
	Urine (At 1-week, 1-month, and 3-month post transplantation	23	Allograft function, immunosuppressive drug levels, and acute rejection by identified miRNA's expression					➢ Three overexpressed urinary exo-miRs (miR-146b, miR-155, andmiR-200a) in recipients are negatively correlated with tacrolimus dose. ➢ MiR-200a is positively correlated with proteinuria.	Freitas et al, 2020 (170)
	Urine and renal allograft tissue (for cause biopsy)	175 kidney transplant recipients undergoing for cause biopsy, with 192 urine samples that have matched biopsy specimens are included.	TCMR, AMR					➢ An exosomal mRNA signature discriminated between biopsy samples from recipients with all-cause rejection and those with non-rejection. ➢ Additional gene signature discriminated recipients with TCMR from those with AMR.	El Fekih et al, 2021 (102)
Chemokines (GRADE certainty rating [a]: LOW)									

(Continued)

TABLE 1 Continued

Biomarkers (Commercial Assay)	Sample	N	Primary outcome(s)	Sensitivity (%)	Specificity (%)	PPV (%)	NPV (%)	Study outcomes	Author, Year [References]
CXCL9, CXCL10	Urine	244	Acute rejection					➢ CXCL9 and CXCL10 are correlated with total inflammation and microvascular inflammation. ➢ Ratio of CXCL10:SCr and DSA in the improved diagnosis of AMR (AUC = 0.83).	Rabant et al, 2015 (114)
CXCL9	Urine	21	Acute rejection					➢ CXCL9 predicts acute rejection by a median of 15 days before clinical presentation of acute rejection	Hricik et al, 2015 (121)

[a]GRADE (Grading of Recommendations, Assessment, Development, and Evaluations) comprises 4 ratings: very low, low, moderate, and high (171). AMR, antibody-mediated rejection; AUC, area under the curve; CXCL, C-terminal amino acid sequence Cystine-X-Cystine motif chemokine ligand; dd-cf-DNA, donor-derived cell-free deoxyribonucleic acid; DSA, donor specific antibodies, eGFR, estimated glomerular filtration rate; IF/TA, interstitial fibrosis and tubular atrophy; iKEA, integrated kidney exosome assay; LC-MS/MS, liquid chromatography–tandem mass spectrometry; NPV, negative predictive value; PPV, positive predictive value; SCr, serum creatinine; TCMR, T cell-mediated rejection

limitations of histology and immunohistology in renal allograft biopsy interpretation. This has highlighted the need for the development of additional diagnostic modalities, including molecular diagnostics.

6 Conclusions

New-generation biomarkers in kidney transplantation are a collection of advanced indicators that provide a more comprehensive understanding of the status of a renal allograft. This has enabled the prognosis of the ultimate long-term renal allograft outcomes through the early detection of renal allograft rejection or dysfunction (Table 1). Although these biomarkers are now promising, further study is required to establish their therapeutic relevance and to find appropriate procedures for measuring and interpreting the data, especially in kidney transplant recipients. The choice of biomarkers may rely on the specific research topic, the type of accessible sample, and the isolation and analysis procedures employed. Interestingly, the integration of numerous indicators for a complete approach may improve accuracy and provide a bird's-eye perspective of the condition of kidney allografts in individual recipients.

Author contributions

The followings are the authors' contribution: conceptualization, WC, OT, and AL. Writing—original draft preparation, WC. Writing—review and editing, WC, OT, AL AT. Funding acquisition, WC; and supervision, AL and AT. All authors contributed to the article and approved the submitted version.

Funding

This research project is supported by the Health System Research Institute (HSRI)-Flagship Project Fund: fiscal year 2020 (HSRI 63-081).

Conflict of interest

The authors declare that the research was conducted in the absence of any commercial or financial relationships that could be construed as a potential conflict of interest.

Publisher's note

References

1. Wolfe RA, Ashby VB, Milford EL, Ojo AO, Ettenger RE, Agodoa LY, et al. Comparison of mortality in all patients on dialysis, patients on dialysis awaiting transplantation, and recipients of a first cadaveric transplant. *N Engl J Med* (1999) 341 (23):1725–30. doi: 10.1056/NEJM199912023412303

2. Poggio ED, Augustine JJ, Arrigain S, Brennan DC, Schold JD. Long-term kidney transplant graft survival-Making progress when most needed. *Am J Transplant* (2021) 21(8):2824–32. doi: 10.1111/ajt.16463

3. Larpparisuth N, Cheungpasitporn W, Lumpaopong A. Global perspective on kidney transplantation: Thailand. *Kidney360* (2021) 2(7):1163–5. doi: 10.34067/KID.0002102021

4. Lamb K, Lodhi S, Meier-Kriesche HU. Long-term renal allograft survival in the United States: a critical reappraisal. *Am J Transplant* (2011) 11(3):450–62. doi: 10.1111/j.1600-6143.2010.03283.x

5. Loupy A, Aubert O, Orandi BJ, Naesens M, Bouatou Y, Raynaud M, et al. Prediction system for risk of allograft loss in patients receiving kidney transplants: international derivation and validation study. *Br Med J* (2019) 366:l4923. doi: 10.1136/bmj.l4923

6. Saengram W, Vadcharavivad S, Poolsup N, Chancharoenthana W. Extended release versus immediate release tacrolimus in kidney transplant recipients: a systematic review and meta-analysis. *Eur J Clin Pharmacol* (2018) 74:1249–60. doi: 10.1007/s00228-018-2512-7

7. Schnitzler MA, Johnston K, Axelrod D, Gheorghian A, Lentine KL. Associations of renal function at 1-year after kidney transplantation with subsequent return to dialysis, mortality, and healthcare costs. *Transplantation* (2011) 91(12):1347–56. doi: 10.1097/TP.0b013e31821ab993

8. Clayton PA, McDonald SP, Russ GR, Chadban SJ. Long-term outcomes after acute rejection in kidney transplant recipients: An ANZDATA analysis. *J Am Soc Nephrol* (2019) 30(9):1697–707. doi: 10.1681/ASN.2018111101

9. Li L, Khatri P, Sigdel TK, Tran T, Ying L, Vitalone MJ, et al. A peripheral blood diagnostic test for acute rejection in renal transplantation. *Am J Transplant* (2012) 12 (10):2710–8. doi: 10.1111/j.1600-6143.2012.04253.x

10. Hirt-Minkowski P, Amico P, Ho J, Gao A, Bestland J, Hopfer H, et al. Detection of clinical and subclinical tubulo-interstitial inflammation by the urinary CXCL10 chemokine in a real-life setting. *Am J Transplant* (2012) 12(7):1811–23. doi: 10.1111/j.1600-6143.2012.03999.x

11. Bestard O, Nickel P, Cruzado JM, Schoenemann C, Boenisch O, Sefrin A, et al. Circulating alloreactive T cells correlate with graft function in longstanding renal transplant recipients. *J Am Soc Nephrol* (2008) 19(7):1419–29. doi: 10.1681/ASN.2007050539

12. Cherkassky L, Lanning M, Lalli PN, Czerr J, Siegel H, Danziger-Isakov L, et al. Evaluation of alloreactivity in kidney transplant recipients treated with antithymocyte globulin versus IL-2 receptor blocker. *Am J Transplant* (2011) 11(7):1388–96. doi: 10.1111/j.1600-6143.2011.03540.x

13. Haas M, Loupy A, Lefaucheur C, Roufosse C, Glotz D, Seron D, et al. The Banff 2017 Kidney Meeting Report: Revised diagnostic criteria for chronic active T cell-mediated rejection, antibody-mediated rejection, and prospects for integrative endpoints for next-generation clinical trials. *Am J Transplant* (2018) 18(2):293–307. doi: 10.1111/ajt.14625

14. Solez K, Colvin RB, Racusen LC, Sis B, Halloran PF, Birk PE, et al. Banff '05 Meeting Report: differential diagnosis of chronic allograft injury and elimination of chronic allograft nephropathy ('CAN'). *Am J Transplant* (2007) 7(3):518–26. doi: 10.1111/j.1600-6143.2006.01688.x

15. Loupy A, Haas M, Roufosse C, Naesens M, Adam B, Afrouzian M, et al. The Banff 2019 Kidney Meeting Report (I): Updates on and clarification of criteria for T cell– and antibody-mediated rejection. *Am J Transplant* (2020) 20(9):2318–31. doi: 10.1111/ajt.15898

16. Loupy A, Mengel M, Haas M. Thirty years of the International Banff Classification for Allograft Pathology: the past, present, and future of kidney transplant diagnostics. *Kidney Int* (2022) 101(4):678–91. doi: 10.1016/j.kint.2021.11.028

17. Callemeyn J, Lamarthée B, Koenig A, Koshy P, Thaunat O, Naesens M. Allorecognition and the spectrum of kidney transplant rejection. *Kidney Int* (2022) 101(4):692–710. doi: 10.1016/j.kint.2021.11.029

18. Roufosse C, Simmonds N, Clahsen-van Groningen M, Haas M, Henriksen KJ, Horsfield C, et al. A 2018 reference guide to the banff classification of renal allograft pathology. *Transplantation* (2018) 102(11):1795–814. doi: 10.1097/TP.0000000000002366

19. Nankivell BJ, Shingde M, Keung KL, Fung CL, Borrows RJ, O'Connell PJ, et al. The causes, significance and consequences of inflammatory fibrosis in kidney transplantation: The Banff i-IFTA lesion. *Am J Transplant* (2018) 18(2):364–76. doi: 10.1111/ajt.14609

20. Nankivell BJ, Agrawal N, Sharma A, Taverniti A, P'Ng CH, Shingde M, et al. The clinical and pathological significance of borderline T cell-mediated rejection. *Am J Transplant* (2019) 19(5):1452–63. doi: 10.1111/ajt.15197

21. Loupy A, Lefaucheur C. Antibody-mediated rejection of solid-organ allografts. *N Engl J Med* (2018) 379(12):1150–60. doi: 10.1056/NEJMra1802677

22. Cornell LD, Smith RN, Colvin RB. Kidney transplantation: mechanisms of rejection and acceptance. *Annu Rev Pathol* (2008) 3:189–220. doi: 10.1146/annurev.pathmechdis.3.121806.151508

23. Wiebe C, Gibson IW, Blydt-Hansen TD, Karpinski M, Ho J, Storsley LJ, et al. Evolution and clinical pathologic correlations of *de novo* donor-specific HLA antibody post kidney transplant. *Am J Transplant* (2012) 12(5):1157–67. doi: 10.1111/j.1600-6143.2012.04013.x

24. Dragun D, Catar R, Philippe A. Non-HLA antibodies against endothelial targets bridging allo- and autoimmunity. *Kidney Int* (2016) 90(2):280–8. doi: 10.1016/j.kint.2016.03.019

25. Cornaby C, Gibbons L, Mayhew V, Sloan CS, Welling A, Poole BD. B cell epitope spreading: mechanisms and contribution to autoimmune diseases. *Immunol Lett* (2015) 163(1):56–68. doi: 10.1016/j.imlet.2014.11.001

26. Valenzuela NM, Reed EF. Antibody-mediated rejection across solid organ transplants: manifestations, mechanisms, and therapies. *J Clin Invest* (2017) 127 (7):2492–504. doi: 10.1172/JCI90597

27. Montgomery RA, Loupy A, Segev DL. Antibody-mediated rejection: New approaches in prevention and management. *Am J Transplant* (2018) 18 Suppl 3:3–17. doi: 10.1111/ajt.14584

28. Wan SS, Ying TD, Wyburn K, Roberts DM, Wyld M, Chadban SJ. The treatment of antibody-mediated rejection in kidney transplantation: An updated systematic review and meta-analysis. *Transplantation* (2018) 102(4):557–68. doi: 10.1097/TP.0000000000002049

29. Bronkhorst AJ, Ungerer V, Holdenrieder S. The emerging role of cell-free DNA as a molecular marker for cancer management. *Biomol Detect Quantif* (2019) 17:100087. doi: 10.1016/j.bdq.2019.100087

30. Diehl F, Schmidt K, Choti MA, Romans K, Goodman S, Li M, et al. Circulating mutant DNA to assess tumor dynamics. *Nat Med* (2008) 14(9):985–90. doi: 10.1038/nm.1789

31. Alekseeva LA, Mironova NL, Brenner EV, Kurilshikov AM, Patutina OA, Zenkova MA. Alteration of the exDNA profile in blood serum of LLC-bearing mice under the decrease of tumour invasion potential by bovine pancreatic DNase I treatment. *PloS One* (2017) 12(2):e0171988. doi: 10.1371/journal.pone.0171988

32. Shen J, Zhou Y, Chen Y, Li X, Lei W, Ge J, et al. Dynamics of early post-operative plasma ddcfDNA levels in kidney transplantation: a single-center pilot study. *Transpl Int* (2019) 32(2):184–92. doi: 10.1111/tri.13341

33. Xie WY, Kim K, Goussous N, Drachenberg CB, Scalea JR, Weir MR, et al. Causes of renal allograft injury in recipients with normal donor-derived cell-free DNA. *Transplant Direct* (2021) 7(4):e679. doi: 10.1097/TXD.0000000000001135

34. Bloom RD, Bromberg JS, Poggio ED, Bunnapradist S, Langone AJ, Sood P, et al. Cell-free DNA and active rejection in kidney allografts. *J Am Soc Nephrol* (2017) 28 (7):2221–32. doi: 10.1681/ASN.2016091034

35. Sigdel TK, Archila FA, Constantin T, Prins SA, Liberto J, Damm I, et al. Optimizing detection of kidney transplant injury by assessment of donor-derived cell-free DNA via massively multiplex PCR. *J Clin Med* (2018) 8(1):19. doi: 10.3390/jcm8010019

36. Oellerich M, Shipkova M, Asendorf T, Walson PD, Schauerte V, Mettenmeyer N, et al. Absolute quantification of donor-derived cell-free DNA as a marker of rejection and graft injury in kidney transplantation: Results from a prospective observational study. *Am J Transplant* (2019) 19(11):3087–99. doi: 10.1111/ajt.15416

37. Stites E, Kumar D, Olaitan O, John Swanson S, Leca N, Weir M, et al. High levels of dd-cfDNA identify patients with TCMR 1A and borderline allograft rejection at elevated risk of graft injury. *Am J Transplant* (2020) 20(9):2491–8. doi: 10.1111/ajt.15822

38. Xiao H, Gao F, Pang Q, Xia Q, Zeng X, Peng J, et al. Diagnostic accuracy of donor-derived cell-free DNA in renal-allograft rejection: A meta-analysis. *Transplantation* (2021) 105(6):1303–10. doi: 10.1097/TP.0000000000003443

39. Garg N, Mandelbrot DA, Parajuli S, Aziz F, Astor BC, Chandraker A, et al. The clinical value of donor-derived cell-free DNA measurements in kidney transplantation. *Transplant Rev* (2021) 35(4):100649. doi: 10.1016/j.trre.2021.100649

40. Huang E, Haas M, Gillespie M, Sethi S, Peng A, Najjar R, et al. An assessment of the value of donor-derived cell-free DNA surveillance in patients with preserved kidney allograft function. *Transplantation* (2023) 107(1):274–82. doi: 10.1097/TP.0000000000004267

41. Bu L, Gupta G, Pai A, Anand S, Stites E, Moinuddin I, et al. Clinical outcomes from the Assessing Donor-derived cell-free DNA Monitoring Insights of kidney Allografts with Longitudinal surveillance (ADMIRAL) study. *Kidney Int* (2022) 101 (4):793–803. doi: 10.1016/j.kint.2021.11.034

42. Gupta G, Moinuddin I, Kamal L, King AL, Winstead R, Demehin M, et al. Correlation of donor-derived cell-free DNA with histology and molecular diagnoses of kidney transplant biopsies. *Transplantation* (2022) 106(5):1061–70. doi: 10.1097/TP.0000000000003838

43. Halloran PF, Reeve J, Madill-Thomsen KS, Demko Z, Prewett A, Billings P. The trifecta study: Comparing plasma levels of donor-derived cell-free DNA with the

molecular phenotype of kidney transplant biopsies. *J Am Soc Nephrol* (2022) 33(2):387–400. doi: 10.1681/ASN.2021091191

44. Huang E, Sethi S, Peng A, Najjar R, Mirocha J, Haas M, et al. Early clinical experience using donor-derived cell-free DNA to detect rejection in kidney transplant recipients. *Am J Transplant* (2019) 19(6):1663–70. doi: 10.1111/ajt.15289

45. Whitlam JB, Ling L, Skene A, Kanellis J, Ierino FL, Slater HR, et al. Diagnostic application of kidney allograft-derived absolute cell-free DNA levels during transplant dysfunction. *Am J Transplant* (2019) 19(4):1037–49. doi: 10.1111/ajt.15142

46. Kyeso Y, Bhalla A, Smith AP, Jia Y, Alakhdhair S, Ogir SC, et al. Donor-derived cell-free DNA kinetics post-kidney transplant biopsy. *Transplant Direct* (2021) 7(6): e703. doi: 10.1097/TXD.0000000000001149

47. Obrișcă B, Butiu M, Sibulesky L, Bakthavatsalam R, Smith KD, Gimferrer I, et al. Combining donor-derived cell-free DNA and donor specific antibody testing as non-invasive biomarkers for rejection in kidney transplantation. *Sci Rep* (2022) 12(1):15061. doi: 10.1038/s41598-022-19017-7

48. Jordan SC, Bunnapradist S, Bromberg JS, Langone AJ, Hiller D, Yee JP, et al. Donor-derived cell-free DNA identifies antibody-mediated rejection in donor specific antibody positive kidney transplant recipients. *Transplant Direct* (2018) 4(9):e379. doi: 10.1097/TXD.0000000000000821

49. Haas M, Sis B, Racusen LC, Solez K, Glotz D, Colvin RB, et al. Banff 2013 meeting report: inclusion of c4d-negative antibody-mediated rejection and antibody-associated arterial lesions. *Am J Transplant* (2014) 14(2):272–83. doi: 10.1111/ajt.12590

50. Venner JM, Hidalgo LG, Famulski KS, Chang J, Halloran PF. The molecular landscape of antibody-mediated kidney transplant rejection: evidence for NK involvement through CD16a Fc receptors. *Am J Transplant* (2015) 15(5):1336–48. doi: 10.1111/ajt.13115

51. Adam B, Afzali B, Dominy KM, Chapman E, Gill R, Hidalgo LG, et al. Multiplexed color-coded probe-based gene expression assessment for clinical molecular diagnostics in forMalin-fixed paraffin-embedded human renal allograft tissue. *Clin Transplant* (2016) 30(3):295–305. doi: 10.1111/ctr.12689

52. Halloran PF, Pereira AB, Chang J, Matas A, Picton M, De Freitas D, et al. Potential impact of microarray diagnosis of T cell-mediated rejection in kidney transplants: The INTERCOM study. *Am J Transplant* (2013) 13(9):2352–63. doi: 10.1111/ajt.12387

53. Halloran PF, Reeve J, Akalin E, Aubert O, Bohmig GA, Brennan D, et al. Real time central assessment of kidney transplant indication biopsies by microarrays: The INTERCOMEX study. *Am J Transplant* (2017) 17(11):2851–62. doi: 10.1111/ajt.14329

54. Geiss GK, Bumgarner RE, Birditt B, Dahl T, Dowidar N, Dunaway DL, et al. Direct multiplexed measurement of gene expression with color-coded probe pairs. *Nat Biotechnol* (2008) 26(3):317–25. doi: 10.1038/nbt1385

55. Loupy A, Haas M, Solez K, Racusen L, Glotz D, Seron D, et al. The banff 2015 kidney meeting report: Current challenges in rejection classification and prospects for adopting molecular pathology. *Am J Transplant* (2017) 17(1):28–41. doi: 10.1111/ajt.14107

56. Mengel M, Loupy A, Haas M, Roufosse C, Naesens M, Akalin E, et al. Banff 2019 Meeting Report: Molecular diagnostics in solid organ transplantation-Consensus for the Banff Human Organ Transplant (B-HOT) gene panel and open source multicenter validation. *Am J Transplant* (2020) 20(9):2305–17. doi: 10.1111/ajt.16059

57. Varol H, Ernst A, Cristoferi I, Arns W, Baan CC, van Baardwijk M, et al. Feasibility and potential of transcriptomic analysis using the nanoString nCounter technology to aid the classification of rejection in kidney transplant biopsies. *Transplantation* (2023) 107(5):903–12. doi: 10.1097/TP.0000000000004372

58. Smith RN, Rosales IA, Tomaszewski KT, Mahowald GT, Araujo-Medina M, Acheampong E, et al. Utility of banff human organ transplant gene panel in human kidney transplant biopsies. *Transplantation* (2023) 107(5):1188–99. doi: 10.1097/TP.0000000000004389

59. Deng MC, Eisen HJ, Mehra MR, Billingham M, Marboe CC, Berry G, et al. Noninvasive discrimination of rejection in cardiac allograft recipients using gene expression profiling. *Am J Transplant* (2006) 6(1):150–60. doi: 10.1111/j.1600-6143.2005.01175.x

60. Kurian SM, Williams AN, Gelbart T, Campbell D, Mondala TS, Head SR, et al. Molecular classifiers for acute kidney transplant rejection in peripheral blood by whole genome gene expression profiling. *Am J Transplant* (2014) 14(5):1164–72. doi: 10.1111/ajt.12671

61. Zhang W, Yi Z, Keung KL, Shang H, Wei C, Cravedi P, et al. A peripheral blood gene expression signature to diagnose subclinical acute rejection. *J Am Soc Nephrol* (2019) 30(8):1481–94. doi: 10.1681/ASN.2018111098

62. Van Loon E, Gazut S, Yazdani S, Lerut E, de Loor H, Coemans M, et al. Development and validation of a peripheral blood mRNA assay for the assessment of antibody-mediated kidney allograft rejection: A multicentre, prospective study. *EBioMedicine* (2019) 46:463–72. doi: 10.1016/j.ebiom.2019.07.028

63. Akalin E, Weir MR, Bunnapradist S, Brennan DC, Delos Santos R, Langone A, et al. Clinical validation of an immune quiescence gene expression signature in kidney transplantation. *Kidney360* (2021) 2(12):1998–2009. doi: 10.34067/KID.0005062021

64. Roedder S, Sigdel T, Salomonis N, Hsieh S, Dai H, Bestard O, et al. The kSORT assay to detect renal transplant patients at high risk for acute rejection: results of the multicenter AART study. *PloS Med* (2014) 11(11):e1001759. doi: 10.1371/journal.pmed.1001759

65. Marsh CL, Kurian SM, Rice JC, Whisenant TC, David J, Rose S, et al. Application of truGraf v1: A novel molecular biomarker for managing kidney transplant recipients with stable renal function. *Transplant Proc* (2019) 51(3):722–8. doi: 10.1016/j.transproceed.2019.01.054

66. Park S, Guo K, Heilman RL, Poggio ED, Taber DJ, Marsh CL, et al. Combining blood gene expression and cellfree DNA to diagnose subclinical rejection in kidney transplant recipients. *Clin J Am Soc Nephrol* (2021) 16(10):1539–51. doi: 10.2215/CJN.05530421

67. Bartel DP. MicroRNAs: genomics, biogenesis, mechanism, and function. *Cell* (2004) 116(2):281–97. doi: 10.1016/S0092-8674(04)00045-5

68. Lorenzen JM, Volkmann I, Fiedler J, Schmidt M, Scheffner I, Haller H, et al. Urinary miR-210 as a mediator of acute T-cell mediated rejection in renal allograft recipients. *Am J Transplant* (2011) 11(10):2221–7. doi: 10.1111/j.1600-6143.2011.03679.x

69. Maluf DG, Dumur CI, Suh JL, Scian MJ, King AL, Cathro H, et al. The urine microRNA profile may help monitor post-transplant renal graft function. *Kidney Int* (2014) 85(2):439–49. doi: 10.1038/ki.2013.338

70. Amrouche L, Desbuissons G, Rabant M, Sauvaget V, Nguyen C, Benon A, et al. MicroRNA-146a in human and experimental ischemic AKI: CXCL8-dependent mechanism of action. *J Am Soc Nephrol* (2017) 28(2):479–93. doi: 10.1681/ASN.2016010045

71. Soltaninejad E, Nicknam MH, Nafar M, Ahmadpoor P, Pourrezagholi F, Sharbafi MH, et al. Differential expression of microRNAs in renal transplant patients with acute T-cell mediated rejection. *Transpl Immunol* (2015) 33(1):1–6. doi: 10.1016/j.trim.2015.05.002

72. Betts G, Shankar S, Sherston S, Friend P, Wood KJ. Examination of serum miRNA levels in kidney transplant recipients with acute rejection. *Transplantation* (2014) 97(4):e28–30. doi: 10.1097/01.TP.0000441098.68212.de

73. Tao J, Yang X, Han Z, Lu P, Wang J, Liu X, et al.Serum microRNA-99a helps detect acute rejection in renal transplantation. *Transplant Proc.* (2015) 47(6):1683–7. doi: 10.1016/j.transproceed.2015.04.094.

74. Anglicheau D, Sharma VK, Ding R, Hummel A, Snopkowski C, Dadhania D, et al. MicroRNA expression profiles predictive of human renal allograft status. *Proc Natl Acad Sci U.S.A.* (2009) 106(13):5330–5. doi: 10.1073/pnas.0813121106

75. Oghumu S, Bracewell A, Nori U, Maclean KH, Balada-Lasat J-M, Brodsky S, et al. Acute pyelonephritis in renal allografts–a new role for MicroRNAs? *Transplantation* (2014) 97(5):559. doi: 10.1097/01.TP.0000441322.95539.b3

76. Matz M, Fabritius K, Lorkowski C, Dürr M, Gaedeke J, Durek P, et al. Identification of T cell–mediated vascular rejection after kidney transplantation by the combined measurement of 5 specific microRNAs in blood. *Transplantation* (2016) 100(4):898–907. doi: 10.1097/TP.0000000000000873

77. Danger R, Paul C, Giral M, Lavault A, Foucher Y, Degauque N, et al. Expression of miR-142-5p in peripheral blood mononuclear cells from renal transplant patients with chronic antibody-mediated rejection. *PloS One* (2013) 8(4):e60702. doi: 10.1371/journal.pone.0060702

78. Millán O, Budde K, Sommerer C, Aliart I, Rissling O, Bardaji B, et al. Urinary miR-155-5p and CXCL10 as prognostic and predictive biomarkers of rejection, graft outcome and treatment response in kidney transplantation. *Br J Clin Pharmacol* (2017) 83(12):2636–50. doi: 10.1111/bcp.13399

79. Scian M, Maluf D, David K, Archer K, Suh J, Wolen A, et al. MicroRNA profiles in allograft tissues and paired urines associate with chronic allograft dysfunction with IF/TA. *Am J Transplant* (2011) 11(10):2110–22. doi: 10.1111/j.1600-6143.2011.03666.x

80. Vahed SZ, Zonouzi AP, Mahmoodpoor F, Samadi N, Ardalan M, Omidi Y. Circulating miR-150, miR-192, miR-200b, and miR-423-3p as non-invasive biomarkers of chronic allograft dysfunction. *Arch Med Res* (2017) 48(1):96–104. doi: 10.1016/j.arcmed.2017.03.004

81. Glowacki F, Savary G, Gnemmi V, Van der Hauwaert C, Lo-Guidice J-M, et al. Increased circulating miR-21 levels are associated with kidney fibrosis. *PloS One* (2013) 8(2):e58014. doi: 10.1371/journal.pone.0058014

82. Pisitkun T, Shen RF, Knepper MA. Identification and proteomic profiling of exosomes in human urine. *Proc Natl Acad Sci U.S.A.* (2004) 101(36):13368–73. doi: 10.1073/pnas.0403453101

83. Robbins PD, Morelli AE. Regulation of immune responses by extracellular vesicles. *Nat Rev Immunol* (2014) 14(3):195–208. doi: 10.1038/nri3622

84. Panich T, Chancharoenthana W, Somparn P, Issara-Amphorn J, HIrankarn N, Leelahavanichkul A. Urinary exosomal activating transcriptional factor 3 as the early diagnostic biomarker for sepsis-induced acute kidney injury. *BMC Nephrol* (2017) 18 (1):10. doi: 10.1186/s12882-016-0415-3

85. Erdbrügger U, Blijdorp CJ, Bijnsdorp IV, Borràs FE, Burger D, Bussolati B, et al. Urinary extracellular vesicles: A position paper by the Urine Task Force of the International Society for Extracellular Vesicles. *J Extracell Vesicles* (2021) 10(7): e12093. doi: 10.1002/jev2.12093

86. Harding C, Heuser J, Stahl P. Receptor-mediated endocytosis of transferrin and recycling of the transferrin receptor in rat reticulocytes. *J Cell Biol* (1983) 97(2):329–39. doi: 10.1083/jcb.97.2.329

87. Veziroglu EM, Mias GI. Characterizing extracellular vesicles and their diverse RNA contents. *Front Genet* (2020) 11:700. doi: 10.3389/fgene.2020.00700

88. Quaglia M, Dellepiane S, Guglielmetti G, Merlotti G, Castellano G, Cantaluppi V. Extracellular vesicles as mediators of cellular crosstalk between immune system and kidney graft. *Front Immunol* (2020) 11:74. doi: 10.3389/fimmu.2020.00074

89. Soekmadji C, Li B, Huang Y, Wang H, An T, Liu C, et al. The future of Extracellular Vesicles as Theranostics - an ISEV meeting report. *J Extracell Vesicles* (2020) 9(1):1809766. doi: 10.1080/20013078.2020.1809766

90. Vykoukal J, Sun N, Aguilar-Bonavides C, Katayama H, Tanaka I, Fahrmann JF, et al. Plasma-derived extracellular vesicle proteins as a source of biomarkers for lung adenocarcinoma. *Oncotarget* (2017) 8(56):95466–80. doi: 10.18632/oncotarget.20748

91. Turco AE, Lam W, Rule AD, Denic A, Lieske JC, Miller VM, et al. Specific renal parenchymal-derived urinary extracellular vesicles identify age-associated structural changes in living donor kidneys. *J Extracell Vesicles* (2016) 5:29642. doi: 10.3402/jev.v5.29642

92. Dimuccio V, Ranghino A, Praticò Barbato L, Fop F, Biancone L, Camussi G, et al. Urinary CD133+ extracellular vesicles are decreased in kidney transplanted patients with slow graft function and vascular damage. *PloS One* (2014) 9(8):e104490. doi: 10.1371/journal.pone.0104490

93. Jung HY, Lee CH, Choi JY, Cho JH, Park SH, Kim YL, et al. Potential urinary extracellular vesicle protein biomarkers of chronic active antibody-mediated rejection in kidney transplant recipients. *J Chromatogr B Analyt Technol BioMed Life Sci* (2020) 1138:121958. doi: 10.1016/j.jchromb.2019.121958

94. Takada Y, Kamimura D, Jiang JJ, Higuchi H, Iwami D, Hotta K, et al. Increased urinary exosomal SYT17 levels in chronic active antibody-mediated rejection after kidney transplantation via the IL-6 amplifier. *Int Immunol* (2020) 32(10):653–62. doi: 10.1093/intimm/dxaa032

95. Pisitkun T, Gandolfo MT, Das S, Knepper MA, Bagnasco SM. Application of systems biology principles to protein biomarker discovery: urinary exosomal proteome in renal transplantation. *Proteomics Clin Appl* (2012) 6(5-6):268–78. doi: 10.1002/prca.201100108

96. Esteva-Font C, Guillén-Gómez E, Diaz JM, Guirado L, Facundo C, Ars E, et al. Renal sodium transporters are increased in urinary exosomes of cyclosporine-treated kidney transplant patients. *Am J Nephrol* (2014) 39(6):528–35. doi: 10.1159/000362905

97. Tutakhel OAZ, Moes AD, Valdez-Flores MA, Kortenoeven MLA, Vrie MVD, Jeleń S, et al. NaCl cotransporter abundance in urinary vesicles is increased by calcineurin inhibitors and predicts thiazide sensitivity. *PloS One* (2017) 12(4):e0176220. doi: 10.1371/journal.pone.0176220

98. Ponticelli C. Ischaemia-reperfusion injury: a major protagonist in kidney transplantation. *Nephrol Dial Transplant* (2014) 29(6):1134–40. doi: 10.1093/ndt/gft488

99. Gatti S, Bruno S, Deregibus MC, Sordi A, Cantaluppi V, Tetta C, et al. Microvesicles derived from human adult mesenchymal stem cells protect against ischaemia-reperfusion-induced acute and chronic kidney injury. *Nephrol Dial Transplant* (2011) 26(5):1474–83. doi: 10.1093/ndt/gfr015

100. Li ZL, Lv LL, Tang TT, Wang B, Feng Y, Zhou LT, et al. HIF-1α inducing exosomal microRNA-23a expression mediates the cross-talk between tubular epithelial cells and macrophages in tubulointerstitial inflammation. *Kidney Int* (2019) 95(2):388–404. doi: 10.1016/j.kint.2018.09.013

101. Park J, Lin HY, Assaker JP, Jeong S, Huang CH, Kurdi T, et al. Integrated kidney exosome analysis for the detection of kidney transplant rejection. *ACS Nano* (2017) 11(11):11041–6. doi: 10.1021/acsnano.7b05083

102. El Fekih R, Hurley J, Tadigotla V, Alghamdi A, Srivastava A, Coticchia C, et al. Discovery and validation of a urinary exosome mRNA signature for the diagnosis of human kidney transplant rejection. *J Am Soc Nephrol* (2021) 32(4):994–1004. doi: 10.1681/ASN.2020060850

103. Woud WW, Arykbaeva AS, Alwayn IPJ, Baan CC, Minnee RC, Hoogduijn MJ, et al. Extracellular vesicles released during normothermic machine perfusion are associated with human donor kidney characteristics. *Transplantation* (2022) 106(12):2360–9. doi: 10.1097/TP.0000000000004215

104. Gregorini M, Corradetti V, Pattonieri EF, Rocca C, Milanesi S, Peloso A, et al. Perfusion of isolated rat kidney with Mesenchymal Stromal Cells/Extracellular Vesicles prevents ischaemic injury. *J Cell Mol Med* (2017) 21(12):3381–93. doi: 10.1111/jcmm.13249

105. Altan-Bonnet N, Perales C, Domingo E. Extracellular vesicles: Vehicles of en bloc viral transmission. *Virus Res* (2019) 265:143–9. doi: 10.1016/j.virusres.2019.03.023

106. Altan-Bonnet N. Extracellular vesicles are the Trojan horses of viral infection. *Curr Opin Microbiol* (2016) 32:77–81. doi: 10.1016/j.mib.2016.05.004

107. Chancharoenthana W, Leelahavanichkul A. Innate immunity response to BK virus infection in polyomavirus-associated nephropathy in kidney transplant recipients. *Transplantology* (2022) 3(1):20–32. doi: 10.3390/transplantology3010003

108. Martelli F, Wu Z, Delbue S, Weissbach FH, Giulioli MC, Ferrante P, et al. BK polyomavirus microRNA levels in exosomes are modulated by non-coding control region activity and down-regulate viral replication when delivered to non-infected cells prior to infection. *Viruses* (2018) 10(9):466. doi: 10.3390/v10090466

109. Kim MH, Lee YH, Seo JW, Moon H, Kim JS, Kim YG, et al. Urinary exosomal viral microRNA as a marker of BK virus nephropathy in kidney transplant recipients. *PloS One* (2017) 12(12):e0190068. doi: 10.1371/journal.pone.0190068

110. Huang Y, Zeng G, Randhawa PS. Detection of BKV encoded mature MicroRNAs in kidney transplant patients: Clinical and biologic insights. *J Clin Virol* (2019) 119:6–10. doi: 10.1016/j.jcv.2019.07.006

111. Ashcroft J, Leighton P, Elliott TR, Hosgood SA, Nicholson ML, Kosmoliaptsis V. Extracellular vesicles in kidney transplantation: a state-of-the-art review. *Kidney Int* (2022) 101(3):485–97. doi: 10.1016/j.kint.2021.10.038

112. Manca S, Upadhyaya B, Mutai E, Desaulniers AT, Cederberg RA, White BR, et al. Milk exosomes are bioavailable and distinct microRNA cargos have unique tissue distribution patterns. *Sci Rep* (2018) 8(1):11321. doi: 10.1038/s41598-018-29780-1

113. Jackson JA, Kim EJ, Begley B, Cheeseman J, Harden T, Perez SD, et al. Urinary chemokines CXCL9 and CXCL10 are noninvasive markers of renal allograft rejection and BK viral infection. *Am J Transplant* (2011) 11(10):2228–34. doi: 10.1111/j.1600-6143.2011.03680.x

114. Rabant M, Amrouche L, Lebreton X, Aulagnon F, Benon A, Sauvaget V, et al. Urinary C-X-C motif chemokine 10 independently improves the noninvasive diagnosis of antibody-mediated kidney allograft rejection. *J Am Soc Nephrol* (2015) 26(11):2840–51. doi: 10.1681/ASN.2014080797

115. Blydt-Hansen TD, Sharma A, Gibson IW, Wiebe C, Sharma AP, Langlois V, et al. Validity and utility of urinary CXCL10/Cr immune monitoring in pediatric kidney transplant recipients. *Am J Transplant* (2021) 21(4):1545–55. doi: 10.1111/ajt.16336

116. Rabant M, Amrouche L, Morin L, Bonifay R, Lebreton X, Aouni L, et al. Early low urinary CXCL9 and CXCL10 might predict immunological quiescence in clinically and histologically stable kidney recipients. *Am J Transplant* (2016) 16(6):1868–81. doi: 10.1111/ajt.13677

117. Schaub S, Nickerson P, Rush D, Mayr M, Hess C, Golian M, et al. Urinary CXCL9 and CXCL10 levels correlate with the extent of subclinical tubulitis. *Am J Transplant* (2009) 9(6):1347–53. doi: 10.1111/j.1600-6143.2009.02645.x

118. Ho J, Schaub S, Wiebe C, Gao A, Wehmeier C, Koller MT, et al. Urinary CXCL10 chemokine is associated with alloimmune and virus compartment-specific renal allograft inflammation. *Transplantation* (2018) 102(3):521–9. doi: 10.1097/TP.0000000000001931

119. Mühlbacher J, Doberer K, Kozakowski N, Regele H, Camovic S, Haindl S, et al. Non-invasive chemokine detection: improved prediction of antibody-mediated rejection in donor-specific antibody-positive renal allograft recipients. *Front Med* (2020) 7:114. doi: 10.3389/fmed.2020.00114

120. Tinel C, Devresse A, Vermorel A, Sauvaget V, Marx D, Avettand-Fenoel V, et al. Development and validation of an optimized integrative model using urinary chemokines for noninvasive diagnosis of acute allograft rejection. *Am J Transplant* (2020) 20(12):3462–76. doi: 10.1111/ajt.15959

121. Hricik DE, Formica RN, Nickerson P, Rush D, Fairchild RL, Poggio E, et al. Adverse outcomes of tacrolimus withdrawal in immune-quiescent kidney transplant recipients. *J Am Soc Nephrol* (2015) 26(12):3114–22. doi: 10.1681/ASN.2014121234

122. Brunet M, Shipkova M, van Gelder T, Wieland E, Sommerer C, Budde K, et al. Barcelona consensus on biomarker-based immunosuppressive drugs management in solid organ transplantation. *Ther Drug Monit* (2016) 38 Suppl 1:S1–20. doi: 10.1097/FTD.0000000000000287

123. Lazzeri E, Rotondi M, Mazzinghi B, Lasagni L, Buonamano A, Rosati A, et al. High CXCL10 expression in rejected kidneys and predictive role of pretransplant serum CXCL10 for acute rejection and chronic allograft nephropathy. *Transplantation* (2005) 79(9):1215–20. doi: 10.1097/01.TP.0000160759.85080.2E

124. Heidt S, Shankar S, Muthusamy AS, San Segundo D, Wood KJ. Pretransplant serum CXCL9 and CXCL10 levels fail to predict acute rejection in kidney transplant recipients receiving induction therapy. *Transplantation* (2011) 91(8):e59–61. doi: 10.1097/TP.0b013e318210de6b

125. Xu C-X, Shi B-Y, Jin Z-K, Hao JJ, Duan WL, Han F, et al. Multiple-biomarkers provide powerful prediction of early acute renal allograft rejection by combination of serum fractalkine, IFN-γ and IP-10. *Transpl Immunol* (2018) 50:68–74. doi: 10.1016/j.trim.2018.08.003

126. Millán O, Rovira J, Guirado L, Espinosa C, Budde K, Sommerer C, et al. Advantages of plasmatic CXCL-10 as a prognostic and diagnostic biomarker for the risk of rejection and subclinical rejection in kidney transplantation. *Clin Immunol* (2021) 229:108792. doi: 10.1016/j.clim.2021.108792

127. Hollmen ME, Kyllönen LE, Inkinen KA, Lalla ML, Merenmies J, Salmela KT. Deceased donor neutrophil gelatinase-associated lipocalin and delayed graft function after kidney transplantation: a prospective study. *Crit Care* (2011) 15(3):R121. doi: 10.1186/cc10220

128. Li YM, Li Y, Yan L, Wang H, Wu XJ, Tang JT, et al. Comparison of urine and blood NGAL for early prediction of delayed graft function in adult kidney transplant recipients: a meta-analysis of observational studies. *BMC Nephrol* (2019) 20(1):291. doi: 10.1186/s12882-019-1491-y

129. Kaufeld JK, Gwinner W, Scheffner I, Haller HG, Schiffer M. Urinary NGAL ratio is not a sensitive biomarker for monitoring acute tubular injury in kidney transplant patients: NGAL and ATI in renal transplant patients. *J Transplant* (2012) 2012:563404. doi: 10.1155/2012/563404

130. Ramirez-Sandoval JC, Barrera-Chimal J, Simancas PE, Correa-Rotter R, Bobadilla NA, Morales-Buenrostro LE. Tubular urinary biomarkers do not identify aetiology of acute kidney injury in kidney transplant recipients. *Nephrol (Carlton)* (2014) 19(6):352–8. doi: 10.1111/nep.12240

131. Ramírez-Sandoval JC, Barrera-Chimal J, Simancas PE, Rojas-Montaño A, Correa-Rotter R, Bobadilla NA, et al. Urinary neutrophil gelatinase-associated lipocalin predicts graft loss after acute kidney injury in kidney transplant. *Biomarkers* (2014) 19(1):63–9. doi: 10.3109/1354750X.2013.867536

132. Cassidy H, Slyne J, O'Kelly P, Traynor C, Conlon PJ, Johnston O, et al. Urinary biomarkers of chronic allograft nephropathy. *Proteomics Clin Appl* (2015) 9(5-6):574–85. doi: 10.1002/prca.201400200

133. Lacquaniti A, Caccamo C, Salis P, Chirico V, Buemi A, Cernaro V, et al. Delayed graft function and chronic allograft nephropathy: diagnostic and prognostic role of neutrophil gelatinase-associated lipocalin. *Biomarkers* (2016) 21(4):371–8. doi: 10.3109/1354750X.2016.1141991

134. Kielar M, Dumnicka P, Gala-Błądzińska A, Będkowska-Prokop A, Ignacak E, Maziarz B, et al. Urinary ngal measured after the first year post kidney transplantation predicts changes in glomerular filtration over one-year follow-up. *J Clin Med* (2020) 10 (1):43. doi: 10.3390/jcm10010043

135. Tabernero G, Pescador M, Ruiz Ferreras E, Morales AI, Prieto M. Evaluation of NAG, NGAL, and KIM-1 as prognostic markers of the initial evolution of kidney transplantation. *Diagnostics (Basel)* (2023) 13(11):1843. doi: 10.3390/diagnostics13111843

136. Zhu M, Chen Z, Wei Y, Yuan Y, Ying L, Zhou H, et al. The predictive value of urinary kidney injury molecular-1 for long-term graft function in kidney transplant patients: a prospective study. *Ann Transl Med* (2021) 9(3):244. doi: 10.21037/atm-20-2215a

137. van Timmeren MM, Vaidya VS, van Ree RM, Oterdoom LH, de Vries AP, Gans RO, et al. High urinary excretion of kidney injury molecule-1 is an independent predictor of graft loss in renal transplant recipients. *Transplantation* (2007) 84 (12):1625–30. doi: 10.1097/01.tp.0000295982.78039.ef

138. Malyszko J, Koc-Zorawska E, Malyszko JS, Mysliwiec M. Kidney injury molecule-1 correlates with kidney function in renal allograft recipients. *Transplant Proc* (2010) 42(10):3957–9. doi: 10.1016/j.transproceed.2010.10.005

139. Verhoeven JG, Boer K, Van Schaik RH, Manintveld OC, Huibers MMH, Baan CC, et al. Liquid biopsies to monitor solid organ transplant function: a review of new biomarkers. *Ther Drug Monit* (2018) 40(5):515–25. doi: 10.1097/FTD.0000000000000549

140. Strahl BD, Allis CD. The language of covalent histone modifications. *Nature* (2000) 403(6765):41–5. doi: 10.1038/47412

141. Chen R, Kang R, Fan X, Tang D. Release and activity of histone in diseases. *Cell Death Dis* (2014) 5(8):e1370–e. doi: 10.1038/cddis.2014.337

142. McAnena P, Brown JA, Kerin MJ. Circulating nucleosomes and nucleosome modifications as biomarkers in cancer. *Cancers* (2017) 9(1):5. doi: 10.3390/cancers9010005

143. Bauden M, Pamart D, Ansari D, Herzog M, Eccleston M, Micallef J, et al. Circulating nucleosomes as epigenetic biomarkers in pancreatic cancer. *Clin Epigenet* (2015) 7(1):1–7. doi: 10.1186/s13148-015-0139-4

144. Verhoeven JG, Baan CC, Peeters AM, Clahsen-van Groningen MC, Nieboer D, Herzog M, et al. Circulating cell-free nucleosomes as biomarker for kidney transplant rejection: a pilot study. *Clin Epigenet* (2021) 13:1–8. doi: 10.1186/s13148-020-00969-4

145. Wang Y, Li M, Stadler S, Correll S, Li P, Wang D, et al. Histone hypercitrullination mediates chromatin decondensation and neutrophil extracellular trap formation. *J Cell Biol* (2009) 184(2):205–13. doi: 10.1083/jcb.200806072

146. Scozzi D, Ibrahim M, Menna C, Krupnick AS, Kreisel D, Gelman AE. The role of neutrophils in transplanted organs. *Am J Tranplant* (2017) 17(2):328–35. doi: 10.1111/ajt.13940

147. Saithong S, Worasilchai N, Saisorn W, Udompornpitak K, Bhunyakarnjanarat T, Chindamporn A, et al. Neutrophil extracellular traps in severe SARS-coV-2 infection: A possible impact of LPS and (1→3)-β-D-glucan in blood from gut translocation. *Cells* (2022) 11(7):1103. doi: 10.3390/cells11071103

148. Henderson LK, Nankivell BJ, Chapman JR. Surveillance protocol kidney transplant biopsies: their evolving role in clinical practice. *Am J Transplant* (2011) 11(8):1570–5. doi: 10.1111/j.1600-6143.2011.03677.x

149. Hariharan S, McBride MA, Cherikh WS, Tolleris CB, Bresnahan BA, Johnson CP. Post-transplant renal function in the first year predicts long-term kidney transplant survival. *Kidney Int* (2002) 62(1):311–8. doi: 10.1046/j.1523-1755.2002.00424.x

150. Amer H, Lieske JC, Rule AD, Kremers WK, Larson TS, Franco Palacios CR, et al. Urine high and low molecular weight proteins one-year post-kidney transplant: relationship to histology and graft survival. *Am J Transplant* (2013) 13(3):676–84. doi: 10.1111/ajt.12044

151. Tsampalieros A, Knoll GA. Evaluation and management of proteinuria after kidney transplantation. *Transplantation* (2015) 99(10):2049–60. doi: 10.1097/TP.0000000000000894

152. Wiebe C, Gibson IW, Blydt-Hansen TD, Pochinco D, Birk PE, Ho J, et al. Rates and determinants of progression to graft failure in kidney allograft recipients with *de novo* donor-specific antibody. *Am J Transplant* (2015) 15(11):2921–30. doi: 10.1111/ajt.13347

153. Cravedi P, Mannon RB. Noninvasive methods to assess the risk of kidney transplant rejection. *Expert Rev Clin Immunol* (2009) 5(5):535–46. doi: 10.1586/eci.09.36

154. Khatri P, Roedder S, Kimura N, De Vusser K, Morgan AA, Gong Y, et al. A common rejection module (CRM) for acute rejection across multiple organs identifies novel therapeutics for organ transplantation. *J Exp Med* (2013) 210(11):2205–21. doi: 10.1084/jem.20122709

155. Sigdel TK, Yang JYC, Bestard O, Schroeder A, Hsieh SC, Liberto JM, et al. A urinary Common Rejection Module (uCRM) score for non-invasive kidney transplant monitoring. *PloS One* (2019) 14(7):e0220052. doi: 10.1371/journal.pone.0220052

156. Yang JYC, Sarwal RD, Sigdel TK, Damm I, Rosenbaum B, Liberto JM, et al. A urine score for noninvasive accurate diagnosis and prediction of kidney transplant rejection. *Sci Transl Med* (2020) 12(535):eaba2501. doi: 10.1126/scitranslmed.aba2501

157. Watson D, Yang JY, Sarwal RD, Sigdel TK, Liberto JM, Damm I, et al. A novel multi-biomarker assay for non-invasive quantitative monitoring of kidney injury. *J Clin Med* (2019) 8(4):499. doi: 10.3390/jcm8040499

158. Mayer KA, Omic H, Weseslindtner L, Doberer K, Reindl-Schwaighofer R, Viard T, et al. Levels of donor-derived cell-free DNA and chemokines in BK polyomavirus-associated nephropathy. *Clin Transplant* (2022) 36(11):e14785. doi: 10.1111/ctr.14785

159. Dauber EM, Kollmann D, Kozakowski N, Rasoul-Rockenschaub S, Soliman T, Berlakovich GA, et al. Quantitative PCR of INDELs to measure donor-derived cell-free DNA-a potential method to detect acute rejection in kidney transplantation: a pilot study. *Transpl Int* (2020) 33(3):298–309. doi: 10.1111/tri.13554

160. Friedewald JJ, Kurian SM, Heilman RL, Whisenant TC, Poggio ED, Marsh C, et al. Development and clinical validity of a novel blood-based molecular biomarker for subclinical acute rejection following kidney transplant. *Am J Transplant* (2019) 19 (1):98–109. doi: 10.1111/ajt.15011

161. Crespo E, Roedder S, Sigdel T, Hsieh SC, Luque S, Cruzado JM, et al. Molecular and functional noninvasive immune monitoring in the ESCAPE study for prediction of subclinical renal allograft rejection. *Transplantation* (2017) 101(6):1400–9. doi: 10.1097/TP.0000000000001287

162. First MR, Peddi VR, Mannon R, Knight R, Marsh CL, Kurian SM, et al. Investigator assessment of the utility of the truGraf molecular diagnostic test in clinical practice. *Transplant Proc* (2019) 51(3):729–33. doi: 10.1016/j.transproceed.2018.10.024

163. Matz M, Lorkowski C, Fabritius K, Durek P, Wu K, Rudolph B, et al. Free microRNA levels in plasma distinguish T-cell mediated rejection from stable graft function after kidney transplantation. *Transpl Immunol* (2016) 39:52–9. doi: 10.1016/j.trim.2016.09.001

164. Matz M, Heinrich F, Lorkowski C, Wu K, Klotsche J, Zhang Q, et al. MicroRNA regulation in blood cells of renal transplanted patients with interstitial fibrosis/tubular atrophy and antibody-mediated rejection. *PloS One* (2018) 13(8): e0201925. doi: 10.1371/journal.pone.0201925

165. Ledeganck KJ, Gielis EM, Abramowicz D, Stenvinkel P, Shiels PG, Van Craenenbroeck AH. MicroRNAs in AKI and kidney transplantation. *Clin J Am Soc Nephrol* (2019) 14(3):454–68. doi: 10.2215/CJN.08020718

166. Qamri Z, Pelletier R, Foster J, Kumar S, Momani H, Ware K, et al. Early posttransplant changes in circulating endothelial microparticles in patients with kidney transplantation. *Transpl Immunol* (2014) 31(2):60–4. doi: 10.1016/j.trim.2014.06.006

167. Sigdel TK, Bestard O, Tran TQ, Hsieh SC, Roedder S, Damm I, et al. A computational gene expression score for predicting immune injury in renal allografts. *PloS One* (2015) 10(9):e0138133. doi: 10.1371/journal.pone.0138133

168. Zhang H, Huang E, Kahwaji J, Nast CC, Li P, Mirocha J, et al. Plasma exosomes from HLA-sensitized kidney transplant recipients contain mRNA transcripts which predict development of antibody-mediated rejection. *Transplantation* (2017) 101 (10):2419–28. doi: 10.1097/TP.0000000000001834

169. Lim JH, Lee CH, Kim KY, Jung HY, Choi JY, Cho JH, et al. Novel urinary exosomal biomarkers of acute T cell-mediated rejection in kidney transplant recipients: A cross-sectional study. *PloS One* (2018) 13(9):e0204204. doi: 10.1371/journal.pone.0204204

170. Freitas RCC, Bortolin RH, Genvigir FDV, Bonezi V, Hirata TDC, Felipe CR, et al. Differentially expressed urinary exo-miRs and clinical outcomes in kidney recipients on short-term tacrolimus therapy: a pilot study. *Epigenomics* (2020) 12 (22):2019–34. doi: 10.2217/epi-2020-0160

171. Guyatt GH, Oxman AD, Vist GE, Kunz R, Falck-Ytter Y, Alonso-Coello P, et al. GRADE: an emerging consensus on rating quality of evidence and strength of recommendations. *BMJ* (2008) 336(7650):924–6. doi: 10.1136/bmj.39489.470347.AD

frontiers | Frontiers in Immunology

TYPE Systematic Review
PUBLISHED 02 October 2023
DOI 10.3389/fimmu.2023.1265796

OPEN ACCESS

EDITED BY
Liping Li,
Geisinger Medical Center, United States

REVIEWED BY
Takayuki Yamamoto,
Massachusetts General Hospital and Harvard Medical School, United States
Alexandre Walencik,
Établissement Français du Sang (EFS), France

*CORRESPONDENCE
Carmen Lefaucheur
carmenlefaucheur4@gmail.com

RECEIVED 23 July 2023
ACCEPTED 07 September 2023
PUBLISHED 02 October 2023

CITATION
Al-Awadhi S, Raynaud M, Louis K, Bouquegneau A, Taupin J-L, Aubert O, Loupy A and Lefaucheur C (2023) Complement-activating donor-specific anti-HLA antibodies in solid organ transplantation: systematic review, meta-analysis, and critical appraisal.
Front. Immunol. 14:1265796.
doi: 10.3389/fimmu.2023.1265796

Complement-activating donor-specific anti-HLA antibodies in solid organ transplantation: systematic review, meta-analysis, and critical appraisal

Solaf Al-Awadhi[1], Marc Raynaud[1], Kevin Louis[1,2], Antoine Bouquegneau[1,3], Jean-Luc Taupin[4], Olivier Aubert[1,5], Alexandre Loupy[1,5] and Carmen Lefaucheur[1,2]*

[1]Université de Paris Cité, Institut National de la Santé et de la Recherche Médicale (INSERM) Unité Mixte de Recherche (UMR)-S970, Paris Cardiovascular Research Center (PARCC), Paris Translational Research Centre for Organ Transplantation, Paris, France, [2]Kidney Transplant Department, Saint-Louis Hospital, Assistance Publique - Hôpitaux de Paris, Paris, France, [3]Department of Nephrology, Dialysis and Transplantation, Centre Hospitalier Universitaire (CHU) de Liège, Liège, Belgium, [4]Department of Immunology and Histocompatibility, Centre Hospitalier Universitaire (CHU) Paris–GH St–Louis Lariboisière, Paris, France, [5]Kidney Transplant Department, Necker Hospital, Assistance Publique – Hôpitaux de Paris, Paris, France

Introduction: Several studies have investigated the impact of circulating complement-activating anti-human leukocyte antigen donor-specific antibodies (anti-HLA DSAs) on organ transplant outcomes. However, a critical appraisal of these studies and a demonstration of the prognostic value of complement-activating status over anti-HLA DSA mean fluorescence intensity (MFI) level are lacking.

Methods: We conducted a systematic review, meta-analysis and critical appraisal evaluating the role of complement-activating anti-HLA DSAs on allograft outcomes in different solid organ transplants. We included studies through Medline, Cochrane, Scopus, and Embase since inception of databases till May 05, 2023. We evaluated allograft loss as the primary outcome, and allograft rejection as the secondary outcome. We used the Newcastle-Ottawa Scale and funnel plots to assess risk of bias and used bias adjustment methods when appropriate. We performed multiple subgroup analyses to account for sources of heterogeneity and studied the added value of complement assays over anti-HLA DSA MFI level.

Results: In total, 52 studies were included in the final meta-analysis (11,035 patients). Complement-activating anti-HLA DSAs were associated with an increased risk of allograft loss (HR 2.77; 95% CI 2.33-3.29, p<0.001; I^2=46.2%), and allograft rejection (HR 4.98; 95% CI 2.96-8.36, p<0.01; I^2=70.9%). These results remained significant after adjustment for potential sources of bias and across multiple subgroup analyses. After adjusting on pan-IgG anti-HLA DSA

10.3389/fimmu.2023.1265796

defined by the MFI levels, complement-activating anti-HLA DSAs were significantly and independently associated with an increased risk of allograft loss.

Discussion: We demonstrated in this systematic review, meta-analysis and critical appraisal the significant deleterious impact and the independent prognostic value of circulating complement-activating anti-HLA DSAs on solid organ transplant risk of allograft loss and rejection.

KEYWORDS

complement-activation, donor specific antibodies, anti-HLA, rejection, transplantation outcomes

1 Introduction

Antibody-mediated rejection has been identified as the main cause for allograft loss (1) and the prognostic role of circulating anti-human leukocyte antigen donor-specific antibodies (anti-HLA DSAs) has been extensively assessed across different solid organ transplants (2–5). One key characteristic of anti-HLA DSAs is their ability to undergo class-switch recombination and activate complement by fixing complement fractions. Several studies have been conducted to evaluate the impact of complement-activating anti-HLA DSAs on allograft outcomes. The reported results were heterogeneous with some studies demonstrating a strong association of complement-activating anti-HLA DSA with adverse allograft outcomes (6, 7) while others showed no or weak associations (8, 9).

As a consequence, our team previously performed a systematic review and meta-analysis to study the role of complement-activating anti-HLA DSAs on adverse allograft outcomes (10) and showed that circulating complement-activating anti-HLA DSAs increased the risk of allograft loss and rejection. However, since the publication of the review in May 2018, major studies assessing the effect of circulating complement-activating anti-HLA DSAs on allograft outcomes have been conducted (11, 12).

In addition, the quality and risk of bias of the previous and recent studies have not been evaluated and a critical appraisal remains to be performed. The Sensitization in transplantation: Assessment of Risk (STAR) working group have recently highlighted several gaps regarding whether ancillary complement-based assays (C1q, C3d, C4d) provide additional useful clinical information compared to mean fluorescence intensity (MFI) values provided by single antigen bead (SAB) pan-IgG assay (6, 8, 13, 14). Therefore, STAR working group recommends verify the role of complement binding assays *in vivo* as potential markers for adverse outcomes before recommending its use in clinical practice.

Therefore, the aim of this article was to provide a comprehensive up-to-date systematic review, meta-analysis and critical appraisal of studies testing the effect of circulating complement-activating anti-HLA DSAs on allograft outcomes and to evaluate and adjust for risk of bias.

2 Methods

This study was an incremental update of a systematic review and a meta-analysis (10), supplemented by a critical appraisal. The study was reported according to the Preferred Reporting Items for Systematic Reviews and Meta-Analyses (PRISMA) (15).

2.1 Data sources

A comprehensive search strategy was conducted on Medline, Cochrane, Scopus and Embase since inception of databases till January 31, 2018 (10). For the period between the closing date of the previous review (10) and May 05, 2023 we created a search strategy using a complementary combination of two PubMed search strategies: 1) narrow Boolean which consists of the main Medical Subject Heading (MeSH) for the population combined with the main MeSH for the intervention (see Supplementary for details), and 2) ranking strategy which consisted of screening all the studies listed under the "similar articles" feature on PubMed of the three largest and three newest studies included in the previous review (16). We opted for a PubMed-only database search for this period because the included articles of the previous review (10), whose search strategy was comprehensive and included multiple databases, were all indexed in PubMed (17). This search strategy was further complemented by a manual search for potential additional studies.

2.2 Study selection

The inclusion criteria were studies evaluating the effect of complement-activating anti-HLA DSAs on allograft loss and rejection in adult and paediatric solid organ transplant recipients. Two independent reviewers (SAA and AB) screened the titles and abstracts of the studies and any disagreement was resolved by consensus.

2.3 Data extraction

We collected the same data variables as the previous review: "author name, year of publication, study size, mean or median follow-up time, mean age of population, type of complement-activating anti-HLA DSA, comparison used (patients with complement-activating anti-HLA DSAs were either compared to patients without complement-activating anti-HLA DSAs, patients with non-complement activating anti-HLA DSAs detected, or a mixed group of patients without anti-HLA DSAs and with non-complement activating anti-HLA DSAs), effect sizes (HR and/or OR) and their 95% confidence intervals, potential confounding factors, and unadjusted and adjusted estimated risks of graft loss or graft rejection." (10).

2.4 Critical appraisal

We used the Newcastle-Ottawa Scale (NOS) to assess the risk of bias in observational studies (18). A high NOS score (≥ 6) represents high methodological quality. Using this quality score, each study is judged on eight items which are divided into three components: selection of the study groups (up to four points), confounding variables adjustment quality (up to two points) and the outcome studied (up to three points). (see Supplementary for details).

Extraction of data and assessment of risk of bias was done by two independent reviewers (SAA and AB) and any disagreement was resolved by consensus.

2.5 Data synthesis and analysis

We performed the meta-analysis through a random-effects model with restricted maximum likelihood approach using an inverse-variance to incorporate a measure of the anticipated heterogeneity into the weight of the studies (19). The index group was complement-activating anti-HLA DSA positive patients. They were compared to either complement-activating anti-HLA DSA negative patients, anti-HLA DSA negative patients, or a mixed group of both. The pooled effect size, study weights and amount of study heterogeneity were represented by forest plots for allograft loss and rejection.

2.6 Statistical heterogeneity and small-study effects

We evaluated statistical heterogeneity using I^2 index which reflects the percentage of variability in the effect size caused by heterogeneity rather than by chance alone. An I^2 above 50% represented substantial heterogeneity (19).

We used a funnel plot to visually assess for the presence of small-size effects which occurs when smaller studies show different, often more pronounced effect size. We statistically assessed any asymmetry in the funnel plot with the Egger's test (20). If this test was significant, we adjusted for small-study effects by using the precision-effect test (PET). This method provided an estimate of the effect size in a study with a hypothetical infinite sample size and thus eliminating small-study effects bias (21).

We tested for publication bias by using a contour-enhanced funnel plot (22). If a bias was observed, we adjusted by using the p-uniform* selection model which assumes that studies with statistically non-significant p-values are published with the same probability as statistically significant results (21).

2.7 Subgroup analyses

We performed the following subgroup analyses to address potential sources of heterogeneity in studies assessing graft loss:

2.7.1 High versus low methodological quality of studies

We separately meta-analysed higher quality studies (NOS scores ≥ 6) (23) versus lower quality studies (NOS score ≤ 5).

2.7.2 Comparator group used

We separately meta-analysed studies comparing complement activating anti-HLA DSA positive patients with complement activating anti-HLA DSA and studies comparing complement activating anti-HLA DSA positive patients with complement activating anti-HLA DSA negative patients and anti-HLA DSA negative patient.

2.7.3 Type of organ transplanted

We separately meta-analysed studies based on the type of the transplanted organ (kidney, liver, lung, heart, pancreas and intestine). We also separately meta-analysed kidney transplants versus all other organs based on the assumption that a low number of studies are available per organ.

2.7.4 Timing of antibody detection

We separately meta-analysed studies testing patients with preformed anti-HLA DSAs (defined as antibodies positive before or at the time of transplantation), *de novo* anti-HLA DSAs (defined as antibodies positive only after transplantation), or a combined group of *de novo* both.

2.7.5 Type of complement-activating capacity of antibodies

We separately meta-analysed anti-HLA DSA according to their C1q-, C3d-, or C4d-, binding capacity or according to their IgG subclass.

2.7.6 Thresholds for complement-activating anti-HLA DSA positivity

We separately meta-analysed studies that considered different MFI thresholds for complement-activating anti-HLA DSA positivity of 300, 500 or 1000.

2.8 Sensitivity analysis

We separately meta-analysed the newly identified studies since the publication of the previous review in 2018 and assessed the association of complement activating anti-HLA DSA with the risk allograft loss and allograft rejection.

2.9 Cumulative meta-analysis

We conducted a cumulative meta-analysis to show the change of hazard ratio of allograft loss as each study is added to the pool (24), which allowed to assess the stability of evidence i.e., whether additional studies change the overall effect of complement-binding anti-HLA DSAs on the outcome, and the sufficiency of evidence i.e., whether additional studies were needed to establish the same conclusion (25). The cumulative meta-analysis was represented on a forest-plot and the studies were arranged in a chronological order by year and month of publication.

2.10 Added prognostic value of complement-activating anti-HLA DSA status over anti-HLA DSA MFI level

We identified studies that showed a correlation between complement-activating anti-HLA DSA status and pan-IgG anti-HLA DSA defined by MFI levels. Then, we identified and separately meta-analysed studies that conducted multivariable analyses adjusting complement-activating anti-HLA DSA status on pan-IgG anti-HLA DSA defined by MFI levels to assess the prognostic value of complement-activating anti-HLA DSA over standard SAB pan-IgG assays.

In addition, to assess the added prognostic value of complement-activating anti-HLA DSA over EDTA treated SAB assays, we identified studies that pre-treated sera with ethylenediaminetetraacetic acid (EDTA) as means to overcome complement interference – a shortcoming of SAB assays caused by complement activation which usually results in underestimating or completely masking strong DSAs (26).

2.11 Added prognostic value of complement-activating anti-HLA DSA status over anti-HLA DSA class

We identified and separately meta-analysed studies that performed multivariable models adjusting complement-activating anti-HLA DSA status on DSA class to assess the independent prognostic value of complement-activating anti-HLA DSA.

The meta-analyses were conducted on R 4.1.1. All tests were two-sided, and a p-value lower than 0.05 was considered significant.

3 Results

3.1 Study identification

The search strategy identified 1,112 potential studies. After removing duplicates (n=91), studies with non-human data or not written in English (n=102), studies with non-solid organ transplant data (n=475), studies with non-complement binding anti-HLA DSAs (n=400), non-original articles (n=19), and studies with different outcomes or without hazard ratio/odds ratio (n=10), 15 new studies were identified, corresponding to 3,099 patients (Figure 1). The previous review (10) included 37 studies, therefore, in this incremental update, 52 studies in total were included in the final meta-analysis, corresponding to 11,035 patients. A descriptive summary of all the included studies is shown in Table 1.

3.2 Study characteristics

In total, 31 (59.6%) studies originated from Europe, 13 (25.0%) from North America, 5 (9.6%) from the United Kingdom, and 3 (5.8%) from Asia. The majority of the patients were kidney recipients (n=8,746; 79.3%), followed by liver recipients (n=1,459; 13.2%), heart recipients (n=546; 4.9%), and lung recipients (n=284; 2.6%). No pancreas or intestine recipients were identified. Complement-activating anti-HLA DSAs were classified by their capacity to bind C1q (28 studies; 53.8%), C3d (12 studies; 23%), or C4d (6 studies; 11.5%) or by their IgG subclass composition (10 studies; 19%).

The median NOS score was 6 (IQR 3-9) with 1.5%, 13%, 15%, 30%, 28%, 13%, and 3% of studies having a NOS score of 3, 4, 5, 6, 7, 8, and 9, respectively. Details on the NOS scoring results are available in Supplementary Table 1.

3.3 Outcomes

3.3.1 Risk for allograft loss

Patients with complement-activating anti-HLA DSAs had a 2.77-fold increase in risk for allograft loss (95% CI 2.33-3.29, $p<0.001$; $I^2=46.2\%$) compared to patients without complement-activating anti-HLA DSA, patients without anti-HLA DSAs, and a mixed group of both (Figure 2).

3.3.2 Risk of allograft rejection

Patients with complement-activating anti-HLA DSAs had a 4.98-fold increase in risk of allograft rejection (95% CI 2.96-8.36, $p<0.001$; $I^2=70.9\%$) compared to patients without complement-activating anti-HLA DSA, patients without anti-HLA DSAs, and a mixed group of both (Figure 3).

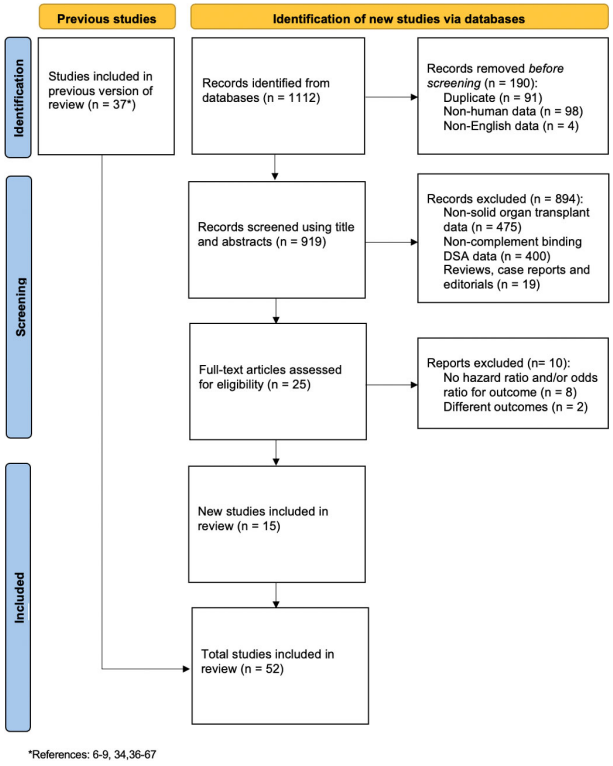

FIGURE 1
Flow chart summarizing study identification and selection process.

3.4 Small-study effects

Visually, the funnel plot presented in Figure 4 showed an asymmetry which was confirmed by Egger's test (p=0.01) indicating the presence of small-study effects. When adjusting using the PET method, the hazard ratio remains significant (HR=1.5, p<0.001) indicating that in a hypothetical infinite sample size, complement-binding anti-HLA DSAs would still increase the risk for allograft loss (Supplementary Figure 3).

Publication bias, as a potential cause for small-study effects, was assessed using the contour-enhanced funnel plot presented in Figure 5 which showed that more studies lie in the statistically significant side of the graph. We adjusted for this bias by using the p-uniform* selection model which yielded a hazard ratio of 2.46 (p=0.01) indicating that taking into account studies with non-significant p-values, complement-binding anti-HLA DSAs would still increase the risk of allograft loss.

3.5 Subgroup analysis

Table 2 summarizes the effect sizes for each subgroup.

3.5.1 Effect of complement-activating anti-HLA DSAs in high methodological quality studies

Analysis done on high methodological quality studies (NOS≥6) showed a significantly increased risk of allograft loss in complement activating anti-HLA DSAs positive patients with a pooled HR of 2.79 (95% CI 2.33-3.35, p<0.001, I^2 = 45.7%). Studies with lower methodological quality (NOS ≤ 5) also showed an increased risk of allograft loss with a HR of 2.46 (CI 1.28-4.70, p<0.001) however, as expected, the heterogeneity level between the lower methodological quality studies was higher (I^2 = 60.5%).

3.5.2 Effect of the complement-activating anti-HLA DSAs using different comparators

The association between complement-activating anti-HLA DSAs and risk of allograft loss remained significant using different comparator groups. When comparing complement-activating anti-HLA DSAs positive patients to complement-activating anti-HLA DSAs negative patients, the pooled HR was 2.56 (95% CI 1.99-3.30, p<0.001, I^2 = 54.2%). When comparing, complement- activating anti-HLA DSA positive patients to a mixed group of complement- activating anti-HLA DSA negative patients and anti-HLA DSA negative patients, the pooled HR was 3.58 (95% CI 2.70-4.74, p<0.001; I^2 = 4.1%).

3.5.3 Effect of complement-activating anti-HLA DSAs according to the type of organ transplantation

Analysis done on kidney allograft recipients versus all other solid organ allograft recipients showed a significant increased risk of allograft loss with HRs of 2.77 (CI 2.25-3.41, p<0.001; I^2 = 49.2%) and 2.74 (CI 2.03-3.69, p<0.001; I^2 = 29.2%) respectively. Analysis specific to other

TABLE 1 Description of the 52 included studies.

First author (date of publication)	Population	Study type	Period of inclusion	Sample size	Type of C′ anti-HLA DSA	MFI threshold for DSA detection	MFI threshold for complement positivity	EDTA pre-treatment	Outcome	Effect size (95% CI)
Wahrmann et al. (2009) (27)	Retrospective, single-centre analysis of consecutive adult renal transplants selected based on the presence of pretransplant DSAs	Cohort	2001-2002	338	C4d	Not reported	Not reported	Not reported	Graft loss Rejection	2.40 (0.90-6.00) 10.10 (3.20-31.00)
Hönger et al. (2010) (28)	Retrospective, single-centre analysis of consecutive adult renal transplant recipients with low levels of pretransplant DSAs	Cohort	1999-2004	64	C4d	>500	Not reported	No	Rejection	0.93 (0.25-3.44)
Sutherland et al. (2011) (29)	Retrospective, single-centre analysis of paediatric renal transplant recipients without DSAs at the time of transplantation	Cohort	2000-2008	35	C1q	>1000	>450	No	Graft loss	5.80 (1.40-22.90)
Hönger et al. (2011) (30)	Retrospective, single-centre analysis of adult renal transplant recipients with high levels of DSAs pre transplant; recipients who developed AMR within 6 months	Cohort	1999-2008	71	IgG3	>500	Not reported	No	Rejection	0.43 (0.17-1.12)
Smith et al. (2011) (31)	Retrospective, single-centre analysis of living heart transplant recipients after 1 year of transplantation without DSAs pre-transplant	Cohort	1995-2004	243	C4d	>1000	Not reported	No	Graft loss	3.02 (1.11-8.23)
Kaneku et al. (2012) (32)	Retrospective (2-centre) analysis of adult liver transplant recipients with liver biopsies showing chronic rejection and DSA analysis at the same time	Case-control	NC	39	IgG3	>5000	Not reported	No	Graft loss	3.35 (1.39-8.05)
Bartel et al. (2013) (33)	Retrospective, single-centre analysis of 68 desensitized renal recipients who had been subjected to peri-transplant desensitization	Cohort	1999-2008	68	C4d	>500	Not reported	No	Rejection	10.10 (1.60-64.20)
Lawrence et al. (2013) (34)	Retrospective, single-centre study of consecutive renal transplant recipients	Cohort	2005-2010	52	C4d	>300	Not reported	No	Rejection	8.90 (1.20-65.86)
Crespo et al. (2013) (8)	Retrospective (2-left) analysis of renal transplant patients with pretransplant DSAs	Cohort	2006-2011	355	C1q	>2000	>500	Yes	Graft loss Rejection	0.83 (0.17-4.14) 1.44 (0.23-9.11)
Loupy et al. (2013) (6)	Consecutive adult patients in a retrospective (2-left) analysis; unselected global population with DSA detection before or after renal transplantation	Cohort	2004-2010	1,016	C1q	>500	>500	No	Graft loss	4.78 (2.69-8.49)
Freitas et al. (2013) (35)	Retrospective, single-centre analysis of renal transplant recipients selected on the basis of DSA detection during follow-up	Cohort	1999-2012	203	IgG3	>1000	>500	No	Graft loss	3.50 (1.30-9.50)

(Continued)

10.3389/fimmu.2023.1265796

TABLE 1 Continued

First author (date of publication)	Population	Study type	Period of inclusion	Sample size	Type of C′ anti-HLA DSA	MFI threshold for DSA detection	MFI threshold for complement positivity	EDTA pre-treatment	Outcome	Effect size (95% CI)
Arnold et al. (2014) (36)	Retrospective, single-centre analysis of renal transplant recipients without DSAs pre transplant and screened for *de novo* DSAs	Cohort	1997-2007	274	IgG3	>1000	>500	No	Graft loss	4.81 (1.65-14.03)
Smith et al. (2014) (37)	Retrospective, single-centre analysis of lung transplant recipients with pretransplant DSA detection	Cohort	1991-2003	63	C4d	500	Not reported	No	Graft loss	6.43 (2.96-13.97)
Everly et al. (2014) (38)	Retrospective, single-centre analysis of primary renal transplant recipients without pretransplant DSA detection	Cohort	1999-2006	179	IgG3	>1000	>1000	No	Graft loss	2.48 (1.02-6.04)
O'Leary et al. (2015) (39)	Retrospective, single-centre analysis of *f*consecutive patients with 1-year survival post liver transplantation; one group analysed pretransplant DSA effects, and another group analysed the impact of *de novo* DSAs	Cohort	2000-2009	1,270	C1q IgG3	>5000	>500	No	Graft loss Graft loss	1.90 (1.62-3.45) 2.40 (1.82-5.75)
Wozniak et al. (2015) (40)	Retrospective, single-centre analysis of paediatric liver transplant patients who were either nontolerant, tolerant, or stable	Cohort	NC	50	C1q	>1000	>1000	No	Rejection	4.30 (1.10-16.40)
Khovanova et al. (2015) (41)	Retrospective, single-centre analysis of HLA-incompatible desensitized renal transplant patients	Cohort	2003-2012	80	IgG3	>1000	Not reported	No	Graft loss	2.09 (0.30-14.60)
Sicard et al. (2015) (14)	Retrospective analysis of consecutive (2-left) adult renal transplant patients who developed AMR	Cohort	2004-2012	69	C3d C1q	>500	Not reported	No	Graft loss Graft loss	2.80 (1.12-6.95) 1.98 (0.95-4.14)
Thammanichanond et al. (2016) (42)	Retrospective, single-centre cohort study of patients with pre-transplant DSAs	Cohort	2009-2013	48	C1q	>1000	>500	No	Rejection	2.20 (0.61-7.85)
Comoli et al. (2016) (43)	Retrospective analysis of consecutive paediatric recipients; single centre; first kidney transplant without any HLA antibodies in sera or at the time of transplantation	Cohort	2002-2013	114	C3d C1q C3d C1q	>1000	>500	No	Rejection RejectionGraft loss Graft loss	6.91 (2.78-17.18) 13.54 (4.95-36.99) 27.80 (5.61-137.72) 11.09 (2.25-54.64)

(Continued)

10.3389/fimmu.2023.1265796

TABLE 1 Continued

First author (date of publication)	Population	Study type	Period of inclusion	Sample size	Type of C′ anti-HLA DSA	MFI threshold for DSA detection	MFI threshold for complement positivity	EDTA pre-treatment	Outcome	Effect size (95% CI)
Yamamoto et al. (2016) (44)	Retrospective analysis of renal transplant patients with *de novo* DSAs and surveillance biopsies	Cohort	2009-2013	43	C1q	>1000	>1000	No	Rejection	2.60 (0.12-53.90)
Calp-Inal et al. (2016) (7)	Retrospective analysis; single centre; consecutive renal transplant patients: Group 1 without pretransplant DSAs and Group 2 with a mix of pre-existing and *de novo* DSAs	Cohort	2009-2012	284	C1q	>1000	>500	No	Graft loss	4.30 (1.10-16.50)
Malheiro et al. (2016) (45)	Retrospective, single-centre analysis of kidney transplant patients with DSAs pre transplant	Cohort	2007-2012	60	C1q	>1000	>500	Yes	Rejection	16.80 (3.18-88.85)
Visentin et al. (2016) (46)	Retrospective, single-centre analysis of lung transplant patients with biopsy (with demonstration of rejection) and serum available	Cohort	1999-2014	53	C1q	>500	>500	No	Graft loss	1.65 (0.68-3.97)
Kauke et al. (2016) (47)	Retrospective, single-centre analysis of patients selected based on renal biopsy-proven rejection during graft dysfunction or viremia with polyomavirus BK	Cohort	2005-2011	611	C3d C1q	1000	Not reported	No	Graft loss Rejection	3.77 (1.40-10.16) 4.52 (1.89-10.37)
Bamoulid et al. (2016) (48)	Retrospective, single-centre analysis of renal transplant consecutive patients without DSAs pre transplant	Cohort	2007-2014	59	C1q	>1000	>300	No	Rejection Graft loss	2.27 (1.05-4.91) 6.78 (0.86-53.50)
Fichtner et al. (2016) (49)	Retrospective, single-centre analysis of prospectively screened renal transplant paediatric patients, non-presensitised	Cohort	1999-2010	62	C1q	>500	>300	No	Graft loss	6.35 (1.33-30.40)
Guidicelli et al. (2016) (50)	Retrospective, single-centre analysis of consecutive non-sensitized kidney transplant patients	Cohort	1998-2005	346	C1q	>500	Not reported	Yes	Graft loss	2.99 (0.94-10.27)
Lefaucheur et al. (2016) (51)	Retrospective analysis of consecutive patients (2-left); renal transplant patients were unselected	Cohort	2008-2010	125	IgG3 C1q	>500	>500	No	Graft loss Graft loss	4.80 (1.70-13.30) 3.60 (1.10-11.70)
Viglietti et al. (2017) (52)	Retrospective analysis of consecutive patients (2-left); renal transplant recipients were unselected	Cohort	2008-2011	851	IgG3 C1q	>1000	>500	No	Graft loss Graft loss	4.25 (1.88-9.61) 3.60 (1.71-7.59)
Wiebe et al. (2017) (53)	Retrospective analysis of consecutive adult and paediatric renal transplant patients, single centre; patients without pretransplant sensitization	Cohort	1999-2012	70	C1q	>300	>300	Yes	Graft loss	1.06 (0.50-2.40)
Moktefi et al. (2017) (9)	Retrospective analysis (2-left) of patients selected based on the development of acute renal AMR and the presence of DSAs	Cohort	2005-2012	48	C1q	>500	>500	No	Graft loss	0.79 (0.25-2.44)

(Continued)

10.3389/fimmu.2023.1265796

TABLE 1 Continued

First author (date of publication)	Population	Study type	Period of inclusion	Sample size	Type of C′ anti-HLA DSA	MFI threshold for DSA detection	MFI threshold for complement positivity	EDTA pre-treatment	Outcome	Effect size (95% CI)
Sicard et al. (2017) (54)	Retrospective analysis of consecutive adult renal transplant patients (2-left) with unselected patients	Cohort	2004-2012	52	C3d	500	>500	No	Graft loss	3.71 (1.27-10.80)
Das et al. (2017) (55)	Retrospective, single-centre analysis of paediatric heart transplant without DSAs pre transplantation and at the time of transplantation	Cohort	2005-2014	127	C1q	>1000	>500	No	Graft loss	3.20 (1.34-7.86)
Couchonnal et al. (2017) (56)	Retrospective analysis; single-centre analysis of consecutive paediatric liver transplant selected on the presence of DSAs during follow-up	Cohort	1990-2014	100	C3d	>500	>500	No	Graft loss	4.12 (0.95-17.89)
Bailly et al. (2017) (57)	Retrospective analysis of multi-centre, prospective, randomized, double-blind, placebo-controlled, parallel-group trials; patients selected on the basis of renal AMR development and DSA detection; patients treated either with standard of care (PP plus IVIg) or rituximab plus standard of care	Cohort	2008-2011	25	C1q	>500	>500	Yes	Graft loss	3.70 (0.80-17.00)
Molina et al. (2017) (58)	Retrospective analysis; single-centre analysis of consecutive adult kidney transplant patients selected on pretransplant DSA detection	Cohort	1995-2009	389	C1q	>1000	>500	No	Graft loss	4.01 (2.33-6.92)
Lan et al. (2018) (11)	Retrospective multi-centre analysis of adult kidney transplant patients selected on the presence of preformed DSA	Cohort	Before 2005	896	C3d	>500	>500	No	Graft loss	1.04 (0.37-2.94)
Courant et al. (2018) (12)	Retrospective single-centre analysis of adult kidney transplant patients selected on pre-transplant DSA detection	Cohort	2004-2013	192	C1q C3d	>500	>300	Yes	Graft loss Graft loss	1.74 (0.94-3.21) 1.01 (0.51-1.98)
Brugière et al. (2018) (59)	Retrospective, three-centre analysis of consecutive adult lung transplant patients selected on the presence of DSA during follow-up	Cohort	2009-2012	168	C1q	>500	>300	Yes	Graft loss	2.98 (1.33-6.66)
Kamburova et al. (2018) (60)	Retrospective multi-centre analysis of adult kidney transplant patients selected on the presence of preformed DSA	Cohort	1995-2005	567	C3d	>750	Not reported	No	Graft loss	1.02 (0.70-1.48)
Viglietti et al. (2018) (61)	Retrospective two-centre analysis of consecutive adult kidney transplant patients selected on the presence of DSA during follow-up	Cohort	2008-2011	139	C1q	>1000	Not reported	No	Graft loss	2.57 (1.29-5.12)
Lee H et al. (2018) (62)	Retrospective single-centre analysis of adult kidney transplant patients selected on the presence of *de novo* DSA	Cohort	1988-2016	161	C1q C3d	>1000	>1000	Yes	Graft loss Graft loss	2.90 (1.43-5.58) 2.82 (1.46-5.43) 18.5 (5.90-58.10) 8.10 (3.00-21.60)

(Continued)

10.3389/fimmu.2023.1265796

TABLE 1 Continued

First author (date of publication)	Population	Study type	Period of inclusion	Sample size	Type of C' anti-HLA DSA	MFI threshold for DSA detection	MFI threshold for complement positivity	EDTA pre-treatment	Outcome	Effect size (95% CI)
					C1q C3d				Rejection Rejection	
Malheiro et al. (2018) (63)	Retrospective single-centre analysis of consecutive adult kidney transplant patients selected on the presence of DSA during follow-up	Cohort	2008-2015	56	C1q	>1000	>500	No	Graft loss	3.94 (1.53-10.18)
Schinstock et al. (2018) (64)	Retrospective multi-centre analysis of adult solitary kidney transplant patients selected on the presence of DSA during follow-up	Cohort	1998-2015	113	C1q IgG3	>1000	>1000	No	Graft loss Graft loss	5.90 (2.30-15.60) 3.80 (1.50-9.30)
Lee DR et al. (2018) (13)	Retrospective single-left analysis of adult solitary kidney transplant patients selected on the presence of DSA during follow-up	Cohort	2013-2016	220	C3d	>500	>500	No	Graft loss	3.02 (1.52-12.12)
Babu et al. (2020) (65)	Retrospective multi-left analysis of adult solitary kidney transplant patients selected on the presence of DSA during follow-up	Cohort	2005-2015	139	C3d	Not reported	Not reported	No	Graft loss	4.56 (1.46-14.4)
Vargas et al. (2020) (66)	Retrospective single-left analysis of adult solitary kidney transplant patients selected on the presence of DSA during follow-up	Cohort	2003-2014	86	C1q	>1000	Not reported	No	Graft loss	1.09 (0.42-2.78)
Zhang et al. (2018) (67)	Retrospective single-centre analysis of paediatric heart transplant patients selected on the presence of DSA during follow-up	Cohort	2010-2013	176	C3d	>1000	>1000	No	Rejection	33.0 (8.10-138)
Cioni et al. (2019) (68)	Retrospective single-centre analysis of consecutive adult kidney transplant patients selected on the presence of *de novo* DSA	Cohort	2002-2014	69	C1q C3d	>1000	>500	No	Rejection Rejection	0.80 (0.20-3.10) 10.10 (1.50-68.30)
Hayde et al. (2020) (69)	Retrospective single-centre analysis of paediatric kidney transplant patients selected on the presence of *de novo* DSA	Cohort	2009-2016	48	C1q	>1000	>500	No	Rejection	10.10 (2.00-51.80)
Pernin et al. (2020) (70)	Retrospective two-centre analysis of adult kidney transplant patients selected on the presence of *de novo* DSA	Cohort	2014-2018	69	IgG3	>1000	Not reported	Yes	Rejection	11.15 (2.24-55.37)

Effect sizes refer to HR for allograft loss and OR for rejection appearance.
C', complement; C1q, complement component 1q; CI, confidence interval; DSA, donor-specific antibody; HR, hazard ratio; IgG3, immunoglobulin G3; OR, odds ratio.

10.3389/fimmu.2023.1265796

10.3389/fimmu.2023.1265796

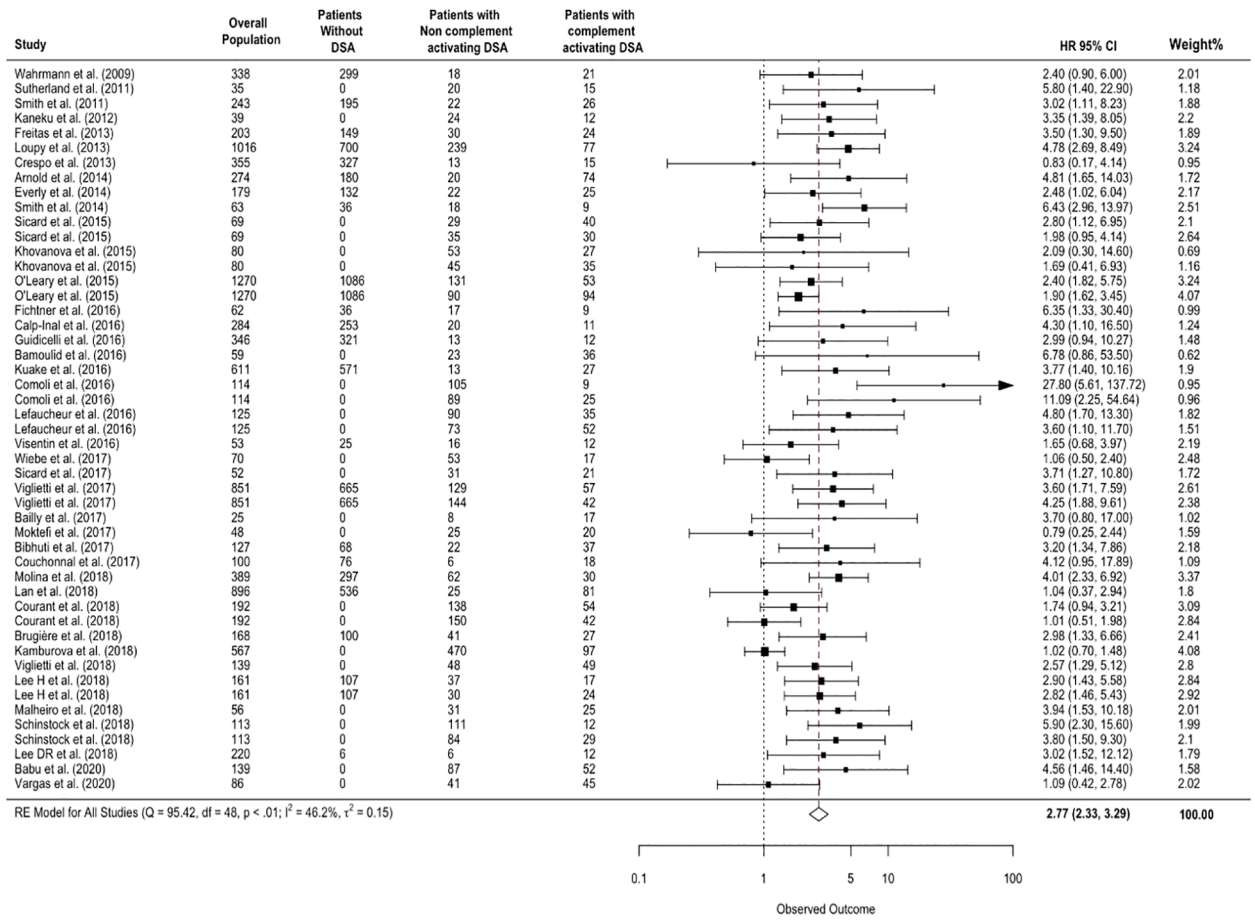

FIGURE 2
Association between circulating complement-activating anti-HLA DSAs and the risk of allograft loss. The figure shows the forest plot of the association between complement-activating anti-HLA DSAs and the risk of allograft loss for each complement binding study and overall (n = 49). Studies are listed by date of publication. Number of patients are listed in the 4 cohort columns. The black square-shaped boxes represent the HR for each individual study. The size of these boxes represents the weight of the study, and lines represent the 95% CI for individual studies. The diamond at the bottom represents the pooled HR. The number of patients in the overall population does not correspond to the sum of the different groups for the studies of Kaneku et al. (32) (3 patients), Sicard et al. (14) (4 patients), and Moktefi et al. (9) (3 patients) either because the data for these patients were missing or because they were not involved in the analysis. CI, confidence interval; DSA, donor-specific antibody; HLA, human leukocyte antigen; HR, hazard ratio.

organs showed an increased risk for allograft loss, however, the results were not statistically significant due to the low number of studies found (Supplementary Table 2).

3.5.4 Effect of complement-activating anti-HLA DSAs according to the timing of antibody detection

Analysis according to the time of antibody detection all showed significant associations with the highest HR of 3.53 for *de novo* DSAs (CI 2.63-4.74, p<0.001; I^2 = 26%).

3.5.5 Analysis according to the type of complement-activating antibodies

Analysis across the different types of complement-activating antibodies showed significant overall effect on allograft loss. The following groups were assessed: (i) C1q-binding capacity (HR 2.72; 95% CI 2.19-3.38, P<0.001; I^2 = 35.8%), (ii) C4d-binding capacity (HR 3.81; 95% CI 2.02-7.20, p<0.001; I^2 = 33%), (iii) C3d-binding capacity (HR 2.50; 95% CI 1.48-4.25, p<0.001; I^2 = 73.1%), (iv) IgG3 subclass (HR 3.17; 95% CI 2.37-4.24, p<0.001; I^2 = 0.0%).

3.5.6 Analysis according to MFI thresholds for complement-activating anti-HLA DSA positivity

6 (15.0%) studies used 300 as an MFI threshold for complement-activating anti-HLA DSA positivity, 1 (2.5%) study used 450, 21 (52.5%) studies used 500, 2 (5.0%) studies used 1000, and 11 (27.5%) studies did not provide the threshold value. The risk of allograft loss remained significantly increased at all complement-activating anti-HLA DSA positivity thresholds: (i) MFI 300 (HR 2.74; 95% CI 1.91-3.93, p<0.001; I^2 = 36.7%), (ii) MFI 500 (HR 2.96; 95% CI 2.29-3.82, p<0.001; I^2 = 47.8%), (iii) MFI 1000 (HR 2.37; 95% CI 1.7-3.29, p<0.001; I^2 = 49.1%).

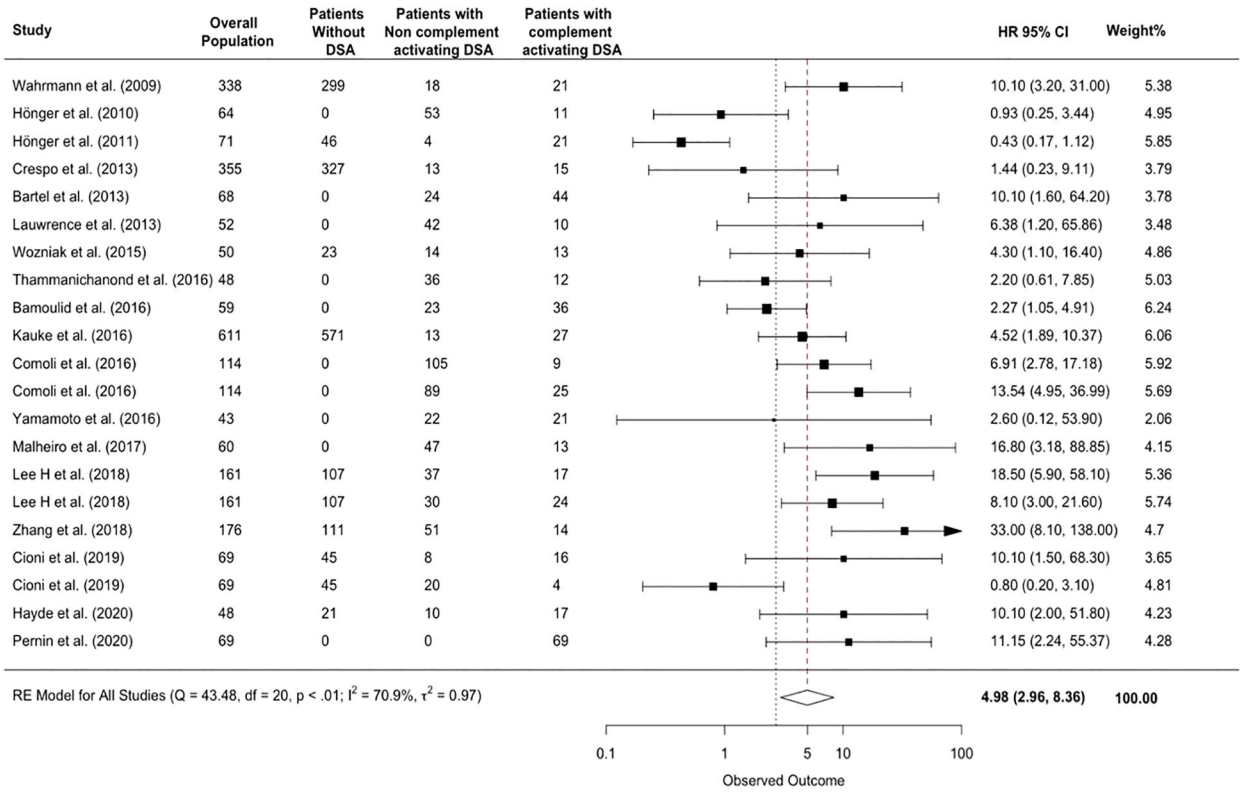

FIGURE 3
Association between complement-activating anti-HLA DSAs and the risk of rejection. The figure shows the forest plot of the association between complement activating anti-HLA DSAs and the risk of rejection for each study and overall (n = 17). Studies are listed by date of publication. The black square-shaped boxes represent the HR for each individual study. The black square-shaped boxes represent the HR for each individual study. The size of these boxes represents the weight of the study, and lines represent the 95% CI for individual studies. The diamond at the bottom represents the overall HR. CI, confidence interval; DSA, donor-specific antibody; HLA, human leukocyte antigen; HR, hazard ratio.

3.6 Sensitivity analysis

The separate meta-analysis of the 15 newly identified studies since the publication of the previous review in 2018 showed that patients with complement-activating anti-HLA DSAs had a 2.21-fold increase in risk for allograft loss (95% CI 1.61-3.04; p<0.001; I^2 = 58.8) (Supplementary Figure 1) and a 8.87-fold increase in risk for allograft rejection (95% CI 3.64-21.6; p<0.001; I^2 = 65.3%) compared to patients without complement-activating anti-HLA DSA, patients without anti-HLA DSAs, and a mixed group of both (Supplementary Figure 2).

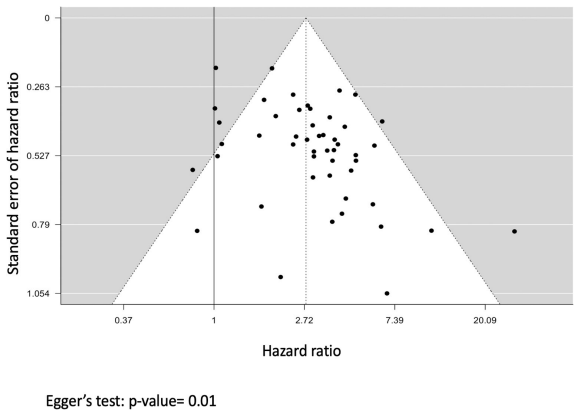

FIGURE 4
Funnel plot representing the analysis for small-study effects. Each black dot represents a study; the x-axis represents the study effect size (hazard ratio), and the y-axis represents the standard error of the hazard ratio. The dashed vertical line represents the overall risk estimate and the black line represents the no intervention effect.

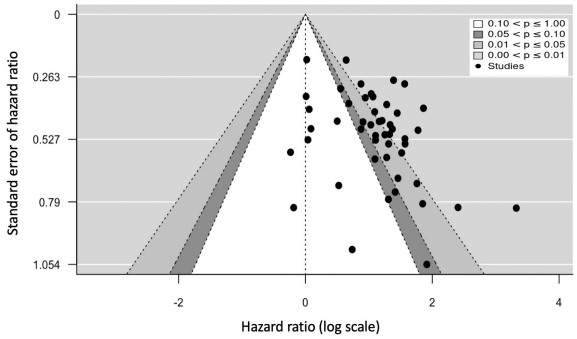

FIGURE 5
Contour-enhanced funnel plot representing the analysis for publication bias according to the statistical significance of studies. Each black dot represents a study; the x-axis represents the study effect size (hazard ratio), and the y-axis represents the standard error of the hazard ratio.

TABLE 2 Effect sizes related to the different subgroup analyses.

Subgroup analyses for allograft survival		Effect size	95% CI	I^2, p-value
Effect of complement-activating anti-HLA DSAs in studies with high or low methodological quality	High-methodological quality studies NOS ≥6	2.79	2.33-3.35	45.7%, p<0.001
	Low-methodological quality studies NOS ≤ 5	2.46	1.28-4.70	60.5%, p<0.001
Effect of complement-activating anti-HLA DSAs in studies with different comparators used	Studies comparing index group and patients with non-complement-activating anti-HLA DSAs	2.56	1.99-3.30	54.2%, p< 0.001
	Studies comparing index group and patients with non-complement-activating anti-HLA DSAs and without anti-HLA DSAs	3.58	2.70-4.74	4.1%, p<0.001
Effect of complement-activating anti-HLA DSAs according to the type of solid organ transplant	Kidney transplantation studies only	2.77	2.25-3.41	49.2%, p< 0.001
	Heart, lung, and liver transplantation studies	2.74	2.03-3.69	29.2%, p<0.001
Effect of complement-activating anti-HLA DSAs according to the timing of antibody detection	Pre-existing DSAs	2.56	1.99-3.30	56.2%, p< 0.001
	Pre-existing and *de novo* DSAs	2.59	2.05-3.26	34.3%, p<0.001
	De novo DSAs	3.53	2.63-4.74	26.0%, p<0.001
Effect of complement-activating anti-HLA DSAs according to the type of test used for detecting complement-activating antibodies	C1q	2.72	2.19-3.38	35.8%, p= 0.001
	C4d	3.81	2.02-7.2	33.0%, p= 0.001
	C3d	2.50	1.48-4.25	73.1%, p< 0.001
	IgG3	3.17	2.37-4.24	0.00%, p<0.001
Effect of complement-activating anti-HLA DSAs according to the MFI thresholds for complement-activating anti-HLA DSA positivity	300	2.74	1.91-3.93	36.7%, p<0.001
	500	2.29	2.29-3.82	47.8%, p<0.001
	1000	2.37	1.7-3.29	49.1%, p<0.001

Effect sizes refer to HR for graft survival and OR for rejection appearance. The Index group refers to patients with complement-activating anti-HLA DSAs.
DSA, donor-specific antibody; C1q, complement component 1q; CI, confidence interval; HR, hazard ratio; HLA, human leukocyte antigen; I^2, heterogeneity; IgG3, immunoglobulin G3; MFI, MFI, Mean fluorescent intensity, NOS, Newcastle-Ottawa scale; OR, odds ratio.

3.7 Cumulative meta-analysis

The cumulative meta-analysis showed the effect of adding new studies in a chronological order on the overall effect size (Supplementary Figure 4). Starting at the second study in 2011 till the end of analysis, there is a consistent and statistically significant risk of allograft loss.

The cumulative meta-analysis demonstrated that adding new studies: i) narrowed the confidence intervals of the overall effect size, ii) reduced the already statistically significant p-values, iii) converged the overall effect size of complement- activating antibodies on allograft loss.

3.8 Added prognostic value of complement-activating anti-HLA DSA status over anti-HLA DSA MFI level on allograft loss

26 (50%) studies reported positive correlation between complement-activating anti-HLA DSA and pan-IgG anti-HLA DSA level defined by the MFI. 15 (37.5%) studies performed multivariable analyses adjusting complement-activating anti-HLA DSA status on pan-IgG anti-HLA DSA defined by the MFI levels as opposed to a linear univariable correlation analysis. The multivariable analysis demonstrated that complement-activating anti-HLA DSA's presence was significantly and independently associated with an increased risk of allograft loss (HR 2.77; 95% CI 2.13-3.6, p=0.017; I^2 = 45.4%) (Figure 6).

Seven (13.5%) studies pre-treated the sera of the studied population, or a sample of the studied population, with EDTA to uncover interfering substances and only 3 studies (5.8%) performed a multivariable analysis models adjusting complement-activating anti-HLA DSA status on EDTA treated pan-IgG anti-HLA DSA assays.

3.9 Added prognostic value of complement-activating anti-HLA DSA status over anti-HLA DSA class type

Among the 29 (55.8%) studies that used multivariate analysis to evaluate the risk of allograft loss, only three (5.8%) studies included DSA class as a predictive variable. Among these three studies, two showed that HLA class II DR was significantly associated with graft loss. Complement activating anti-HLA DSA remained independently associated with an increased risk for graft loss HR=3.76 (CI=2.33-6.06;

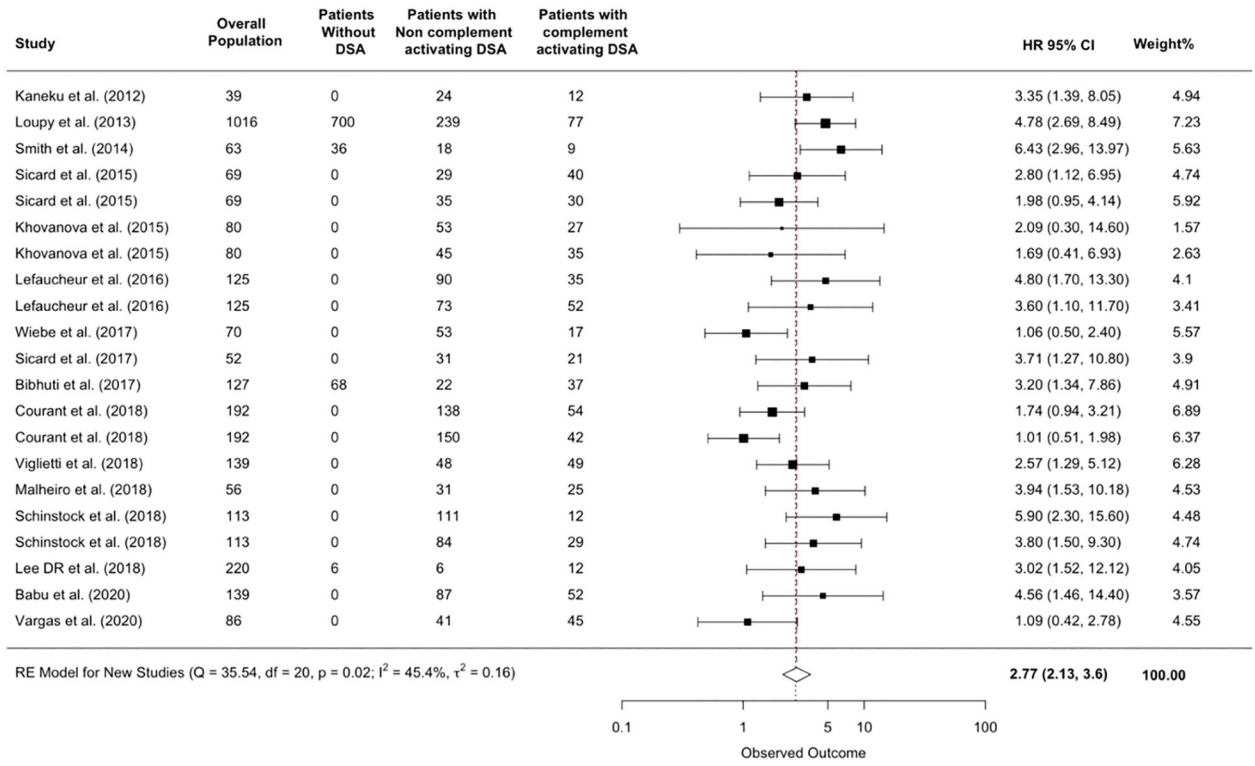

FIGURE 6
Added prognostic value of complement-activating anti-HLA DSA status over anti-HLA DSA MFI level on allograft loss. The figure shows the forest plot of the association between complement-activating anti-HLA DSAs and the risk of allograft loss for each c study that included the anti-HLA DSA MFI level in their evaluation of the prognostic value of complement-activating anti-HLA DSA. Number of patients are listed in the 4 cohort columns. The black square-shaped boxes represent the HR for each individual study. The size of these boxes represents the weight of the study, and lines represent the 95% CI for individual studies. The diamond at the bottom represents the pooled HR. CI, confidence interval; DSA, donor-specific antibody; HLA, human leukocyte antigen; HR, hazard ratio.

p=0.626; I2 = 0%) however, the results were statistically insignificant due to the low number of studies that included DSA type in the multivariable models.

4 Discussion

4.1 Study overview

In this systematic review, meta-analysis, and critical appraisal including 11,035 solid organ recipients, we confirmed the increased risk of allograft failure and rejection associated with complement-binding anti-HLA DSAs. To the best of our knowledge, this is the first comprehensive systematic review and meta-analysis on the topic and the first in-depth critical appraisal assessing for the risk of bias, adjusting for it and providing several subgroup analyses to study the association of complement-binding anti-HLA DSAs with allograft outcomes. We also addressed the utility of complement-activating anti-HLA DSAs assessment over anti-HLA DSA MFI levels.

4.2 Subgroup analyses findings

This meta-analysis showed consistent results in multiple subgroup analyses. Complement-activating anti-HLA DSA were associated with an increased risk for allograft loss in higher quality studies, in different types of complement-activating anti-HLA DSAs (C1q, C3d, C4d and IgG3), at different times of evaluation for complement-activating anti-HLA DSA status (before and after transplantation) and at different MFI thresholds for complement-activating anti-HLA DSA positivity.

4.3 Cumulative meta-analysis findings

The cumulative meta-analysis further illustrated the significant overall effect of complement activating anti-HLA DSAs on allograft loss. Combining this finding with our findings from the subgroup analyses, we can perceive saturation of knowledge in particular in kidney transplant recipients and C1q evaluations. This is due to the fact that the majority of patients assessed were kidney recipients (78%) who were tested for C1q (54%) and therefore further research in this particular area could be redundant. However, there remains some areas that could benefit from further exploration, for instance, we did not identify any studies on the effect of complement-binding anti-HLA DSAs in pancreas and intestine transplants. In addition, more studies in liver, lung and heart recipients could be beneficial to confirm the initial findings by increasing the sample size and by comparing the risk of allograft loss across different organ transplants.

4.4 Added prognostic value of complement-activating anti-HLA DSA status over anti-HLA DSA MFI level

Several studies in this meta-analysis and in the literature (53, 71, 72) indicated a strong correlation between complement-activating antibody status and anti-HLA DSA MFI level. Interestingly, studies included in this meta-analysis that performed multivariable analyses for the assessment of the independent prognostic value of complement-activating anti-HLA DSA adjusted on pan-IgG anti-HLA DSA defined by the MFI levels, showed that the association between C1q, C3d, C4d-binding tests or IgG3 test and allograft lost was independent of anti-HLA DSA MFI levels.

Although the absence of DSA complement binding antibodies should not be considered as a lack of the harmful effects of DSA *in vivo*, our meta-analysis supports a clinical utility of performing complement-binding assays. Indeed, the clinical impact remains significantly associated with graft loss independent of anti-HLA DSA MFI levels.

In addition to the uncertain association between the MFI levels and the clinical significance of an antibody, SAB pan-IgG assay remains a semi-quantitative test and technical limitations have been raised such as significant variations in repeated testing, between different laboratories (73), and due to various interfering substances (74). In addition, even though some studies addressed interfering substances by pretreatment of sera with EDTA (12, 13, 50, 53, 59), several limitations were noted; the EDTA concentrations were inconsistent across the studies, two studies only pretreated a small sample of the studied populations (4-8 patients), and the prognostic advantage of EDTA treated sera over complement assays was not demonstrated.

Therefore, our study shows that the use of complement binding anti-HLA DSA in clinical practice, in complement to MFI levels, which remains gold standard, could enhance risk stratification.

4.5 Added prognostic value of complement-activating anti-HLA DSA status over anti-HLA DSA class

We could not show independent association of complement-activating anti-HLA DSA status over HLA-DSA class due insufficient data published so far (only 3 studies). Further studies should therefore investigate the independent impact of class I or class II anti-HLA DSA regardless of their ability to activate complement, but also investigate the clinical impact of class I versus class II complement-activating anti-HLA DSA.

4.6 Implications

This study addresses several gaps highlighted by the STAR working group including the strong evidence regarding the prognostic role of complement-activating anti-HLA DSA in allograft rejection and loss, in complement to HLA-DSA titre and MFI assessment. This strongly supports a potential role for this test in clinical practice. and encourages interventional research regarding the role of certain drugs that target complement-dependent cytotoxicity as a prophylaxis and/or treatment of antibody-mediated rejection and the value of a complement-activating anti-HLA DSA based strategy to monitor organ transplant patients to demonstrate clinical benefit and improvement of allograft survival.

4.7 Limitations

This study has the following limitations. First, we only included studies that provided a clear effect size for allograft loss or rejection (hazard or odds ratio). Second, No data was available from South America, Africa and Australia to reinforce the generalizability of the results. Third, all of the included studies were observational and retrospective. Finally, the review only included studies written in English.

5 Conclusion

The results of this systematic review, meta-analysis and critical appraisal support the significant and independent detrimental effects of complement-activating anti-HLA DSAs on allograft outcomes. This study highlights areas that need further exploration in complement-activating anti-HLA DSAs research, and encourages the clinical evaluation of complement-activating anti-HLA DSA testing to improve risk stratification and tailoring treatment regimens.

Data availability statement

The raw data supporting the conclusions of this article will be made available upon reasonable request.

Author contributions

S-AA: Conceptualization, Data curation, Formal analysis, Investigation, Methodology, Software, Writing- original draft, Writing- review & editing. MR: Formal analysis, Methodology, Supervision, Validation, Writing- review & editing. KL: Methodology, Supervision, Validation, Writing- review & editing. AB: Data curation, Formal analysis, Investigation, Methodology, Validation, Writing- original draft, Writing- review & editing. J-LT: Validation, Writing- review & editing. OA: Methodology, Validation, Writing- review & editing. AL: Conceptualization, Methodology, Project administration, Supervision, Validation, Writing- review & editing. CL: Conceptualization, Funding acquisition, Methodology, Project administration, Resources, Supervision, Writing- review & editing.

Funding

The authors declare that no financial support was received for the research, authorship, and/or publication of this article.

Conflict of interest

The authors declare that the research was conducted in the absence of any commercial or financial relationships that could be construed as a potential conflict of interest.

Publisher's note

Supplementary material

The Supplementary Material for this article can be found online at: https://www.frontiersin.org/articles/10.3389/fimmu.2023.1265796/full#supplementary-material

References

1. Sellarés J, de Freitas DG, Mengel M, Reeve J, Einecke G, Sis B, et al. Understanding the causes of kidney transplant failure: the dominant role of antibody-mediated rejection and nonadherence. *Am J Transplant Off J Am Soc Transplant Am Soc Transpl Surg* (2012) 12(2):388–99. doi: 10.1111/j.1600-6143.2011.03840.x

2. Loupy A, Hill GS, Jordan SC. The impact of donor-specific anti-HLA antibodies on late kidney allograft failure. *Nat Rev Nephrol* (2012) 8(6):348–57. doi: 10.1038/nrneph.2012.81

3. Morrell MR, Pilewski JM, Gries CJ, Pipeling MR, Crespo MM, Ensor CR, et al. *De novo* donor-specific HLA antibodies are associated with early and high-grade bronchiolitis obliterans syndrome and death after lung transplantation. *J Heart Lung Transplant Off Publ Int Soc Heart Transplant* (2014) 33(12):1288–94. doi: 10.1016/j.healun.2014.07.018

4. Ho EK, Vlad G, Vasilescu ER, de la Torre L, Colovai AI, Burke E, et al. Pre- and posttransplantation allosensitisation in heart allograft recipients: major impact of *de novo* alloantibody production on allograft survival. *Hum Immunol* (2011) 72(1):5–10. doi: 10.1016/j.humimm.2010.10.013

5. O'Leary JG, Kaneku H, Susskind BM, Jennings LW, Neri MA, Davis GL, et al. High mean fluorescence intensity donor-specific anti-HLA antibodies associated with chronic rejection Postliver transplant. *Am J Transplant Off J Am Soc Transplant Am Soc Transpl Surg* (2011) 11(9):1868–76. doi: 10.1111/j.1600-6143.2011.03593.x

6. Loupy A, Lefaucheur C, Vernerey D, Prugger C, van Huyen JPD, Mooney N, et al. Complement-binding anti-HLA antibodies and kidney-allograft survival. *N Engl J Med* (2013) 369(13):1215–26. doi: 10.1056/NEJMoa1302506

7. Calp-Inal S, Ajaimy M, Melamed ML, Savchik C, Masiakos P, Colovai A, et al. The prevalence and clinical significance of C1q-binding donor-specific anti-HLA antibodies early and late after kidney transplantation. *Kidney Int* (2016) 89(1):209–16. doi: 10.1038/ki.2015.275

8. Crespo M, Torio A, Mas V, Redondo D, Pérez-Sáez MJ, Mir M, et al. Clinical relevance of pretransplant anti-HLA donor-specific antibodies: does C1q-fixation matter? *Transpl Immunol* (2013) 29(1–4):28–33. doi: 10.1016/j.trim.2013.07.002

9. Moktefi A, Parisot J, Desvaux D, Canoui-Poitrine F, Brocheriou I, Peltier J, et al. C1q binding is not an independent risk factor for kidney allograft loss after an acute antibody-mediated rejection episode: a retrospective cohort study. *Transpl Int Off J Eur Soc Organ Transplant* (2017) 30(3):277–87. doi: 10.1111/tri.12905

10. Bouquegneau A, Loheac C, Aubert O, Bouatou Y, Viglietti D, Empana JP, et al. Complement-activating donor-specific anti-HLA antibodies and solid organ transplant

survival: A systematic review and meta-analysis. *PloS Med* (2018) 15(5):e1002572. doi: 10.1371/journal.pmed.1002572

11. Lan JH, Gjertson D, Zheng Y, Clark SDeKAF Investigators, , Reed EF, et al. Clinical utility of complement-dependent C3d assay in kidney recipients presenting with late allograft dysfunction. *Am J Transplant Off J Am Soc Transplant Am Soc Transpl Surg* (2018) 18(12):2934–44. doi: 10.1111/ajt.14871

12. Courant M, Visentin J, Linares G, Dubois V, Lepreux S, Guidicelli G, et al. The disappointing contribution of anti-human leukocyte antigen donor-specific antibodies characteristics for predicting allograft loss. *Nephrol Dial Transplant* (2018) 33 (10):1853–63. doi: 10.1093/ndt/gfy088

13. Lee DR, Kim BC, Kim JP, Kim IG, Jeon MY. C3d-binding donor-specific HLA antibody is associated with a high risk of antibody-mediated rejection and graft loss in stable kidney transplant recipients: A single-centre cohort study. *Transplant Proc* (2018) 50(10):3452–9. doi: 10.1016/j.transproceed.2018.06.037

14. Sicard A, Ducreux S, Rabeyrin M, Couzi L, McGregor B, Badet L, et al. Detection of C3d-binding donor-specific anti-HLA antibodies at diagnosis of humoral rejection predicts renal graft loss. *J Am Soc Nephrol JASN* (2015) 26(2):457–67. doi: 10.1681/ASN.2013101144

15. Moher D, Liberati A, Tetzlaff J, Altman DG. Preferred reporting items for systematic reviews and meta-analyses: the PRISMA statement. *BMJ* (2009) 339:b2535. doi: 10.1371/journal.pmed.1000097

16. Sampson M, de Bruijn B, Urquhart C, Shojania K. Complementary approaches to searching MEDLINE may be sufficient for updating systematic reviews. *J Clin Epidemiol* (2016) 78:108–15. doi: 10.1016/j.jclinepi.2016.03.004

17. Garner P, Hopewell S, Chandler J, MacLehose H, Akl EA, Beyene J, et al. When and how to update systematic reviews: consensus and checklist. *BMJ* (2016) 354:i3507. doi: 10.1136/bmj.i3507

18. Ottawa Hospital Research Institute. (2021). Available at: http://www.ohri.ca/programs/clinical_epidemiology/oxford.asp.

19. *Cochrane handbook for systematic reviews of interventions* (2021). Available at: https://training.cochrane.org/handbook.

20. Egger M, Smith GD, Schneider M, Minder C. Bias in meta-analysis detected by a simple, graphical test. *BMJ* (1997) 315(7109):629–34. doi: 10.1136/bmj.315.7109.629

21. van Aert RCM, Wicherts JM, van Assen MALM. Publication bias examined in meta-analyses from psychology and medicine: A meta-meta-analysis. *PloS One* (2019) 14(4):e0215052.

22. Peters JL, Sutton AJ, Jones DR, Abrams KR, Rushton L. Contour-enhanced meta-analysis funnel plots help distinguish publication bias from other causes of asymmetry. *J Clin Epidemiol* (2008) 61(10):991–6. doi: 10.1016/j.jclinepi.2007.11.010

23. McPheeters ML, Kripalani S, Peterson NB, Idowu RT, Jerome RN, Potter SA, et al. Closing the quality gap: revisiting the state of the science (vol. 3: quality improvement interventions to address health disparities). *Evid ReportTechnology Assess* (2012) 208.3):1–475.

24. Lau J, Schmid CH, Chalmers TC. Cumulative meta-analysis of clinical trials builds evidence for exemplary medical care. *J Clin Epidemiol* (1995) 48(1):45–57; discussion 59-60. doi: 10.1016/0895-4356(94)00106-Z

25. Mullen B, Muellerleile P, Bryant B. Cumulative meta-analysis: A consideration of indicators of sufficiency and stability. *Sage Journals* (2001) 27(11). doi: 10.1177/01461672012711006

26. Konvalinka A, Tinckam K. Utility of HLA antibody testing in kidney transplantation. *J Am Soc Nephrol* (2015) 26(7):1489–502. doi: 10.1681/ASN.2014080837

27. Wahrmann M, Bartel G, Exner M, Regele H, Körmöczi GF, Fischer GF, et al. Clinical relevance of preformed C4d-fixing and non-C4d-fixing HLA single antigen reactivity in renal allograft recipients. *Transpl Int Off J Eur Soc Organ Transplant* (2009) 22(10):982–9. doi: 10.1111/j.1432-2277.2009.00912.x

28. Hönger G, Wahrmann M, Amico P, Hopfer H, Böhmig GA, Schaub S. C4d-fixing capability of low-level donor-specific HLA antibodies is not predictive for early antibody-mediated rejection. *Transplantation* (2010) 89(12):1471–5. doi: 10.1097/TP.0b013e3181dc13e7

29. Sutherland SM, Chen G, Sequeira FA, Lou CD, Alexander SR, Tyan DB. Complement-fixing donor-specific antibodies identified by a novel C1q assay are associated with allograft loss. *Pediatr Transplant* (2012) 16(1):12–7. doi: 10.1111/j.1399-3046.2011.01599.x

30. Hönger G, Hopfer H, Arnold ML, Spriewald BM, Schaub S, Amico P. Pretransplant IgG subclasses of donor-specific human leukocyte antigen antibodies and development of antibody-mediated rejection. *Transplantation* (2011) 92(1):41–7. doi: 10.1097/TP.0b013e31821cdf0d

31. Smith JD, Banner NR, Hamour IM, Ozawa M, Goh A, Robinson D, et al. *De novo* donor HLA-specific antibodies after heart transplantation are an independent predictor of poor patient survival. *Am J Transplant* (2011) 11(2):312–9. doi: 10.1111/j.1600-6143.2010.03383.x

32. Kaneku H, O'Leary JG, Taniguchi M, Susskind BM, Terasaki PI, Klintmalm GB. Donor-specific human leukocyte antigen antibodies of the immunoglobulin G3 subclass are associated with Chronic rejection and graft loss after liver transplantation. *Liver Transpl* (2012) 18(8):984–92. doi: 10.1002/lt.23451

33. Bartel G, Wahrmann M, Schwaiger E, Kikić Ž, Winzer C, Hörl WH, et al. Solid phase detection of C4d-fixing HLA antibodies to predict rejection in high immunological risk kidney transplant recipients. *Transpl Int* (2013) 26(2):121–30. doi: 10.1111/tri.12000

34. Lawrence C, Willicombe M, Brookes PA, Santos-Nunez E, Bajaj R, Cook T, et al. Preformed complement-activating low-level donor-specific antibody predicts early antibody-mediated rejection in renal allografts. *Transplantation* (2013) 95(2):341–6. doi: 10.1097/TP.0b013e3182743cfa

35. Freitas MCS, Rebellato LM, Ozawa M, Nguyen A, Sasaki N, Everly M, et al. The role of immunoglobulin-G subclasses and C1q in *de novo* HLA-DQ donor-specific antibody kidney transplantation outcomes. *Transplantation* (2013) 95(9):1113–9. doi: 10.1097/TP.0b013e3182888db6

36. Arnold ML, Ntokou IS, Doxiadis IIN, Spriewald BM, Boletis JN, Iniotaki AG. Donor-specific HLA antibodies: evaluating the risk for graft loss in renal transplant recipients with isotype switch from complement fixing IgG1/IgG3 to noncomplement fixing IgG2/IgG4 anti-HLA alloantibodies. *Transpl Int* (2014) 27(3):253–61. doi: 10.1111/tri.12206

37. Smith JD, Ibrahim MW, Newell H, Danskine AJ, Soresi S, Burke MM, et al. Pre-transplant donor HLA-specific antibodies: Characteristics causing detrimental effects on survival after lung transplantation. *J Heart Lung Transplant* (2014) 33(10):1074–82. doi: 10.1016/j.healun.2014.02.033

38. Everly MJ, Rebellato LM, Haisch CE, Briley KP, Bolin P, Kendrick WT, et al. Impact of IgM and IgG3 anti-HLA alloantibodies in primary renal allograft recipients. *Transplantation* (2014) 97(5):494–501. doi: 10.1097/01.TP.0000441362.11232.48

39. O'Leary JG, Kaneku H, Banuelos N, Jennings LW, Klintmalm GB, Terasaki PI. Impact of igG3 subclass and C1q-fixing donor-specific HLA alloantibodies on rejection and survival in liver transplantation. *Am J Transplant* (2015) 15(4):1003–13. doi: 10.1111/ajt.13153

40. Wozniak LJ, Hickey MJ, Venick RS, Vargas JH, Farmer DG, Busuttil RW, et al. Donor-specific HLA antibodies are associated with late allograft dysfunction after paediatric liver transplantation. *Transplantation* (2015) 99(7):1416–22. doi: 10.1097/TP.0000000000000796

41. Khovanova N, Daga S, Shaikhina T, Krishnan N, Jones J, Zehnder D, et al. Subclass analysis of donor HLA-specific IgG in antibody-incompatible renal transplantation reveals a significant association of IgG4 with rejection and graft failure. *Transpl Int* (2015) 28(12):1405–15. doi: 10.1111/tri.12648

42. Thammanichanond D, Wiwattanathum P, Mongkolsuk T, Kantachuvesiri S, Worawichawong S, Vallipakorn SA, et al. Role of pretransplant complement-fixing donor-specific antibodies identified by C1q assay in kidney transplantation. *Transplant Proc* (2016) 48(3):756–60. doi: 10.1016/j.transproceed.2015.12.116

43. Comoli P, Cioni M, Tagliamacco A, Quartuccio G, Innocente A, Fontana I, et al. Acquisition of C3d-binding activity by *de novo* donor-specific HLA antibodies correlates with graft loss in nonsensitised pediatric kidney recipients. *Am J Transplant Off J Am Soc Transplant Am Soc Transpl Surg* (2016) 16(7):2106–16. doi: 10.1111/ajt.13700

44. Yamamoto T, Watarai Y, Takeda A, Tsujita M, Hiramitsu T, Goto N, et al. *De novo* anti-HLA DSA characteristics and subclinical antibody-mediated kidney allograft injury. *Transplantation* (2016) 100(10):2194–202. doi: 10.1097/TP.0000000000001012

45. Malheiro J, Tafulo S, Dias L, Martins LS, Fonseca I, Beirão I, et al. Determining donor-specific antibody C1q-binding ability improves the prediction of antibody-mediated rejection in human leucocyte antigen-incompatible kidney transplantation. *Transpl Int* (2017) 30(4):347–59. doi: 10.1111/tri.12873

46. Visentin J, Chartier A, Massara L, Linares G, Guidicelli G, Blanchard E, et al. Lung intragraft donor-specific antibodies as a risk factor for graft loss. *J Heart Lung Transplant* (2016) 35(12):1418–26. doi: 10.1016/j.healun.2016.06.010

47. Kauke T, Oberhauser C, Lin V, Coenen M, Fischereder M, Dick A, et al. *De novo* donor-specific anti-HLA antibodies after kidney transplantation are associated with impaired graft outcome independently of their C1q-binding ability. *Transpl Int* (2017) 30(4):360–70. doi: 10.1111/tri.12887

48. Bamoulid J, Roodenburg A, Staeck O, Wu K, Rudolph B, Brakemeier S, et al. Clinical outcome of patients with *de novo* C1q-binding donor-specific HLA antibodies after renal transplantation. *Transplantation* (2017) 101(9):2165–74. doi: 10.1097/TP.0000000000001487

49. Fichtner A, Süsal C, Höcker B, Rieger S, Waldherr R, Westhoff JH, et al. Association of C1q-fixing DSA with late graft failure in paediatric renal transplant recipients. *Pediatr Nephrol* (2016) 31(7):1157–66. doi: 10.1007/s00467-016-3322-8

50. Guidicelli G, Guerville F, Lepreux S, Wiebe C, Thaunat O, Dubois V, et al. Non-complement–binding *de novo* donor-specific anti-HLA antibodies and kidney allograft survival. *J Am Soc Nephrol* (2016) 27(2):615–25. doi: 10.1681/ASN.2014040326

51. Lefaucheur C, Viglietti D, Bentlejewski C, van Huyen JPD, Vernerey D, Aubert O, et al. IgG donor-specific anti-human HLA antibody subclasses and kidney allograft antibody-mediated injury. *J Am Soc Nephrol* (2016) 27(1):293–304. doi: 10.1681/ASN.2014111120

52. Viglietti D, Loupy A, Vernerey D, Bentlejewski C, Gosset C, Aubert O, et al. Value of donor–specific anti–HLA antibody monitoring and characterization for risk stratification of kidney allograft loss. *J Am Soc Nephrol* (2017) 28(2):702–15. doi: 10.1681/ASN.2016030368

53. Wiebe C, Gareau AJ, Pochinco D, Gibson IW, Ho J, Birk PE, et al. Evaluation of C1q status and titer of *de novo* donor-specific antibodies as predictors of allograft survival. *Am J Transplant* (2017) 17(3):703–11. doi: 10.1111/ajt.14015

54. Sicard A, Meas-Yedid V, Rabeyrin M, Koenig A, Ducreux S, Dijoud F, et al. Computer-assisted topological analysis of renal allograft inflammation adds to risk evaluation at diagnosis of humoral rejection. *Kidney Int* (2017) 92(1):214–26. doi: 10.1016/j.kint.2017.01.011

55. Das BB, Lacelle C, Zhang S, Gao A, Fixler D. Complement (C1q) binding *de novo* donor-specific antibodies and cardiac-allograft vasculopathy in pediatric heart transplant recipients. *Transplantation* (2018) 102(3):502–9. doi: 10.1097/TP.0000000000001944

56. Couchonnal E, Rivet C, Ducreux S, Dumortier J, Bosch A, Boillot O, et al. Deleterious impact of C3d-binding donor-specific anti-HLA antibodies after pediatric liver transplantation. *Transpl Immunol* (2017) 45:8–14. doi: 10.1016/j.trim.2017.08.001

57. Bailly E, Anglicheau D, Blancho G, Gatault P, Vuiblet V, Chatelet V, et al. Prognostic value of the persistence of C1q-binding anti-HLA antibodies in acute antibody-mediated rejection in kidney transplantation. *Transplantation* (2018) 102 (4):688–98. doi: 10.1097/TP.0000000000002002

58. Molina J, Navas A, Agüera ML, Rodelo-Haad C, Alonso C, Rodríguez-Benot A, et al. Impact of preformed donor-specific anti-human leukocyte antigen antibody C1q-binding ability on kidney allograft outcome. *Front Immunol* (2017) 8:1310. doi: 10.3389/fimmu.2017.01310

59. Brugière O, Roux A, Le Pavec J, Sroussi D, Parquin F, Pradère P, et al. Role of C1q-binding anti-HLA antibodies as a predictor of lung allograft outcome. *Eur Respir J* (2018) 52(2):1701898. doi: 10.1183/13993003.01898-2017

60. Kamburova EG, Wisse BW, Joosten I, Allebes WA, van der Meer A, Hilbrands LB, et al. Pretransplant C3d-fixing donor-specific anti-HLA antibodies are not associated with increased risk for kidney graft failure. *J Am Soc Nephrol* (2018) 29 (9):2279–85. doi: 10.1681/ASN.2018020205

61. Viglietti D, Bouatou Y, Kheav VD, Aubert O, Suberbielle-Boissel C, Glotz D, et al. Complement-binding anti-HLA antibodies are independent predictors of response to treatment in kidney recipients with antibody-mediated rejection. *Kidney Int* (2018) 94(4):773–87. doi: 10.1016/j.kint.2018.03.015

62. Lee H, Han E, Choi AR, Ban TH, Chung BH, Yang CW, et al. Clinical impact of complement (C1q, C3d) binding *De Novo* donor-specific HLA antibody in kidney transplant recipients. *PloS One* (2018) 13(11):e0207434. doi: 10.1371/journal.pone.0207434

63. Malheiro J, Santos S, Tafulo S, Dias L, Martins LS, Fonseca I, et al. Detection of complement-binding donor-specific antibodies, not IgG-antibody strength nor C4d status, at antibody-mediated rejection diagnosis is an independent predictor of kidney graft failure. *Transplantation* (2018) 102(11):1943–54. doi: 10.1097/TP.0000000000002265

64. Schinstock CA, Dadhania DM, Everly MJ, Smith B, Gandhi M, Farkash E, et al. Factors at *de novo* donor-specific antibody initial detection associated with allograft loss: a multicentre study. *Transpl Int* (2019) 32(5):502–15. doi: 10.1111/tri.13395

65. Babu A, Khovanova N, Shaw O, Griffin S, Briggs D, Krishnan NS, et al. C3d-positive donor-specific antibodies have a role in pretransplant risk stratification of cross-match-positive HLA-incompatible renal transplantation: United Kingdom multicentre study. *Transpl Int Off J Eur Soc Organ Transplant* (2020) 33(9):1128–39. doi: 10.1111/tri.13663

66. Gautier Vargas G, Olagne J, Parissiadis A, Joly M, Cognard N, Perrin P, et al. Does a useful test exist to properly evaluate the pathogenicity of donor-specific antibodies? Lessons from a comprehensive analysis in a well-studied single-centre kidney transplant cohort. *Transplantation* (2020) 104(10):2148–57. doi: 10.1097/TP.0000000000003080

67. Zhang Q, Hickey M, Drogalis-Kim D, Zheng Y, Gjertson D, Cadeiras M, et al. Understanding the correlation between DSA, complement activation, and antibody-mediated rejection in heart transplant recipients. *Transplantation* (2018) 102(10):e431. doi: 10.1097/TP.0000000000002333

68. Cioni M, Nocera A, Tagliamacco A, Basso S, Innocente A, Fontana I, et al. Failure to remove *de novo* donor-specific HLA antibodies is influenced by antibody properties and identifies kidney recipients with late antibody-mediated rejection destined to graft loss – a retrospective study. *Transpl Int* (2019) 32(1):38–48. doi: 10.1111/tri.13325

69. Hayde N, Solomon S, Caglar E, Ge J, Qama E, Colovai A. C1q-binding DSA and allograft outcomes in pediatric kidney transplant recipients. *Pediatr Transplant* (2021) 25(2):e13885. doi: 10.1111/petr.13885

70. Pernin V, Beyze A, Szwarc I, Bec N, Salsac C, Perez-Garcia E, et al. Distribution of *de novo* Donor-Specific Antibody Subclasses Quantified by Mass Spectrometry: High IgG3 Proportion Is Associated With Antibody-Mediated Rejection Occurrence and Severity. *Front Immunol* (2020) 11:919. doi: 10.3389/fimmu.2020.00919

71. Schaub S, Hönger G, Koller MT, Liwski R, Amico P. Determinants of C1q binding in the single antigen bead assay. *Transplantation* (2014) 98(4):387–93. doi: 10.1097/TP.0000000000000203

72. Yell M, Muth BL, Kaufman DB, Djamali A, Ellis TM. C1q binding activity of *de novo* donor-specific HLA antibodies in renal transplant recipients with and without antibody-mediated rejection. *Transplantation* (2015) 99(6):1151–5. doi: 10.1097/TP.0000000000000699

73. Reed EF, Rao P, Zhang Z, Gebel H, Bray RA, Guleria I, et al. Comprehensive assessment and standardization of solid phase multiplex-bead arrays for the detection of antibodies to HLA. *Am J Transplant Off J Am Soc Transplant Am Soc Transpl Surg* (2013) 13(7):1859–70. doi: 10.1111/ajt.12287

74. Zachary AA, Lucas DP, Detrick B, Leffell MS. Naturally occurring interference in Luminex assays for HLA-specific antibodies: characteristics and resolution. *Hum Immunol* (2009) 70(7):496–501. doi: 10.1016/j.humimm.2009.04.001

Frontiers in Immunology

Explores novel approaches and diagnoses to treat immune disorders.

The official journal of the International Union of Immunological Societies (IUIS) and the most cited in its field, leading the way for research across basic, translational and clinical immunology.

Discover the latest Research Topics

See more →

Frontiers

Avenue du Tribunal-Fédéral 34
1005 Lausanne, Switzerland
frontiersin.org

Contact us

+41 (0)21 510 17 00
frontiersin.org/about/contact